Effect of climate change on permafrost microbiome at the Pleistocene-Holocene and Holocene-Anthropocene transitions

by

Alireza Saidi-Mehrabad

A thesis submitted in partial fulfillment of the requirements for the degree of

Doctor of Philosophy

in

Microbiology and Biotechnology

Department of Biological Sciences

University of Alberta

Abstract

Understanding past and future responses of Arctic soil microbes to climate change is critical to an understanding of ecosystem function and climate change feedbacks; the goal of my thesis was to obtain a clearer understanding of these feedbacks. The remnants of the Pleistocene and early Holocene biota, including microorganisms, are preserved in the permafrost of Eastern Beringia, which could potentially show how soil microbes were shaped in Eastern Beringia by the ancient climate change that occurred at the end of the last ice age. However, contamination, low biomass, and physical complexity of permafrost samples create difficulties for molecular analyses. My results show that none of the widely used permafrost decontamination methods fully removed intentionally added biological tracer; hence, I introduced a novel method based on bleaching and scraping. Further, I showed that while permafrost chemical parameters and age did not affect decontamination, they influenced DNA extraction efficiency. I tested multiple widely used DNA extraction kits and modified one to acquire sufficient DNA from difficult permafrost samples. Using this optimized sampling and extraction protocol, I examined whether relict permafrost microbial communities provide a window into past soil microbial communities or not. Microbial community composition and soil chemistry at the Pleistocene-Holocene transition indicated that these parameters were stable until the climate system crossed a threshold, after which there was an abrupt shift to a new steady state. These findings may provide insights into possible future shifts in modern soils. I also examined the response of Arctic methanotrophs (microbes that use CH_4 as their sole source of energy) to increases in temperature and active layer disturbance, which both parameters are going to be wide spread in Anthropocene. Soil disturbance had a more significant effect on methanotroph community structure than temperature. There was a strong linear relationship between CH_4 oxidation rate and temperature;

furthermore, CH_4 oxidation rates significantly increased in disturbed soils. The active methanotrophs shifted in response to temperature in undisturbed samples, but not in disturbed samples. The results of my thesis complement the previous studies regarding the carbon cycle in the fragile Arctic, and could lead to generation of effective strategies for better management of novel fragile ecosystems in a warmer world.

Preface

All the figures and tables in this thesis are designed by **Alireza Saidi-Mehrabad**, except Figures 1.1-1.5 of the chapter 1 and Figure 2.1 of the chapter 2. Figures obtained from other publications have been cited and acknowledged.

Chapter 2 of this thesis has been published in the journal "Scientific Reports" as "**Saidi-Mehrabad, A.**, Neuberger, P., Cavaco, M., Froese, D., Lanoil, B. (2020). Optimization of subsampling, decontamination, and DNA extraction of difficult peat and silt permafrost samples. *Scientific Reports.* 10:14295".

Chapter 3 of this thesis has been published in the journal of "Frontiers in Environmental Science" as "**Saidi-Mehrabad, A.**, Neuberger, P., Hajihosseini, M., Froese, D., Lanoil, B. (2020). Permafrost microbial community structure changes across the Pleistocene-Holocene boundary. *Frontiers in Environmental Science.* 8:133".

Chapter 4 of this thesis is in preparation for publication. No specific journal has been selected yet. The potential title for the publication is going to be "**Saidi-Mehrabad, A**., Strilets, T., Forster, M., Froese, D., Lanoil, B. (2021). A major shift in activity and composition of methanotrophs in permafrost active layer soil in response to soil disturbance and temperature changes".

In all these chapters, I was responsible for conceptualizing the projects, sample collection, performing the experiments, data analysis, designing of the figures and tables (except Figures

1.1-1.5 and 2.1), article review, and lead authorship of the manuscripts. Lanoil and Froese obtained the funding for all the projects, conceptualized the projects, and aided with the formulation of the manuscripts. Neuberger, Cavaco, Strilets, and Forster, assisted with the experiments and data analysis. Hajihosseini aided with the statistical tests.

This project was made possible with the generous support of University of Alberta (UANRA grant, obtained by **Alireza Saidi-Mehrabad**), the Polar Knowledge Canada (NSTP grant, obtained by **Alireza Saidi-Mehrabad**), Queen Elizabeth II graduate scholarship (QEII, obtained by **Alireza Saidi-Mehrabad**), Alberta Graduate Excellence Scholarship (obtained by **Alireza Saidi-Mehrabad**), Alberta Innovates Graduate Student Scholarship (obtained by **Alireza Saidi-Mehrabad**), Steve and Elaine Antoniuk Graduate Scholarship in Arctic research in biological sciences (obtained by **Alireza Saidi-Mehrabad**), NSERC Discovery Grant (obtained by **Brian Lanoil** and **Duane Froese**), NSERC Northern Research Supplements (obtained by **Duane Froese**) and ArcticNet project (obtained by **Brian Lanoil**).

Some components of this project have been used in the following posters and presentations:

Saidi-Mehrabad, A., Neuberger, P., Hajihosseini, M., Froese, D., and Lanoil, B. (2019). Soil chemistry, not age, is the primary driving factor correlated to difference in Pleistocene-aged and Holocene-aged permafrost microbiomes. ASM-Arctic Net, Halifax Canada (Oral and poster presentations).

Saidi-Mehrabad, A., Neuberger, P., Hajihosseini, M., Froese, D., and Lanoil, B. (2017). Microbial community structure is distinct across the Holocene-Pleistocene boundary in ancient Beringian permafrost. ASM-Arctic Net, Québec Canada (Poster presentation).

Lanoil, B., Neuberger, P., **Saidi-Mehrabad, A**., and Froese, D. (2019). AGU conference, San Francisco USA. (Oral and poster presentations).

Saidi-Mehrabad, A. (2019). ACUNS conference, Edmonton Canada. (Guest speaker).

Saidi-Mehrabad, A. (2019). RENR GSA Conference, Edmonton Canada. (Guest speaker).

My findings have been also featured at the University of Alberta's scientific news under the title "A climatic crystal ball: How changes in ancient soil microbes could predict the future of the Arctic".
https://www.ualberta.ca/science/news/2020/august/arctic-soil-climate-change.html.

CTV EDMONTON NEWS "Soil microbes may be 'crystal ball' in future climate".
(https://www.facebook.com/watch/?v=365633934429447)

University of Alberta's CJSR-FM campus radio station "Ice age microbes" (Broadcasted in Persian/Farsi language).

توانا بود هر که دانا بود

ز دانش دل پیر برنا بود

“Mighty is he who has knowledge; from knowledge the old heart becomes young”

Ferdowsi

Shahnameh (The book of kings)

I dedicate this work to my family and friends. I am forever grateful for their compassion and support.

Acknowledgment

First and foremost, I would like to sincerely thank my advisor, Dr. Brian Lanoil, for his guidance, for his patience, and for all the opportunities that he provided me. Joining his lab was a dream come true. Brian, it was an honor working with you.

Furthermore, I would like to thank Dr. Duane Froese for his support and guidance. Thank you so much Duane for sharing your immense knowledge with me. I would have never thought one day I can go beyond all those documentaries and posters about the ice age and mammoth and tag along with your awesome lab on a journey to wonderful Yukon for collecting samples. I thank you Brian and Duane for providing me this once in a lifetime opportunity.

I would like to extend my thanks to the members of my supervisory committee: Dr. Suzanne Tank, Dr. Maya Bhatia, and Dr. Lyle Whyte. I sincerely appreciate you taking the time to get involved in my Ph.D. project and your insightful comments that helped to perfect my project.

I thank my past and present fellow lab mates in Lanoil lab and Froese lab, especially Patrick Neuberger, William Kirby, Juan Camilo Santana, Angelica Aguirre, Julian Ariel Cabrera, Helena Magaldi, Joseph Young, Sasiri Bandara, Joel Pumple, and Casey Buchanan.

Of course, I will never forget my amazing friends at the University of Alberta, Morteza Hajihosseini, Peyman Derik Vand, Maria Cavaco, Dillon Lee, Tania Strilets, Helen Trinh, Natalie Leung, Erin Macdonald, Sarah Shakil, Sattar Soltani, Dimitri Kits, and Philip Sun.

The Department of Biological Sciences has been a great environment, I thank each and everyone in the graduate office, the 265 microbiology lab, the microscopy lab, and the MBSU lab for helping me with my research. Thank you University of Alberta for shaping my career and being my second home for five years.

I finish this acknowledgment section by thanking my wonderful family for their unquestionable support and love throughout my life.

GOD, thank you for your amazing power and work in our lives, thank you for your goodness and for your blessings over us. Thank you for your great love and care. Thank you for your mercy and grace.

Table of content

List of Tables

List of Figures

viability in Holocene aged and Pleistocene aged soils. These depths were selected based on their close proximity to the Pleistocene-Holocene transition zone of 244 cm. The statistical significance (Student's t-test) of fold change in cell counts from Holocene to Pleistocene is as follows: fold change in viable cells ($p < 0.001$), fold change in dead cells ($p < 0.001$), and fold change in total cells ($p < 0.001$).

Figure 3.2. PCoA biplot of the OTU composition in Holocene (n = 3) and Pleistocene (n = 3) aged samples. Combined Axis 1 (PCOA1) and Axis 2 (PCOA2) components explained a total of 84.7% of the dissimilarity between the clusters in the system ($p = 0.022$). Samples 174–179, 179–184, 189–194 cm formed the Holocene cluster (8–10 k cal yr BP) and 296–301, 305–310, 314–319 cm formed the Pleistocene aged cluster (14–15 k cal yr BP). In the ordination space, samples (5 cm segments of DHL_16-1 and 2) have been shown with white circles and OTUs with colored squares. Colors of OTUs represent their taxonomic identity at the phylum level.

Figure 3.3. Relative abundance analyses of the OTUs detected in Holocene-aged and Pleistocene-aged permafrost samples at the phylum level.

Figure 4.1. Linear relationship between CH_4 oxidation rates and temperature.

Figure 4.2. Non-metric Multidimensional Scaling (NMDS) biplot of (A) the entire dataset and (B) methanotroph dataset. Filled black circles represent undisturbed active layer samples (DC5 and DC6) and open circles represent disturbed samples (DC7 and DC8). Values in parentheses represent the incubated temperatures. The large gray ovals separate the undisturbed (DC5 and DC6) samples (open circles) from disturbed (DC7 and DC8) samples (filled circles) based on Bray-Curtis dissimilarity matrix. Small light green and dark purple clusters separate the samples based on the incubated temperatures. Clusters were designed based on hierarchical trees (see the main text and Supplementary **Figures 4.5 A, B; 4.6 A, B; 4.8 A, B; and 4.9 A, B**).

Figure 4.3. The relative abundance of active strains detected in the heaviest ^{13}C fractions of the composite undisturbed (DC5 and DC6) (A-C) and composite disturbed (DC7 and DC8) (D-F) samples incubated at 0 ^{o}C (A and D), 4 ^{o}C (B and E) and 22 ^{o}C (C and F). The pie charts only represent the top two ASVs with the highest percent relative abundance, the rest are grouped in "Other".

Supplementary Figure 2.1. Sample preparation for decontamination protocols (a-g). Step 1: Initial dry cut. DH-1 and DH-2 cores cut into 1/3 and 2/3 sections. Step 2: Cutting into subsections. The upper portion of the 2/3 section cut horizontally for decontamination protocols (a-f). For protocol (g), the 2/3 section was cut into three rectangular pieces. Step 3: Intentional contamination of the samples. For protocols (a-f), one side of the sample was painted with the spike in the lab (LS) and the other side only contained the sprayed field spike (FS). For protocol g, one rectangular piece only contained the sprayed field spike (FS); one piece was painted with the spike in the lab (LS), and one piece was painted with pure vector (VS).

Supplementary Figure 2.2. Chemical profiles of DH_1 and DH_2 permafrost samples in relation to depth. Depth (cm) is relative to the permafrost table. Dashed lines indicate depth of sample used for noted decontamination protocol labeled as in Table 2.2. The solid line depicts the boundary between permafrost with high peat (DH_1, filled dots) and high silt content (DH_2, hollow triangles). A. Organic matter content (mass %), B. Gravimetric water content (mass %),

C. pH. The observed gap between sample d and sample e for DH_1 is due to the presence of ice pockets or not measured.

Supplementary Figure 3.1. Supplementary Figure 3.1. Chemical parameters in DHL16-1 (Holocene-aged) and DHL16-2 and DHL16-3 (Pleistocene-aged). The gray bar is the Pleistocene-Holocene boundary that started at a depth of 244 cm. (A) Organic matter (OM) and gravimetric water content. (B) pH. (C) Electrical Conductivity. (D) Nutrients, including Fe, K, Mg, P, S, and total nitrogen (TN). (E) NO_3^-/NO_2^-. (F) Ca and total carbon. (G) Cations, including Cu, Mn, Zn, Na, and NH_4^+. All measured chemical parameters demonstrated a statistically significant change ($P < 0.001$-0.05) from Holocene to Pleistocene soils except NH_4^+ ($p=0.16$).

Supplementary Figure 3.2. Relative abundance analysis of the 14 lab strains (lab constructed mock community) used as a positive sequencing control. The strains are shown at the genus level only.

Supplementary Figure 3.3. Rarefaction curve based on the observed OTUs (OTU richness) at 97% cutoff value. Samples were rarefied to 1768 sequences per samples. In parenthesis H = Holocene aged and P= Pleistocene aged samples.

Supplementary Figure 3.4. A-D Micrograph of a Pleistocene (~14-15 k cal yr BP) and Holocene (~8-10 k cal yr BP) aged Eastern Beringian permafrost soil samples after 48 h of drying at 70 ^oC. Image A depicts a silty Pleistocene aged soil with no traces of organic material, selected from the depth of 296 cm under 4.5 × magnification. Image B depicts a peaty Holocene aged soil sample from a depth of 210 cm under 4.5 × magnification. Image C and D depict the same soil samples shown in images A and B under 67 × magnification respectively.

Supplementary Figure 3.5. PCA biplot of the measured soil chemistry from segments associated to Holocene aged DHL-16_1 core (n=3) and Pleistocene aged DHL-16_2 core (n=3). Clustering was based on epoch ($p = 0.021$) and PCA1 and 2 components were able to explain 97.89% of the variation in the system. R^2 of each vector: OM: 0.88, TC: 0.96, TN: 0.79, H_2O: 0.66, pH: 0.97, Ca: 0.88, Cu: 0.84, Fe: 0.97, K: 0.97, Mg: 0.94, Mn: 0.84, Zn: 0.96, Na: 0.96, P: 0.97, S: 0.96, NO^-_3/NO^-_2: 0.88, EC: 0.91, and NH_4^+: 0.99. In the biplot: large white circles represent the samples, TC = total carbon, TN = total nitrogen, and EC = electrical conductivity.

Supplementary Figure 3.6. Co-occurrence net connectivity analysis of shared OTU and core OTUs between and within composite Holocene and Pleistocene samples. Core H OTUs (unique to Holocene aged samples) are shown with red circles (n=284). Core P OTUs (unique to Pleistocene aged samples) are shown with blue circles (n=276). Shared OTUs (n=52) are shown with green circles. H = Holocene, P = Pleistocene, and P-H = shared between Holocene and Pleistocene.

Supplementary Figure 3.7. Differential abundance analysis of the top 10 dominant phyla that were statistically significantly driving the taxonomic difference in abundance between the composite Holocene and Pleistocene samples. Differential abundance was calculated with DEseq2 method.

Supplementary Figure 3.8. Difference in taxonomic composition between Pleistocene aged cluster (small gray oval on the right) and Holocene aged cluster (large gray oval on the left) at phylum level. Samples 174-179, 179-184,189-194 cm formed the Holocene cluster (8-10 k cal yr BP) and 296-301, 305-310, 314-319 cm formed the Pleistocene aged cluster (14-15 k cal yr BP).

Each small circle represents a taxon. Axis 1 and Axis 2 combined explained 84.7% of the variation in the system ($p = 0.022$).

Supplementary Figure 3.9. Relative abundance analysis of composite Holocene and Pleistocene permafrost samples at taxonomic level of class.

Supplementary Figure 3.10a. Rank abundance analysis of P-H shared group at taxonomic level of phylum. P-H shared = Pleistocene-Holocene shared.

Supplementary Figure 3.10b. Relative abundance analysis of P-H shared group at taxonomic level of phylum. P-H shared = Pleistocene-Holocene shared.

Supplementary Figure 4.1. Active layer sampling sites. A. Undisturbed site (DC5 and DC6). B. Disturbed site (DC7 and DC8).

Supplementary Figure 4.2. DNA density gradients of control samples prepared from pure cultures of *Methylomicrobium album* BG8 (strain ACM 3308) grown under ^{13}C (black circles) and ^{12}C (open circles) CH_4 atmosphere. A. Control sample included at 0 ^{o}C SIP run. B. Control sample included at 4 ^{o}C SIP run, C. Control sample included at 22 ^{o}C SIP run.

Supplementary Figure 4.3. 15 known bacterial strains used as a positive control in 16S rRNA sequencing.

Supplementary Figure 4.4. CH_4 oxidation rates in composite undisturbed (DC5 and DC6) and composite disturbed (DC7 and DC8) samples incubated at 22 ^{o}C (A), 4 ^{o}C (B) and 0 ^{o}C (C). $*p < 0.05$ and $**p < 0.01$.

Supplementary Figure 4.5. Measured alpha diversity indices between composite disturbed (DC7 and DC8) and undisturbed (DC5 and DC6) active layer soils, A. for complete dataset, B. for the methanotroph dataset and C. time zero samples with no history of laboratory incubation. Probability values were measured with Mann Whitney U-test between and within samples.

Supplementary Figure 4.6. Optimal number of clusters for the complete dataset was determined based on the "elbow method" by the aid of Gap statistics. A. Optimal number of clusters determined in undisturbed samples (DC5 and DC6) from the entire dataset and B. Optimal number of clusters determined in disturbed samples (DC 7 and DC8) from the entire dataset. The dash lines depict the optimum number of clusters.

Supplementary Figure 4.7. Hierarchical trees of the undisturbed (DC5 and DC6) (A) and disturbed (DC7 and DC8) (B) active layer samples from the entire dataset. The distance matrix used was Manhattan, and the clustering was performed with the ward.d2 algorithm. The optimum number of clusters (in green for undisturbed samples and purple in disturbed samples) were determined based on the "elbow method" by the aid of Gap statistics (see **Supplementary Figure 4.5 A, B**).

Supplementary Figure 4.8. A. NMDS biplot of the time zero samples. B. The "elbow method" used by the aid of Gap statistics for determining the number of optimum clusters and, C. hierarchical tree designed based on the distance matrix of Manhattan, and clustering based on ward.d2 algorithm. In figure (A) large gray ovals separate the undisturbed (DC5 and DC6) (depicted with filled black circles) samples from disturbed (DC7 and DC8) (depicted with open circles) samples based on Bray-Curtis dissimilarity matrix. Small circles in green (DC5 and

DC6) and purple (DC7 and DC8) separate the samples based on the optimum number of clusters based on the "elbow method" (determined based on C). In (B) the dashed line depicts the optimum number of clusters. In (C) the coloured boxes represent a cluster, which was determined based on (B).

Supplementary Figure 4.9. The Gap statistics method used for evaluating the optimum number of clusters in the methanotroph dataset. The "elbow method" was used in order to cut the hierarchical trees (see **Figure S9 A, B**) of the methanotrophs dataset in undisturbed (DC5 and DC6) (A) and disturbed (DC7 and DC8) (B) active layer samples.

Supplementary Figure 4.10. Hierarchical cluster trees of the methanotroph dataset in (A) undisturbed (DC5 and DC6), and (B) disturbed (DC7 and DC8) active layer samples. In figure, the coloured boxes represent a cluster which was determined based on **Supplementary Figure 4.8 A, B.**

Supplementary Figure 4.11. Venn diagrams of methanotroph dataset based on observed ASVs. Shared and unique ASVs between undisturbed (DC5 and DC6) and disturbed (DC7 and DC8) samples incubated at 22 ºC (A), 4 ºC (B) and 0 ºC (C).

Supplementary Figure 4.12. DESeq2 differential abundance analysis of the entire dataset (A) and methanotroph dataset (B) based on soil disturbance. In both figures coloured circles depict species that were differentially abundant (log2 fold change) between soil types ($p < 0.01$). In A, color of the circles shows the phylogenetic affiliation of a particular species to a phylum. Benjamini-Hochberg algorithm was used for controlling the false discovery rate of the analysis.

Supplementary Figure 4.13. Relative abundance analysis of the entire database (A) undisturbed (DC5 and DC6) and (B) disturbed samples (DC7 and DC8) at phylum level. In A and B the orange bars show 0 ºC, black bars 4 ºC and green bars 22 ºC samples. The "NA" group did not match any known phyla.

Supplementary Figure 4.14. Relative abundance analysis of the methanotroph dataset (A) undisturbed (DC5 and DC6) and (B) disturbed (DC7 and DC8) samples at class level. In A and B the orange bars show 0 ºC, black bars 4 ºC and green bars 22 ºC samples.

Supplementary Figure 4.15. Relative abundance analysis of the methanotroph dataset (A) undisturbed (DC5 and DC6) and (B) disturbed (DC7 and DC8) samples at genus level. In A and B the orange bars show 0 ºC, black bars 4 ºC and green bars 22 ºC samples.

Supplementary Figure 4.16. The relative abundance of the strains detected in the heaviest ^{12}C fractions of the composite undisturbed (DC5 and DC6) (A-C) and composite disturbed (DC7 and DC8) (D-F) samples incubated at 0 ºC (A and D), 4 ºC (B and E) and 22 ºC (C and F). The group "Other" represents the composite relative abundance of the species with less than 4% abundance.

Supplementary Figure 4.17. DNA density gradients of composite undisturbed (DC5 and DC6) (A-C) and disturbed (DC7 and DC8) (D-F) samples incubated at 0 ºC (A and D), 4 ºC (B and E) and 22 ºC (C and F).

Chapter 1

1.1. Climate change and Anthropocene

This section intends to provide a general overview of the thesis background by introducing the readers to definitions of "climate change" and "Anthropocene".

Climate on Earth naturally changes from one season to another or from one geographical location to another, however, any significant changes in the mean state of the climate that persists for a long meaningful geological time scale is referred to as climate change (Kuria, 2012). Climate change is a defining environmental crisis of our time (Kuria, 2012; Marques, 2012). It is a growing crisis with a capacity to affect the phenology, physiology, and community structures of most life forms on Earth (Nunez *et al.*, 2019; Pecl *et al.*, 2017; Van der Putten, 2012).

Climate change is not a new concept to scientists because geological proxies (see **section 1.4**) around the globe and studies of the Earth's rotation around its axis demonstrate signs of major climatic oscillations throughout the Earth's history (see **sections 1.3 and 1.4**). For example, the Earth's orbital cycles around the sun and the effect of the eccentricity (a parameter that determines the amount of deviation from the orbiting pattern) of Jupiter's orbit, all could trigger major forcing on Earth's climate and shift climate in and out of ice age conditions (Milankovitch cycles) (Paillard, 2001; Rahmstorf, 2002; Spiegel *et al.*, 2010). Milankovitch cycles are very slow and gradual; as a result, their effects on climate are only noticeable over thousands of years (Paillard, 2001; Rahmstorf, 2002; Thomson, 1995) (for more information see **section 1.3**). Milankovitch cycles play a key role in Earth's long-term climate (Bennett, 1990). For example,

at the Last Glaciation Maximum (LGM; ~31 kyr - ~16 kyr) (see **section 1.3**) the continental surface temperatures were 40-2.5 ^{o}C cooler than today (depending on the geographical location) (Bennett, 1990).

Another example of proxy records that hint at past climate changes is the volcanic deposits (tephra ash grains; see **section 1.4**) of North Island of New Zealand and the adjacent ocean basins, which demonstrate that the oceans of the ice age were very poorly mixed and ventilated. However, at the end of the Pleistocene epoch (see **section 1.3**) the strength of oceanic ventilation increased (Sikes *et al.*, 2000; Toggweiler & Russell, 2008). This increase in ocean ventilation has been hypothesized to have released large quantities of carbon dioxide (CO_2) to the atmosphere and helped to terminate the last age by shifting the global climate to Holocene conditions (The current geological epoch) (Sikes *et al.*, 2000; Toggweiler & Russell, 2008).

Most of our knowledge of the Earth's past 800 kyr of climatic conditions has been obtained from the ice cores of Greenland and Antarctica (Alley, 2000; Cuffey & Clow, 1997; Vinther *et al.*, 2009). Analysis of these ice cores demonstrates a strong linear relationship between an increase in greenhouse gases (in particular CO_2) and an increase in atmospheric temperature (Alley, 2000; Cuffey & Clow, 1997; Elsig *et al.*, 2009; Vinther *et al.*, 2009). Through paleoclimatological construction of these ice cores, scientists have noticed a significant increase in atmospheric CO_2 levels since the industrial revolution (from ~280 ppmv (parts per million by volume) to ~368 ppmv at present) (Monnin *et al.*, 2001). Amongst all major greenhouse gases in atmosphere, CO_2 dominates total forcing with 2.076 Wm^{-2} followed by CH_4 with 0.156 Wm^{-2} and N_2O with 0.202 Wm^{-2} respectively (Butler & Montzka, 2016). The greenhouse gas effect of CO_2 was originally

identified by Tyndall in 1861 and it is widely reported as the most important greenhouse gas generated due to human activities since the industrial revolution (Lewis & Maslin, 2015; Retallack, 2002). Human's insatiable need for energy since the industrial revolution has resulted in increased use of coal, oil, and gas, collectively known as fossil fuels. Fossil fuels are long term storage of organic carbon and have a biological origin, which are derived from the buried ancient biota of Cenozoic (~10 million years ago) and Mesozoic (~180 million years ago) eras—burning them return the sequestered carbon mainly in the form of CO_2 to the atmosphere (Berner, 2003).

Greenhouse gases have high potential in trapping the Sun's energy, which could lead to reduction in the Earth's albedo (Cao, 2003). The Earth's albedo is a fundamental parameter of the global energy balance, thus decrease or increase in global albedo could have major consequences on Earth's climate (Wielicki *et al.*, 2005). Major greenhouse gases with high potential in influencing the Earth's albedo include CO_2, which is the by-product of complete combustion, and carbon monoxide (CO), nitrogen oxide (NO_x), sulfur dioxide (SO_2), water vapor (H_2O) and methane (CH_4), which are either by-products of incomplete combustion or products of biological activities (Heilig, 1994; Ramanathan & Feng, 2009).

CH_4 is second to CO_2, which is biologically produced by methanogens (see **sections 1.5, 1.6, 1.7 and chapter 5**) in shallow anoxic subsurface systems. It can also be naturally present in deep geological strata. On a time, scale of 100 years, CH_4 has heat-trapping potential per molecule that is 34 × higher than CO_2 (IPCC 2007) (Arthur & Cole, 2014). In addition to the combustion of fossil fuels, other human activities such as habitat degradation, disturbance of natural ecosystems, nutrient loading, and overexploitation of biological resources have directly

amplified climate change and still continue to amplify it (Ballhausen *et al.*, 2020; Cao, 2003; Leadley, 2010; Zimov *et al.*, 2006). Such human activates are permanently disturbing the Earth systems to a point of no return to the prior state (tipping point/ecological threshold hypothesis; see below), thus, it has led scientists to suggest the beginning of a new geological epoch, the Anthropocene (Johnson, 2013; Lewis & Maslin, 2015). There is no consensus agreement among scientists exactly when the Anthropocene began, but its signs are observable in geological proxy records (such as traces of fire fossil charcoal, agriculture and overkill of some species) and will be observable for millions of years into the future (Zalasiewicz & Freedman, 2009).

Some noticeable features of the Anthropocene, which differentiates this epoch from other late Quaternary epochs include drastic changes in nitrogen cycle due to overuse of ammonia-based fertilizers (not seen since 2.5 Gy (giga annum/billion years ago)) (Canfield *et al.*, 2010), substantial increase in concertation of the greenhouse (to a level not seen for at least several Myr (million years ago)) (Stocker *et al.*, 2013a), substantial increase in ocean water acidity (not seen since 300 Myr) (Broadgate *et al.*, 2013), and mass-scale selective species extinction directly linked to human activities (100 -1000 × higher than natural scale) (Barnosky *et al.*, 2011). As a result scientists believe that all these observations match with the criteria for recognizing a shift in an epoch, which strongly suggests that we no longer live in the Holocene (Palumbi, 2001; Zalasiewicz & Freedman, 2009). Some scientists propose that the Holocene-Anthropocene transition occurred at the end of the LGM, some propose the industrial revolution, some the 1960s, and others that we are currently experiencing it now (Lewis & Maslin, 2015).

Climate change and Earth's biodiversity are deeply interconnected (Ho, 2010; Nunez *et al.*, 2019). Biodiversity forecast models show that climate change could have abrupt and catastrophic effects on Earth's life forms if permanent changes in the climate system crosses an ecosystem threshold. The crossing of the threshold, also known as a tipping point, would drastically reorganize ecosystems and lead to species extinctions and loss of biomes or irreversible alteration in ecosystem function with unknown consequences (Alley *et al.*, 2003; Leadley, 2010; Scheffer *et al.*, 2001; Trisos *et al.*, 2020).

The relationship between climate change and loss of organisms and biomes has been very well documented and publicized; however, microorganisms, particularly those in the soil, are generally overlooked and not discussed in the context of climate change, global process models, or policy development (Allison & Martiny, 2008; Cavicchioli *et al.*, 2019). Relatively little is known about the effect of climate change on microbial community structure or metabolic activity (Classen *et al.*, 2015). Soil microorganisms are an essential player in ecosystem functioning and because of their vital role, they have been termed by Cavicchioli and colleagues as "the life support system of the biosphere" (Cavicchioli *et al.*, 2019; Cavigelli & Robertson, 2000; Classen *et al.*, 2015; Fatima *et al.*, 2014; Fierer & Schimel, 2002; Gulledge & Schimel, 1998; Lundquist *et al.*, 1999).

Previous studies investigated the relationship between changes in soil microbial community and increase in temperature; however, these studies have failed to produce a consensus result (Biasi *et al.*, 2008; Lamb *et al.*, 2011; Rinnan *et al.*, 2007) (for more information see **section 1.2**). For example, some studies demonstrated that microbial community structure changes in parallel to

changes in soil physicochemical parameters (Lamb *et al.*, 2011). As a result, it is important to disentangle the effect of soil physicochemical parameters and temperature on microbial community structure.

However, as mentioned above this is not the first time the Earth is experiencing rapid global climate change. The most recent major shift in climatic conditions occurred ~10 kyr, at the Pleistocene-Holocene transition, which coincided with the glacial retreat, change in plant community composition, and disappearance of the ancient megafauna (Hoffecker *et al.*, 2014; Lacelle *et al.*, 2019; Sandom *et al.*, 2014). The remnants of this ancient biota in the form of intact fossils, ancient DNA, pollen and even viable soil microorganisms are well-preserved in permafrost, particularly that of un-glaciated eastern Beringia (D'Costa *et al.*, 2011; Froese *et al.*, 2009b; Gaglioti *et al.*, 2016; Haile *et al.*, 2009; Lorenzen *et al.*, 2011; Opel *et al.*, 2018; Peteet, 2000; Porter *et al.*, 2019; Shapiro & Cooper, 2003; Willerslev *et al.*, 2014; Zazula *et al.*, 2003a; Zazula *et al.*, 2007). At the end of the Pleistocene epoch, Beringia encompassed Eastern unglaciated Siberia, Alaska, and westernmost Northwest Canada and was located between the colossal Laurentide and Scandinavian ice sheets (Strauss et al., 2017). Since no major climate shifts similar in scale to Pleistocene-Holocene have occurred after the most recent epoch transiting, the permafrost of Beringia has remained intact and is an archive of the direct effects of the most recent global climate change e.g. (Mackelprang *et al.*, 2017; Willerslev *et al.*, 2003). Permafrost in general is protected from the influence of the atmosphere, plants, animals, and even microbes in the surrounding unfrozen soil (Ponder *et al.*, 2004; Willerslev *et al.*, 2003) (for more information see **sections 1.2, 1.3**, and **1.4**). Hence, permafrost that was deposited across the Pleistocene-Holocene could provide a snapshot of microbes that formed under two different

climatic conditions, e.g. (Burkert *et al.*, 2019). However, obtaining clean samples devoid of environmental contaminants from a low biomass sample like permafrost is very challenging and requires rigorous authentication processes. Currently, effective DNA extraction and contamination monitoring protocols are missing in the field of permafrost microbiology (for more information see **chapter 2**).

By using Eastern Beringian permafrost and active layer microbial communities as a model, my Ph.D. thesis focuses on the following questions: 1) "how confident are we that the DNA extracted from permafrost is truly representing the ancient microbes and not contaminating contemporary microbes?" 2) "what was the impact of abrupt climate change at Pleistocene-Holocene transition on soil microorganisms?" and; 3) "If we assume that modern climate change is analogous to the Pleistocene-Holocene transition, how will disturbance of the active layer soil along with an increase in temperature shape active layer microbial community structure, and in particular, the methanotrophic community?" Methanotrophs are an important functional guild of microbes that are capable of acting as natural bio filters by consuming CH_4 as their sole source of energy (for more information see **section 1.7** and **chapter 4**). To answer these questions, I investigated the microbial community structure of Eastern Beringian permafrost that formed at the time of the Pleistocene-Holocene transition. The relict microbial DNA (DNA preserved in late Pleistocene aged permafrost; see **chapter 3**) can provide important insight into how the microbial community was structured in a colder world. Concurrently, live members of the microbial community found in early Holocene aged permafrost can demonstrate how the extant community responds to changing soil physicochemical parameters within permafrost.

In order to understand how the entire microbial community and less-studied methanotrophs might respond to the future climate change (Holocene-Anthropocene), I compared both the entire microbial community and the methanotrophic community structure from a disturbed active layer site with methanotrophs and with microbial communities found in an undisturbed site in Eastern Beringia. Active layer overlays the permafrost table and undergoes seasonal freeze and thaw cycles (Hinzman *et al.*, 1991). Samples were incubated at a series of below and above sub-zero temperatures to study the relationship between changes in CH_4 oxidation rates, and active layer soil disturbance. Subsequently, DNA Stable Isotope Probing (SIP) was employed to see how the active members of the methanotrophic community responded to drastic changes in temperature and disturbance.

The overall goal of this thesis project is to further the science of microbial ecology in the context of climate change and aid to fulfill one of the major goals of environmental microbiology, which is predicting microbial community dynamics in complex environments. Finally, this thesis attempts to answer the bigger question of "what is the effect of climate change on soil microbes?" Studies such as this project are important because, although soil microorganisms show high metabolic capacity/flexibility, rapid growth rate, and high abundance, they have been shown to be sensitive to climate change-driven disturbances (Fenchel & Finlay, 2004). Hence, to create an environmentally sustainable future in a warmer world it is pivotal to consider the microscopic portion of the Earth's biosphere and its community composition in the climate models.

1.2. Drivers of soil microbial community structure and soil warming experiments

The objectives of this section are to introduce the reader to 1) ecological parameters that shape the soil microbial community structure, 2) describe the potential pitfalls associated with the soil warming experiments, and 3) why the archival capacity of permafrost could help us to circumvent most of the issues associated with soil warming experiments.

Since soil microbes are essential in ecosystem functioning it is important to consider their ecological dynamics in the context of climate change. To achieve this, a clear understanding of the climate-based and soil physicochemical (edaphic) based parameters that shape the microbial community structure is required. This knowledge is important because any disturbances that could change these parameters could ultimately cause a shift in soil microbial community composition or metabolic rates, which could subsequently affect dynamics of carbon degradation, carbon feedback rate to the atmosphere and in general soil processes and ecosystem services (Allison & Martiny, 2008; Balser & Firestone, 2005; Cavigelli & Robertson, 2000; Fierer & Schimel, 2002; Frey *et al.*, 2013; Gulledge & Schimel, 1998; Johnson *et al.*, 2007; Lundquist *et al.*, 1999; Schimel *et al.*, 1999; Waldrop & Firestone, 2004).

Factors that influence the soil microorganisms' temporal dynamics in a local community have been recently broadly classified into historical contingencies, internal dynamics (previously known as autogenic succession), and external forcing factors (previously known as allogenic succession), which all are interconnected (Stegen *et al.*, 2018). The historical contingency has been defined as "constraints on microbial responses created by prior conditions that result in aggregate functional responses to environmental change dependent on either previous biota or

environments" (Hawkes & Keitt, 2015). In other words, the community is structured by the history of the environment. Hence, if the community was shaped by certain parameters in the past, it is more likely to have residual members that are resistant to a similar disturbance in the future (Fierer & Schimel, 2002; Gulledge & Schimel, 1998; Lundquist *et al.*, 1999; Stegen *et al.*, 2018).

Internal dynamics are a combination of processes associated with intraspecific and interspecific species interactions. These dynamics are important for maintaining stable communities and changes in internal dynamics can result in a change in community composition and structure. (Kampichler *et al.*, 1998; Kowalchuk *et al.*, 2002; Ringelberg *et al.*, 1997; Stegen *et al.*, 2018). Although multiple factors have been recognized to influence the internal dynamics of the microbial populations, resource depletion followed by competition seems to be the most common factor (Hawkes & Keitt, 2015).

External forcing factors are abiotic stochastic (random disturbances) or deterministic factors (selection pressures) that shape the community structure by selecting species within a community that are able to cope with these factors imposed by the environment (Binu *et al.*, 2018; Chave, 2004; Cody, 2002; Stegen *et al.*, 2018; Wang *et al.*, 2013). These forcing factors are also known as environmental filters, which control the spatial patterns of microbial communities.

In soil environments, the deterministic selection pressures are mainly climate-driven or soil edaphic-driven, which both act concurrently in shaping the microbial community structure (Chase & Myers, 2011; Langenheder & Székely, 2011; Stegen *et al.*, 2013; Zhou *et al.*, 2014),

although their influence on microbial community changes from one system to another (Chisholm & Pacala, 2011; Dini-Andreote *et al.*, 2015; Evans *et al.*, 2017). For example, in comparison to aquatic systems, soils are generally heterogeneous, hence microbes in soil systems are under constant pressure by numerous environmental filters that might not be present in the aquatic systems (Ettema & Wardle, 2002; Zhou *et al.*, 2002). Although there are numerous climate-driven parameters that influence the microbial community structure, two important ones are temperature and moisture content of the soil (Hutchins *et al.*, 2019; Waldrop & Firestone, 2006). In many terrestrial environments, low temperature has been highlighted as a limiting factor for microbial degradation of organic carbon material (Hutchins *et al.*, 2019; Waldrop & Firestone, 2006). Earth is a cold planet with ~85% of the biosphere permanently exposed to low temperatures (< 5 ^{o}C), with a mean annual temperature of 15 ^{o}C (Rampelotto, 2014; Trotsenko & Khmelenina, 2005), which makes degradation of complex recalcitrant compounds in soil difficult for microbes (Davidson & Janssens, 2006). In general, the vulnerability of soil organic material to temperature and increased microbial decomposition is dependent on the chemical and physical properties of these materials (Abbott *et al.*, 2014; Schädel *et al.*, 2014; Tanski *et al.*, 2017). The temperature sensitivity of organic matter degradation has been studied extensively in soils, demonstrating that increasing temperature has a linear relation with increase in the microbial degradation rate of recalcitrant organic matter, e.g. (Davidson & Trumbore; Davidson & Janssens, 2006). To better understand this relationship soil microbiologists rely on the Arrhenius equation. The Arrhenius equation ($k=Ae^{-Ea/RT}$) measures the temperature dependence of reaction rates (Logan, 1982). In the formula: k = rate constant, A = pre-exponential factor, E_a = activation energy, R = universal gas constant, and T = temperature (Logan, 1982). According to the Arrhenius equation, the k of a reaction ("a coefficient of proportionality directly related to

the rate of a chemical reaction at a given temperature to the concentration of reactant") increases exponentially when E_a decreases. Because the rate of a reaction is directly proportional to the k value of a reaction, the rate increases exponentially as well. Hence, a reaction with a small E_a only requires a very small amount of energy to reach the transition state, and as a result should proceed faster than a reaction with a larger E_a (Logan, 1982).

In general, more complex substrates have a higher E_a and high temperature sensitivity in comparison to simple compounds (Davidson & Janssens, 2006). As a result, it could be understood that the lability of a substrate can be defined by the change in the Ea needed in order for the degradation to take place. The more recalcitrant the compound, the higher its Ea, according to the Arrhenius equation higher its temperature sensitivity to microbial degradation (Davidson & Trumbore; DavidsonEA, 2006; Sierra, 2012). Thus, in general microbes tend to utilize organic carbon that has a lower molecular weight, which contains a higher C:H ratio (more aliphatic), and lower O:C ratio (less oxidized) (Sun et al., 1997; Vallino et al., 1996). However, some studies disagree that increased temperature enhances the degradation of soil organic material, e.g. (Wei *et al.*, 2014). They highlight this fact that this observation is only true in a short term and they argue that soil microbial community structure shift in response to increased temperature and the degradation rates depends on the new community members' ability in degrading these organic materials, hence the underlying mechanisms are not clear (Conant *et al.*, 2011; Crowther & Bradford, 2013; Hartley & Ineson, 2008). Some scientists also argue that the Arrhenius equation might not be applicable to the soil environment, because soil contains a large number of organic compounds with differing molecular structure and

complexity. Thus, the heterogeneity of soils results in unique inherent kinetic properties (Davidson & Janssens, 2006).

Like all microbially-mediated reactions, water is required for organic carbon degradation and the amount of water in the soil could drastically alter the microbial community structure and carbon feedback to the atmosphere (Davidson & Janssens, 2006; Li *et al.*, 2012; Wang *et al.*, 2010). Microbes consistently responded to soil wetting events by increased expression of pathways involved in the production of a variety of sugars and osmolytes (Chowdhury *et al.*, 2019). In contrast, reduced soil water content negatively affects enzymes that are involved in carbon cycling, such as beta-glucosidase and aminopeptidase, or those involved in nutrient cycling, such as phosphatase and arylsulfatase (Bouskill *et al.*, 2016; Hinojosa *et al.*, 2016; McHale *et al.*, 2005; McKew *et al.*, 2011). However, some enzymes involved in carbon metabolism such as cellobiohydrolase, N-acetylglucosaminidase, and xylanase could significantly increase under drying scenarios (Bouskill *et al.*, 2016). Soil water content controls the osmotic status of the cells and the availability of substrates for microbes by affecting the diffusion rate of nutrients (Kieft *et al.*, 1993; Konings *et al.*, 2002; Potts, 1994). Hence, the moisture content of the soil plays a key role in shaping the microbial community structure and their metabolic responses to climate change.

Flooding of the soil reduces the diffusion of the oxygen into deeper soil layers and causes a shift from aerobic to anaerobic conditions (Davidson & Janssens, 2006). Anaerobic conditions are conducive to methanogenesis (Wagner, 2017). This phenomenon is more important in permafrost affected regions of the northern hemisphere, because it has been predicted that the permafrost of this region is going to substantially thaw in near future due to increased

atmospheric temperatures resulting from anthropogenic climate change (see **chapter 4** for more details). For example, the Community Climate System Model (version 3.0) has predicted that of the approximately 10.5 million km^2 of the near-surface permafrost, only 1 million km^2 will remain in Anthropocene (Lawrence & Slater, 2005).

The physical and chemical aspects of soil, collectively known as edaphic parameters, have a substantial influence on the alpha, beta, and functional diversity of soil microbes (Deng *et al.*, 2015; Docherty *et al.*, 2015; Papke & Ward, 2004; Waldrop & Firestone, 2006). Scientists believe that Microbial community structure and diversity are under the direct control of the soil edaphic parameters around the globe, unlike higher trophic life forms, whose diversity is dependent on geographical location (e.g. their diversity decreases from the equator to the higher latitudes) (Falge *et al.*, 2002; Fierer *et al.*, 2011; Fisher, 1936; Hackl *et al.*, 2004; King *et al.*, 2010; Lauber *et al.*, 2009a; Prevost-Boure *et al.*, 2014). For example, soil physical properties, such as particle size distribution, aggregate size, and porosity, profoundly influence water holding capacity, nutrient retention, nutrient availability, drainage, and leaching in soils (Brady *et al.*, 2008; Wei *et al.*, 2018). Soil texture influences the microbial enzymatic activity; a decrease in the size of the soil particles was associated with an increase in enzymatic activity (Waldrop & Firestone, 2006).

Among all soil edaphic parameters, soil pH showed the strongest regulatory effect on microbial community structure and enzymatic activities across various landscapes and it is a key index of soil properties (Downie & Taskey, 1997; Kandeler *et al.*, 1998; Razanamalala *et al.*, 2018; Slessarev *et al.*, 2016; Stark *et al.*, 2014; Zhang *et al.*, 2019). One known mechanism that

controls the soil pH is change in the ratio of two secondary minerals of $CaCO_3$ (calcite) and $Al(OH)_3$ (gibbsite) (Slessarev *et al.*, 2016). Both calcite and gibbsite act like proton sponges in the soil, by dissolving in the water they absorb the protons from the soil matrix and release them when they precipitate due to lack of water, buffering soil pH (Chadwick & Chorover, 2001; Van Breemen *et al.*, 1983). Local studies have shown that in soils where evaporation is higher than precipitation, leaching rates are low, hence it allows calcium ions (Ca^{2+}) to accumulate and result in the formation of calcite, which increases the soil pH to the alkaline end of the spectrum (near pH 8.5) (Jenny, 1994). Conversely, in soils where precipitation is higher than evaporation, the excess water in the soil removes calcium ions and allows the aluminum ions (Al^{3+}) to accumulate and result in the formation of gibbsite decreasing the soil pH to the acidic end of the spectrum (near pH 5.1) (Jenny, 1994). In general soils with neutral pH are uncommon in the terrestrial environments and are either acidic, which are rich in trace elements such as Ba and Pb, or basic, which are rich in elements such Co, Ni, Zn and Cr in comparison to acidic soils (Brady *et al.*, 2008; Vitousek *et al.*, 2004; West, 1981). Trace elements such as Cu, Mn, B, Mo and Se are somewhat evenly distributed between acidic and basic soils worldwide (West, 1981).

Another common mechanism involved in the buffering of the soil pH is the decarboxylation of organic matter (Yan *et al.*, 1996). When soil microorganisms degrade carbohydrates they release carboxylic groups to their environment via glycolytic pathway, decreasing the soil pH to the acidic end of the spectrum (Yan *et al.*, 1996). On the other hand when the organic anions get decarboxylated in the citrate cycle an equivalent amount of protons is required, which results in the increase of the pH to the basic end of the spectrum (Yan *et al.*, 1996). Other parameters such

as the underlying geological material (parent material) have also been seen to substantially influence the soil pH (Fabian *et al.*, 2014; Reuter *et al.*, 2008).

Because of the strong influence of soil edaphic parameters on microbial community structure and function many scientists were motivated to understand the effect of climate change, in particular warming of the soil, on microbial community structure, resilience, resistance, organic carbon degradation rates, and rate of carbon feedback to the atmosphere (Ågren, 2010; Conant *et al.*, 2011; Docherty *et al.*, 2015; Heimann & Reichstein, 2008; Hutchins *et al.*, 2019; Melillo *et al.*, 2017; Waldrop & Firestone, 2006; Williams & Jackson, 2007). Results obtained from soil warming experiments have not presented a consistent pattern (Davidson & Janssens, 2006; Waldrop & Firestone, 2006), with some demonstrating a shift in microbial community composition in a short period of time (e.g. 3 years; (Yergeau *et al.*, 2012)) and others no major directional shift in microbial community structure after a decade (e.g. 16 years; (Lamb *et al.*, 2011)).

In general, in the initial phase of the soil warming experiments, soil respiration rate significantly increases in comparison to controls, but within 2-3 years this rate decreases and becomes similar to the controls (Eliasson *et al.*, 2005; Luo *et al.*, 2001; Melillo *et al.*, 2002). This apparent physiological response in CO_2 flux across biomes seems to be consistent, but the response of soil microbial community structure is not (DeAngelis *et al.*, 2015). Few scenarios could possibly explain this observation.

Scenario 1: high resilience of soil microorganisms to disturbance. A disturbance is "any event that is relatively discrete in time and space that disrupts the structure of an ecosystem, community, or population, and changes resource availability or the physical environment" (Newman, 2019). Soil microbial communities show high stability in time and space, and drastic shifts in community structure are usually associated with major ecological and environmental disturbances (Baldrian *et al.*, 2012; Griffiths & Philippot, 2013; Lauber *et al.*, 2009b; Rousk *et al.*, 2010; Shade *et al.*, 2013). Soil warming experiments might not create enough disturbance for microbes to respond and they are able to gradually acclimate to moderate warming and the community resists shifts in composition (Allison & Martiny, 2008; Bradford *et al.*, 2008; Metcalfe, 2017; Rousk *et al.*, 2012). Thus, the duration of the soil warming experiments could also cause discrepancies between studies (Conant *et al.*, 2011; Wang *et al.*, 2006). For example, one to four years does not seem to be enough to observe significant changes in the soil microbial community structure in response to warming, e.g. (Biasi *et al.*, 2008; Conant *et al.*, 2011; Kuffner *et al.*, 2012; Rousk *et al.*, 2012; Zhang *et al.*, 2014). Studies have shown that the microbial community members could acclaim to increased soil temperature, e.g. (Bradford et al., 2010), meaning that microbes could still show high plasticity to increase in temperature as long as they can survive. In addition, the mean residence time of soil organic matter cycling is very slow in comparison to the duration of most soil warming experiments (Conant *et al.*, 2011).

Scenario 2: Another possibility is change in soil edaphic parameters (such as changes in the pH profile of the soil) accompanied by changes in microbial community structure (Docherty *et al.*, 2015). For example, Biasi and colleagues did not see a major change in soil microbial community structure in a course of 2 years of soil warming experiment. Inertia in the community

structure was correlated with inertia in soil edaphic parameters such as moisture content (Biasi *et al.*, 2008). In contrast, Rinnan and colleagues demonstrated major alterations in microbial biomass accompanied by a significant change in water content at a higher temperatures (Rinnan *et al.*, 2007). Such observations remain to be further tested with laboratory-based manipulation of the soil edaphic parameters accompanied by increase in temperature.

Scenario 3: Some portion of the labile organic material in soil are encapsulated in aggregates of different size, which stabilizes the organic matter by protecting them from microbial enzymes (Goebel *et al.*, 2009). After the initial phase of the experiment, the fast depletion of the labile and easy to access organic material, which microbes prefer over more recalcitrant compounds might explain the significant reduction in metabolic rates, e.g. (Eliasson *et al.*, 2005; Hartley *et al.*, 2008). Shift in microbial community structure and reduction in biomass has also been observed in parallel with a reduction in microbial degradation rates and increased soil temperature (Frey *et al.*, 2008; T. Weedon *et al.*, 2012). The new dominant microbial community members that have been selected due to the experimental conditions may show different temperature dependencies and abilities in degrading the organic material in response to increased temperature (Luo, 2007).

Scenario 4: Extracellular DNA released from the dead cells have been shown to be dominant in soil and could obscure estimates of soil microbial diversity (Carini *et al.*, 2016; Nocker *et al.*, 2007). A study by the use of propidium monoazide a DNA intercalating agent, which could prevent the amplification of the extracellular DNA, demonstrated that 40% of the obtained DNA from both prokaryotic and eukaryotic microbes in soil were extracellular DAN (Carini *et al.*, 2016; Nocker *et al.*, 2007). However, as long the species abundance distribution of the

extracellular and intact DNA pools are equivalent, it is less likely that the extracellular DNA could cause significant changes in estimates of microbial alpha diversity (Lennon *et al.*, 2018).

Such scenarios increase the complexity of microbial response to climate change and reduce the ability of the global climate models to predict future carbon dynamics from the biosphere to the atmosphere (Wei *et al.*, 2014). The majority of global climate models do not consider the microbial response to climate change and only a hand full of models such as the Century Model (Parton *et al.*, 1987), Multiple Element Limitation model (Rastetter *et al.*, 1997), and Terrestrial Ecosystem Model (McGuire *et al.*, 1993) consider microbial processes; however, these models do not account for shifts in the community composition (Allison & Martiny, 2008). One reason behind this shortcoming is the high complexity of ecosystem processes, and most notably microbial community members are too diverse to catalog and model (Allison & Martiny, 2008; Schmidt *et al.*, 2011). In addition, there is still no clear connection between community structure and function.

One environment that could help to study the relationship between climate change, soil edaphic parameters, and shifts in microbial community structure is permafrost. Permafrost is an example of an environment with a capacity to harbor relict DNA, as well as dead and viable microorganisms (Willerslev & Cooper, 2005; Willerslev *et al.*, 2004b). In addition, permafrost is isolated from atmospheric inputs and modern root growth and soil microorganisms do not penetrate into the permafrost table, hence permafrost is a snapshot of the above ground and possibly below ground conditions of cold and warm periods that occurred during the Quaternary ice age (Ponder *et al.*, 2004; Willerslev *et al.*, 2003). Although permafrost is not able to directly

preserve the signs of the past climatic events, it does preserve proxy records, including preserved soil physicochemical parameters that formed in response to the past climatic oscillations. Soil physicochemical parameters are directly influenced by the climate, e.g. (Lawrence & Hornberger, 2007), hence, by studying changes in preserved soil edaphic parameters and microbial community structure that had formed at the Pleistocene-Holocene transition, we could observe how microbial community structure has formed over a long geological time period in response to above and below ground conditions. **Chapter 3** of the current thesis will provide more information regarding the archival capacity of permafrost in preserving both soil edaphic parameters and microbial community structures across the Pleistocene-Holocene transition. The next section (**section 1.3**) delves deeper into the climatic conditions of the late Pleistocene and early Holocene epochs and also provides more information regarding the archival capacity of the Eastern Beringian permafrost that formed at the Pleistocene-Holocene transition. Section 1.4 highlights the main findings in the literature that explains why the permafrost of Beringia is a snapshot of two different worlds.

1.3. The Quaternary ice age and the Pleistocene-Holocene transition

This section intends to provide information about 1) the most recent climate change at the Pleistocene-Holocene transition, which coincided with major reorganization in Earth's systems, and 2) signs of this major climatic transition archived in an exceptional state in the permafrost of Eastern Beringia.

The Anthropocene era is not the first time that the Earth has experienced rapid global climate change; multiple major climatic oscillations and glacial conditions periodically occurred during the 4.6 Gya BP (Before Present) history of the Earth (Gargaud *et al.*, 2013; Macdonald *et al.*, 2010; Montañez & Poulsen, 2013; Tang & Chen, 2013). The most recent major climatic oscillations in Earth's history began with the ending of the Neogene period and the beginning of the Quaternary, in which the Arctic ice cap became established and marked the beginning of 100 kyr cycles of stadial (colder climate) and interstadial (warmer climate) periods (Gargaud *et al.*, 2013). According to the Milankovitch theory, variations in the Earth's orbital pattern around the sun result in changes in the amount of solar radiation reaching the Earth, which in return strongly influences the climate and cause the stadial and interstadial cycles every 100 kyr (Gargaud *et al.*, 2013; Repenning & Brouwers, 1992). The stadial and interstadial cycles became more dramatic, frequent, and abrupt at the end of the Pleistocene epoch (Dokken *et al.*, 2013).

Oxygen isotopes ($\delta^{18}O$) (which are an important proxy for palaeoclimatological studies of a region) entrapped in Northern Greenland ice cores (known as NGRIP cores) drilled in 1999 demonstrated that every 1-2 kyr, the mean annual temperature (MAT) abruptly (in less than 10 years) rose by as much as 15-16.5 ^{o}C, which then persisted for 200-400 yr. At the end of these warm periods, the MAT cooled in a short period of 50-200 yr. The temperature then remained

cold for about 1 kyr. These cycles of abrupt climatic oscillation are known as Dansgaard-Oeschger events (DO cycle/oscillation events) (Alley *et al.*, 2003; Boers *et al.*, 2018; Bond *et al.*, 1993; Dansgaard *et al.*, 1993; Dokken *et al.*, 2013) **(Figure 1.1)**.

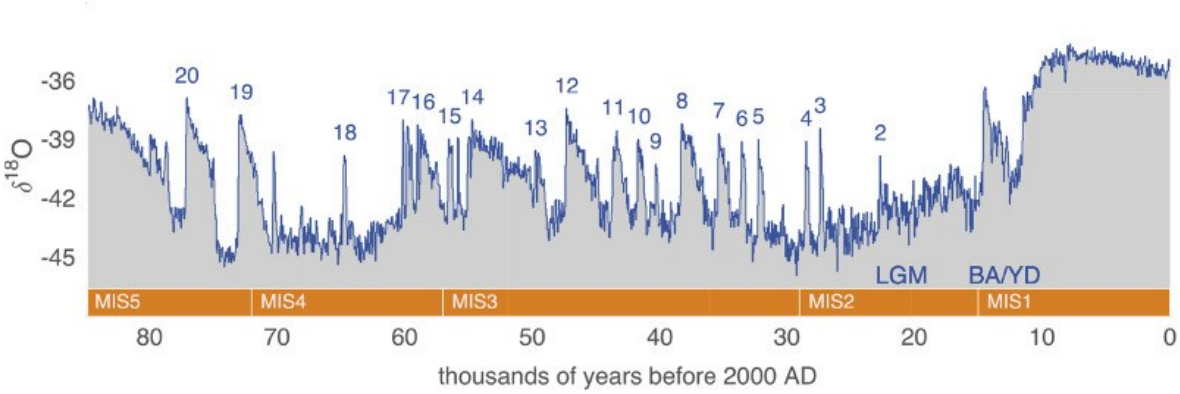

Figure 1.1. Dansgaard-Oeschger climatic oscillation events (shown with blue numbers) assessed based on the preserved oxygen isotopes ($\delta^{18}O$) in Greenland ice cores (thousands of years before 2000 A.D). In the figure, the horizontal orange line depicts the Marine Isotope Stages (MIS), LGM = last glaciation maximum, and BA/YD = Bølling-Allerød (interstadial)/Younger-Dryas (stadial) transition. MIS 1-14 (kyr), MIS 2-29 (kyr), MIS 3-57 (kyr), MIS 4-71 (kyr), MIS 5-130 (kyr). The figure has been reprinted with permission from (Li & Born, 2019).

It should be mentioned that the oxygen isotopes ($\delta^{18}O$) are a powerful tool for reconstructing the past climatic oscillations of a particular region (Bowen, 1991; Sklash et al., 1976). Water molecules with ^{16}O isotope are much lighter than the water with ^{18}O isotope, allowing it to

evaporate faster than the water molecules enriched with ^{18}O isotopes. However, when water vapor condenses to form rain it is mainly enriched in ^{18}O water, leaving a greater percentage of the ^{16}O water molecule in the atmosphere. As ^{16}O enriched water vapor travels toward the Earth's pols/colder regions it freezes and forms glaciers or helps form permafrost mainly made of ^{16}O isotopes and a small amount of ^{18}O isotopes. The extent of the ^{16}O enrichment and ^{18}O depletion depends on how cold the atmospheric temperature is, because colder the temperature greater the loss of ^{18}O isotopes (Bowen, 1991). This difference in ^{16}O: ^{18}O ratio in response to temperature allows indirect estimation of the climatic conditions of a region since the time of the glacial/permafrost deposition.

In addition to these DO cycles, the Younger Dryas (12,800 yr BP) near glaciation event is another example of a very abrupt shift in global climate close to the Pleistocene-Holocene epoch transition (Alley *et al.*, 2003; Rasmussen *et al.*, 2006). The Earth's MAT started to gradually increase after the LGM when colossal ice sheets started to retreat; however, a sharp decline in temperature terminated the warm Bølling/Allerød interstadial (last interstadial period before Holocene; ~14,700 yr BP) and initiated a cold near glacial condition known as the Younger Dryas (named after *Dryas integrifoliao/octopetala*, a type of Arctic alpine flowering plant) (Clark *et al.*, 1993; Thiagarajan *et al.*, 2014). The Younger Dryas abruptly ended ~11,550 yr BP after ~1,200 yr. The abrupt termination of the Younger Dryas marked the end of the cold Pleistocene epoch and the beginning of the warm, current Holocene epoch. During this transition, the MAT increased by 10 ºC in just 10 yr (Wanner *et al.*, 2011). One possible explanation regarding the sudden termination of the Younger Dryas is due to DO oscillation (Stocker, 2000); however, a recent climate model has highlighted ocean circulation, ice shelf and

sea ice interactions as another plausible cause for Younger Dryas termination and the amplification of the DO cycles (Boers *et al.*, 2018).

The Pleistocene-Holocene transition coincided with a series of major changes at both global and ecosystem levels, including human migration into North America, global mass extinction of large ice age mammals (also known as megafauna (animals > 45 kg body weight)), reorganization in plant communities, and accompanying changes in soil chemistry and sedimentation (Hoffecker *et al.*, 2014; Lacelle *et al.*, 2019; Sandom *et al.*, 2014).

Not only Pleistocene terminus coincided with major ecosystem changes it was also accompanied with rapid and extensive increase in global atmospheric CO_2 and CH_4. It is unclear why this occurred, although there are at least three hypotheses that attempt to explain it. The first hypothesis, known as the "thermokarst lake hypothesis" (permafrost thaw pond formation; see **section 1.6**), posits that at Pleistocene-Holocene transition, sudden extensive permafrost thaw, which affected 70% of permafrost deposits, caused a dramatic increase in atmospheric CH_4 (30-87% released to the atmosphere) and CO_2 concentrations (Kanevskiy *et al.*, 2014; Köhler *et al.*, 2014; Strauss *et al.*, 2013; Walter *et al.*, 2007). This pulse of greenhouse gasses was estimated to cause a net climate warming of +0.06 Wm^{-2}, and may have played an important role in the termination of the Pleistocene epoch (Anthony *et al.*, 2014). The second hypothesis, known as the "wetland hypothesis" (Chappellaz *et al.*, 1993; MacDonald *et al.*, 2006; Smith *et al.*, 2004), proposes that widespread wetland/peatland establishment in lower latitudes led to increases in methanogenic activity. This hypothesis is different than the "thermokarst lake hypothesis" because the mechanism of CH_4 released from the thaw ponds is mainly via ebullition (CH_4

trapped in bubbles), which is now recognized as one of the major routes of CH_4 escaping to the atmosphere (see below) (Walter *et al.*, 2007; Walter *et al.*, 2006). The third hypothesis, is known as the "clathrate gun hypothesis"(Kennett *et al.*, 2000), which states that CH_4 entrapped in oceanic clathrates was periodically destabilized and released to the atmosphere (Kennett *et al.*, 2000). CH_4 clathrates are crystalline structures with CH_4 gas entrapped inside them, which are primarily found in permafrost and marine sediments (Kvenvolden, 1993; Buffett, 2000). However, the plausibility of this hypothesis has been challenged in several studies (Cannariato & Stott, 2004; Maslin *et al.*, 2004). For example, one study demonstrated that the "clathrate gun hypothesis" is unable to explain the DO oscillations (Maslin *et al.*, 2004) and it has also been suggested that the foraminiferal (single cell Eukaryotes) $\delta^{13}C$ records acquired from the Santa Barbara Basin sediments, which were used for proposing this hypothesis, might have been contaminated (Cannariato & Stott, 2004).

While Pleistocene-Holocene transition occurred recently enough that records are preserved around the globe, they are particularly well preserved in the Beringian region (Barnes *et al.*, 2002; Froese *et al.*, 2009b). In 1930, Eric Hultén, while investigating the distribution of the shrub tundra community around the Bering Strait (65º 40' N of the Arctic Circle), proposed the possible existence of an ice-free refugium. This region was not impacted by glaciation and deglaciation of North American continental ice sheets during the stadial and interstadial events (Froese *et al.*, 2009b; Hoffecker *et al.*, 2014). This region, which he termed Beringia, encompassed Eastern unglaciated Siberia, Alaska, and westernmost Northwest Canada and was located between the colossal Laurentide and Scandinavian ice sheets (Strauss *et al.*, 2017).

The main reason for Beringia remaining ice-free under the glacier conditions was because of the rain shadow effect caused by the St. Elias Mountain of western Canada, Alaska Range and Wrangell Mountains of southern Alaska (Froese *et al.*, 2000a; White *et al.*, 1997). The resulting dry climate system prevented snow and ice accumulation and prevented the ice sheets from covering this area. During stadial conditions, an herb and forbs dominated grassland (steppe) with a large variety of megafauna flourished in this region (Froese *et al.*, 2009b). The major megafauna of the late Quaternary of Eastern Beringia were Gray wolf (*Canis lupus*), woolly mammoth (*Mammuthus primigenius*), scimitar cat (*Homotherium serum*), American lion (*Panthera atrox*), steppe horse (*Equus lambei*), brown bear (*Ursus arctos*), short-faced bear (*Arctodus simus*), reindeer/caribou (*Rangifer tarandus*), bison (*Bison bison*), yak (*Bos grunniens*), and woodland muskox (*Symbos cavifrons*) (Fox-Dobbs *et al.*, 2008). The Eastern part of the ancient Beringian subcontinent contained a productive ecosystem of prairie sages related to genera *Artemisia*, herb families of *Asteraceae, Poaceae, Antirrhinaceae, Campanulaceae, Rosaceae*, all resembling a subarctic steppe ecosystem, which sustained the ice age mammalian community (Willerslev *et al.*, 2003; Zazula *et al.*, 2003b). In the late Pleistocene, approximately 50,000 yr BP, much of the late Quaternary megafauna's population such as the steppe bison, woolly mammoth and steppe horses started to decline. By the time of the Pleistocene-Holocene transition around the Younger Dryas, they completely disappeared (15,000-13,000 yr BP) (Froese *et al.*, 2009b; Lorenzen *et al.*, 2011) except for a small declining population of woolly mammoths and horses, which survived until ~10,500 yr BP (Haile *et al.*, 2009).

Factors contributing to the mass extinction of the ice age late Quaternary mammals are still not clear. Some studies have proposed climate change leading to a shift from a steppe ecosystem to a shrub ecosystem, while others point to over hunting by early humans of North America, disease, extraterrestrial impact, or some combination of these factors (Burney & Flannery, 2005; Firestone *et al.*, 2007; Guthrie, 2006; Kennett *et al.*, 2009; Koch & Barnosky, 2006; Martínez-Meyer *et al.*, 2004). However, mounting evidence indicates that climate change is the most plausible cause (Haile *et al.*, 2009). The DO cycles and Younger Dryas at Pleistocene-Holocene was as a major tipping point event in the Earth's climate system, rapidly leading to a change in all ecosystem components (Boers *et al.*, 2018). Understanding the underlying mechanisms that led to the Pleistocene-Holocene transition could enable us to predict similar abrupt climate changes in the future in order to prevent diversity loss (Boers *et al.*, 2018).

1.4. Eastern Beringian permafrost, a "Pleistocene genetic museum", challenges and perspectives

The objectives of this section are to introduce the reader to 1) the value of proxy records in reconstructing late Quaternary climate and ecosystems, 2) the value of ancient DNA (aDNA) as a powerful molecular tool for reconstructing past biomes and ecosystems, 3) the archival capacity of permafrost (in particular the permafrost of Eastern Beringia) in preserving aDNA and viable microorganisms, 4) challenges associated with aDNA studies in general, 5) challenges associated with aDNA and microbiological studies in permafrost, and 6) the lack of standardized DNA extraction protocols and decontamination methods in the field of permafrost microbiology.

Much of the knowledge of the Beringian paleoecosystem and climate has been reconstructed based on various climate and ecosystem proxies preserved in the permafrost of this region (D'Costa *et al.*, 2011; Froese *et al.*, 2009b; Gaglioti *et al.*, 2016; Haile *et al.*, 2009; Lorenzen *et al.*, 2011; Opel *et al.*, 2018; Peteet, 2000; Porter *et al.*, 2019; Shapiro & Cooper, 2003; Willerslev *et al.*, 2014; Zazula *et al.*, 2003a; Zazula *et al.*, 2007). Some of the ecosystem proxies include fossils, extracellular DNA fragments, organic material, pollen, and Arctic ground squirrel (*Spermopbilus parryii*) middens (Bradley, 1999). These proxies are used to directly construct the past ecosystems.

Some examples of climate proxies include frozen ice lenses, ice wedges, and distal silicic tephra beds (glassy particles that originated from a volcanic eruption) (Bradley, 1999), and oxygen isotopes ($\delta^{18}O$) preserved in water molecules of ancient ice or ice lenses, e.g. (Porter *et al.*, 2019). One common method extensively used in Quaternary studies of Beringia is ^{14}C-carbon (^{14}C) dating (e.g. (Porter *et al.*, 2019). On Earth, trace quantities of ^{14}C is generated in the upper atmosphere due to the interaction between thermal neutrons and nitrogen (^{14}N), which occurs as

a result of cosmic rays (Hajdas, 2008). In a course of 1-2 yr, ^{14}C gets oxidized into CO (^{14}CO) and CO_2 ($^{14}CO_2$), eventually entering into terrestrial and aquatic ecosystems via the carbon cycle (Hajdas, 2008). Autotrophic organisms fix the ^{14}C into biomass, which is then transferred into the rest of the food web by heterotrophs. While an organism is alive and metabolically active, it will continue to exchange ^{14}C with its environment; however, as soon as it dies, the amount of ^{14}C in its biomass starts to decrease due to radioisotope decay. As a result, measurements of ^{14}C beta decay rate (conversion rate of ^{14}C to nitrogen) or remaining ^{14}C atoms in a sample could help to indirectly estimate the time period (only able to measure up to 50 kyr) since the ^{14}C started to decay in a biological sample (Hajdas, 2008). Thus, these proxies are a mechanism to assist with accurate dating of the ecosystem proxies or indirectly help to construct the past climatic conditions (Bradley, 1999; Froese *et al.*, 2002).

For a paleo proxy preserved in permafrost to be useful in reconstructing ancient ecosystems, it is important to pay attention to how the surrounding permafrost has formed because it could indirectly allow us to assess its age relative to the time of permafrost deposition. Permafrost forms via two mechanisms: 1) syngeneic formation, where the sedimentation process occurs concomitantly with freezing of the soil material, and 2) epigenetic formation, where the freezing of ground material occurs after the sedimentation process (Rivkina *et al.*, 2018). The age of the paleo proxy signals preserved in syngeneic permafrost is usually equal to the age of the sediments; in contrast, the age of the paleo proxy signals in the epigenetic permafrost is related to the last glaciation condition (Rivkina *et al.*, 2018). The oldest syngeneic permafrost found in North America is in the Yukon valley (located in Beringia), where tephrochronology-based dating has estimated the age of these deposits as 60-740 kyr (BP) (Froese *et al.*, 2009a; Millar &

Lambert, 2013). This finding strongly suggests the survival of some portion of the Northern hemisphere permafrost since the time of stadial and interstitial cycles of the Pleistocene epoch and the early Holocene thermal maximum (which persisting for tens of thousands of years in Beringia) (Froese *et al.*, 2008; Kaufman *et al.*, 2004; Porter *et al.*, 2019).

The use of ancient DNA (aDNA) preserved in permafrost is a recent method in mapping the paleoecosystems in comparison to other well-established proxies (Barnes *et al.*, 2002; Bellemain *et al.*, 2013; Haile *et al.*, 2009; Lydolph *et al.*, 2005; Shapiro *et al.*, 2004; Willerslev *et al.*, 2003). aDNA in general is defined as DNA obtained from an ancient organism. In permafrost, aDNA could have originated from dead/viable microbial cells or higher trophic life forms. Due to the high archival capacity of permafrost in preserving extracellular DNA and the absence of clear parameters in the literature to help distinguish viable microbial cells that have remained metabolically active since the last ice age (see **section 1.5**) from the microbes that are possibly the offspring of the ancient ice age community, all challenges and features common to aDNA research, including the permafrost microbiology have been included in this section.

The use of aDNA has paved the path for major discoveries that otherwise was not possible by just relying on other types of paleo and ecosystem proxies (Haile *et al.*, 2009). For example, aDNA was first used by Higuchi and colleagues to address evolutionary and ecological questions regarding extinct quagga (*Equus quagga*) (Higuchi *et al.*, 1984). The 140 yr skin mitochondrial DNA demonstrated that quagga is phylogenetically more similar to African zebra (*Equus zebra*) than to horses (Higuchi *et al.*, 1984). In 1985 Pääbo successfully colonized aDNA fragments obtained from a 2,400 yr Egyptian mummy, demonstrating the possibility of using aDNA as a

reliable molecular genetic tool (Pääbo, 1985). Thomas and colleagues used aDNA to investigate the phylogeny of the extinct marsupial wolf (*Thy-lacinus cynocephalus*), which once used to roam the Australian mainland (Thomas *et al.*, 1989). A combination of aDNA and Polymerase Chain Reaction (PCR) allowed them to show that the marsupial wolf was more closely related to other Australian marsupial carnivores than to those of South America (Thomas *et al.*, 1989). **Figure 1.2** demonstrates a timeline of major discoveries made possible with aDNA.

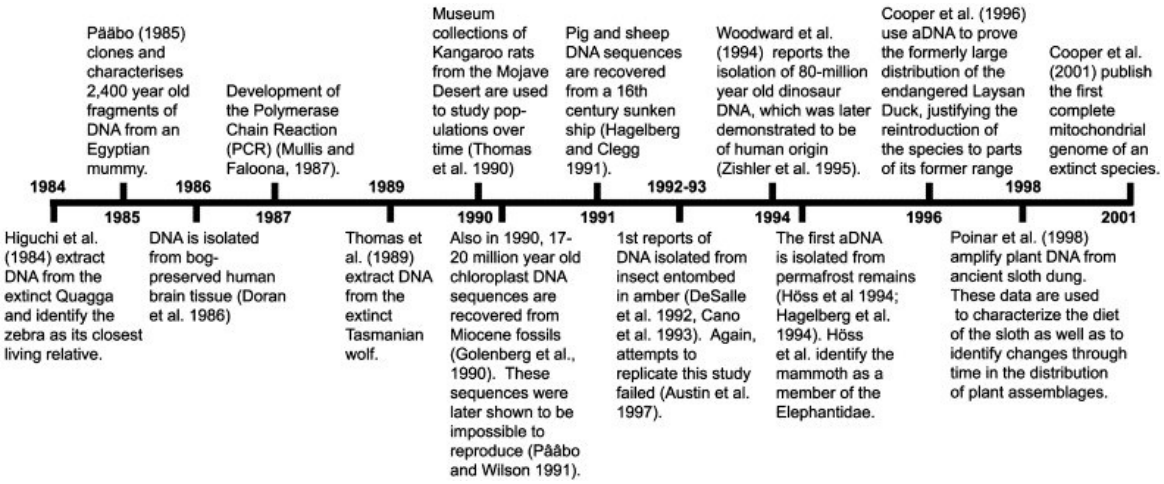

Figure 1.2. History of early studies that employed aDNA as a molecular tool before and after the advent of the PCR. The figure has been reprinted with permission from (Shapiro & Cooper, 2003).

The first DNA ever extracted from permafrost was from a frozen mammoth bone, which based on the obtained sequences, Höss and colleagues were able to identify the phylogenetic relation of the mammoth to the family Elephantidae (Hagelberg *et al.*, 1994; Hoss *et al.*, 1994).

A large number of aDNA studies from Beringian permafrost demonstrates its high archival capacity in preserving DNA that is suitable and reproducible for molecular studies, which has resulted in major discoveries about the ice age biota's population dynamics before and after major climatic oscillations of late Pleistocene and early Holocene. For example, fungal aDNA sequencing of 300-400 kyr permafrost samples revealed the presence of a wide variety of fungal species such as dark pigmented fungi and plant parasitic fungi (Lydolph *et al.*, 2005). However, a major change in the fungal community structure was observed when the sequences from the ancient samples were compared to modern tundra communities. Authors concluded that the observed changes in the fungal diversity occurred in parallel with changes in plants, which occurred in response to rapidly changing climatic conditions during the Pleistocene terminus (Lydolph *et al.*, 2005). Another study by targeting the aDNA of brown bear (*Ursus arctos*) preserved in 60 kyr permafrost from eastern Beringia, demonstrated interspecies competition with the short-faced bear (*Arctodus simus*) and relatively a stable community close to the LGM (Barnes *et al.*, 2002). The authors demonstrated major phylogeographic changes in the brown bear population close to the LGM (occurred 35 to 21 kyr) and re-establishment of a stable community after that time period (Barnes *et al.*, 2002). Willerslev and colleagues demonstrated that Beringian permafrost has the capacity to preserve plant and animal aDNA for up to 400 kyr even in the absence of conventional ecosystem proxies (Willerslev *et al.*, 2003). In addition, based on aDNA records they demonstrated dramatic changes in the taxonomic diversity and

composition of Beringian vegetation and fauna closer to the Holocene epoch (Willerslev *et al.*, 2003). Haile and colleagues with the aid of aDNA preserved in Beringian permafrost demonstrated that woolly mammoth and horse persisted in interior Alaska until the early Holocene (10,500 yr BP) (Haile *et al.*, 2009). This finding is several thousands of years later than the dates estimated from macrofossil surveys (Haile *et al.*, 2009). In the absence of plant macrofossils, Zimmermann and colleagues by relying on plant aDNA preserved in Western Beringian permafrost were able to provide a comprehensive late Quaternary history of the vegetation that persisted in North-eastern Siberia closer to the Holocene epoch (Zimmermann *et al.*, 2016).

While aDNA has been extensively used to reconstruct the ice age vegetation, and ice age mammalian communities, soil microorganisms in permafrost have received very little attention, e.g. (D'Costa *et al.*, 2011; Porter *et al.*, 2013). It is fairly well established that closer to the Pleistocene-Holocene transition the diversity of plants, and ice age mammals drastically changed, however, we still do not know how soil microbial communities have responded to this epoch transitioning (Lydolph et al., 2005; Willerslev et al., 2003; (Porter *et al.*, 2013). Also, it is still not known if the permafrost has the capacity to preserve possible changes in microbial community structure across the Pleistocene-Holocene transition. A study by Willerslev and colleague demonstrated that bacterial DNA under sub-zero conditions could survive for 400 kyr to 1.5 Myr (Willerslev & Cooper, 2005). Moreover, microbes have been cultivated from permafrost and have demonstrated active metabolism at sub-zero temperatures; thus, some microbes appear to be viable and metabolically active under deep-freeze and harsh conditions of ancient permafrost (see **section 1.5**) (Carpenter *et al.*, 2000; Christner, 2002; Drotz *et al.*, 2010;

Junge *et al.*, 2006; Lacelle *et al.*, 2011; Mackelprang *et al.*, 2017; McMahon *et al.*, 2009; Rivkina *et al.*, 2000). However, there are several issues related to aDNA studies, which some are common to all aDNA research areas and some are only related to permafrost aDNA studies. Next paragraphs delve deeper into some of these problems.

One common issue related to all aDNA-based studies is the inability of the PCR in distinguishing contaminant DNA, originating from the environment (eDNA), from aDNA. As a result, scientists became suspicious of the authenticity of some aDNA studies specially conducted in the 80s and 90s due to their non-reproducible nature; as a result, several high impact aDNA publications were discredited (Willerslev & Cooper, 2005) (**Figure 1.3**).

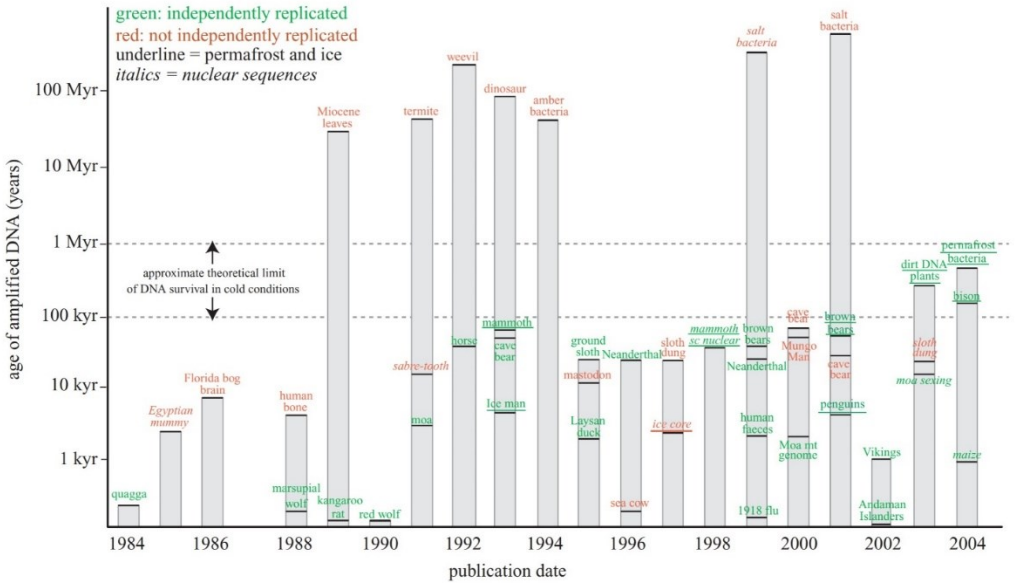

Figure 1.3. Major discoveries made possible using aDNA over the past two decades and whether they were authenticated by repeating the experiments. The figure has been reprinted with permission from (Willerslev & Cooper, 2005).

Ironically, one major source of contamination in an aDNA dedicated laboratory has been attributed to the PCR generated aerosols (Willerslev & Cooper, 2005). Aerosolized PCR droplets could contain more than a million copies of amplified DNA per 5 µl, which could easily disperse across the laboratory surfaces or even the entire facility via air movement (Willerslev & Cooper, 2005).

In addition to the PCR generated contaminants, human- and microbial-associated DNA, which form a large portion of the eDNA, are ubiquitous in laboratories; hence, all reagents and tools used in aDNA studies should be assumed to be contaminated (Willerslev & Cooper, 2005).

Even if we tackle the contamination problem, studying aDNA is not an easy task due to its fragmented nature (Dabney *et al.*, 2013). Usually, aDNA acquired from 4-13 kyr remains are heavily fragmented, with most fragments in the range of 40-500 bp due to hydrolytic and oxidative damage (Lindahl, 1993; Poinar *et al.*, 1996). Fragmented extracellular DNA of 100-500 base pairs (bp) does not survive more than 10^4 years in temperate soils (Lindahl, 1993; Poinar *et al.*, 1996). Hydrolytic damage can directly cause strand breakage of the phosphodiester backbone of the aDNA or cause depurination by removing the purine bases followed by β-elimination of the sugar backbone (Abe & Sasaki, 2016; Briggs *et al.*, 2007; Willerslev & Cooper, 2005). Hydrolytic damage can also result in the reorganization of nucleobases or their derivatives such as adenine, cytosine, 5-methylcytosine, and guanine and result in the formation of miscoding bases of hypoxanthine, uracil, thymine, and xanthine respectively (Willerslev *et al.*, 2004a). Among all nucleobases, cytosine is the most prone to hydrolytic damage and reconfiguration (Willerslev *et al.*, 2004a). Hydrolytic lesions could prevent the polymerase

enzyme from amplifying the aDNA segments or result in chimeric sequences through a phenomenon known as “jumping PCR” (Pääbo *et al.*, 1990; Willerslev & Cooper, 2005). Jumping PCR occurs when each primer is extended until a damaged site on the template DNA is encountered. In the next cycle, the newly synthesized strands interact with undamaged templates, creating chimeric strands (Pääbo *et al.*, 1990).

Oxidative damage is mainly mediated by highly reactive free radicals such as hydroxyl radical (•OH), superoxide radical (•O2) and hydrogen peroxide (H_2O_2). Free radicals cause blocking lesions that prevent the polymerase enzyme from interacting with the damaged aDNA and reduces PCR amplifiablity (Pääbo *et al.*, 1989). These free radicals are generated as by-products of oxygen interacting with various metal ions or biological molecules, ultraviolet radiation (UV) and alkylating agents (Cadet & Davies, 2017; Rastogi *et al.*, 2010). Oxidative damage includes single as well as double DNA strand lesions, which the latter damage can break the entire aDNA structure (Rastogi *et al.*, 2010). Among all known classes of free radicals, hydroxyl radicals have the potential to damage all the components of the aDNA strands, including the deoxyribose backbone (Halliwell & Gutteridge, 2015; Valko *et al.*, 2006).

In general, aDNA damage is highly dependent on the environment and the state of aDNA preservation. For example, lesions of the phosphodiester backbone in a fully hydrated system can happen every 2.5 h at 37 ºC (Willerslev *et al.*, 2004a). Hydrolytic cleavage of the β-N-glycosidic bond and associated depurination and depyrimidination can happen at every 10 h at 37 ºC in a fully hydrated system (Willerslev *et al.*, 2004a). In contrast, in frozen environments such as permafrost, water activity is very low and 92-97% of it is in ice form; hence, the chance of lesion

formation due to hydrolytic damage is very low (Gilichinsky, 2002). In addition, the measured redox potential of permafrost (in permafrost of Northern hemisphere) soil ranges from +40 to -250 mV, which is indicative of an oxygen-depleted environment (suboxic); hence, the rate of oxidative damage of preserved DNA is relatively low (Vishnivetskaya *et al.*, 2001). Moreover, permafrost is dark and the aDNA is encased in ice and soil, hence the possibility of oxidative damages caused by UV rays is very low, although other electromagnetic radiation, such as X-rays and gamma rays, could eventually contribute to aDNA damage in permafrost but the rate of damage is very slow (Brouchkov *et al.*, 2016). The main contributors to natural permafrost radiation are decaying uranium, potassium, and thorium (Van Schmus, 1995). In the absence of hydrolytic and oxidative damage, extracellular DNA has been estimated to survive up to 1 Myr under frozen conditions (Hofreiter *et al.*, 2001). Thus, DNA could survive much longer in permafrost in comparison to temperate environments.

One specific issue related to aDNA studies in permafrost is low DNA yield, which has been attributed to the physicochemical properties of the frozen soil and low cell abundance of microbial cells. Permafrost contains 10^7-10^9 microbial cells (g dry weight)$^{-1}$, irrespective of its age (cell concentration is also reported to be 10-100 times lower than the active layer), however, DNA yield is usually very low (Johnson *et al.*, 2007; Vishnivetskaya *et al.*, 2000; Vishnivetskaya *et al.*, 2006). DNA extraction from permafrost has been proven to be very challenging (Bang-Andreasen *et al.*, 2017; Fatima *et al.*, 2014; Schneegurt *et al.*, 2003). For permafrost microbiology, there are no standardized DNA extraction methods between laboratories and none of the commercially available DNA extraction kits have been compared to show, which is ideal for extracting DNA from peaty or silty permafrost with drastically different ^{14}C ages.

One major issue with all soil DNA extraction protocols is the co-extraction of humic substances (depending on the soil type they could form 5-7 $mg/_{g}$ of the soil) with the DNA (Hazen *et al.*, 2013; Matheson *et al.*, 2010; Smalla *et al.*, 1993; Tsai & Olson, 1992). Humic substances prevent PCR amplification via two mechanisms; crosslinking with the template DNA used for amplification and direct inhibition of the DNA polymerase enzymes by the ability to absorb soil metal ions (Masini *et al.*, 1998; Matheson *et al.*, 2010). Humic substances are formed from the polycondensation of organic material as a by-product of microbial mineralization of organic matter (Whitehouse & Hottel, 2007). Humic and fulvic acids are derivatives of humic substances, which are characterized as high molecular weight organic matters, alkali-soluble, and acid-insoluble (Matheson *et al.*, 2010). Usually, after each soil DNA extraction (depending on soil type and the DNA extraction protocol) ~0.7-3 $\mu g/_{\mu L}$ of humic acid gets co-extracted (which accounts for only 0.21-0.99% of the total humic acid composition of the soil) with DNA (Matheson *et al.*, 2010). Although DNA extraction protocols are constantly evolving and becoming more effective at removing a large fraction of humic and fulvic acids, no DNA extraction protocol has proven to be able to remove all humic substances in eluted DNA. Therefore, all DNA extraction protocols require further purification, since as little as 10 ng of humic substances is enough to prevent a PCR reaction (Matheson *et al.*, 2010). Although methods such as the use of powdered milk, gel extraction, size exclusion chromatography, gel filtration chromatography, and a series of chelation based (e.g. ethylenediaminetetraacetic acid, and polyvinylpolypyrrolidone) reactions have been used for removing humic substances, however, these methods all could result in loss of DNA (Matheson *et al.*, 2010; Volossiouk *et al.*, 1995). Loss of DNA might be irreparable in sequence-based studies of permafrost microbiome due to the low yield of DNA extraction protocols.

In general, in samples that produce low DNA concentrations, contamination has a higher impact and next-generation sequencing platforms are unable to distinguish contaminant sequences (Bang-Andreasen *et al.*, 2017; Burkert *et al.*, 2019; Gilbert *et al.*, 2005; Johnson *et al.*, 2007; Porter *et al.*, 2013; Rampelotto, 2014; Shade *et al.*, 2013; Willerslev *et al.*, 2004a). In microbiome studies of permafrost, contaminant sequences could cause overestimation of microbial diversity or richness and even distort permafrost microbiology research if they get recorded in reference databases (such as GenBank) as core permafrost sequences (Kunin *et al.*, 2010; Porter *et al.*, 2013). Currently, there is no standard protocol for contamination tracing and decontamination of permafrost cores; rather, every lab either uses their own protocol or no decontamination is performed (Porter *et al.*, 2013). The field of permafrost microbiology has been categorized as a high contamination risk research and requires full validation of the contaminant DNA from authentic DNA (Gilbert *et al.*, 2005).

1.5. Microbial survival strategies in permafrost

The objective of this section is to demonstrate that, unlike other known ecosystem and climate proxies preserved in permafrost, some soil microorganisms detected in permafrost are alive and metabolically active. In addition, the goal of the section was to introduce readers to several key survival strategies used by soil microbes to proliferate or survive under the harsh conditions of the permafrost.

Unlike other biological paleo proxy signals preserved in cold permafrost, some soil microorganisms are alive and metabolically active (Johnson *et al.*, 2007; Rivkina *et al.*, 2018). Omelansky reported the first microbial cultures from the Siberian permafrost in 1911 while searching for frozen mammoth remains and the first *in situ* metabolic activity at sub-zero temperature was measured in cryptoendolithic lichens (lichens that proliferate in rocks) of Antarctica (Kappen, 1993; Ponder *et al.*, 2004). Since that time, multiple studies based on soil respiration assays or CH_4 flux measurements have shown the presence of viable microbial cells in frozen permafrost, including -16 ºC in West Siberian permafrost (Panikov & Dedysh, 2000), -39 ºC in tundra soil microcosms of Barrow, Alaska (Panikov et al., 2006), -18 ºC in Greenland tundra soil (Elberling & Brandt, 2003), and -5 ºC in microcosms of McMurdo Dry Valley, Antarctic (Bakermans *et al.*, 2014). In addition to soil respiration experiments, the consumption of the ^{14}C labeled glucose in -15 ºC cryopegs (salty supercooled water brines) (**see below**) (Gilichinsky *et al.*, 2003), DNA stable isotope analysis (DNA-SIP) of frozen permafrost samples incubated at 0 ºC to -20 ºC (Tuorto *et al.*, 2014), measurement of RNA/DNA ratios (Hultman *et al.*, 2015) all hint at active microorganisms with active genome replication machinery under the harsh permafrost conditions.

Permafrost in general is a thermal phenomenon, which can encompass any ground material that has been frozen for more than 2 years (Van Everdingen & Association, 1998). Hence, permafrost

is a unique habitat for microbial proliferation because it is not heterogeneous and contains distinct geomorphological features that each could create challenges for microbial life (Hugelius & Kuhry, 2009). As a result, permafrost soils around the globe are distinguished from each other based on soil physicochemical characteristics, carbon content, ice content, and not temperature alone (Bottos *et al.*, 2018; Schuur *et al.*, 2008; Steven *et al.*, 2006). As a result, permafrost is a unique ecosystem and harbours a distinct microbiome. For example, permafrost deposits of the Northern hemisphere are both peaty (high in organic material) and silty (high in mineral content). Closer to the polar deserts of High Arctic region permafrost becomes poor in organic content, but in contrast the permafrost of the Arctic circumpolar region is rich in Pleistocene aged organic material (> 90% organic matter; **see section 1.6**) (Altshuler *et al.*, 2017). In addition, some permafrost soils are acidic such as permafrost deposits of High Arctic wetland (e.g. Axel Heiberg Island in Canadian High Arctic) (Wilhelm *et al.*, 2011) or Eastern Beringian permafrost in Yukon (**see Chapters 2 and 3**) and some have near neutral pH (e.g. Pleistocene aged permafrost of Yukon**; see Chapters 2 and 3**). In comparison to Northern hemisphere permafrost deposits, the permafrost soils of McMurdo Dry valleys of Antarctica are very dry with < 3% water content, which is mainly found in a form of ice lenses or vines in sand wedges (Altshuler *et al.*, 2017). Also the permafrost of Antarctica is poor in organic material (0.01% in the Dry Valleys and 1.5% in the coastal oases) and is highly oligotrophic (Gilichinsky *et al.*, 2007).

As mentioned above, in addition to differences in permafrost soil chemical parameters around the globe, permafrost contains unique geomorphological features such as cryopegs, taliks (unfrozen ground in permafrost affected regions), ice-wedges (ice formed in the ground cracks),

thermokarst systems (a type of terrain formed due to permafrost thaw; see **section 1.6**), frost boils (a type of ground formation caused by cryoturbation), broken soil horizons, which all could play an important role in shaping the microbial community structure and function (**see below**). As a result, the extent to which the soil edaphic parameters' influence the permafrost microbiome in comparison to temperate soils is still not well understood. Some studies have shown the influence of permafrost age (Burkert et al., 2019; Liang et al., 2019; Mackelprang et al., 2017), ice content (Burkert et al., 2019), dispersal limitation and physical/thermodynamic constraints (Bottos et al., 2018) on the structuring of the microbial community with minor correlation with soil edaphic parameters. For example, Mackelprang and colleagues found that microbes within three Pleistocene-aged permafrost chronosequences (similar samples with different age) changed in composition in response to increasing age, with a corresponding increase in survival strategies (Mackelprang et al., 2017). A parallel increase in the survival strategies with increasing permafrost age implies that environmental pressures, arising from harsh permafrost conditions, selects for a subset of species, which no longer correlate with the soil edaphic parameters (Kraft et al., 2015b; Liang et al., 2019; Mackelprang et al., 2017; Willerslev et al., 2004b). However, another study performed on two Pleistocene-aged permafrost samples of a similar age but of differing origins (lake-alluvial sediments and Yedoma/ice complex sediments) demonstrated that two distinct microbial communities, belonging to each sediment type formed in response to differing environmental settings and not due to the age of the samples alone (Rivkina et al., 2016). Chapter 3 will provide more information regarding the influence of the soil edaphic parameters on the soil microbial community of permafrost that has formed across the Pleistocene-Holocene transition.

In general permafrost is a very unique and harsh environment for microbial metabolism and growth. However, both culture based and non-culture based approaches have demonstrated a globally diverse and viable microorganisms in frozen permafrost, although in different physiological and metabolic states. Viable cells in permafrost might exist in different physiological and metabolic states such as viable but non-culturable (VBNC) state; a dormant state with no active DNA repair mechanism and no metabolic activity; and viable state with active metabolic machinery (Johnson *et al.*, 2007; Puspita *et al.*, 2015). VBNC cells are unable to form colonies and proliferate on culture media, however, they have intact cell membranes, are capable of carrying out respiration, metabolic activity and gene expression, which all are features of a viable cell (Li *et al.*, 2014). Interestingly, VBNC cells have some morphological, and physiological features that are different from non-VBNC cells. For example, VBNC cells tend to be smaller (dwarf cells) than non-VBNC cells, which is believed to be a strategy to minimize energy requirements in an oligotrophic environment such as permafrost (Biosca *et al.*, 1996; Du *et al.*, 2007). In addition, VBNC cells change their cellular shape to coccoid, which increases the surface area to volume ratio for acquiring more nutrients under stressful conditions (Cook & Bolster, 2007). VBNC cells have lower metabolic rates and a different gene expression profile than cells in a non-VBNC state (Shleeva *et al.*, 2004). For example, a study about VBNC of *Vibrio cholerae* showed a fivefold increase in the expression of 58 genes involved in regulatory functions, energy metabolism, cellular processes, transport and binding proteins in comparison to its normal sister cells (Asakura *et al.*, 2007). The cell wall structure of the VBNC cells is strengthened by increased peptidoglycan cross-linking in comparison to the normal cells (Signoretto *et al.*, 2000). Such cell wall modifications have attributed to the VBNC cells' resistance to mechanical disruption (as seen in VBNC cells of *Vibrio vulnificus*) (Weichart &

Kjelleberg, 1996), to high temperature (as seen in VBNC cells of *Mycobacterium smegmatis*), high tolerance against acidic pH, ethanol, chlorine, antibiotics and heavy metals (as seen in VBNC cells of *Vibrio parahaemolyticus, Vibrio vulnificus, Campylobacter jejuni,* and *Enterococcus faecalis* respectively) (Anuchin *et al.*, 2009; del Mar Lleò *et al.*, 2007; Nowakowska & Oliver, 2013; Rowe *et al.*, 1998; Weichart & Kjelleberg, 1996). However, it is not known if the VBNC state is due to the recovery of cells from damage caused by environmental stressors or they are simply the remnants of cells that are unable to cope and they are in a state of dying (Lennon & Jones, 2011; Li *et al.*, 2014).

Permafrost is a very harsh environment for microbial life mainly because of low temperatures and low water availability in a liquid state (1.5-7%), and high salinity in the liquid water that is available (Gilichinsky *et al.*, 2003). These salty liquid waters in permafrost are found in forms of saline brine veins or supercooled cryopegs (Gilichinsky *et al.*, 2003). These stressors and geomorphological features can drastically affect the nutrient and waste product diffusion and availability, protein structure, gas diffusion (estimated to be ~1 $m/_{10^5\ years^{-1}}$), cell enzymatic activity, membrane fluidity, and kinetic energy availability (Bakermans et al., 2003; Bottos et al., 2018; Brouchkov et al., 2016; Burkert et al., 2019; Ershov, 1998; Gilichinsky et al., 2003; Gilichinsky et al., 2002; Hinsa-Leasure et al., 2010; Mangelsdorf et al., 2007; Rivkina et al., 2018). In addition, permafrost imposes a strong limitation on microbial movement, limiting their ability to scavenge for nutrients and moving away from undesirable conditions (Bottos et al., 2018). Moreover, microbes in permafrost are constantly exposed to high concentrations of mercury (Hg) and high dosages of ionizing radiation (Schaefer *et al.*, 2020).

Hg has accumulated in permafrost over thousands of years and has the ability to change the cell membrane permeability by binding to sulfhydryls (thiol groups) and inhibiting the osmotic water permeability of aquaporins or it could lead to enzyme deficiency by binding to cysteine residues (Aduayom *et al.*, 2005; Ajsuvakova *et al.*, 2020; Rice *et al.*, 2014; Schuster *et al.*, 2018). It has been suggested that Hg, by directly binding to the Na^+, K^+ and Cl^- cotransporters in the cell membrane, could cause changes in the cell volume and act as a direct killing mechanism (Isenring & Forbush, 2001). Permafrost and the active layer, are believed to be a substantial source of Hg on Earth. The permafrost of the northern hemisphere has been estimated to contain 1656 Gg_{Hg}, which is ~2 × the concentration of Hg found in non-permafrost affected soils, oceans, and atmosphere combined (Schuster *et al.*, 2018).

Among all pressures of the permafrost environment, radiation has been highlighted as the most dangerous parameter to microbial life forms (Brouchkov *et al.*, 2016). X- and gamma rays generated from radioisotope decay in frozen minerals produce ~1-4 $mGy_{yr\text{-}1}$ exposure in Arctic permafrost. DNA encased in the endospore in spore-forming bacteria is partially protected from that radiation; however, radiation-based damage accumulates and can inhibit germination over time (Gilichinsky *et al.*, 2008; Gittel *et al.*, 2014; Margesin *et al.*, 2008; Nicholson *et al.*, 2000). As a result, microbes capable of endospore formation can not stay in a dormant state with no active DNA repair mechanisms for more than 10^2-10^4 years, or earlier than the late Pleistocene (Brouchkov *et al.*, 2016; Burkert *et al.*, 2019).

The nature of extreme longevity of entrapped microbes in permafrost and their exact age is still not clear to scientists; it has been suggested that microbes lose viability over the course of

hundreds of years (Brouchkov *et al.*, 2016; Lindahl, 1993). In addition, molecular bonds in polymer chains have been estimated to break in less than 300 years and frozen water is unable to support cell division (Levy & Miller, 1998; Rivkina *et al.*, 2018). Although salty liquid water films around soil particles might provide water for cell division, these water films are small, with a thickness ranging from 5-75 Å (10^{-10} m) in size, depending on salt concentration in the system, the charges on the mineral particles, and the temperature of the permafrost. Cells are several orders of magnitude larger than these layers; thus, they are likely insufficient for cell growth and movement (Anderson, 1967; Ponder *et al.*, 2004; Rivkina *et al.*, 2018).

Despite all these harsh conditions of permafrost, it is clear that the viable cells in permafrost have developed physiological and genetic adaptation mechanisms to survive under the harsh permanent freezing conditions (Mackelprang *et al.*, 2017). Direct microscopic cell counts from permafrost samples obtained from Siberia have shown a total of 10^7-10^8 cells/$_g$, of which 10^2-10^6 cells/$_g$ were determined to be viable, demonstrating that ancient cold permafrost is not devoid of microbial life (Ponder *et al.*, 2004; Rivkina *et al.*, 2000; Rivkina *et al.*, 1998; Vishnivetskaya *et al.*, 2000). For example, permafrost cores of the Mackenzie River region in Canada contain viable microbial cells to a depth of 400 m and permafrost samples acquired from the Tibetan Plateau at an altitude of 4,700 m also have viable microbes (Gilichinsky, 2002). Viable microbial cells ($4.8 \times 10^1 – 9.1 \times 10^1$ cells/$_g$) were also detected down to a depth of ~17 m in Antarctic permafrost samples cored from McMurdo Dry Valleys' polar desert (Gilichinsky *et al.*, 2007). Total microscopic cell counts from Antarctica permafrost have been estimated to be 10^5-10^6 cell/$_g$ (Cowan *et al.*, 2002; Gilichinsky *et al.*, 2007; Horowitz *et al.*, 1972).

How do these viable microbes adapt to allow metabolism in the difficult conditions found in permafrost? Earth is a cold planet with 25% of terrestrial biosphere permafrost affected and 85% permanently exposed to temperatures < 5 ºC. Hence, microbial psychrophiles and psychrotolerant are the most successful colonizers on Earth (Carr, 2007; Ponder *et al.*, 2004; Rampelotto, 2014; Sandle & Skinner, 2013; Trotsenko & Khmelenina, 2005; Williams & Smith, 1989). Psychrophiles are obligate low temperatures organisms capable of growing and remaining metabolically active at $\geq$ 0 ºC (minimum temperature) and $\leq$ 20 ºC (maximum temperature) with an optimum temperature for growth at $\leq$ 15 ºC. One example of a psychrophilic strain isolated from a supercooled brine in permafrost of Kolyma Lowland is *Clostridium algoriphilum*, which is able to grow down to -5 ºC with optimum temperature for growth at +5 ºC (Shcherbakova *et al.*, 2005).

In contrast, psychrotolerant organisms only tolerate the freezing conditions but prefer a temperature of $\geq$ 20 ºC for growth (optimum) (Moyer & Morita, 2007). For example, *Psychrobacter cryopegella* isolated from a cryopeg (from a 40,000 yr Siberian permafrost sample) is capable of growing in a wide temperature range (-10 ºC to +28 ºC) with optimum growth at +22 ºC (Bakermans *et al.*, 2003). Most microbes isolated from permafrost are psychrotolerant—not obligate psychrophiles (Rivkina *et al.*, 2000).

The majority of the permafrost psychrotolerant and psychrophiles detected in permafrost deposits of the Northern hemisphere are taxonomically associated with domain Bacteria, which includes Gram-positive aerobes (mainly Actinobacteria), Gram-negative aerobes (mainly Proteobacteria), anaerobic spore formers (Firmicutes), and non-spore-forming bacteria (Liang *et*

al., 2019; Pikuta *et al.*, 2005; Vorobyova *et al.*, 1997). The study of the microbial genetic material directly recovered from permafrost (metagenomics) has shown the dominance of phyla Proteobacteria, Firmicutes, Acidobacteria, Chlorofexi, Bacteroidetes and Actinobacteria in permafrost samples obtained from Hess Creek (Alaska) (Mackelprang et al., 2011), Nome (Alaska) (Taş et al., 2014), the Canadian High Arctic (Steven et al., 2007; Steven et al., 2008), Toolik (Alaska) (Coolen & Orsi, 2015), Tanana Flats (Alaska) (Hultman et al., 2015), and Eastern Siberia (Brouchkov et al., 2017). It seems that the domain Archaea is a minor component of the microbial community in frozen permafrost of the Northern hemisphere (~1%; a total of 10^5-10^7 cells/$_g$), however, 97% of this small group has been associated with an important guild of CH_4 producing microbes within the phylum Euryarchaeota, collectively known as methanogens (see **section 1.7**) (Bottos *et al.*, 2018; Coolen & Orsi, 2015). In addition to methanogenic Archaea, halophilic Archaea taxonomically affiliated with phylum Euryarchaeota (Steven *et al.*, 2007) and high acidophilic Archaea affiliated with phylum Crenarchaeota (Wilhelm *et al.*, 2011) have also been observed in permafrost. Microorganisms from the domain Eukarya, such as algae (10^3-10^5 cells/$_g$), protists (10^3 cells/$_g$), filamentous and ascomycetous fungi (mainly detected in the upper permafrost layers) and yeast (together 10^3 cells/$_g$) are also found in the permafrost of the Northern hemisphere (Coolen & Orsi, 2015; Ponder *et al.*, 2004). In general, in addition to being more abundant, the diversity of Bacteria in permafrost in the Northern hemisphere is greater than Eukarya and Archaea (Jansson & Taş, 2014).

From a microbial functional perspective, Northern hemisphere permafrost is a habitat for ammonia oxidizers, fermenters, Iron (III) reducers, methanogens, methanotrophs, nitrifiers, nitrogen fixers, sulfur reducers, sulfate reducers and thiosulfate oxidizers (Deng *et al.*, 2015; Hu *et al.*, 2019; Wu *et al.*, 2012; Yun *et al.*, 2014; Zhang *et al.*, 2009).

The permafrost in Antarctica is less studied in comparison to the permafrost deposits of the Northern hemisphere and it is believed to be much harsher for microbial proliferation in comparison to permafrost of the High Arctic (Altshuler *et al.*, 2017). The microbial community of Antarctic permafrost deposits are primarily associated with phyla Proteobacteria, Nitrospirae, Fibrobacteres, Acidobacteria, Actinobacteria, and Bacteroidetes (Gilichinsky *et al.*, 2007). Methanogenic Archaea seem to form a small fraction of the Antarctic permafrost microbial community (10^3 viable cells from a total of 10^5-10^6 cell/$_g$) (Cowan *et al.*, 2002). Mycelial fungi, yeast and green algal species associated with phylum Chlorophyta have also been detected from Antarctic permafrost (Gilichinsky *et al.*, 2007). Antarctic permafrost deposits have demonstrated microbial activities such as methanogenesis, sulfate reduction and denitrification (Gilichinsky *et al.*, 2007). In general, in addition to known phyla, permafrost around the globe also contains uncultured species associated with less characterized candidate phyla such as Patescibacteria (candidate superphylum), OP5, SR1, MVP-21, WS5, and Kazan-3B-28 (Altshuler *et al.*, 2017; Frey *et al.*, 2016).

There is no clear, reported evidence for the existence of minimum temperature for microbial metabolism in permafrost (Nikrad *et al.*, 2016; Ponder *et al.*, 2004; Song *et al.*, 2014). Some studies have shown that below freezing temperature is not a major limiting factor in microbial metabolism and growth since the majority of isolates (~ 67%) from permafrost resulted in colony formation within three weeks at -2.5 ^oC , and at -10 ^oC with added glycerol (Gilichinsky *et al.*, 1993; Vishnivetskaya *et al.*, 2000). Some examples of permafrost isolates that are capable of growing at sub-zero temperatures include *Exiguobacterium sibiricum* (minimum of -2.5 ^oC),

Psychrobacter sp. 273-4 (minimum of -2.5 ºC) (Ponder *et al.*, 2005), and *Planococcus halocryophilus* (minimum of -15 ºC) (Mykytczuk *et al.*, 2013).

These findings are not surprising since the majority of studied microbial enzymes are able to remain active down to -20 ºC (Coolen *et al.*, 2011). The reason is that the psychrophilic enzymes have unique molecular features that allow them to remain active in frozen conditions. There is a strong linear relationship between a decrease in temperature and reduced catalytic reaction activity of enzymes (Feller, 2013). Mesophilic enzymes have shown 20-80 fold reduction in catalytic reaction activity when the temperature drops from 37 ºC to 0 ºC, as a result, mesophilic microorganisms are unable to remain metabolically active in permafrost (Feller, 2013). One molecular adaption of psychrophilic enzymes is significant structural changes at their active site. For example, in the protease enzyme of psychrophilic *Pseudomonas* species, a Ca^{2+} ion widens the entrance of the active site increasing accessibility of the site to substrates (Aghajari *et al.*, 2003). Such configuration substantially reduces the Ea requirement for the formation of the enzyme-substrate complex and furthermore makes the release of products easier and faster, which could increase the enzymatic activity rate (De Vos *et al.*, 2006). Another example regarding the changes in the active site of the psychrophilic enzymes is the difference in the electrostatic potential of their enzyme active sites in comparison to mesophilic enzymes (Feller, 2013). The electrostatic potential generated by charged polar groups could orient a substrate and pull it toward the enzymes' active site, hence increasing the chance of survival in an environment such as permafrost, where molecular movement is very low (Feller, 2013). Examples of psychrophilic enzymes with different electrostatic potentials in comparison to their mesophilic counterpart include citrate synthase, malate dehydrogenase, uracil-DNA glycosylase, elastase,

and trypsin (Feller, 2013). Moreover, psychrophilic enzymes have a broader specificity their active site in comparison to their mesophilic counterparts, making them more flexible and dynamic under oligotrophic conditions in permafrost (Feller, 2013). Hence, the active site of the psychrophilic enzymes is able to accept substrates with slightly distinct structures (Feller, 2013). A highly dynamic active site then results in higher K_m (Michaelis–Menten kinetics; which is the concentration of substrate that allows the enzyme to reach ½ V_{max}). In return higher K_m lowers the enzymatic affinity to its substrate, making the enzyme less specific (Feller, 2013). Also, such enzymes are not easily saturated with small concentrations of substrate (Feller, 2013). Another interesting mechanism of adaption in psychrophilic enzymes is an increase in the number of active sites. For example, psychrophilic β-galactosidases have 6 active (homohexamer) sites in comparison to their mesophilic counterparts, which with few exceptions possess 4 active sites (Skalova *et al.*, 2005). Additional enzymatic active sites could increase the chance of enzyme-substrate interaction, hence cell survival in permafrost.

In general, psychrophilic proteins show high structural stability at sub-zero temperatures. The reason could be due to clustering of glycine residues, which provides local mobility (Kulakova *et al.*, 2004); reduction in proline residues, which enhances the flexibility of the protein's secondary structure (Sakaguchi *et al.*, 2007); reduction in arginine residues, which are involved in the formation of salt bridges and hydrogen bonds (which are considered as weak molecular bonds) (Siddiqui *et al.*, 2006); reduction in weak molecular bonds (e.g. hydrogen bonds, hydrophobic and inter-subunit interactions, and ion-pairing), which could easily dissociate at freezing temperatures (Feller *et al.*, 1996; Russell, 2000). In addition, cavity sizes in the structure of the psychrophilic proteins are larger than their mesophilic counterparts allowing water molecules to

move easily. These large cavities and embedded water molecules can significantly increase the structural flexibility of the psychrophilic proteins (Paredes *et al.*, 2011).

Protein synthesis and folding are highly sensitive to temperature fluctuations and it is known to be one of the major factors in restricting the growth of mesophilic microorganisms at sub-zero temperatures (Piette *et al.*, 2011). Also, all components of the microbial protein-synthesizing machinery could be heavy affected under cold temperatures, especially due to reduced molecular diffusion rates, and reduced activity of ribosomes as a result of increased cytoplasmic viscosity (Piette *et al.*, 2011). One mechanism of adaption in response to issues mentioned above is an increase in A:U pairing in RNA, which improves the folded ribosome function in psychrophilic microorganisms (Khachane *et al.*, 2005). Another mechanism includes high levels of post-transcriptional modification in the structure of transfer RNA (tRNA), which occurs via the activity of dihydrouridine (Dalluge *et al.*, 1997). Dihydrouridine is generated as the result of carbon-carbon reduction at positions 5 and 6 in uridine molecule by dihydrouridine synthase family of enzymes. Dihydrouridine is found in the D-loop of tRNA and stabilizes the tRNA under frozen conditions (Kasprzak *et al.*, 2012; Yu *et al.*, 2011). Helicase proteins have seen to be generated in high numbers in some psychrophilic microorganisms in comparison to their mesophilic counterparts (Piette *et al.*, 2011). A high number of helicases are essential for the efficient unwinding of the RNA at sub-zero temperatures and the rapid translation of proteins required for survival (Piette *et al.*, 2011).

Low temperatures could also drastically reduce the rate of protein folding (Piette *et al.*, 2011). As a result, psychrophilic protein folding is highly dependent on chaperones, which do not have any

effect on the speed of folding but rather optimizes the efficiency of the folding by preventing aggradations and misfolding of the proteins at sub-zero temperatures (Piette *et al.*, 2011). For example, Antarctic *Psychrobacter* sp. PAMC 21119 isolate is able to grow and remain metabolically active at -5 ^{o}C by relying on an efficient psychrophilic protein folding mechanism (Koh *et al.*, 2017). In addition, chaperone proteins such as cold shock proteins (Csp) or DEAD-box helicase are upregulated to relax the DNA and prevent secondary structure formation due to sub-zero temperatures (Margesin *et al.*, 2008). Cold shock proteins or cold-induced proteins (Cips) are a broad class of proteins that have regulatory roles in the cellular protein-synthesizing machinery produced in response to rapid temperature drop (cold shock) (Lindquist & Mertens, 2018; Phadtare, 2004). There is a strong linear relationship between an increase in the severity of the cold shock and an increase in production of the cold shock proteins (Hébraud & Potier, 1999). These proteins are among the most evolutionary preserved class of proteins in microorganisms (Lindquist & Mertens, 2018; Phadtare, 2004). In addition, psychrophilic microbes by upregulating genes such as *clpB* (disaggregating chaperone) enable the discard of the denatured and aggregated proteins under cold temperatures to prevent hindering of the cellular protein machinery (Margesin, 2008). These microbes are also capable of efficient recycling of the damaged or not needed cellular compounds to increase resource use efficiency (Margesin, 2008). Some examples of well-studied cold adapted chaperones include: trigger factor (TF), peptidyl-prolyl *cis-trans* isomerase (PPiase), GroEL/ES and ClpB (Piette *et al.*, 2011; Strocchi *et al.*, 2006). Among all chaperones, TF seems to be the most important, since it interacts with almost all of the newly synthesized polypeptides in the microbial cell (Piette *et al.*, 2011). TF has also been categorized as a cold-shock protein (Piette *et al.*, 2011).

In addition to maintaining protein function at sub-zero temperatures, microbes entrapped in permafrost need to maintain cell membrane fluidity as well. In order to maintain membrane fluidity, psychrophilic bacteria have been seen to alter the ratio of fatty acids of $C_{18:1}/C_{16}$, increase in the number of unsaturated lipids, reorganize the polar head groups, increase the amount of the compatible solutes, and decrease the length of the acyl chain and iso fatty acids from the branched-chain fatty acid family (Margesin *et al.*, 2008). All these adaptive traits are known as homeoviscous adaption, which is very important for the proper functioning and integrity of the microbial cells at very low temperatures of permafrost (Ernst *et al.*, 2016). The most fundamental homeoviscous adaption in response to temperature fluctuations is the balance between saturated and unsaturated membrane fatty acids (Erimban & Daschakraborty, 2020; Sinensky, 1974). Microbes regulate the membrane fluidity by directly sensing the temperature changes in their putative environment by relying on their histidine kinases membrane sensors (Ernst *et al.*, 2016). For example, when temperature rapidly drops around the bacterium *Bacillus subtilis,* membrane-associated DesK protein switches its role from a phosphatase to a kinase sensor (Aguilar *et al.*, 2001). DesK activates the DesR protein (a transcriptional regulator of the *des* gene) via autophosphorylation, which results in the generation of Δ5-Des lipid desaturase. Δ5-Des lipid desaturase shifts the saturated lipid acyl chains to unsaturated ones, restoring the membrane fluidity under cold temperature (Porrini *et al.*, 2014; Saita *et al.*, 2016). Homeoviscous adaption to the cold temperatures in permafrost have also been seen in *Exiguobacterium sibiricum* and *Psychrobacter* sp. 273-4 as well (Ponder *et al.*, 2005).

Sub-zero temperatures and low water activity of the permafrost could drop the cellular turgor pressure and result in inhibition of cell division (Whatmore *et al.*, 1990). However, the

accumulation of the compatible solutes could maintain the osmotic balance in cells. Compatible solutes are organic compounds that are generated in response to increased salinity, osmolarity and significant reduction in available water (Hoffmann & Bremer, 2011). Some examples of well-studied compatible solutes in *Bacillus subtilis* are proline and glycine betaine (Boch *et al.*, 1994; Whatmore *et al.*, 1990). Microbes either generate compatible solutes (e.g. in *B. subtilis* by the rapid uptake of K^+) or acquired them from dead cells or animal and plant originated products around them (BREMER, 2000; Kempf & Bremer, 1998; Spiegelhalter & Bremer, 1998; Welsh, 2000; Ziegler *et al.*, 2010). Since the concentrations of compatible solutes are very low in the environment (nM or μM) and the demand is high in case of severe osmotic stress (in molar concentrations), a very efficient mechanism to scavenge these compounds are required (BREMER, 2000; Kempf & Bremer, 1998; Welsh, 2000; Ziegler *et al.*, 2010). For example, *B. subtilis* can acquire proline from the environment via a group of special compatible solutes transporters (e.g. OpuA, OpuB, OpuC, OpuD, and OpuE) (Von Blohn *et al.*, 1997; Whatmore *et al.*, 1990). These transporters are part of the universal ATP-binding cassette systems (ABC systems) (Teichmann *et al.*, 2018; Tillotson & Tillotson, 2010). Compatible solutes have also been shown to act as a growth-promoting factor. For example, in *B. subtilis* glycine betaine has been seen to act as a growth factor when the temperature rises to about +52 ^{o}C or drops below +15 ^{o}C (Brigulla *et al.*, 2003; Holtmann & Bremer, 2004).

Some of the major genomic adaptations to frozen conditions in parallel with phenotypic adaptions include overexpression (relative to mesophilic microbes) of genes involved in Amino acid transport and metabolism, energy production, and DNA repair, replication and recombination (Coolen & Orsi, 2015). Adaptation genes such as those associated with virulence

and horizontal gene transfer were also highly expressed (Coolen & Orsi, 2015). Genes associated with Type II restriction modification system and virulence factors (Coolen & Orsi, 2015) act as a defense mechanism against foreign DNA and phages/viruses, implying a relatively high activity of phages/viruses in permafrost (Coolen & Orsi, 2015; Pingoud *et al.*, 2005). Overexpression of the type IV secretion system genes raises the possibility that the spread of the adaptive traits via horizontal gene transfer might be common among the entrapped microbes in permafrost (Mackelprang *et al.*, 2017). In permafrost, horizontal gene transfer has been reported to be faster than in mesophilic soils where horizontal gene transfer is slow in comparison to asexual reproduction (Mackelprang *et al.*, 2017). Genes associated with uracil-DNA glycosylases, which are involved in DNA repair, are also overexpressed in permafrost relative to non-permafrost affected microbes (Coolen & Orsi, 2015). Uracil-DNA glycosylases are able to recognize and remove uracil bases in damaged DNA without affecting the natural thymine bases (Visnes *et al.*, 2009). In addition, a gene related to RecA-mediated autopeptidase was also overexpressed, suggesting the presence of an active SOS response machinery in frozen permafrost (Coolen & Orsi, 2015). SOS response is a global response that is usually triggered when DNA is damaged and is activated by the RecA protein and deactivated by the LexA protein (Michel, 2005). The overexpression of these DNA repair mechanism in permafrost may be a response to the exposure to high dosages of ionizing radiation discussed above. **Figure 1.4** summarizes some of the major genes involved in the survival of the permafrost microbes that are overexpressed under frozen conditions.

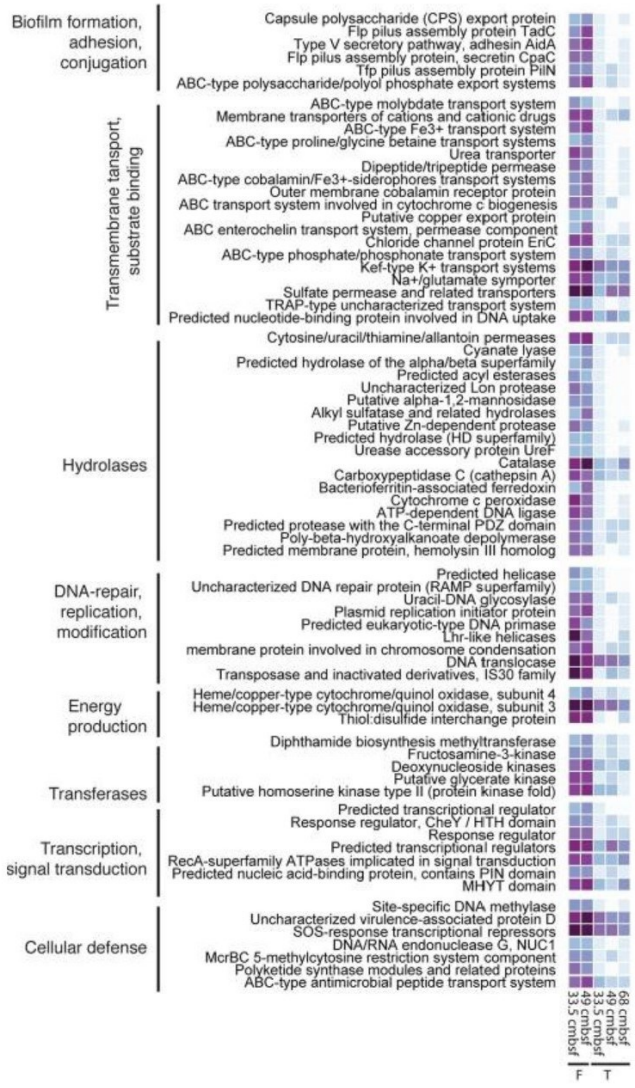

Figure 1.4. Abundance heatmap of genes upregulated in frozen permafrost. Colored boxes represent log-transformed and normalized read abundance. The threshold used for identifying the gene function was set to 60% amino acid identity. In the figure T = thawed, F= frozen, cmbsf = cm below seafloor. The figure has been reprinted with permission from (Coolen & Orsi, 2015).

Although metagenomics studies are unable to link the sequenced genes to activity, they have provided valuable information regarding the potential microbial activity in permafrost. Genes associated with nitrogen fixation and alcohol, sugar, aminosugar, and polysaccharide degradation in high abundance (Yergeau *et al.*, 2010a) and sulfate and iron (III) reduction are likely at low levels in permafrost (Hultman *et al.*, 2015). With an increase in age of the permafrost, genes involved in survival strategies, chemotaxis (movement in response to changes in chemical gradient) and aromatic hydrocarbon degradation significantly increase (Mackelprang *et al.*, 2017). All these demonstrate that microbes entrapped in ancient permafrost have developed a series of adaptations to not only survive but also remain metabolically active for long periods of time.

In addition to genotypic and phenotypic adaptions mentioned above, permafrost microbes also demonstrate physiological adaptations and are equipped with a series of unique life strategies to deal with the harsh frozen conditions of permafrost. One well-studied example is the spore formation and entering into a dormant resting stage by some bacteria to survive unfavorable environments such as permafrost, starvation, viral attack, or in general extinction. However, this mechanism of survival is not beneficial in a long term due to damage accumulation, and there is a high probability of missing signals associated with favorable conditions (Lennon & Jones, 2011). In addition, spore formation is energetically a costly process especially in low energy environments like permafrost, but sometimes it is preferred since the metabolic demand for maintaining an active microbial cell is three orders of magnitude higher than maintaining a spore (Lennon & Jones, 2011).

Another physiological adaptation to oligotrophic conditions in permafrost in the absence of active metabolic machinery is the use of glycogen, polyphosphates, and polyhydroxyalkanoates, which are produced during the growth phase and usually stored as energy compounds (Lennon & Jones, 2011). Consumption of sister cells (cannibalism) under starvation is another adaptation mechanism. Cannibalism occurs in cells that have initiated sporulation, however, when they run very low on energy, they halt spore formation and instead produce killing factors that prevent their sister cells from forming spores and cause them to lyse. The released nutrients could be used as a food source (González-Pastor *et al.*, 2003). Extracellular polymeric substances (EPSs; mainly used in biofilm production) can also be used as a carbon source under unfavorable environments such as permafrost for a short period of time. Large quantities of organic carbon are used by microbes in order to make EPS, hence it is a valuable labile carbon source in nutrient-limited conditions (Junge et al., 2006). EPS generation can happen when the microbes have access to large quantities of carbon, hence this strategy might not be preferred in comparison to other strategies of survival. In addition to the nutritional value of EPS, it could help to stabilize the cell membrane under sub-zero conditions or protect cells against ionizing radiation and assist in scavenging for metals and other nutrients necessary for cell survival (Anesio et al., 2017). Low metabolic activity sometimes (e.g. low DNA synthesis observed at -15 ºC) is preferred in comparison to long term survival strategies such spore formation (Mackelprang *et al.*, 2017). For example, genome studies of the model psychrophilic bacteria *Psychrobacter arcticus* (273-4) (isolated from Siberian permafrost) have shown down regulation of energetically costly ATP synthase, NADH dehydrogenase and TCA in order to maintain a basal metabolism (Bakermans *et al.*, 2006; Margesin, 2008). *Planococcus halocryophilus* Or1 isolated from high Arctic permafrost is also able to remain metabolically active at -25 ºC by just

relying on a basal metabolism (Mykytczuk *et al.*, 2013). Basal metabolism is believed to able to produce enough energy to repair DNA lesions caused by background radiation (Mackelprang *et al.*, 2017; Mehta & Haber, 2014).

1.6. Microbes in Permafrost: The Pandora's Box of climate change

The objective of this section is to demonstrate that 1) permafrost is not only an archive of viable microorganisms, but it is also a substantial source of sequestered organic material, 2) permafrost thaw could release a substantial amount of organic material to the surrounding environment, which could subsequently lead to increased release of CH_4 and CO_2 due to higher microbial activity, and 3) permafrost thaw could not only influence the climate change, but it could also drastically affect the hydrology and nutrient flow in the Arctic region.

The permafrost environment and the microorganisms that successfully survive there are part of the Earth's cryobiosphere, which includes snow, ice, and supercool clouds (Sattler *et al.*, 2001). Permafrost is also part of the cryolithosphere, which is defined as an environment where the majority of its constituent water is in ice form (Rivkina *et al.*, 2018). Permafrost is an archive of viable microorganisms entrapped since the last ice age and possibly could provide an invaluable opportunity to study the microbes of past periods at a phylogenetic and genome level for possible biotechnological applications or for expanding our knowledge regarding bacterial evolution, adaption mechanisms and ecology over a long meaningful geological time scale. However, by the aid of soil microorganisms in response to climate change, permafrost could act as a modern day "Pandora's Box" (Mascarelli, 2009; Strauss *et al.*, 2017; Treat & Frolking, 2013; Walter *et al.*, 2007). This phenomenon occurs either by providing an environment conducive to methanogens or by releasing the sequestered organic matter into the environment.

Currently, there is ~ 23 million km^2 of permafrost (24%-27% of the Earth's terrestrial environment), which contains a total of ~1673 Pg of organic carbon (accounting for 50% of the global carbon pool) (Brown *et al.*, 1997; Jansson & Taş, 2014; Mackelprang *et al.*, 2011; Ponder

et al., 2004; Tarnocai *et al.*, 2009). Approximately 500 Pg of this permafrost-associated organic carbon is entrapped in Yedoma permafrost (a Russian word for muck) and the rest is found in non-Yedoma domains (~ 400 Pg) including the peatlands of western Siberia (50-70 Pg) (Assessment, 2004; Smith *et al.*, 2004). Permafrost is also a substantial source of natural CH_4, which is entrapped in a form of temperature-sensitive clathrates (frozen pockets of CH_4) and have been estimated to add another extra ~5-400 Gt_C to the permafrost carbon pool (Maslin *et al.*, 2010; McGuire *et al.*, 2009)

Currently, the Yedoma domain is limited to Eastern Siberia (mainly Yakutia/Republic of Sakha), interior Alaska and Yukon (all part of Beringia) (Strauss *et al.*, 2017). Yedoma permafrost contains large quantities of partially degraded plant material of the Pleistocene epoch (grass and root), which forms ~400-500 Gt_C of sequestered organic carbon (2-5% organic carbon to the depth of 25 m) and a large volume of frozen ice (50-90% by volume) in the form of ice lenses or ice wedges. This high amount of sequestered organic matter in Yedoma is 10-30 × higher than the amount of organic matter that is sequestered in silty permafrost of the northern hemisphere and permafrost of Antarctica (Knoblauch *et al.*, 2013; Nikrad *et al.*, 2016; Schädel *et al.*, 2014; Zimov *et al.*, 2006). These features set Yedoma permafrost apart from the other type of peaty or silt permafrost in Beringia (Schirrmeister *et al.*, 2013; Schuur *et al.*, 2008; Strauss *et al.*, 2017; Walter *et al.*, 2007; Walter *et al.*, 2006). Radioisotopic signatures of the organic carbon in Yedoma permafrost indicates a deposition age around the LGM (**Figure 1.1**); no Yedoma permafrost has been found to be older than the Eemian interstadial period (130-115 kyr) (Schirrmeister *et al.*, 2013; Shackleton *et al.*, 2003). There is no consensus agreement regarding the Yedoma genesis of eastern and western Beringia, however, processes such as alluvial,

glaciolacustrine (originated from glacial lake sediments), deltaic (originated from an active or abandoned delta), and aeolian (windblown sediments) have been proposed in Yedoma genesis (Murton *et al.*, 2015; Schirrmeister *et al.*, 2013). The extent of the Yedoma permafrost has been estimated to be around 3.3 million km^2 (45^{o}N in Europe and 40^{o}N in North America) during the LGM, however, its deposition and expansion was abruptly terminated at the end of the Younger Dryas, and instead, thawing was intensified (Strauss *et al.*, 2017; Walter *et al.*, 2007; Zimov *et al.*, 2006).

Irrespective of the permafrost type, thaw could occur either very abruptly (pulse thaw) or gradually and slowly (press thaw) (Vonk *et al.*, 2015). The pulse type of thaw can release large quantities of particulate material suddenly and press type of thaw can release large quantities of nutrients, base cations, and dissolved organic carbon (DOC) over time (Vonk *et al.*, 2015). Either type of thaw can result in major landscape changes, and are divided into three categories:1) hillslope processes (also known as thermoerosional features), 2) wetland processes and 3) thermokarst lake processes (Vonk *et al.*, 2015). All these disturbances are collectively known as thermokarst formations (Vonk *et al.*, 2015).

Hillslope processes might occur very abruptly (in matter hours), and usually progress slowly over the years (Vonk *et al.*, 2015). The three most important hillslope processes include: retrogressive thaw slumps (Lantuit & Pollard, 2008), active layer detachment (Lewkowicz & Harris, 2005) and thermal erosional gullies (Godin & Fortier, 2012). Retrogressive thaw slumps are a change of ground material due to the thawing of ice into mud slurry and forming U shaped landslides (Lantuit & Pollard, 2008). Active layer detachment, on the other hand, does not

involve a change in the ground material, but rather is a "transitional landslide of active layer overlaying permafrost" (Lewkowicz & Harris, 2005). Thermal erosional gullies are "a steep sided trench or channel, often (several meters) deep, that is cut into poorly consolidated bedrock, weathered sediment or soil"(Godin & Fortier, 2012). Although the scale of hillslope processes are local but it could introduce large quantities of organic matter into aquatic systems, thus strongly influence the greenhouse gas generation (Vonk *et al.*, 2015).

Wetland processes include peatland collapse and bog/fen formation (Tarnocai, 2009). Peatlands and bogs form due to the accumulation of organic material derived from plants. The organic matter accumulates due to low turnover rates in anoxic, saturated soils resulting from the thawing of ice-rich permafrost (Craft & Richardson, 2008; Tarnocai, 2009).

Thermokarst lake processes, which include thaw ponds (a.k.a. thermokarst ponds), are a manifestation of abrupt pulse thaw, with the potential to dramatically alter the hydrology of the system and persist for thousands of years (Åkerman & Johansson, 2008; Deng *et al.*, 2015; Guérin, 1983; Osterkamp, 2007; Romanovskii *et al.*, 2000; Schuur *et al.*, 2008). Thaw ponds originating from Yedoma usually form deep ponds due to high ice content in comparison to non-Yedoma permafrost (Grosse *et al.*, 2013). Yedoma thaw ponds gradually lose oxygen in the bottom layers (they are highly stratified) and become anoxic, which provides a suitable environment for methanogenic activity (see **section 1.7**) and an increase in CO_2 and CH_4 generation (Knoblauch *et al.*, 2018). There are approximately 140,000 thaw ponds of different sizes (0.1-50 km^2) in the Arctic circumpolar region, which altogether cover 400,000 km^2 of this region (Smith *et al.*, 2007).

In addition, to the thermokarst formations mentioned above, vertical gradual thawing of permafrost with low ice content could result in the deepening of the active layer and formation of talik (Schuur *et al.*, 2008). Talik formation is defined as a layer of unfrozen ground in permafrost affected regions, which no longer freezes (Connon *et al.*, 2018). The deepening of the active layer and talik formation can cover a large area (Åkerman & Johansson, 2008).

Thermokarst formations are a major concern for Arctic nations (the majority of their land surface is permafrost affected) such as Alaska (85%), Russia (50-55%), Canada (50-55%) and China (20%), due to the socioeconomic burden that it could cause (Oliva & Fritz, 2018; Ponder *et al.*, 2004; Streletskiy *et al.*, 2019). For example, permafrost subsidence causes major damage to roads, equipment and infrastructure (Guo & Sun, 2015; Hope & Schaefer, 2016; Melvin *et al.*, 2017). Thermokarst formations can not only drastically alter the landscape topography, but it can also have a major impact on riverine and oceanic environments by introducing labile organic matter to the microbial hotspots of these aquatic systems (Berhe *et al.*, 2007). In addition, thermokarst formations could cause tree cover loss and subsequently reorganize the plant community (favoring sedge and fen vegetation) (Jorgenson *et al.*, 2001). Furthermore, by controlling the emission of the secondary aerosols formed due to microbial activity, it could directly affect cloud formation (Ehn *et al.*, 2014). As a result thermokarst formations under anthropogenic climate change needs to be closely monitored for accurate climate modeling and policy development (Romanovsky *et al.*, 2010).

One major concern regarding the thermokarst formations is that they have been hypothesized to lift many of the constraints (e.g. low temperature, oxygen, and nutrients) that had limited

microbial metabolism (see previous section) and release the sequestered organic material (Coolen & Orsi, 2015; Coolen *et al.*, 2011; Ernakovich *et al.*, 2015; Grannas *et al.*, 2013; Jansson & Taş, 2014; Ping *et al.*, 2015). Such a wealth of easily accessible carbon source and reduced barriers, may increase the microbial metabolic activity (increase in overall flux or increase in respiration rate) (Sjögersten *et al.*, 2016; Wei *et al.*, 2018). The net result of microbial degradation is the formation of greenhouse gases, mainly in the forms of CO_2 and CH_4, potentially leading to exacerbation of climate change through positive feedback (with more warming, permafrost releases more greenhouse gasses, which leads to further warming) (Coolen & Orsi, 2015; Mackelprang *et al.*, 2011; Oliva & Fritz, 2018; Schuur *et al.*, 2008). For example, one metatranscriptome-based (RNA transcripts directly collected from the environmental samples) study of thawing permafrost has shown an increase in abundance of genes associate with extracellular protein degradation, carbohydrate metabolism, and hydrolase class of enzymes (Coolen & Orsi, 2015). Some examples of genes upregulated after thawing of permafrost have been shown in **Figure 1.5**.

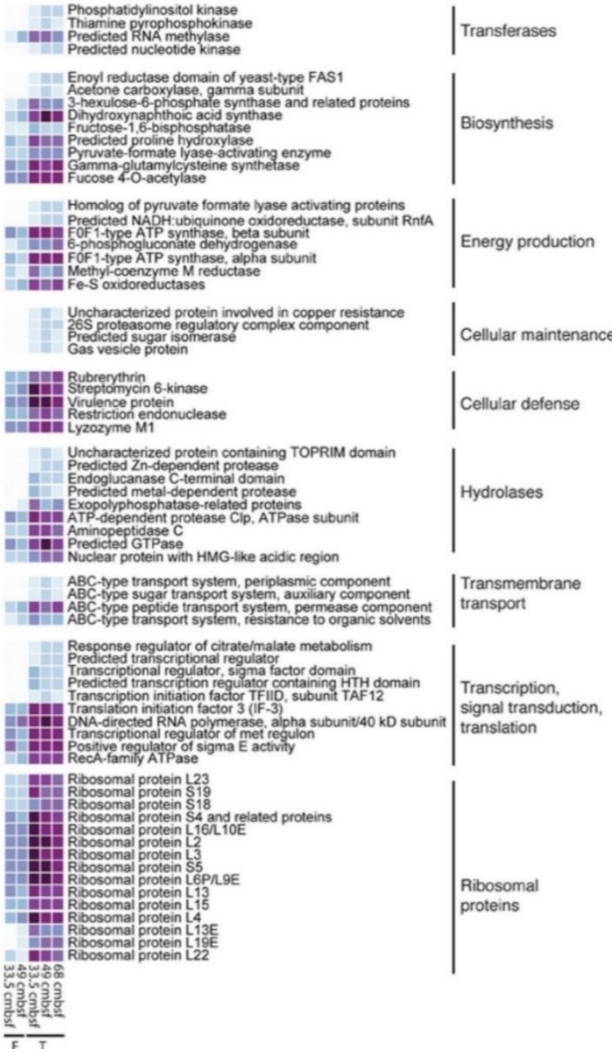

Figure 1.5. Abundance heatmap of genes upregulated after thawing of permafrost. Colored boxes represent log transformed and normalized read abundance. The threshold used for identifying the gene function was set to 60% amino acid identity. In the figure T = thawed, F= frozen, cmbsf = cm below sea floor. The figure has been reprinted with permission from (Coolen & Orsi, 2015)

Microcosm-based experiments have shown that the sequestered carbon in permafrost (in particular Yedoma) is highly labile and, initially, microbes could degrade 10-40 g of carbon.m^3.day^{-1}. However, this respiration rate decreases steadily until it remains constant at 0.5-5 g of carbon.m^3.day^{-1} over a course of several years (Zimov *et al.*, 2006). The majority of the permafrost DOC seem to be more aliphatic, hence it is labile and readily mineralized by microbes (see **section 1.2**) (Hodgkins *et al.*, 2014; Sun *et al.*, 1997; Vallino *et al.*, 1996; Waldrop *et al.*, 2010; Ward & Cory, 2015). Even in a case that the released carbon content is not favorable for microbial mineralization, photooxidation can increase the degradability of less labile carbon content, although it could also make these compounds more recalcitrant (Tank *et al.*, 2012; Vonk *et al.*, 2015). Exposure of organic material to light could stimulate the light-absorbing chromophoric part of these compounds (CDOM), which CDOM could later interact with oxygen or water molecules to generate free radicals (Kaplan & Cory, 2016). These free radicals could result in the degradation of organic material (Kaplan & Cory, 2016). Light can also generate CO_2 from thawing permafrost via photomineralization (Tank *et al.*, 2012; Vonk *et al.*, 2015; Wang *et al.*, 2020).

With an increase in atmospheric temperature and continuous erosion of the permafrost (e.g. Yedoma permafrost), thermokarst formations will continue to become enriched in freshly released labile organic material, which under anaerobic conditions may increase methanogenesis. For example, increased methanogenesis has been observed in Siberian thaw ponds and has been estimated to account for 90% of CH_4 emission from this region (Rivkina *et al.*, 2016; Schaefer *et al.*, 2011) (For more information, refer to **section 1.7**). Warming experiments of permafrost microcosms obtained from Arctic demonstrated a strong linear relationship with increase in

temperature and increase in CO_2 production (Mu *et al.*, 2016; Stackhouse *et al.*, 2015). Moreover, a microcosm warming experiment has shown a significant amount of N_2O release from thawing permafrost (Elberling *et al.*, 2010); demonstrating that thermokarst formations could allow a substantial N_2O feedback to the atmosphere in a warmer world. The latter experiment demonstrated that with the increase in drying and wetting cycles, the rate of the released N_2O also significantly increased (Elberling *et al.*, 2010). In permafrost-affected regions of Antarctica, the relationship between permafrost thaw and the increase in microbial activity is still not well understood (Altshuler *et al.*, 2017).

Although a large body of literature is showing an increase in greenhouse gas emissions from thermokarst systems, however, carbon-climate feedback models from these systems are not showing any consensus results. The inconsistency between models is believed to be arising due to the complex geomorphology and the heterogenic nature of the permafrost (see above) (Chen *et al.*, 2016). For example, it has been seen that old sequestered organic material in deep permafrost results in low CO_2 release after thawing in comparison to shallow permafrost thawing. This is mainly due to the recalcitrant nature of the deep (old) carbon (Song *et al.*, 2014). Also, there is a large uncertainty amongst scientists concerning the proportion of sequestered organic material in thawing permafrost that will be converted to CO_2 versus CH_4 (Mackelprang *et al.*, 2016). Hence, it is important to study the changes associated with the microbial community structure and function occurring in response to permafrost thaw.

Thawing of the Yedoma permafrost may be one of the most important elements that could trigger another major tipping point event in the ecosystem (**see section 1.1**) similar to the one at

the Pleistocene terminus (Lenton, 2012). The extent of Anthropocene climate change and atmospheric warming has been predicted to be unprecedented in scale in comparison to the early Holocene climate change (Walther *et al.*, 2002).

1.7. Methanotrophs: the unknown piece of the permafrost climate change puzzle

The objective of this section is to introduce the CH_4 oxidizing bacteria and their capacity to assimilate the CH_4 generated in thermokarst formations. Much emphasis has been given to the point that our knowledge of methanotrophs and their CH_4 oxidizing capacity in a changing Arctic is very limited in comparison to methanogens, which has been extensively studied.

Approximately 20-25% of the global biogenic CH_4 emission (~15-50 $Tg/_{year}$) is attributed to the cold northern hemisphere, where the ground is mainly permafrost affected (Bischoff *et al.*, 2013; Saunois *et al.*, 2016b). Two prevalent methanogenesis pathways responsible for CH_4 release in thermokarst systems of the Northern hemisphere are hydrogenotrophic methanogenesis (resulting in a $\delta^{13}CH_4$ of -110 to -60‰, overall reaction: $4H_2 + CO_2 \rightarrow CH_4 + 2\ H_2O$) and acetoclastic methanogenesis (resulting in a $\delta^{13}CH_4$ of -70 to -30‰, overall reaction: $CH_3COOH \rightarrow CO_2 + CH_4$) (Doelle, 2014; Hodgkins *et al.*, 2014). More depleted $\delta^{13}CH_4$ indicates hydrogenotrophic pathway and, in contrast, less depleted $\delta^{13}CH_4$ implies methanogenesis activity via the acetoclastic pathway (Hodgkins *et al.*, 2014). Continuous permafrost erosion and deepening of the thermokarst lakes leads to a shift from the acetoclastic to the hydrogenotrophic methanogenesis (Taş *et al.*, 2014), accelerating CH_4 generation (Anthony *et al.*, 2014; Walter *et al.*, 2006; Zimov *et al.*, 1997). However, some studies have also demonstrated a concurrent shift from hydrogenotrophic to acetoclastic pathways with an increase in CO_2 emissions after the thawing of peaty permafrost (McCalley *et al.*, 2014). In general, it seems that hydrogenotrophic methanogens, mainly affiliated with class Methanobacteria are more abundant in the upper layers of permafrost in comparison to acetoclastic members of the same class, which are more abundant in deeper layers (Barbier *et al.*, 2012; Deng *et al.*, 2015). Hence, the type of thermokarst formation and geomorphology of the permafrost could play an important role in selecting one

methanogenic pathway over another. Studies have shown that under the current climate change regime, Arctic wetland areas have been identified as methanogenic hotspots (biogenic CH_4 source) while High Arctic mineral cryosols (icy mineral soils) are acting as CH_4 sinks (**see below**) (Christiansen *et al.*, 2015; Lau *et al.*, 2015). However, an increase in the prevalence of thermokarst formations and climate change could favor methanogens irrespective of the permafrost type and turn the entire permafrost affected regions of the Northern hemisphere into a major CH_4 source (Altshuler *et al.*, 2017). However, Methanogenesis in permafrost affected regions is not limited to thermokarst formations. Studies have shown that methanogenesis could also occur in frozen permafrost, although at a lower rate (**see below**) (Mackelprang *et al.*, 2011; Rivkina *et al.*, 2007).

Studies of cryosols have shown the dominance of methanogens taxonomically affiliated with orders of Methanococcales and Methanomicrobiales, while deep Pleistocene aged permafrost samples of High Arctic with large concentrations of entrapped CH_4 demonstrated the dominance of genera *Methanosarcina*, *Methanoregula*, and *Methanobacterium* (Allan *et al.*, 2014; Shcherbakova *et al.*, 2016). In contrast to permafrost, the analysis of active layer soil samples demonstrated the dominance of methanogens taxonomically associated with orders Methanosarcinales, Methanocellaceae, and Methanomicrobiales (Ganzert *et al.*, 2007).

In general, methanogens are adapted to thrive under energetically stressful environments with low requirements of redox potential and have a narrow substrate requirement; however, their methanogenesis capacity is directly influenced by the aliphatic/oxidative state of the organic

material, water regime, and increase in temperature of the thermokarst systems such as the thaw ponds (Ganzert *et al.*, 2007; Høj *et al.*, 2006; Wagner *et al.*, 2007).

Methanogenesis significantly decreases at freezing temperatures; however, based on the recent greenhouse gas trajectory model RCP 8.5, 30-99% (~10^6-10^7 km^2) of the permafrost will thaw and release ~37-174 Pg of labile carbon by the year 2100 in response to ~10 ^oC increase in Arctic air temperature (Ponder *et al.*, 2004; Romanovsky *et al.*, 2010; Schuur *et al.*, 2015). Other models have estimated 16-20% permafrost loss in Canada by the year 2100, 40-57% in the Northern hemisphere in general, and some have even predicted 100% permafrost thaw (Jung & Kunstmann, 2007; Lawrence & Slater, 2005; Zhang *et al.*, 2008a, 2008b). Although the projections are different, there is an agreement that the CH_4 generated from the thawing permafrost by the end of this century will contribute substantially (predicted to be an extra ~25%) to the northern hemisphere CH_4 budget (Schaefer *et al.*, 2011; Schneider & Hook, 2010; Strauss *et al.*, 2017). Although deep permafrost does not harbor a large number of methanogens in comparison to bacterial species (**see section 1.5**), it seems that with gradual thawing of the permafrost they become abundant later on (Hultman *et al.*, 2015).

Not all volatile organic compounds generated from thermokarst systems enter the atmosphere; plants and CH_4 oxidizing microbes act as a biofilter, removing some of these gasses before they escape. Increased CO_2 concentration in the Arctic promotes plant productivity (photosynthesis), which could increase the CO_2 sink capacity of this region. However, CH_4 emissions are somewhat more problematic since CH_4 oxidation is limited to a narrow guild of microorganisms (Angert *et al.*, 2005; Anthony *et al.*, 2014; Black *et al.*, 2000; Friend *et al.*, 2014; Hicks Pries *et al.*, 2013; McGuire *et al.*, 2010; Negandhi *et al.*, 2014; Oechel *et al.*, 1994; Van Huissteden &

Dolman, 2012). CH_4 is not an easy energy source to consume because it has a very stable molecular structure and a high Ea is required for overcoming this stability (Strous, 2010).

Aerobic methane oxidizing bacteria (MOB) use CH_4 as their sole source of carbon and energy with the aid of their specialized methane monooxygenase enzymes (MMO) (Hanson & Hanson, 1996). Methanotrophy is initiated by activating the CH_4 molecule via the catalytic activity of particulate or soluble methane monooxygenase enzymes (pMMO/sMMO) and an oxygen molecule (Khmelenina *et al.*, 2018). The particulate copper-containing form of the enzyme (pMMO) is almost universal in known MOB (except genera *Methylocella* and *Methyloferula*) and consists of three polypeptide subunits of α (49 kDa), β (27 kDa) and γ (22 kDa) expressed by *pmoCAB* operon (Chen *et al.*, 2010; Khmelenina *et al.*, 2018; Vorobev *et al.*, 2011). The enzyme has a $(\alpha\beta\gamma)_3$ homotrimer 3D structure. The *pmoA* gene, which encodes the α subunit is often used as a functional biomarker for screening the MOB in the environmental samples via PCR (Luesken *et al.*, 2011).

The soluble di-iron (III) form of the enzyme (sMMO) is only present in some MOB and usually acts as a secondary enzyme in the absence of copper required for pMMO activity (Khmelenina *et al.*, 2018). The enzyme has a dimer structure of $(\alpha\beta\gamma)_2$, which is encoded by the operon *mmoXYZ* (Lawton & Rosenzweig, 2016). Similar to *pmoA* gene, *mmoX* (encodes the α subunit) could be used as a biomarker for detecting MOB with sMMO activity (McDonald *et al.*, 2008).

Methanotrophy was initially thought to only happen under aerobic conditions, because of the involvement of the oxygen in the first step of the pathway for activating the CH_4 molecule

(Strous, 2010). It is important to mention that aerobic MOB can also carry out CH_4 oxidation under oxygen limited conditions by partial oxidation of CH_4 to acetate and subsequently shuttling the acetate to a denitrifier (Costa *et al.*, 2000). It has been suggested that under anaerobic conditions archaeal strains distantly related to acetoclastic methanogens are able to carry out methanotrophy with a mechanism known as "reverse methanogenesis" coupled with the activity of sulfate reducing bacteria (e.g. *Desulfosarcina*, *Desulfococcus*, and *Desulfobulbus*) (Strous, 2010). Although it is difficult to calculate the exact Gibbs free energy for the anaerobic methane oxidation (ANME) *in situ* (due to the high sensitivity of the reaction to environmental perturbations), it has been estimated to proceed at -20 to -40 $kJ/_{mol}$ (less than one $ATP/_{CH\hat{}4}$ oxidized) close to -10 $kJ/_{mol}$ of thermodynamic lower limit for life (Jackson & McInerney, 2002; Scheller *et al.*, 2020). However, some studies do not agree with this mechanism of "reverse methanogenesis" with syntrophic association (beneficial cross-feeding) with sulfate reducers. For examples, two studies demonstrated ANME activity in the absence of sulfate reducing partners (Eller *et al.*, 2005; Orphan *et al.*, 2002).

ANME has also been seen to be coupled to nitrate reduction (Raghoebarsing et al., 2006; Scheller et al., 2020), and to metal (iron and manganese) oxide reduction (Beal *et al.*, 2009). In ANME coupled to nitrate reduction, the syntrophic partners are two methanotrophs, "*Candidatus* (*Ca.) Methylomirabilis oxyfera"* (Ettwig *et al.*, 2010; Raghoebarsing *et al.*, 2006; Scheller *et al.*, 2020) and "*Ca. Methyanoperedens nitroreducens*" (Lu *et al.*, 2019). "*Ca. M. nitroreducens*" reduced nitrate to nitrite and "*Ca. M. oxyfera"* reduces the generated nitrite to nitrogen molecule, which also acts as a detoxifying step for the "*Ca. M. nitroreducens*" (Ettwig *et al.*, 2008; Haroon *et al.*, 2013).

Currently very little is know about the syntrophic partners and the exact route of electron transfer and sink source in ANME coupled with iron oxidation (Scheller *et al.*, 2020). However, it has been proposed that multiple members of ANME are involved in this type of methanotrophy, which some members transfer the CH_4 driven electron to sulfate reducing bacteria and some might transfer the electron to metals such as iron or manganese (Scheller *et al.*, 2020). This type of methanotrophy might explain the activity of some ANME archaea in the absence of bacterial partners (Orphan *et al.*, 2002).

In general, the exact ecological importance and capacity of ANME are not well understood and they are only known as ANME-1, ANME-2 and ANME-3 (paraphyletic with methanogens). Although they have been cultured individually in a laboratory setting but no isolate of ANME and their sulfate reducing partner(s) exist (Strous, 2010). Two reasons that have been suggested for why ANME are hard to isolate are **i)** their extremely slow doubling time (e.g. in the order of months-yeas) and **ii)** our limited knowledge regarding the nature of the electron transport mechanism between ANME and their sulfate reducing partner (Girguis *et al.*, 2003; Wegener *et al.*, 2008).

The majority of the known MOB are aerobic and are associated with either Gammaproteobacteria (Type I) or Alphaproteobacteria (Type II) based on their morphological, physiological, and phylogenetic features (Khmelenina *et al.*, 2018). Outside of the proteobacterial MOB three genera *Methylacidiphilum*, *Methylacidimicrobium* and *Methyloacida* are associated with phylum Verrucomicrobia, and "*Ca. M. oxyfera"* is associated with phylum

NC10 (Ettwig *et al.*, 2010; Islam *et al.*, 2008; Khmelenina *et al.*, 2018; van Teeseling *et al.*, 2014).

Type I MOB are obligatory methanotrophs (only able to consume C1 compounds such as CH_4 or methanol (CH_3OH) as an energy source) and their primary route of CH_4 assimilation is the ribulose monophosphate pathway (RuMP) (Khmelenina *et al.*, 2018). Type I MOB are phylogenetically associated with two families of *Methylococcaceae* and *Methylothermaceae* (Khmelenina *et al.*, 2018). In contrast, some members of the Type II MOB are facultative MOB capable of consuming a number of multi-carbon compounds in addition to the CH_4, which they primarily assimilate via serine pathway and some strains (associated with *Beijerinckiaceae*) via Calvin-Benson Bassham cycle (CBB) (Chistoserdova *et al.*, 2009; Dunfield & Dedysh, 2014; Khmelenina *et al.*, 2018). Type II MOB are scattered between *Methylocystaceae* and *Beijerinckiaceae* families (Khmelenina *et al.*, 2018). Verrucomicrobial methanotrophs prefer to proliferate at pH of 0.5-5 and temperatures of 30-65 ^oC a typical feature of geothermal and highly acidic habitats, e.g. (Dunfield *et al.*, 2007). Methanotrophs of this phylum are autotrophs, which they oxidize the CH_4 all the way to CO_2 and then using the generated CO_2 in CBB for organic matter production (Khadem *et al.*, 2011). NC10 related "*Ca. M. oxyfera"* couples anaerobic CH_4 oxidation to nitrification via the activity of a novel enzyme NO dismutase, which generates oxygen for the MMO enzyme to carry out the methanotrophy (Ettwig *et al.*, 2010).

In addition to their taxonomical classification, Proteobacterial MOB have been broadly divided into two major groups based on their affinity to CH_4 (a^0_s); low-affinity methanotrophs (LAM), which are unable to colonize in the presence of CH_4 at atmospheric levels and high-affinity

methanotrophs (HAM), which are capable of growing in the presence of trace CH_4 at atmospheric levels (Tveit *et al.*, 2019). However, there are some exceptions to this broad classification of MOB. For example, *Methylobacter album* BG8 (Type I MOB; formerly known as *M. albus*) although characterized as LAM, is able to carry out methanotrophy at atmospheric levels when the strain is supplemented with methanol (Benstead *et al.*, 1998). Some *Methylocystis* strains (Type II MOB), by relying on a high CH_4 affinity variant of the pMMO enzyme known as pMMO2, are able to survive by oxidizing CH_4 at atmospheric levels (Baani & Liesack, 2008).

In general, HAM are less well known than LAM; currently, there is only one cultivated HAM (strain MG08 affiliated with the otherwise uncultivated methanotroph group USCα). HAM are designated as aerobic upland soil clusters (USC), which are found phylogenetically in either Gammaproteobacteria (USCγ) and Alphaproteobacteria (USCα) (Dunfield, 2007; Tveit *et al.*, 2019). USCα prefer to proliferate in neutral to acidic soils and while USCγ prefer neutral to alkaline soils (Knief, 2015; Knief *et al.*, 2003). Because of such differences in their physiology, HAM MOB seem to be highly sensitive to anthropogenic disturbances in comparison to conventional MOB (Tveit et al., 2019). HAM has been recently characterized in permafrost-affected regions (Lau *et al.*, 2015; Martineau *et al.*, 2014; Tveit *et al.*, 2019). However, the possibility of CH_4 oxidation at the atmospheric levels in permafrost (deposits of Alaskan permafrost) was first reported by Whalen and Reeburgh in 1990 (Whalen & Reeburgh, 1990). Simulated soil warming experiments show that boreal forest, tundra biome and Arctic polar desert are potential HAM MOB hotspots (Martineau *et al.*, 2014). Microarray analysis of *pmoA* genes detected in acidic active layer soils of Axel Heiberg Island (Canadian High Arctic)

demonstrated the abundance of HAM MOB affiliated with USCα in the top 15 cm layer. In contrast, the USCγ MOB was more abundant in upland tundra soil from the same region mentioned above (Martineau *et al.*, 2014). In general, the highest CH_4 oxidation activity related to HAM MOB is in the upper layers of the soil where access to atmospheric CH_4 is easy (Kolb, 2009; Martineau *et al.*, 2014). MOB associated with USCα has been seen to favour bog and palsa systems (Singleton *et al.*, 2018). It has been suggested that the USCα are facultative MOB capable of surviving by living on acetate in the absence of CH_4, which explains their dominance in acidic bogs when CH_4 is very limited (Semrau *et al.*, 2011). Two studies show that the peaty permafrost of the Northern hemisphere (Yedoma and organic rich permafrost) is currently acting as a CH_4 source, while silty permafrost is acting as a CH_4 sink, mainly due to the activity of the HAM MOB (Christiansen *et al.*, 2015; Lau *et al.*, 2015). Interestingly across the High Arctic region, the CH_4 oxidation activity of the HAM MOB was significantly different between different geographical regions mainly due to the geomorphology of the permafrost. For example, cryosols demonstrate the lowest atmospheric level CH_4 oxidation activity (-0.02 to -17.8 mg CH_4.C m^{-2}.day^{-1}) in comparison to other sites of the High and sub-Arctic permafrost affected regions (Lau *et al.*, 2015). The reason for this observation was attributed to low soil organic carbon, vegetation cover and water content in cryosols (Lau *et al.*, 2015).

In permafrost affected regions, LAM are often found in close proximity to methanogens in the anoxic or sub-oxic ($\leq$ 2.2 $mg_{O\hat{}2}$ L^{-1}) zones of thermokarst systems such as thaw ponds (Crevecoeur *et al.*, 2017; Mackelprang *et al.*, 2016; Vonk *et al.*, 2015). Permafrost in both frozen states and in active layer contains Type I and Type II classes of MOB, including MOB associated with Verrucomicrobia; however, these important functional guilds of microbes are not

prevalent in permafrost affected regions and their abundance decrease with increase in depth of the permafrost. This is possibly due to a reduction in available oxygen (Christiansen *et al.*, 2015; Stackhouse *et al.*, 2015; Yergeau *et al.*, 2010b). Similar to methanogens, it seems that thermokarst formations can select for a certain species of MOB. A comprehensive study conducted by Singleton and colleagues on a permafrost thaw gradient from Stordalen Mire demonstrated that LAM MOB community structure and activity significantly changed in parallel with an increase in permafrost thaw (Singleton *et al.*, 2018). The partially thawed bog demonstrated the highest dominance of MOB, in particular, Type II MOB whereas Type I MOB was the most dominant MOB in fully thawed fen (Singleton *et al.*, 2018).

The methanotrophic capacity of the permafrost affected regions is still not well understood; however, 40-70% of CH_4 produced in thermokarst formations is believed to be oxidized by methanotrophs before escaping to the atmosphere (Crevecoeur *et al.*, 2017; Megonigal *et al.*, 2004). Two main reasons for CH_4 escaping the MMO enzymes of the MOB are ebullition of CH_4 and CH_4 transfer through aerenchyma (air channels) of plants, which both phenomenon often occurs in the thaw ponds (Bischoff *et al.*, 2013; Walter *et al.*, 2006).

It seems that permafrost affected regions are mainly dominated by LAM taxonomically associated with Type I. Some examples include genera *Methylobacter* and *Methylocystis* (Type II MOB), which were the most dominant MOB in Sanjiang wetlands of China (Zhang *et al.*, 2020a); *Methylobacter* and *Methylosarcina* in Haibei wetlands of china (Zhang *et al.*, 2020a); *Methylobacter* in thaw ponds of Sub Arctic Québec (Crevecoeur *et al.*, 2017); *Methylobacter* and

Methylosarcina in active layer soil from Ellesmere island in the Canadian high Arctic (Martineau *et al.*, 2010).

The community structure of the dominant MOB strain have been seen to change in response to increased temperature or permafrost thaw (e.g. 2 to 5 days of incubation at 4, 10 and 21 ºC) (He *et al.*, 2012b; Singleton *et al.*, 2018). However, the combination of both an increase in temperature and permafrost/active layer soil disturbance (such as thermokarst formations) on MOB community structure and activity is not well understood. Limited studies have predicted that with an increase in atmospheric temperature and drastic changes in the hydrology of the permafrost affected regions due to thaw, methanotrophic activity is going to increase (especially in well-drained cryosol permafrost deposits of the Northern hemisphere), while methanogenesis will remain constant (Emmerton *et al.*, 2014; Mackelprang *et al.*, 2017).

Although methanotrophs are an important functional guild of microbes, they are under-characterised relative to methanogens in permafrost affected regions. Due to limited knowledge of the methanotrophic capacity of the thawing permafrost, it is not clear what percentage of the CH_4 escapes the methanotrophs and reaches the atmosphere. Two recent studies show that the current CH_4 emission models overestimate the amount of CH_4 reaching the atmosphere (Mayr *et al.*, 2020b; Oh *et al.*, 2020). These studies concluded that HAM MOB are capable of adapting to changing Arctic environments and can rapidly respond to a large increase in the concentration of CH_4 emitted to only allow a relatively small percentage (~18%) of CH_4 to escape into the atmosphere (Mayr *et al.*, 2020a; Oh *et al.*, 2020). Hence, for developing accurate CH_4 emission models from permafrost affected regions, it is essential to consider methanotrophic community

and activity along with the methanogens under rapidly increasing temperatures and permafrost thaw (Song *et al.*, 2014). In addition, in order to gain a better understanding of the Arctic CH_4 cycle, it is important to understand what parameters in permafrost and active layer are influencing methanotrophic community structure. Limited studies have been conducted in the past; however, none have resulted in any consensus results. For example, a study conducted by Liebner and colleagues on active layer MOB showed that the diversity of the MOB were not influenced by the depth or physical and geochemical gradient of the soil (Liebner *et al.*, 2009). However, another study demonstrated that in the same geographical location (conducted in High Arctic Canada) from one site to another the MOB structure and abundance were significantly different. The authors attributed local soil characteristics and sampling depth as key parameters causing differences in abundance and structure of the detected MOB (Martineau *et al.*, 2014). From these contradictory studies, two questions arise "how would permafrost or active layer soil disturbance and increases in atmospheric temperature might impact MOB?" and; "how much of a role does soil disturbance play in driving MOB community structure in comparison to key soil indices such as organic carbon content, pH and moisture?"

1.8. Summary of Chapter 1 and the main research questions

Soil microorganisms are catalysts of ecosystem function and different guilds of microbes are able to differentially influence nutrient mobilization and mineralization, and thus, local and global biogeochemical cycling. For example, methanogenic archaea are responsible for transforming organic matter released from thawing permafrost into the potent greenhouse gas CH_4 under anaerobic conditions, while CH_4 oxidizing bacteria (MOB) are responsible for controlling the flux of that CH_4 to the atmosphere by transforming it to the less potent greenhouse gas CO_2 under aerobic conditions. Anthropogenic activities have been identified as a major driver of climate change, which in return has increased the risk of abrupt loss of above-ground biodiversity on Earth. By contrast, below ground microorganisms have relatively rarely been the focus of research in the context of climate change. Climate change induced alterations in soil microbial community structure or function have been speculated to subsequently alter soil processes with a possible negative impact on higher trophic levels. Soil microorganisms have the capacity to change a carbon rich ecosystem like permafrost to a giant, time-sensitive "carbon bomb" (Strauss *et al.*, 2017). Hence, it is clear that it is essential to incorporate the knowledge of microbial response to climate change in order to create accurate carbon-climate feedback models and an environmentally sustainable future. Although soil warming experiments have contributed a lot to our knowledge regarding both microbial response towards increases in temperature and the extent at which soil edaphic parameters influence microbial community structure, we still have yet to learn and agree upon.

According to the preserved paleoclimatic proxy records, the Earth has experienced multiple profound climatic oscillations with the most recent having occurred ~10,000 yr at the Pleistocene-Holocene transition. This latest epoch transition coincided with multiple events including: glacial retreat, shifts in plant community composition, changes from a cold and dry ecosystem to a warm and wet ecosystem, and disappearance of the ancient megafauna, most notably populations of bison, horse and mammoth. The remnants of this ancient biota in the form of intact fossils, ancient DNA, pollen and microorganisms are very well preserved in permafrost, particularly permafrost of the un-glaciated eastern Beringia, which has never been affected by glacial retreat (may profoundly alter the soils structure via physical perturbation and mixing). The permafrost of this land mass has therefore remained pristine since the time of last glaciation maximum and is representative of the direct effect of past climate change. Permafrost samples from this location dated to the Pleistocene-Holocene boundary thus provide me with an excellent opportunity to not only study the potential changes in microbial community structure across two different epochs but also allows study of the changes in soil edaphic parameters. The Pleistocene-Holocene geological boundary might be a potential analog for the current Holocene-Anthropocene transition and may aid in the prediction of possible future change in the microbial community structure of permafrost/soil in a warmer world.

Despite being one of the coldest oxygen and nutrient-limited geological settings on Earth, high latitude permafrost contains 10^7-10^8 cells/$_{g\ of\ soil}$, of which some are known to be alive and metabolically functional or in a state of dormancy. Methanogenic Archaea are viable and highly active within the permafrost. Thawing of massive ice triggered by climate change within the permafrost can lead to the formation of thermokarst. Thermokarst is highly anoxic, with

conditions suitable for methanogenesis, resulting in generation of CH_4. This increase in CH_4 production stimulates methanotrophs that use the generated CH_4 as their sole source of carbon, acting as natural CH_4 biofilters. Hence, the changes in the community structure of these two ecologically important microorganisms could determine whether permafrost is a biological CH_4 source or sink. Extensive studies have been done regarding identifying the taxonomy of methanogens in permafrost and their CH_4 generating capacity and population structure prior to and following permafrost thaw. Studies of the methanotrophs in permafrost and Arctic environments are limited. In particular, it is not known how MOB are going to respond to permafrost or active layer soil disturbance in parallel to an increase in temperature. An increase in atmospheric temperature and an increase in the disturbance of permafrost/active layer soil are two key markers of the Anthropocene.

By using permafrost and active layer bacteria of the Beringia as a model, my Ph.D. thesis focuses on the following questions: 1) “how confident are we that the DNA extracted from permafrost is truly representing the ancient microbes and not contaminating contemporary microbes?” 2) “what was the impact of abrupt climate change at Pleistocene-Holocene transition on soil microorganisms?” and; 3) “If we assume that modern climate change is analogous to the Pleistocene-Holocene transition, how will disturbance of the active layer soil along with an increase in temperature shape active layer microbial community structure, and in particular, the methanotrophic community?”

Chapter 2

Optimization of subsampling, decontamination, and DNA extraction of difficult peat and silt permafrost samples

This chapter has been published in the journal "Scientific Reports" as "Saidi-Mehrabad, A., Neuberger, P., Cavaco, M., Froese, D., Lanoil, B. (2020). Optimization of subsampling, decontamination, and DNA extraction of difficult peat and silt permafrost samples. *Scientific Reports.* 10:14295".

2.1. Introduction

Permafrost, i.e. Earth materials below 0 °C for at least two years and up to millions of years, acts as an archive of past environments and ecosystems, preserving biological material as a result of its isolation from atmospheric inputs, low temperatures, and low water activity (Willerslev *et al.*, 2003). Ancient DNA derived from long-dead organisms is an important example of such material and has been used for a variety of purposes, ranging from reconstructing human migration patterns to reconstituting the genomes of extinct organisms such as the woolly mammoth and North American horses (Birks & Birks, 2016; Froese *et al.*, 2002; Orlando *et al.*, 2013; Poinar *et al.*, 2006; Waters & Stafford, 2007). Furthermore, permafrost-dwelling microbes may also play important roles in carbon cycling by conversion of permafrost organic carbon to CH_4 and CO_2, both important greenhouse gasses (Davidson & Janssens, 2006; Mackelprang *et al.*, 2011; Nikrad *et al.*, 2016; Schuur *et al.*, 2008).

The use of high-throughput sequencing technologies has enriched our understanding of microbial communities in permafrost and ancient DNA. However, these technologies require the extraction of high yields of DNA devoid of contaminants (Shendure *et al.*, 2017). External contamination is particularly problematic in DNA-based approaches due to the high sensitivity in detecting, amplifying and sequencing of DNA. The nature of these contaminants are primarily DNA from humans and background or exogenous DNA of microorganisms (Skoglund *et al.*, 2014; Weyrich *et al.*, 2019).

Obtaining DNA devoid of contaminants from environmental samples, especially from those with low biomass such as permafrost, is often challenging. Such samples are prone to external contamination during drilling and collection in the field and handling in the laboratory, which could lead to misinterpretation of microbial diversity, activity, or ancient DNA studies (Bang-Andreasen *et al.*, 2017; Salter *et al.*, 2014; Willerslev *et al.*, 2004a). Several methods have been used for permafrost decontamination, such as scraping the outer surface of cores, fracturing of cores followed by clean subsampling from the interior of the core sections (i.e. "disk sampling"), or washing the cores with DNase (e.g. (Barbato *et al.*, 2016; D'Costa *et al.*, 2011; Rivkina *et al.*, 2016) (**Supplementary Table 1.1**). Either scraping or disk sampling are the most commonly used protocols (**Supplementary Table 1.1**); however, the efficacy of these methods in removing external contaminants is not well characterized (e.g. (Bang-Andreasen *et al.*, 2017).

Ancient DNA (aDNA) and deep subsurface (both sediment and ice) microbiology studies face similar challenges to permafrost DNA studies, with high potential for contamination due to low endogenous cell and DNA abundance in the samples. Such studies have formalized highly

stringent sampling and decontamination protocols, with protocols to minimize contamination and controls to monitor contamination at all stages from sampling to downstream analyses (e.g. (Bollongino *et al.*, 2008; Kallmeyer, 2017; Kallmeyer *et al.*, 2006; Korlević *et al.*, 2015; Llamas *et al.*, 2017; Yanagawa *et al.*, 2013; Yang & Watt, 2005). Similar approaches may be beneficial for permafrost studies. For example, a unique tracer or combination of tracers added during drilling is used to monitor contamination in deep subsurface microbiology studies (e.g. (Smith *et al.*, 2000). Similar tracers have also been used in permafrost microbiology, but only rarely (e.g. (Krivushin *et al.*, 2015; Vishnivetskaya *et al.*, 2006; Wright & Poinar, 2012). Likewise, many decontamination methods have been systematically tested for ancient DNA studies of skeletal remains. Some of these methods, such as scraping (Kalmár *et al.*, 2000) and disk sampling (Palmirotta *et al.*, 1997), have been used for permafrost decontamination as well. However, other methods used for aDNA studies of bone, including UV irradiation (González-Oliver *et al.*, 2001), and treatment with household bleach (Kemp & Smith, 2005) have not been tested on permafrost intended for microbial work. Bleaching, in particular, has proven to be highly effective in removing external contaminants without damaging the genomic material within the samples in both ancient remains and ice cores (Korlević *et al.*, 2015; Rogers *et al.*, 2004a; Salamon *et al.*, 2005).

Another major issue in permafrost molecular studies is low DNA yield and poor quality of isolated DNA due to co-extracted chemical inhibitors (Mackelprang *et al.*, 2017; Vishnivetskaya *et al.*, 2000; Yergeau *et al.*, 2010a). Permafrost researchers have utilized either commercial DNA extraction kits, most of which are based on mechanical disruption followed by DNA purification, or chemical DNA extraction protocols. Commercial mechanical disruption-based kits provide

consistent DNA yield (although yield differs significantly between kits) and similar community composition, while chemical DNA extraction approaches are less consistent (Vishnivetskaya *et al.*, 2014). Issues with co-extraction of chemical inhibitors have led some researchers to add extra purification steps. In some cases (e.g. (Braid *et al.*, 2003; Griffiths & Whiteley, 2000; Porter *et al.*, 2013), additional purification can lead to a loss of DNA or biases in the evaluation of community structure, although observable bias is not always seen (e.g. (Vishnivetskaya *et al.*, 2014). To our knowledge, there have been no comparative studies assessing the efficacy of commercial kits for DNA extraction of difficult permafrost samples of different textures,chemistry and age.

In this study, we tested the efficacy of several decontamination methods on permafrost with the aid of a microbial tracer. In addition, we compared DNA yield and purity for four widely used commercially available soil DNA extraction kits with peaty and silty permafrost samples, with and without modifications of the manufacturer's protocol. We developed recommendations for permafrost researchers for sample handling and processing, contamination detection and control, and DNA extraction.

2.2. Material and Methods

2.2.1. Site description and sampling strategies

A 3.97 m long, 10 cm diameter continuous permafrost core (termed DHL-16) was collected in May, 2016 adjacent to cores collected and presented previously (1.5 m lateral; GPS: 65.21061 N, and 138.32208 W; **Figure 2.1**) (Porter *et al.*, 2019). Two intervals of this core were sampled for this study. The first was a lower silt unit (from a depth of 254 cm to 336 cm, here called DH_2) dating to the Pleistocene, between 11,650 and 15,710 cal yr BP based on radiocarbon dating and age modelling (Porter *et al.*, 2019). The second was an upper peat unit (from a depth of 105 cm to 212 cm, here called DH_1) dating to the early Holocene between 8,190 and 10,380 cal yr BP. The organic/silt boundary was determined at 244 cm (~ 10,400 cal yr BP), placing the DH_2 core segment right around the start of the Holocene geological epoch.

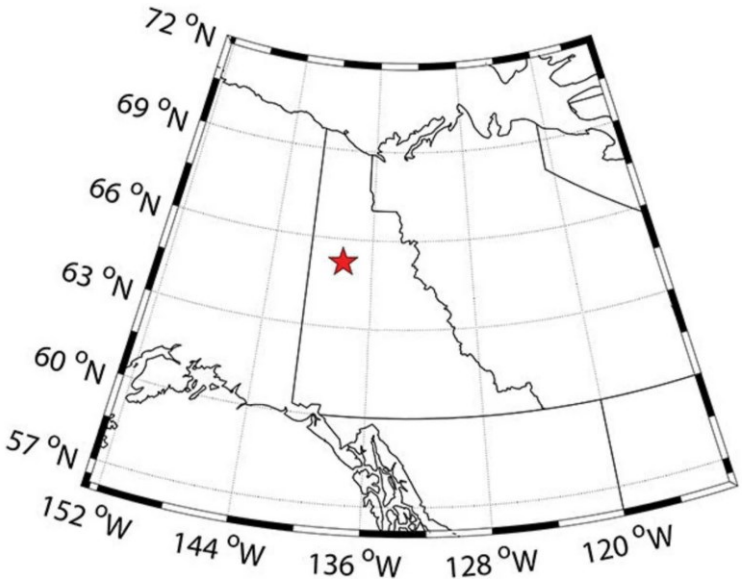

Figure 2.1. Map of Yukon region showing the coring location (DHP174-13L) for DHL_16 core (Porter *et al.*, 2019). The location was within the continuous permafrost zone (90–100% permafrost extent). The map has been reprinted with permission from (Porter *et al.*, 2019).

The surface material at our sampling site was approximately 2.5 m below the surface of surrounding undisturbed sites. The reason for this difference was due to the removal of the active layer soil in our sampling site by the Yukon government to be used in road maintenance. To access the frozen permafrost table, we removed approximately 10–20 cm of thawed material with a shovel. The core was extracted by vertical drilling with a hand-held gas-powered drill with a custom-made diamond bit. Cores were extracted from the ground in an average of ~ 25 cm segments. Upon removing the core segments from the core catcher, the organic materials stuck to the surface of the core were scraped off with a clean pocket knife and the core was immediately sprayed with our contamination tracer (see below). Frozen core segments were placed in heat-sealed clear plastic bags (ULine, Canada), placed in coolers with ice packs for the duration of coring, and then stored at − 20 °C during transportation and subsequent analyses. At the University of Alberta, the DH_1 and DH_2 core segments were cut vertically into 1/3 and 2/3 subsections with the aid of a masonry saw. The 2/3 section was used to test decontamination and DNA extraction protocols, while the 1/3 section was used for chemical analyses.

2.2.2. Contamination tracer

Approximately 2.8×10^7 cells/ml of *Escherichia coli* (*E. coli*) strain DH10B harboring a pBAD vector (Thermofisher Scientific, Canada), suspended in a total of 50 ml 1 × PBS, was sprayed from a spray bottle on the core catcher, diamond bits, and the surface of the frozen cores (Durfee *et al.*, 2008; Guzman *et al.*, 1995; Shaner *et al.*, 2013). pBAD is an expression vector that codes for the mNeonGreen protein. This vector and its product were targeted as the main contamination tracer in this study via PCR of vector sequences and macro-photography of the mNeonGreen protein fluorescence under 470 nm wavelength using a xenon arc lamp (Sutter Instruments, USA).

2.2.3. Sterilization procedure of the tools and work areas

To maintain cleanliness in the sub-sampling laboratory environment, we followed recommendations for ancient DNA and deep subsurface microbiological work (Llamas et al., 2017(Cooper & Poinar, 2000). These recommendations include the use of Tyvek clothing covers, masks, and gloves; sterilization of all equipment via baking, bleaching, or both; subsampling in a class 1,000 clean space with no history of DNA extraction or PCR amplification of DNA; and monitoring of the space for potential contaminants. For full details, see supplemental methods in **Appendix 1**.

2.2.4. Basic chemical parameter analyses of the core segments

The 1/3 core sections of DH_1 and DH_2 were cut into 1-cm^3 cubes with a handsaw in a 4 °C cold room. The analyses of water content, organic matter, and pH were determined based on standard methods (see **Appendix 1** for details).

2.2.5. Decontamination and subsampling methods

To prepare the samples for intentional contamination and decontamination, the 2/3 section of each core segment was cut horizontally into multiple disks (**Supplementary Figure 2.1**). Except for the piece selected for the decontamination protocol g (see below), one side of the disks was painted with a total of 5.3×10^8 cells ml^{-1} of *E.coli* with pBAD suspended in 1 × PBS using a 25 mm paintbrush. The other side was not painted in the laboratory and thus any spike present was the result of spraying in the field. For decontamination protocol g, the disk was cut into three rectangular subsections (**Supplementary Figure 2.1**). One rectangular piece was painted with the spike as above, another painted with a total of 18 µg of pBAD vector DNA isolated using QIAprep Spin Miniprep Kit, by the manufacturer's instructions (MO Bio, Qiagen Canada), and the third piece was not painted in the laboratory (**Supplementary Figure 2.1**).

Seven decontamination methods were tested in this study: (a) scraping off external, potentially contaminated material by shaving the exterior of the cores 4–5 times, which removed ~ 2–3 mm of material with a series of 0.012"/0.30 mm single edge blades (i.e. "scraping", modified from (Rivkina *et al.*, 2016)). (b) Sampling of a fresh, uncontaminated face with brass pipe connectors

(1/2" O.D. × 1/2" O.D.) (similar to (D'Costa *et al.*, 2011) with the only difference being that brass pipe connectors were used instead of a stationary drill press (i.e. "disk sampling"); (c) disk sampling as in protocol b, but using a manual soil press device for volumetric subsampling (similar to (Bottos *et al.*, 2018). Protocol c was performed with a set of custom-made high-pressure 30 cm long and 1.5 mm thick stainless-steel tubing. (d) Disk sampling as in protocol b, but using a hammer, chisel and a hand saw to remove the outer, contaminated material (similar to (Hultman *et al.*, 2015), with the only difference being that a manual hand saw was used instead of an electric jigsaw, no clamps were utilized, and the cores were not cut into cubes. (e) A combination of scraping and disk sampling with chisels and blades (similar to (Mackelprang *et al.*, 2017), with the only difference being that single edge blades were used instead of knives. (f) UV irradiation of the disk (modified from (Kalmár *et al.*, 2000). In protocol f, a disk was placed in a clean, closed UV box (UVP C-70G Chromato-Vue Cabinet; Analytik Jena, USA) ~ 6 cm from the UV lamp of 15 watts and was subjected to UV light at 254 nm for 5 min (8.45×10^{-17} $J/m^2_{UV\ dosage}$), 10 min (1.69×10^{-16} $J/m^2_{UV\ dosage}$), 20 min (3.38×10^{-16} $J/m^2_{UV\ dosage}$) or 30 min (5.07×10^{-16} $J/m^2_{UV\ dosage}$) intervals. (g) Scraping and bleaching (developed for this study based on (Kemp & Smith, 2005; Rogers *et al.*, 2004b).

Unlike protocols a-f, protocol g started with subsampling first and then decontamination (**Supplementary Figure 2.1**). In protocol g, the surface of the rectangular piece was first washed with pre-chilled (4 °C), full strength concentrated household bleach solution with no phosphorus compounds. Bleach was rinsed off with pre-chilled (4 °C) Milli-Q water. The resulting loosened surface materials were removed via scraping with 0.012"/0.30 mm heavy duty single edge blades (Richard Ltd, Canada). This entire process was then repeated a second time (**Figure 2.2**).

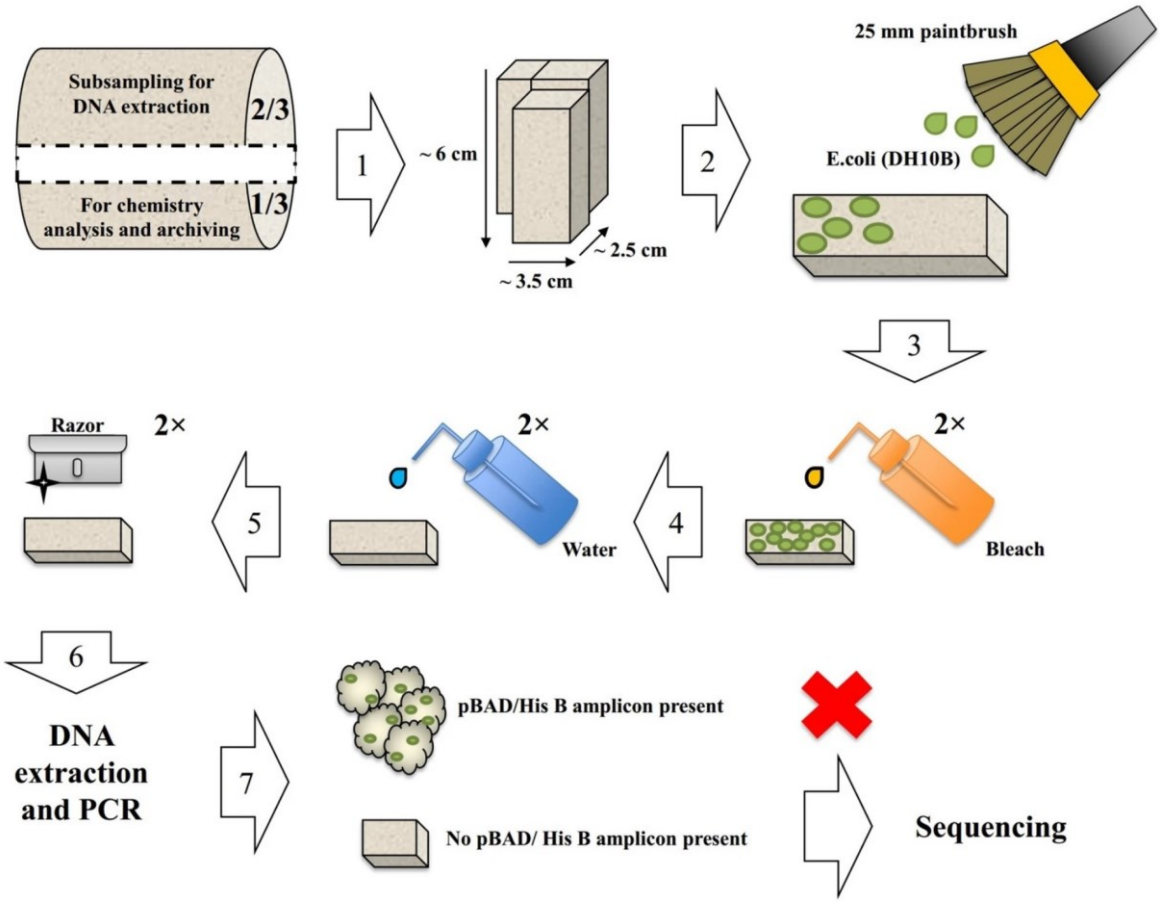

Figure 2.2. Schematic of our recommended protocol (decontamination protocol g). Step 1: A 2/3 section of each core segment is horizontally dry cut into multiple rectangular pieces. Step 2: Each rectangular piece is intentionally surface contaminated by painting with an *E.coli* strain (DH10B) carrying a known plasmid vector (e.g. pBAD/His B). Step 3: Intentionally contaminated rectangular pieces are thoroughly washed with 4 °C pre-chilled full strength household bleach with no phosphorus compounds. Step 4: Bleach residues are rinsed off with pre-chilled 4 °C Milli-Q water. Step 5: Loosened surface materials are removed via scraping with a 0.012"/0.30 mm heavy duty single edge blade razor. Steps 3–5 are repeated to ensure decontamination. Step 6: The DNA is extracted. Step 7: Samples are screened for the presence of

the plasmid vector via PCR. If the plasmid vector is detected, the sample is discarded; if not detected, the sample is sent for sequencing.

Decontaminated samples were stored at − 20 °C prior to DNA extraction. Decontaminated samples obtained from protocols (a and c–f) were crushed into smaller pieces with a sterile chisel and hammer and prior to DNA extraction, they were allowed to thaw at room temperature. Thawed material was homogenized by mixing and the resulting material was subsampled for DNA work. Soils in brass pipe connectors obtained via protocol (b) were left at room temperature prior to DNA extraction to allow easy removal of the material with the aid of a sterilized spatula and were later mixed and subsampled.

2.2.6. DNA extraction

We compared seven DNA extraction protocols: four commercially available, well-established soil DNA extraction kits as recommended by the manufacturers as well as simple modifications to three of these commercial kits (see **Appendix 1** for details of the modifications). The protocols used for soil DNA extraction were as follows: 1) Fast DNA SPIN kit for soil (MP Biomedicals, USA) by the manufacturer's protocol; 2) Fast DNA SPIN kit for soil (MP Biomedicals, USA) with modifications; 3) OMEGA E.Z.N.A so il DNA kit (OMEGA-Bio-Tek, USA) by the manufacturer's protocol; 4) Powersoil Isolation kit (MO Bio Laboratories/Qiagen, Canada) by the manufacturer's protocol; 5) Powersoil Isolation kit (MO Bio Laboratories/Qiagen, Canada) with modifications; 6) ZymoBIOMICS DNA Microprep kit

(Zymo Research, USA), by the manufacturer's protocol; and 7) ZymoBIOMICS DNA Microprep kit (Zymo Research, USA) with modifications. DNA yield was determined using a Qubit fluorometer device (Invitrogen, Canada) via Quant-iT dsDNA HS Assay Kit (Invitrogen, Canada), calibrated using the manufacturer's protocol. DNA was extracted from triplicate 1 g subsamples for DH_1 and DH_2, and triplicate 0.5 g subsamples from the control soil (CS; see below).

To ensure that similar amounts of permafrost sediment were being used, water was removed as much as possible following thaw and homogenization. Samples differed dramatically in pH, which can affect DNA extraction yield. To minimize the effect of pH on DNA yield, most kits and chemical extraction methods utilize a buffer. To confirm that the buffers were effective in neutralizing samples, the provided buffers from each DNA extraction kit were mixed in a 1:1 ratio with samples from DH_1 and DH_2 prior to each DNA extraction. Samples were thoroughly mixed by vortexing for 30 s. The supernatant was collected after a 16,000 × g centrifugation step for 1 min. The pH of the supernatant was measured. pH was always 7–7.5 irrespective of the DNA extraction kit.

A positive control soil sample (termed CS in this manuscript) was used to test the efficiency of each DNA extraction protocol (mentioned below) in obtaining contaminant free and PCR amplifiable DNA from a non-permafrost sample. The CS sample was an 8:1 ratio of peat and mineral subsoils from the rhizosphere of *Populus tremuloides*, mixed using a clean cement mixer

for 10 min. Two blank negative controls with no soil added were prepared from each kit to trace possible contamination originating from kit reagents.

2.2.7. Contamination detection

To determine if a decontamination procedure was successful, the isolated DNA was tested for the presence of pBAD-vector via PCR. 1–2 µl of the 1:2, 1:5 and 1:10 diluted DNA in triplicates was used as the template (see **Appendix 1** for PCR protocol details). When no PCR product is indicated, none of the replicates produced a detectable PCR product; when a PCR product is indicated, all replicates produced a detectable PCR product.

2.2.8. 16S rRNA gene-targeted PCR protocol

16S rRNA genes were PCR amplified in triplicate from the DNA obtained from the decontaminated samples to test for their PCR amplifiability, here used as a proxy for DNA purity. In order to reduce the PCR inhibitory effect of some compounds which might have escaped the purification steps, 1–2 µl of the 1:2, 1:5 and 1:10 diluted DNA was used as the template (For more information, refer to **Appendix 1**). As mentioned above reported positive results were positive for all replicates and in case of negative results, none of the replicates resulted in PCR product.

2.3. Results

2.3.1. Chemical characteristics of core sections DH_1 and DH_2

The DH_1 segment was a peaty unit with high organic matter content (mean = 95.7% w/w dried (± 1.82%), n = 23), high gravimetric water content (mean = 91.8% w/w (± 3.01), n = 23), and low pH (mean = 3.68 (± 0.102), n = 24). DH_2 segment was a silty unit with lower organic matter content (mean = 39.58% w/w dried (± 21.85%), n = 21), lower gravimetric water content (mean = 74.48% w/w (±18.02%), n = 21), and higher pH (mean = 6.04 (± 0.54), n = 30) **(Supplementary Figure 2.2)**. The organic matter content range for DH_1 was relatively consistent (90.56%—98.02%) **(Supplementary Figure 2.2)**. However, DH_2 varied widely in organic content (9.91%—68.36%). A similar trend was observed regarding gravimetric water content, with the DH_1 fairly consistent (80.88–98.33%), but DH_2 samples varying dramatically (8.15–97.61%). pH did not change significantly in DH_1 with depth; however, the pH increased significantly with depth for DH_2, from 5.17 to 6.9 **(Supplementary Figure 2.2)**.

2.3.2. Decontamination testing

To test our decontamination protocol, we applied *E. coli* carrying a mNeonGreen protein expression vector to our core sections as a tracer. The tracer was applied by spraying the corer and the core sections in the field and/or by painting the core sections in the lab. Painting of the tracer on the core sections showed a uniform distribution of cells based on fluorescence of mNeonGreen protein as well as consistent amplification of the pBAD vector PCR product from all samples prior to decontamination (data not shown). The side of the disk where tracer was

only applied in the field resulted in patches of spike and inconsistent amplification of the vector. However, the crystallized ice from the interior of the bags used for transporting the core sections always showed positive PCR amplification of the vector, indicating that the tracer was easily removed from the surface of the core. In addition, we noticed cutting the samples and handling in the lab resulted in the loss of the contamination tracer. Hence, we recommend the application of the tracer by painting prior to decontamination, as well as field application by spraying, to ensure decontamination is as thorough as possible.

Of the seven decontamination methods tested, scraping (protocol a) and UV irradiation (protocol f) retained the most material for subsequent biological work (**Table 2.1**). Conversely, disk decontamination with brass pipe connectors (protocol b) was the most destructive, resulting in a very small quantity of decontaminated material. The soil press method (protocol c) did not perform well, resulting in crushing and thawing of the disk and bending of the tubes. Protocols d (disk sampling with chisel removal of outer material), e (disk sampling with scraping), and g (scraping and bleaching) resulted in a moderate quantity of samples for biological work (**Table 2.1**).

Table 2.1. Decontamination methods on permafrost samples DH_1 and DH_2.

Protocol[a]	Fraction retained (mass %)		Colonies (<1 m away)		Colonies (> 1 m away)[e]		pBAD amplification[f]	
	DH_1	DH_2	DH_1	DH_2	DH_1	DH_2	DH_1	DH_2
a	94	92	+[d]	+	+/-	+/-	+	+
b	7	6	+	+	+/-	+/-	-	-
c[b]	0	0	n.d.[d]	n.d.	+/-	+/-	+/-	+/-
d	40	47	+	+	+/-	+/-	+/-	+/-
e	37	45	+	+	+/-	+/-	+/-	+/-
f	100	100	+	+	+/-	+/-	+/-	+/-
g[c]	40	32	-[f]	-	-	-	-	-

[a] Protocols: a = scraping, b = disk sampling with brass pipe connectors, c = disk sampling with a soil press, d = disk sampling with a chisel, hammer and a hand saw, e = combination of scraping and disk sampling, f = UV irradiation, g = bleach and scraping. See methods for details.

[b] This protocol failed to acquire any samples due to bending of the tubing.

[c] NOTE: In this protocol, permafrost is first subsampled and then decontaminated; for other protocols, decontamination occurs before subsampling (see **Supplementary Figure 2.1**).

[d] n.d. = not done, + = detected, - = not detected, +/- = inconsistent detection.

[e] Colonies formed on nutrient rich media plates placed near work station.

[f] PCR amplification of the pBAD plasmid carried by the intentional contaminant. Indicates contamination. DNA templates for PCR were diluted 1:2, 1:5, and 1:10 and PCR amplification of these dilutions were performed in triplicate.

The DNA from the soil samples was extracted via DNA extraction protocol 7 and tested via PCR of the pBAD vector. The decontaminated samples from protocols b and g were devoid of PCR amplifiable pBAD vector, indicating effective decontamination (**Table 2.1**). Decontaminated samples from protocols (a) and (c–f) resulted in amplification of the pBAD vector when tested with PCR, indicating incomplete decontamination. Protocols a-f resulted in colony formation on growth media left open in the room during decontamination, indicating contamination of the local environment. Such contamination could lead to subsequent cross-contamination of other

samples. Protocol (g) was the only method that did not show colony formation on nearby growth media (**Table 2.1**). Thus, protocol (g) provided complete decontamination and a moderate amount of decontaminated material remaining, and therefore seems to be the best decontamination protocol for permafrost samples and was used for subsequent DNA extraction testing.

2.3.3. DNA extraction testing

Following decontamination with protocol (g), DNA was extracted from the two permafrost samples as well as a positive control temperate soil (CS). The kits and protocols tested displayed varying efficiency and effectiveness in extracting DNA (**Table 2.2**). Protocol 1 did not result in any detectable DNA when it was used on either permafrost sample, but it resulted in the highest yield of DNA from CS (**Table 2.2**). Detectable, but low, DNA yield from DH_2 was obtained with Protocol 2 and Protocol 5; however, neither of these protocols provided detectable DNA from DH_1 (**Table 2.2**). Protocol 3 resulted in DNA yield from DH_1, DH_2, and CS (**Table 2.2**). Protocol 6, in contrast to other methods, was able to obtain detectable DNA from DH_1 and CS, but not DH_2 (**Table 2.2**). Protocol 7 produced DNA from both DH_1 and DH_2 (**Table 2.2**). All of the DNA extraction protocols provided high yields of DNA for the positive control temperate soil, (CS). The CS samples provided 2–3 orders of magnitude more DNA (47×–754×) than the permafrost samples, no matter which extraction protocol was utilized (**Table 2.2**).

Table 2.2. DNA extraction protocol on samples DH_1, DH_2, and CS.

Protocol[a]	DNA yield (ng/g)[b]				PCR amplification†			
	DH_1* (±SD)	DH_2 (±SD)	CS (±SD)	Kit blank[c] (±SD)	DH_1	DH_2	CS	PCR blank
1	BDL	BDL	6633*,[NS] (2310)	BDL	-[d]	-	+++	-
2	BDL	2.5*,[NS] (0.1)	n.d.	BDL	-	-	n.d.[d]	-
3	24.6* (0.2)	31.8* (0.2)	1517*,[NS] (16)	60.1 (3)	+[d]	+	+	+
4	BDL	10 (0.1)	660* (6.4)	BDL	+	++[d]	++	-
5	BDL	4.6*,[NS] (0.4)	n.d.	BDL	-	++	n.d.	-
6	0.7* (0.1)	BDL	513* (14)	BDL	+++[d]	+	+	-
7	1.1* (0.2)	17* (0.2)	n.d.	BDL	+++	+++	n.d.	-

† DNA templates for 16S rRNA gene PCR were diluted 1:2, 1:5, and 1:10 and PCR amplification of these dilutions were performed in triplicate. Results marked as positive yielded PCR product for all replicates; no amplification product was detected for any replicate for those marked as negative.

[a]DNA extraction protocols: 1 = Fast DNA SPIN kit for soil (manufacturer's protocol), 2 = Fast DNATM SPIN kit for soil (modified), 3 = OMEGA E.Z.N.A soil DNA kit (manufacturer's protocol), 4 = Powersoxil Isolation kit (manufacturer's protocol), 5 = Powersoil Isolation kit (modified), 6 = ZymoBIOMICSTM DNA Microprep kit (manufacturer's protocol), and 7 = ZymoBIOMICSTM DNA Microprep kit (modified).

[b]DNA was extracted from triplicate 1 g subsamples for DH_1 and DH_2, and triplicate 0.5 g subsamples from CS.

[c]Measured in ng of DNA.

[d]BDL = below the detection limit, n.d. = not done, + = weak PCR band, ++ = medium PCR band, +++ = strong PCR band, - = not detected.

*$p < 0.05$ (based on Student's t test).

[NS] Not Statistically Significant ($p \geq 0.05$), DH_2: Protocol 2 vs 5 and CS: Protocol 1 vs 3.

Protocol 3 consistently resulted in PCR amplification from blank extractions, both with different kit lot numbers and different researchers; as a result, I did not test this protocol further (**Table 2.2**). We tested the purity of DNA obtained from unmodified kit protocols (i.e. protocols 1, 4, and 6) on the CS soil; all kits provided DNA pure enough to PCR amplify 16S rRNA genes (**Table 2.2**). However, on permafrost soils, DNA from protocols 1 and 2 was not PCR amplifiable for either permafrost sample (**Table 2.2**). Several protocols gave differential results for the two different samples, with protocols 4 and 5 showing better PCR amplifiability with DH_2 and protocol 6 showing better PCR amplifiability with DH_1 (**Table 2.2**). For protocols 4 and 6, DNA yield was below the detection limit; however, PCR product was obtained (**Table 2.2**). Only protocol 7 provided consistently strong PCR amplification from both permafrost samples (**Table 2.2**).

2.4. Discussion

Deep subsurface microbiology studies have demonstrated the importance of contamination detection through the use of tracers (D'Costa *et al.*, 2011; Smith *et al.*, 2000). Fluorescent latex beads similar in size to microbes have been used extensively in deep subsurface microbiology (e.g. (Kallmeyer *et al.*, 2012)) and to a lesser extent in permafrost studies (e.g. (Bang-Andreasen *et al.*, 2017; Juck *et al.*, 2005) to track potential contamination during sample acquisition. However, these beads do not mimic microbes well (Bang-Andreasen et al., 2017(Colwell *et al.*, 1994), are subject to quenching and bleaching of fluorescence (Yanagawa *et al.*, 2013), are labor-intensive to detect (Friese *et al.*, 2017), and cannot be detected easily at low levels of contamination (Kallmeyer *et al.*, 2006). Biological tracers have two major advantages relative to

beads: they are biological particles and thus mimic contaminants better and they can be easily detected at very low levels by PCR (Juck *et al.*, 2005). Intact cells that are not found in permafrost that carry a well-characterized target DNA molecule, such as a plasmid, are an ideal contamination tracer. In this study, we utilized *E.coli* mNeonGreen-expressing cells, which are a commercial product and thus are not found in permafrost. This tracer can be visualized by fluorescence of the mNeonGreen protein and the pBAD plasmid is easily detected at low levels by PCR.

Applying the tracer to the wrong sampling component or at the wrong time may lead to a false negative, i.e. the presumption that decontamination is complete when the lack of detection of the tracer is actually due to loss during handling (Bang-Andreasen *et al.*, 2017; Juck *et al.*, 2005; Kallmeyer, 2017). Based on our observations, tracer should be applied both to the drilling apparatus and cores in the field and again in the laboratory; application solely in the field led to inconsistent detection of tracer even before decontamination. Furthermore, we found that applying the tracer by painting rather than by spraying provided a more consistent coverage of samples.

Our results showed that none of the tested decontamination methods were able to completely remove the tracer except the bleach wash method and disk sampling method with brass pipe connectors. Bleach is cheap and readily available in comparison to costlier DNAse and RNAse decontamination solutions used in some studies (Barbato *et al.*, 2016; Kemp & Smith, 2005). Bleach was effective in removing our tracer and left a moderate amount of the material available

for subsequent work without damaging the indigenous DNA. In contrast, while the brass pipe connector-based protocol used a clean subsampling approach, it yielded a low quantity of subsamples.

One possible disadvantage of using bleach for decontaminating permafrost segments is changes to the chemistry of the samples. We addressed this potential issue by splitting the core section into separate samples for chemistry and biology (e.g. 1/3 and 2/3 sections), which allowed preservation of samples for chemistry work, and a sufficient amount of material for decontamination and DNA extraction. However, if the amount of material available is restricted, this approach may not be tenable. It should be noted that the amount of the material required for archiving and microbiological analysis could vary based on the drilling strategy used for obtaining samples and should be adjusted based on the experimental design.

The rest of the tested methods, based on the most commonly used method in published permafrost studies (e.g. disk sampling or scraping; **Supplementary Table 1.1**) resulted in inconsistent PCR amplification of the tracer from decontaminated samples. One possible reason for a lack of decontamination was physical contact of the clean interior pieces with contaminated materials and dust generation during the subsampling. We noted that our test plates were contaminated with tracers and other cells during disk sampling methods, likely indicating the production of contaminated dust or aerosols during processing, similar to previous findings (Knapp *et al.*, 2012; Yang & Watt, 2005). Thus, methods that minimize dust and aerosol generation are recommended to decrease the possibility of re-contaminating cleaned samples.

In the case of scraping, insufficient removal of the contaminated surface of the core section may have been another reason for detecting the tracer. Bang-Andreasen and colleagues (Bang-Andreasen *et al.*, 2017) demonstrated that their intentional contamination spike was still detectable down to 17 mm depth after coring; thus, scraping, which in our experiment only removed 2–3 mm after 4–5 scrapes, is insufficient to decontaminate the core. The ineffectiveness of the scraping method has also been reported in ancient DNA studies (Kemp & Smith, 2005). Thus, we strongly recommend against scraping as the sole decontamination method for permafrost cores.

In general, a major difference between protocol (g) in comparison to protocols (a-f) was that our developed protocol (g) uses a different approach and that our goal was not to modify or improve the widely used protocols (a-f), but rather to compare efficacy between widely used permafrost decontamination methods and our novel protocol (g).

In our experiment, commercial DNA extraction kits vary in both DNA yield and purity. In a previous study, the Fast DNA SPIN kit for soil (MP Biomedicals, USA) provided the highest DNA yield from permafrost, although it required further purification (Vishnivetskaya *et al.*, 2014). However, in our experiment while the Fast DNA SPIN kit for soil gave the highest yield in the control soil, no detectable DNA was obtained from the permafrost. The modified protocol for ZymoBIOMICS DNA Microprep kit (Zymo Research, USA) was the only protocol able to yield sufficient PCR amplifiable DNA. It is unclear whether the same kit or the same modifications will always provide optimal results; thus, when there is sufficient sample, we

recommend testing of several commercially available kits and modification of those protocols (e.g. see **Appendix 1**) to obtain the maximum amount of pure DNA from permafrost.

It is critical to utilize DNA extraction blank controls since the kit reagents could introduce contamination. In one protocol, the negative control for the kit always showed amplification, indicating contamination from the kit reagents. Contamination via kit reagents has been observed in other studies as well (e.g. (Eisenhofer *et al.*, 2019). Eisenhofer and colleagues (Eisenhofer *et al.*, 2019) have noted and summarized some species from a large variety of microbiome studies that are regularly found in DNA extraction kits. Thus, it is clear that extraction kits can and often do introduce contaminants: kits should be selected with care for low biomass samples such as permafrost that are prone to contamination. Furthermore, extractions should include extensive positive (control soils) and negative (blank extraction) controls.

Our results indicate that basic soil chemical parameters did not influence the spike penetration or decontamination procedures; however, these parameters did affect DNA extraction yield. The silty core generally provided a higher DNA yield than the peaty core, indicating that permafrost chemical and physical parameters can affect DNA extraction.

2.5. Conclusions and recommendations

We recommend the following to prevent contamination of permafrost samples intended for microbial work:

1: A biological spike should be applied both in the field via spraying and in the lab by painting of the core sections. The spike should be allowed to fully freeze onto the core. PCR should be

used to detect the applied biological tracer: clean samples should be negative; removed material should be positive.

2: Ancient DNA protocols for sample handling should be followed whenever possible (e.g. (Cooper & Poinar, 2000; Llamas *et al.*, 2017). These protocols were developed to minimize external contamination and cross-contamination between samples. These protocols are evolving and should be updated regularly. We have provided a summary of these guidelines in this manuscript (see **Appendix 1** for details).

3: Combined bleach wash and shaving is the most effective method for decontaminating permafrost samples intended for DNA work. We recommend against utilizing only disk decontamination or scraping, as these approaches did not remove our tracer. Since this method is destructive, we suggest acquiring large quantities of permafrost sample for both microbial/ancient DNA work and archiving.

4: Multiple DNA extraction kits should be tested for the specific samples, with both positive (temperate soil) and negative (reagents only) controls. In our experiment, modified ZymoBIOMICS DNA Microprep kit (Zymo Research, USA) was the most effective method in extracting DNA from silty permafrost and to some extent from peaty permafrost; however, other samples may respond better to other DNA extraction protocols.

5: A serial dilution of the DNA template intended for PCR should be performed to ensure that the absence of amplicons (from the contamination marker or 16S rRNA genes) is not due to PCR inhibitory compounds, which might have escaped the purification steps of DNA extraction protocols.

6: Positive controls should never be processed together with permafrost samples or at all in a lab intended for ancient DNA or permafrost microbiome work. The risk of cross contamination is too high.

2.6. Summary of chapter 2

This chapter aimed to act as a methodological guide for contamination monitoring, decontamination, and DNA extraction for peaty and silty permafrost samples with low biomass or difficult to extract DNA. I applied a biological tracer, either only in the field or both in the field and in the lab, via either spraying or painting. Spraying in the field followed by painting in the lab resulted in a uniform layer of the tracer on the core sections. A combination of bleaching, washing, and scraping resulted in complete removal of the tracer leaving sufficient material for DNA extraction, while other widely used decontamination methods did not remove all detectable tracer. In addition, of four widely used commercially available DNA extraction kits, only a modified ZymoBIOMICS DNA Microprep kit was able to acquire PCR amplifiable DNA. Permafrost chemical parameters, age, and soil texture did not have an effect on decontamination efficacy; however, the permafrost type did influence DNA extraction. Based on these findings, I developed recommendations for permafrost researchers to acquire contaminant-free DNA from permafrost with low biomass.

Chapter 3

Permafrost Microbial Community Structure Changes Across the Pleistocene-Holocene Boundary

This chapter has been published in the journal of "Frontiers in Environmental Science" as "Saidi-Mehrabad, A., Neuberger, P., Hajihosseini, M., Froese, D., Lanoil, B. (2020). Permafrost microbial community structure changes across the Pleistocene-Holocene boundary. Frontiers in Environmental Science. 8:133".

3.1. Introduction

The Pleistocene – Holocene transition was accompanied by rapid, extensive global climate and ecosystem changes (Barnosky *et al.*, 2004; Guthrie, 2006). These rapid changes forced the Earth system to cross a climate threshold causing a major transition in terrestrial biosphere and pedogenesis from one stable state to another stable state and coincided with extinction of megafauna, reorganization of plant communities, and accompanying changes in soil chemistry and sedimentation (Alley *et al.*, 2003; Lacelle *et al.*, 2019; Steffen *et al.*, 2018). At high latitudes, these changes may be preserved in relict permafrost (Froese *et al.*, 2009b; Gaglioti *et al.*, 2016; Shapiro & Cooper, 2003). Relict permafrost is defined as "permafrost existing in areas where permafrost can not form under present climatic conditions; reflecting past climatic conditions that were colder" (National Snow and Ice Data Center). In this chapter whenever the word "relict permafrost" is used, it refers to permafrost that has survived the Pleistocene-Holocene transition, and contains fossil records of the late Pleistocene and early Holocene biota. These natural biological and chemical archives have been used to reconstruct late Quaternary paleoclimate (Porter *et al.*, 2019), vegetation (Willerslev *et al.*, 2014), and faunal communities (Haile *et al.*,

2009; Lorenzen *et al.*, 2011). Despite the presence of well-documented changes in vegetation and faunal community structure across the Pleistocene-Holocene transition (Guthrie, 2006; Mann *et al.*, 2016), it is still unclear whether these changes were associated with concomitant restructuring of soil microbial communities.

Recent studies have shown that the main factors governing microbial community structure in permafrost appear to be the age of the samples (Burkert *et al.*, 2019; Liang *et al.*, 2019; Mackelprang *et al.*, 2017), ice content (Burkert *et al.*, 2019), dispersal limitation and physical/thermodynamic constraints (Bottos *et al.*, 2018), with little to no correlation with soil chemical parameters. For example, one recent study indicated that microbes within three Pleistocene-aged permafrost chronosequences changed in composition in response to increasing age, with a corresponding increase in survival strategies (Mackelprang *et al.*, 2017). These correlations suggest that these environmental pressures, arising from harsh permafrost conditions, select for a subset of species and that the community structure deviates from the community present at the time the permafrost was formed (Kraft *et al.*, 2015b; Liang *et al.*, 2019; Mackelprang *et al.*, 2017; Willerslev *et al.*, 2004b). However, another study performed on two Pleistocene-aged permafrost samples of a similar age but differing origins (lake-alluvial sediments and Yedoma/ice complex sediments) indicated the presence of two distinct microbial communities, which were formed in response to differing environmental settings and not due to the age of the samples alone (Rivkina *et al.*, 2016). As a result, it is not clear whether relict permafrost microbial communities provide a window into past soil microbial communities, or are the strict remnants of selective pressures of the permafrost environment, or some combination of the two. The word “relict” in ecology is defined as “either geographical or phylogenetic, a

species or a group of species remaining from a large group that is mainly extinct and/or having no constraints on the time frame and extinctions date to either the Holocene or the Paleocene" (Grandcolas *et al.*, 2014). In this chapter "relict microbial community" refers to the community that formed at the Pleistocene-Holocene transition and could include both dead and viable microbial cells that have remained metabolically active since the late Pleistocene or are the offspring of the cells that were once active at the Pleistocene terminus.

In this study, we selected samples on either side of the Pleistocene-Holocene transition from a permafrost core extracted from central Yukon, a part of Eastern Beringia. The permafrost of Eastern Beringia contains exceptional proxy records of climate change (Froese *et al.*, 2009b). Furthermore, the Pleistocene-Holocene transition zone preserved in Eastern Beringian permafrost is prominent in the core stratigraphy, allowing for detailed microbiological and soil physicochemical analyses (Porter *et al.*, 2019). The core in this study was collected about 1.5 m adjacent to, and shares stratigraphy with a well-dated and chemically and physically characterized core spanning the last ca. 16,000 years (Davies *et al.*, 2018; Porter *et al.*, 2019).

3.2. Material and methods

3.2.1. Permafrost coring location and analysis of the soil texture

The topography of our sampling site (DHP174-13L) along with the paleoenvironmental setting, stratigraphy and coring strategies were described previously (Davies *et al.*, 2018; Porter *et al.*, 2019). We obtained a 3.97 m long permafrost core (called DHL_16, collected in May 2016) about 1.5 m lateral to the core reported by (Porter *et al.*, 2019). Three intervals from depths of 174–210, 296–319, and 327–365 cm (termed DHL_16_1, DHL_16_2, and DHL_16_3 in this manuscript, respectively) were selected from the DHL_16 core for microbiological and chemical analyses. We were careful to sample near the Pleistocene-Holocene transition zone while avoiding the transition zone itself to minimize any effects of water migration in the paleoactive layer [detailed in (Porter *et al.*, 2019) for the stable isotopes of the pore waters in that study]. Active layer (or seasonally thawed soils) can allow water leaching from the paleo-surface to deeper depths (< ∼50 cm at this site today) and result in mixing of the surface water, potentially impacting microbial and edaphic properties. We used the depleted water isotopes to provide further support that the waters (and thus the microbes) have not been mobilized since they froze (detailed in (Porter *et al.*, 2019).

The core stratigraphy, reported by (Davies *et al.*, 2018; Porter *et al.*, 2019), documents three prominent units that are readily recognized in both cores: units 1, 2, and 3 from the bottom of the core to the surface. The youngest unit sampled, corresponding to unit 3 of (Porter *et al.*, 2019) consists of peat (sampled interval 174–210 cm; DHL_16_1) and dates to the early Holocene (∼8–10.5 k cal yr BP), whereas DHL_16_2 and DHL_16_ 3 are loessal silts (eolian silt)

(sampled at 296–319 cm and 327–365 cm respectively) both associated with the late Pleistocene (~14.3–15 k cal yr BP, and ~15–16 k cal yr BP, respectively), based on the age model of (Porter *et al.*, 2019). At the site, the peat/silt boundary was determined to be at 244 cm (which was dated to ~10.5 k cal yr BP, **Supplementary Figure 3.1**). These three selected intervals were vertically cut into 1/3 and 2/3 subsections with the aid of a masonry saw. The 2/3 sections were used for DNA extraction, while the 1/3 sections were used for chemical analyses (See **chapter 2**).

Soil textures of Holocene-aged samples from 210 cm depth and Pleistocene-aged samples from 296 cm depth were examined and photographed under 4.5 × and 67 × magnifications of a zoom stereomicroscope (Olympus-Life Sciences SZ61, Japan). These two depths were near the 244 cm peat/silt boundary. Samples were allowed to thaw and dry at 70 °C in a table top oven for 48 h prior to microscopy.

3.2.2. Permafrost edaphic parameter analysis

Selected intervals of DHL_16_1, DHL_16_2, and DHL_16_3 were sub-sectioned for soil chemical analysis based on a previously described method (see **chapter 2**). Briefly, the 1/3 core sections were cut into 1-cm^3 cubes with a hand saw in a 4 °C cold room for measuring the basic chemical parameters of these samples, including soil organic matter (OM), pH and gravimetric water content (GW) (see **chapter 2**). Total carbon (TC) and total nitrogen (TN) were measured from 0.5 g of subsections based on a dry combustion method with the aid of an Elemental Analyzer (EA 4010; Costech International Strumatzione, Italy) (Sparks *et al.*, 2020).

Nitrate/nitrite (NO^{-}_{3}/NO_{2}^{-}) was analyzed using ~ 5 g of soil material with a colorimetric diazo coupling method by a SmartChem Discrete Wet Chemistry analyzer (model 200, Westco Scientific, USA (Maynard *et al.*, 1993). Ammonium (NH_4^+) was measured from 0.5 g of subsections based on a colorimetric Berthelot protocol (Maynard *et al.*, 1993). Electrical conductivity (EC) was measured at 1:5 soil:water (w/v) ratio, calibrated at 20 °C with 0.01M KCl solution (Hardie & Doyle, 2012) using an EC500 ExStik® II conductivity measuring device (EXTECH instruments, USA). Dissolved metals were extracted from 0.5 g of sample by HNO_3/HCl digestion and measured via inductively coupled plasma-optical emission spectroscopy (iCAP6300, Thermofisher Scientific, Canada) (Skoog *et al.*, 2017).

3.2.3. DNA extraction and sequencing

Prior to DNA extraction the 2/3 sections associated with the DHL_16_1, DHL_16_2, and DHL_16_3 intervals were cut into ~6 × 3.5 × 2.5 cm rectangular pieces (n = 16) and the exterior of these rectangles were painted with a total of 3×10^8 cells/ml of *Escherichia coli* (*E. coli*) (strain DH10B) suspended in 50 ml of 1 × PBS using a 25 mm paintbrush (see **chapter 2**). The *E. coli* strain used in our contamination monitoring procedure harbored a mNeonGreen - expressing and ampicillin-resistant pBAD/His B vector, which allowed us to trace the contamination at a much smaller levels via direct PCR targeting the vector or macro-photography of the glowing mNeonGreen protein under 470 nm wavelength (see **chapter 2**). All rectangular pieces were decontaminated by the combination of bleach washing and scraping under sterilize conditions designed for ancient DNA analysis in a class 1000 clean lab with no history of sample processing (see **chapter 2**). Genomic DNA was extracted from a total of ~10 g

of homogenized thawed soil at room temperature from each 6 cm subsection using a modified ZymoBIOMICS DNA Microprep kit (Zymo Research, USA) protocol (see **chapter 2**). DNA concentration was measured with a Qubit dsDNA HS Assay Kit according to manufacturer's protocol (Thermofisher Scientific, Canada). The extracted DNA was tested for the presence of the biological tracer used in our contamination monitoring procedure via PCR (performed in triplicate and in a variety of dilutions) as described in **chapter 2**. We were unable to obtain sufficient DNA devoid of the contamination tracer for sequencing from DHL_16_3 sub-sections, as a result, these samples were excluded from further molecular analysis. Thus, a total of six segments, three from DHL_16_1 (174–179, 179–184, and 189–194 cm) and three from DHL_16_2 (296–301, 305–310, and 314–319 cm), passed our quality control steps (see **chapter 2**) for microbial community analysis.

Clean genomic DNA extracted from the permafrost samples, a lab-constructed mock community (**Supplementary Figure 3.2**), and DNA extraction blanks (**Supplementary Table 3.1**) were sequenced based on the V4 region of the 16S rRNA genes by using standard Earth Microbiome Project (EMP) primers 515F and 806R (Caporaso *et al.*, 2011). The platform used by the commercial sequencing provider (Microbiome Insights, Canada) was an Illumina MiSeq machine using a 250-bp paired-end kit (V2 500-cycle PE Chemistry; Illumina, USA). No additional library preparation kits were used, as the libraries were constructed in a single PCR step. Generated sequences were demultiplexed via bcl2fastq2 2.20 according to Illumina guidelines (Illumina, USA).

3.2.4. Quality control of raw sequences and OTU construction

A combination of USEARCH 10.0.240 (Edgar, 2010) and Mothur 1.39.5 (Schloss *et al.*, 2009) pipelines were utilized for analyzing the sequences. USEARCH was used to merge the reads and to form contigs based on the criteria recommended in USEARCH 10 manual for analyzing sequences generated from the V4 region of the 16S rRNA genes. Mothur was used to merge the raw reads into a single merge file and to normalize the reads to the lowest read counts via random subsampling. OTU picking, chimera, and universal singleton checks were performed with the UPARSE pipeline via de novo/greedy heuristic algorithm (Edgar, 2013). The threshold used for OTU clustering was 97% similarity. Constructed OTUs were mapped to taxonomy via SINTAX algorithm by using a trained V4 16S rRNA RDP (v16; 13k sequences) database (recommended for SINTAX algorithm) (Cole *et al.*, 2014; Edgar, 2016a). The confidence level cut-off at each taxonomic level was set to 0 to prevent data loss. In addition to the bootstrap values obtained from SINTAX algorithm, the taxonomic identity of the sequences were manually investigated via Basic Local Alignment Search Tool (BLAST) in the NCBI database (Altschul *et al.*, 1990). The SINTAX algorithm uses k-mer similarity to identify the top taxonomy (Edgar, 2016a), hence it is very fast and computationally less expensive for taxonomic assignment of OTUs. However, the algorithm is unable to assess taxonomy with high accuracy down to the species level. Hence, the BLAST algorithm was used to compensate for this shortcoming.

All strains detected in the blank controls, Eukarya, Archaea species and Cyanobacteria/Chloroplast (termed anomalous sequences) were removed from downstream

community analyses (**Supplementary Table 3.2**). Archaeal species were mainly removed to prevent overestimation or underestimation of their diversity since the universal Earth microbiome primers used in this study might not be suitable to assess Archaeal diversity (Wear *et al.*, 2018). Universal Earth microbiome primers targeting the V4 region of the 16S rRNA gene have shown to over-represent species associated with Euryarchaeota and Thaumarchaeota but accurately present all bacterial species (Wear *et al.*, 2018). Archaea will be studied in the future by relying on Archaeal specific primers and metagenomics to prevent diversity biases.

In summary, 98.1% of the reads passed the filtering Q score parameters (with expected error < 1.0) and resulted in 87843 filtered reads. Of these, 11417 reads were unique (de-replicated) and 8287 were singletons (72.6%). OTU counts were rarified to 1768 sequences per sample by random subsampling. UPARSE picked 778 OTUs, with 612 OTUs assigned to domain Bacteria via SINTAX after removal of anomalous sequences. Despite a relatively small number of OTUs and sample size, the constructed rarefaction curve demonstrated enough sampling depth for downstream diversity analyses (**Supplementary Figure 3.3**). Raw sequences obtained in this study have been archived in NCBI Sequence Read Archive under the ascension number of PRJNA607368, and BioSample accession of SAMN14130768.

3.2.5. Community Analysis

All the statistical computations that utilized the R language were performed in R Studio environment 1.1.442. The soil parameters were $\log_{10}(x + 1)$ transformed and were later used to create a variable matrix for PcOrd version 6.22 (Wild Blueberry Media, Inc., USA) and a Phyloseq 1.16.2 object for alpha and beta diversity analyses (McMurdie & Holmes, 2013). The possible differences in OTU structure between groups were calculated with Bray-Curtis dissimilarity matrix and clustering was calculated based on average linkage in PcOrd version 6.22. Results were visualized in a principal coordinate analysis biplot (PCoA) and statistical support for differences between groups was calculated with the aid of Multi-Response Permutation Procedure (MRPP) with 999 randomized permutation tests in PcOrd version 6.22 (Mielke Jr *et al.*, 1976). The coefficient of determination of chemical parameters to sample groups (Holocene or Pleistocene) were assessed based on the "envfit" function of vegan ver 2.4-2 package with max $p < 0.05$ and 999 permutation tests (Oksanen *et al.*, 2007). Differences in chemical composition between samples were visualized in a principal component biplot (PCA). Samples were clustered based on average linkage and statistical significance between clusters were assessed based on MRPP in PcOrd version 6.22 (Mielke Jr *et al.*, 1976). The shared and unique OTUs between and within clusters detected in PCoA analysis were investigated with a co-occurrence network test based on a maximum ecological distance of 0.8 and distance matrix of Jaccard by the aid of Phyloseq 1.16.2 package (McMurdie & Holmes, 2013). To assess which taxa were significantly differentially abundant in Pleistocene and Holocene groups, the DESeq2 differential abundance method (Love *et al.*, 2014) with a threshold of 0.01 and $p < 0.05$ was used on the top 10 dominant phyla within all samples combined (microbiomeSeq package 0.1). In order to assess the sequence similarity of the Pleistocene- and Holocene-aged bacteria to

published bacteria, each representative sequence of an OTU was compared to publicly available sequences via BLAST in NCBI (standard nucleotide (nr/nt) database). Uncultured/environmental sample sequences were excluded from our search criteria. The top sequence hit similarity values for each individual group were averaged and compared with each other. The possible effect of epoch-based separation on the relationship between soil chemistry and changes in OTU structure were investigated using a negative binomial many-generalized linear model (ManyGLM) (Warton *et al.*, 2012). The model performed multiple random re-samplings via Monte Carlo algorithm to investigate many correlated variables while considering the strong mean-variance relationship due to the presence of rare species and high zero inflation (Warton, 2011; Warton *et al.*, 2012). The statistical significance of this model was based on Wald's test, which employed a generalized estimating equations approach (Warton *et al.*, 2012). The model was executed with the mvabund 4.0.1 package (Wang *et al.*, 2012). This model was also used to assess the differential abundance of OTUs shared between Pleistocene- and Holocene-aged samples with the same criteria described above.

3.2.6. Live/Dead Microscopy Assay

The viability assay was performed with a Live/Dead BacLight Bacterial Viability Kit (Invitrogen Thermo Fisher, Canada) and a DM RXA fluorescence microscope (Leica Microsystems, Germany). The viable cells were enumerated via green fluorescence at 470 nm excitation and the dead cells were enumerated via red fluorescence at 530 nm excitation. A 36 cm section from DHL_16_1 and a 23 cm section from DHL_16_2 were cut, homogenized and subsampled in quadruplicate as representative Holocene and Pleistocene samples, respectively. For each

replicate subsample, 15 fields of view were counted under both wavelengths and the resulting n = 60 mean observation was used to calculate the abundance and live/dead proportion of the cells. The detailed protocol is available in **Appendix 2**.

3.3. Results

The Holocene-aged permafrost sediments had properties distinct from Pleistocene-aged permafrost sediments, matching the descriptions of (Fraser & Burn, 1997) and (Kotler & Burn, 2000). The most noticeable difference was Holocene sediments were dominated by peat, while Pleistocene sediments were comprised of silty loess with frozen rare lenses of ice and largely lacking visible plant remains (**Supplementary Figure 3.4**). No clear differences in texture were observed for samples within each epoch (**Supplementary Figure 3.4**). The presence of well-preserved plant macroremains from the peat suggest a relatively uninterrupted aggradation of permafrost with the plant material since the time of deposition, and that the permafrost of our sampling region formed syngenetically, or as the surface aggraded, without signs of previous thaw; this is also reflected by the water isotopes from these cores reported by (Porter *et al.*, 2019).

All measured chemical parameters differed significantly between Pleistocene and Holocene sediments (**Tables 3.1, 3.2** and **Supplementary Figures 3.1**, **3.5**). Similar to texture, none of the measured chemical parameters showed statistically significant changes within epochs. Holocene samples had significantly higher organic matter ($p < 0.001$), nitrate/nitrite ($p < 0.01$), water ($p <$

0.01), and total nitrogen ($p < 0.01$) as well as significantly lower metals ($p < 0.05$), electrical conductivity ($p < 0.05$), and pH ($p < 0.001$) than Pleistocene samples (**Tables 3.1, 3.2**).

Table 3.1. Basic soil edaphic parameters of the selected segments for microbial analysis.

Epoch	Depth (cm)	OM[1**] (±SD)	TC[1*] (±SD)	TN[1*] (±SD)	GW[1*] (±SD)	pH** (±SD)	NO_3^-/NO_2^{-d*} (±SD)	EC[e*] (±SD)	NH_4^{+d*} (±SD)
H[a]	174-179	95 (3)	47 (4)	1 (0.2)	92 (0.8)	3.7 (0.06)	0.9 (0.12)	370 (55)	15.5 (3.2)
H	179-184	96 (0.4)	48 (3.6)	1 (0.2)	90 (1.4)	3.7 (0.08)	1 (0.1)	405 (5)	19 (2.8)
H	189-194	96 (0.7)	45 (0.6)	0.8 (0.05)	91 (1.8)	3.73 (0.03)	1.18 (0.01)	342 (22)	21 (0.07)
P[b]	296-301	22 (16)	7 (0.9)	0.6 (0.07)	77 (18)	6 (0.15)	0.1 (0.01)	671 (186)	136 (24)
P	305-310	16 (12)	7 (1)	0.5 (0.08)	62 (18)	6.46 (0.04)	0.1 (0.1)	701 (150)	90 (41)
P	314-319	6 (0.3)	5 (1.4)	0.4 (0.1)	45 (6.2)	6.71 (0.16)	0.3 (0.04)	1106 (422)	90 (42)

Segments 174-194 cm were associated with Holocene aged DHL_16_1 core and 296-319 cm were associated with Pleistocene aged DHL_16_2 core. ** $p < 0.001$, * $p < 0.01$. (±SD) = standard deviation. 1 OM = Organic Matter, TC = Total Carbon, TN = Total Nitrogen, GW = Gravimetric Water content, EC = Electrical Conductivity. [a] H, Holocene age, [b] Pleistocene age, [c] % (w/w), [d] mg/kg [e] µS/cm.

Table 3.2. Measured dissolved metals of the selected segments for microbial analysis.

Epoch	Depth (cm)	Ca[c]* (±SD)	Cu[d]* (±SD)	Fe[c]* (±SD)	K[c]* (±SD)	Mg[c]* (±SD)	Mn[d]* (±SD)	Zn[d]* (±SD)	Na[d]* (±SD)	P[c]* (±SD)	S[a]** (±SD)
H[a]	174-179	0.23 (0.07)	18.26 (11.7)	0.33 (0.19)	0.02 (0.01)	0.05 (0.02)	19.51 (0.5)	21 (5)	129 (69)	0.02 (0.0)	0.17 (0.006)
H	179-184	0.27 (0.13)	9 (1.25)	0.19 (0.3)	0.02 (0.0)	0.05 (0.02)	18.33 (1.08)	22 (6)	109 (40)	0.02 (0.004)	0.16 (0.03)
H	189-194	0.4 (0.02)	9.65 (2)	0.32 (0.03)	0.01 (0.001)	0.08 (0.007)	19 (2)	28 (2)	146 (12)	0.02 (0.0)	0.12 (0.01)
P[b]	296-301	0.83 (0.08)	68 (30)	1.7 (0.24)	0.13 (0.01)	0.5 (0.07)	153 (57)	137 (9.4)	224 (15)	0.09 (0.0)	0.22 (0.02)
P	305-310	0.8 (0.03)	82 (9.5)	1.71 (0.02)	0.14 (0.03)	0.47 (0.03)	136 (33)	139 (12)	261 (66)	0.09 (0.002)	0.21 (0.03)
P	314-319	1.60 (1)	62.(19)	1.96 (0.22)	0.13 (0.006)	0.75 (0.34)	194 (47)	148 (1.4)	261 (65)	0.1 (0.01)	0.16 (0.02)

Segments 174-194 cm were associated with Holocene aged DHL_16_1 core and 296-319 cm were associated with Pleistocene aged DHL_16_2 core. *$p < 0.01$, ** $p < 0.05$, (±SD) = standard deviation, [a] Holocene age, [b] Pleistocene age, [c] % (w/w), [d] mg/kg.

In addition to dramatic changes in soil composition and chemistry, there was significantly higher cell viability and cell abundance in Holocene samples than in Pleistocene samples, with ~8 fold higher viable cells ($p < 0.001$), ~2 fold fewer dead cells ($p < 0.001$) and ~2 fold higher total cells ($p < 0.001$) (**Figure 3.1**). Direct microscopic cell counts demonstrated Holocene samples had a total of 1.12×10^7 ($\pm 4.44 \times 10^6$) cells g^{-1} of wet soil, with 84% viable cells and 16% non-viable cells. Pleistocene samples had a total of 6.47×10^6 ($\pm 9.57 \times 10^5$) cells g^{-1} of wet soil, with 17% viable cells and 83% non-viable cells (**Figure 3.1**).

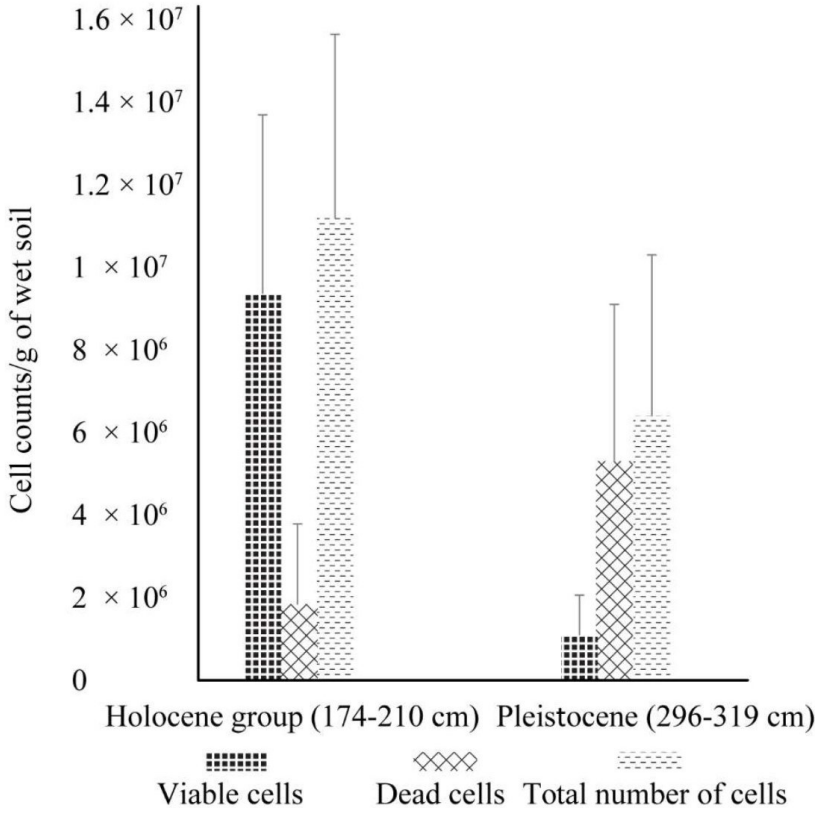

Figure 3.1. Live/dead cell counts of Holocene and Pleistocene aged samples. Error bars represent one standard deviation from the mean (n = 60 mean observation). For this experiment, samples from 174–210 cm (n = 4) and 296–319 cm (n = 4) were selected to investigate cell viability in Holocene aged and Pleistocene aged soils. These depths were selected based on their close proximity to the Pleistocene-Holocene transition zone of 244 cm. The statistical significance (Student's t-test) of fold change in cell counts from Holocene to Pleistocene is as follows: fold change in viable cells ($p < 0.001$), fold change in dead cells ($p < 0.001$), and fold change in total cells ($p < 0.001$).

Overall microbial diversity based on 16S rRNA genes was either not significantly different between Holocene and Pleistocene samples (as measured by observed OTUs, Shannon diversity index, Chao1 richness estimator, Simpson evenness, and Fisher's alpha diversity index), or the statistical support for differences was weak (as for the Mann–Whitney U test) (**Supplementary Table 3.3**). In a PCoA biplot, composite Holocene and Pleistocene samples demonstrated a dramatic dissimilarity in OTU composition. The microbial communities formed two clusters based on epoch; there was no clear differentiation within the epoch-based groups (**Figure 3.2**).

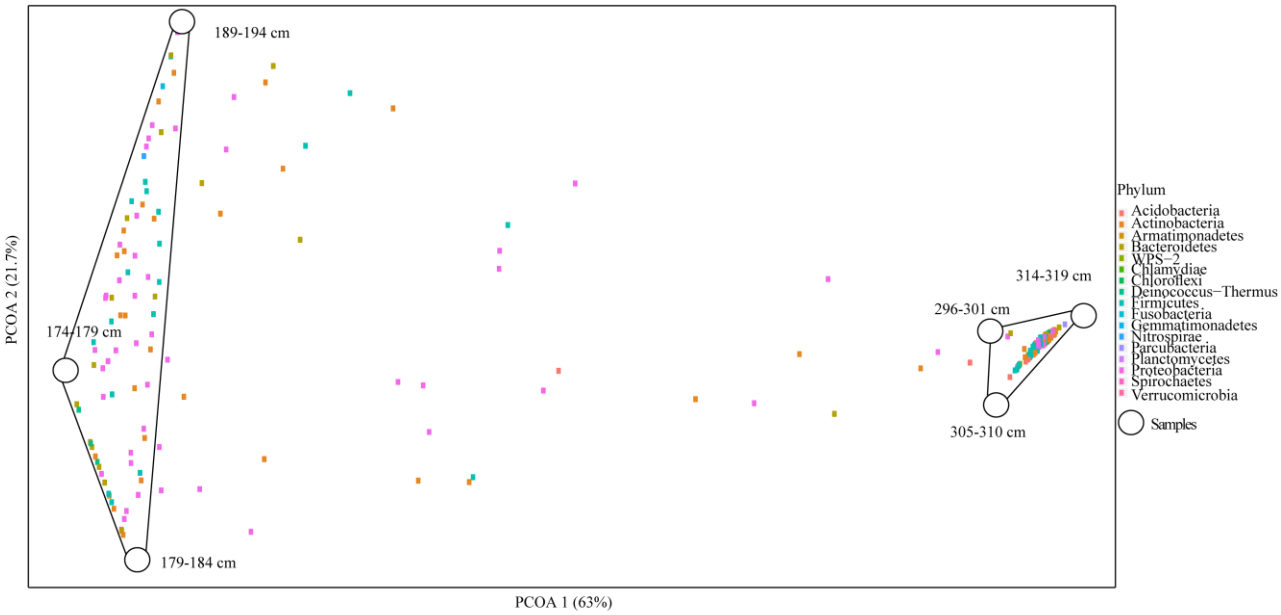

Figure 3.2. PCoA biplot of the OTU composition in Holocene (n = 3) and Pleistocene (n = 3) aged samples. Combined Axis 1 (PCOA1) and Axis 2 (PCOA2) components explained a total of 84.7% of the dissimilarity between the clusters in the system (p = 0.022). Samples 174–179, 179–184, 189–194 cm formed the Holocene cluster (8–10 k cal yr BP) and 296–301, 305–310, 314–319 cm formed the Pleistocene aged cluster (14–15 k cal yr BP). In the ordination space,

samples (5 cm segments of DHL_16-1 and 2) have been shown with white circles and OTUs with colored squares. Colors of OTUs represent their taxonomic identity at the phylum level.

Similar to soil texture, chemistry and cell abundance, each epoch-based cluster had a unique set of OTUs not present in the other epoch, which are probably selected by the environmental condition of each permafrost soil. The OTUs within and between epochs demonstrated that of 336 OTUs within Holocene samples, 84.5% were unique to this group (which we termed core Holocene OTUs, 284 OTUs), and only 15.5% were shared with the Pleistocene group (which we termed Pleistocene-Holocene shared, 52 OTUs) (**Supplementary Figure 3.6.**). Similarly, of a total of 328 OTUs within the Pleistocene cluster, 84.1% of the OTUs were unique to this group (which we termed core Pleistocene OTUs, 276 OTUs), and only 15.8% of the OTUs were in Pleistocene-Holocene shared group (**Supplementary Figure 3.6.**). The three dominant OTUs that formed the top 30% of the composite Pleistocene and Holocene samples were associated with the Pleistocene-Holocene shared group. In general, OTUs found within this cluster were slightly more dominant in Pleistocene samples (52.1%) than Holocene samples (47.8%).

Core Pleistocene and Holocene sequences were individually compared to the standard reference DNA sequence database in NCBI via BLAST. The average percent similarity of core Pleistocene OTU 16S rRNA gene sequences to published bacterial sequences was 92.1% (±0.05%; n = 276 OTUs) in comparison to Holocene OTUs, which was 97.5% (±0.03%; n = 284 OTUs) ($p < 0.001$). Since the average of the 16S rRNA gene sequence similarity value of Pleistocene OTUs were less than the 97% identity boundary between unknown and known species (Stackebrandt &

Goebel, 1994), they are uncharacterized and are more different from extant bacterial communities in databases than are Holocene OTUs. Pleistocene-Holocene shared OTUs (n = 52) demonstrated similarity to characterized strains similar to that for the Holocene OTUs (97.3% ± 0.05%) ($p > 0.05$) and not Pleistocene OTUs ($p < 0.001$).

Differential abundance analysis of the top 10 dominant phyla in composite Holocene and Pleistocene samples identified five phyla (Actinobacteria, Acidobacteria, Proteobacteria, Deinococcus-Thermus and Fusobacteria) as the main drivers of differences in taxonomy ($p < 0.001$) between Pleistocene and Holocene samples (**Supplementary Figures 3.7, 3.8**). In composite Holocene samples, 94% of the sequences fell within the Proteobacteria (56%), Actinobacteria (17%), Firmicutes (15%), and Bacteroidetes (5%) (**Figure 3.3**). Deinococcus-Thermus and Fusobacteria were part of the core Holocene samples and together constituted 3.58% of the community. On the other hand, 98% of the composite Pleistocene sequences were Actinobacteria (43%), Firmicutes (24%), Proteobacteria (16%), Acidobacteria (8%), and Bacteroidetes (6%). A similar distinction in taxonomic composition between composite Holocene and Pleistocene samples was also evident at the class level (**Supplementary Figure 3.9**). In the Pleistocene-Holocene shared group, 98% of the OTUs were associated with Proteobacteria (88%), Actinobacteria (8%), Firmicutes (2%) and Bacteroidetes (1%) respectively (**Supplementary Figure 3.10a**). Although these OTUs were shared between Pleistocene and Holocene samples the abundance of these OTUs were significantly different between epochs ($p < 0.001$) (**Supplementary Figure 3.10b**).

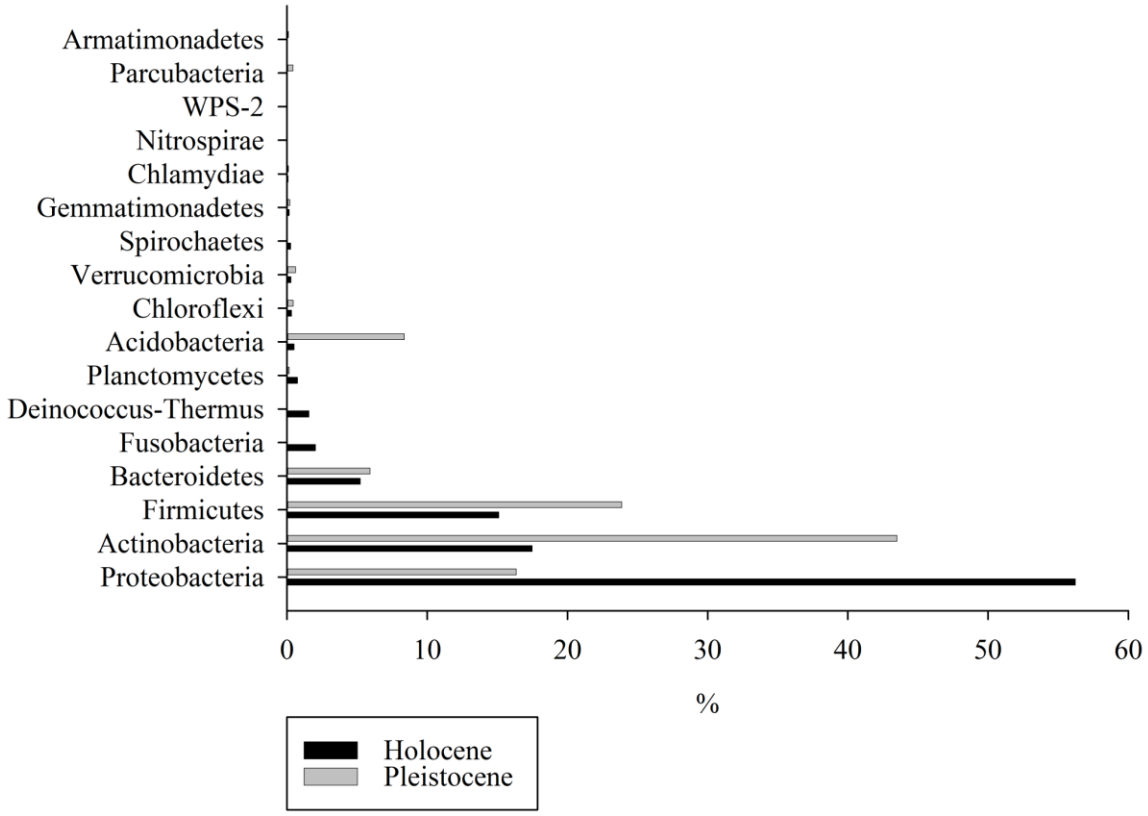

Figure 3.3. Relative abundance analyses of the OTUs detected in Holocene-aged and Pleistocene-aged permafrost samples at the phylum level.

To test for possible correlation between epoch-based separation of the microbial community structure and changes in soil chemical parameters, a ManyGLM model was utilized. The ManyGLM indicated that within the composited Holocene samples, only Ca and Mn had a statistically significant correlation ($p < 0.05$) to the core OTUs. The other 20 measured variables, including depth of the samples, did not show any significant relationship to the core OTUs

(**Table 3.3**). Within Pleistocene samples, no significant correlation was found between core OTUs and any measured variable, including depth of the samples. However, between the Pleistocene and Holocene groups, there was a clear correlation between shift in epoch, changes in soil chemical parameters and reorganization in core OTU compositions (**Table 3.3**).

Table 3.3. The probability values calculated based on Wald's generalized estimating equation in the context of a negative binomial many generalized linear model (MGLM).

Measured Variables	Holocene	Pleistocene	Between Epoch
Depth	0.605	0.184	0.009*
TC[a]	0.394	0.32	0.021*
TN[a]	0.219	0.444	0.005*[c]
NO_3^-/NO_2^-	0.531	0.385	0.012*
NH_4^+	0.151	0.072	0.003**
EC[a]	0.391	0.494	0.021*
pH	0.081	0.294	0.014*
H2O	0.379	0.226	0.044*
OM[a]	0.469	0.287	0.033*
Ca	0.039*[b]	0.349	0.022*
Cu	0.417	0.225	0.016*
Fe	0.3	0.505	0.027*
K	0.108	0.604	0.032*
Mg	0.12	0.271	0.014*
Mn	0.037*	0.567	0.016*
Zn	0.165	0.383	0.014*

Na	0.435	0.596	0.031*
P	0.074	0.239	0.008**
S	0.097	0.672	0.003**

[a] TC: Total carbon, TN: Total nitrogen, EC: Electric conductivity, OM: Organic matter. [b] * $p < 0.05$, [c]** $p < 0.01$. Note: within an epoch, degrees of freedom remaining after fitting each variable was 1 and degrees of freedom attributed to each variable was also 1. Between epochs, degrees of freedom remaining after fitting each variable was 4 and degrees of freedom attributed to each variable was 1.

3.4. Discussion

The perennially frozen nature of permafrost prevents movement of entrapped bacteria, creating a dispersal limitation. Furthermore, it is a challenging environment in terms of energy and nutrient availability (thermodynamic constraints) and damage to cells (physical constraints) (Bottos *et al.*, 2018; Burkert *et al.*, 2019; Liang *et al.*, 2019; Mackelprang *et al.*, 2017). Therefore, permafrost creates an environmental filter that only allows species resistant to these effects to survive, dramatically changing the composition of the community (Bottos et al., 2018; Mackelprang et al., 2017). Furthermore, these effects are compounded with time, further shifting the communities as the permafrost ages (Mackelprang et al., 2017). Hence, it is not clear if the surviving community members can be used as a paleoenvironmental tool.

Most previous studies of permafrost microbial community structure or community-level function have been conducted on permafrost chronosequences from a single epoch (e.g. (Hultman *et al.*, 2015; Mackelprang *et al.*, 2017; Mackelprang *et al.*, 2011). Therefore, it is not known whether

there is a shift in the permafrost microbial community structure close to the Pleistocene-Holocene transition. We observed dramatic differences in soil chemistry and OTU composition in samples from either side of the Pleistocene-Holocene transition (**Figure 3.2**, **Supplementary Figures 3.1, 3.5, 3.6, and Tables 3.1, 3.2**). A small number of OTUs (n = 52) that were able to persist despite the dramatic change during the Pleistocene-Holocene transition and the permafrost freezing-filtering effect were shared among the Pleistocene and Holocene samples (Pleistocene-Holocene shared group; **Supplementary Figure 3.6**). However, their abundance differed dramatically between epochs (**Supplementary Figure 3.10b**). No significant differences were observed between samples within an epoch (despite a difference in age between the samples). The lack of clear observable correlations between chemistry and microbiology within epochs is consistent with prior observations (e.g. (Bottos *et al.*, 2018; Mackelprang *et al.*, 2017).

Based on our data, microbial community structure within an epoch (despite few hundreds of years of an age difference between subsamples) is relatively stable over time, likely due to physiological flexibility and community stability of the microbial community (Shade *et al.*, 2013). Thus, the environmental filter of the frozen and isolated conditions in the permafrost creates a strong selection pressure on microbial communities that are initially similar. Any relatively small signal of microbial community differences at the time of formation are lost. However, once the system surpasses a threshold, both chemical and microbial parameters rapidly shift to a new stable state. Some OTUs are able to persist, despite the dramatic change during the Pleistocene-Holocene transition and the permafrost freezing filtering effect, and were shared among the Pleistocene and Holocene samples (Pleistocene-Holocene shared group;

Supplementary Figure 3.6) (Mandakovic *et al.*, 2018). This scenario resembles the threshold hypothesis (also known as the tipping point hypothesis) (Scheffer *et al.*, 2001), wherein a critical threshold exists in a system beyond which perturbations cause extensive changes (called "catastrophic" by Scheffer et al., 2001) and the system shifts from one stable state to another (Allison & Martiny, 2008; Mikkelson *et al.*, 2016; Shade *et al.*, 2012). Many paleoclimatic records indicate that the Pleistocene-Holocene transition was rapid and caused the climate system to cross a threshold, triggering a rapid transition to a warmer Holocene climate (Alley *et al.*, 2003; Boers *et al.*, 2018; Guthrie, 2006). Such an abrupt change is consistent with our ManyGLM model (**Table 3.3**), which did not detect any statistically significant correlation between OTU composition and soil chemical parameters within an epoch, with the exception of weak statistical support for correlations with Mn and Ca in Holocene samples (**Table 3.3**). However, between epochs, the ManyGLM model indicated a statistically significant change in microbial community structure and chemical profile (**Table 3.3**). Hence, we hypothesize that both soil chemical and microbial parameters were relatively stable until a threshold was reached at the Pleistocene-Holocene transition, after which there was a drastic shift to a new set of chemical and microbial parameters.

One implication of the threshold hypothesis described above is that it may explain why some decades-long in situ soil warming experiments have shown little or no change in microbial community structure (e.g. (Kuffner *et al.*, 2012), while lab-based incubations have shown dramatic shifts in community structure in a matter of days (e.g. (Mackelprang *et al.*, 2011). This difference between field and lab outcomes is likely because field-based studies generally involve moderate heating of the surface-active layer of soil and thus do not strongly affect the underlying

permafrost. In these experiments, microbes are able to gradually acclimate to moderate warming and the community resists shifts in composition (Allison & Martiny, 2008; Bradford *et al.*, 2008; Metcalfe, 2017; Rousk *et al.*, 2012). In contrast, in laboratory-based experiments, small amounts of permafrost thaw rapidly in response to increased temperature, leading to significant changes in the physicochemical parameters of the soil (Vonk *et al.*, 2015) accompanied by dramatic changes in microbial community structure (e.g. (Mackelprang *et al.*, 2011; Schostag *et al.*, 2019). Even changes at subzero temperatures in laboratory microcosms have been reported to alter microbial community structure (Tuorto *et al.*, 2014).

Changes in OTU and chemical composition between epochs were accompanied by major changes in taxonomy (**Supplementary Figures 3.7, 3.8**). Proteobacteria-related species were dominant in Holocene samples, whereas Actinobacteria-related species dominated Pleistocene samples (**Figure 3.3 and Supplementary Figures 3.7, 3.8**). Species associated with phyla Proteobacteria and Actinobacteria are the most dominant species in soil worldwide (Janssen, 2006), including cold environments such as permafrost (e.g. (Gittel *et al.*, 2014; Zhang *et al.*, 2016). Although phylogeny cannot be used to directly infer physiology and broad taxonomic groups (such as phyla) can include organisms with many different physiological features, strains affiliated with Actinobacteria have been characterized as oligotrophs adapted to nutrient-poor environments, while strains associated with Proteobacteria have been characterized as copiotrophs adapted to carbon-rich systems (De Vries & Shade, 2013; Itcus *et al.*, 2018). Competition for nutrients among species associated with these two phyla have been reported (Goldfarb *et al.*, 2011). According to a recent revision in environmental filtering theory, abiotic factors initially select certain strains, and then the second phase of selection pressure occurs

based on species competition for resources (Freedman & Zak, 2015; Kraft *et al.*, 2015a). Hence, competition for resources could be a major consequence of threshold-crossing events, which might drastically alter ecosystem services, in particular when Pleistocene-aged permafrost thaws and releases the entrapped microorganisms to the surrounding environment due to climate warming (Castro *et al.*, 2010; De Vries & Shade, 2013; Schostag *et al.*, 2019; Strauss *et al.*, 2017). Based on metatranscriptome analysis of frozen permafrost, Coolen and Orsi (Coolen & Orsi, 2015) demonstrated a shift in microbial community structure from Firmicutes, Acidobacteria, Actinobacteria and Proteobacteria dominant community to a Firmicutes, Bacteroidetes, and Euryarchaeota dominant community upon thaw. Permafrost thaw in their study was in parallel in increase in complex biopolymer degradation, translation and biogenesis transcripts, indicating a general increase in microbial activity (Coolen & Orsi, 2015).

Another, less likely, scenario to explain the microbial community shift between epochs is the effect of the relict extracellular DNA on our diversity analyses. In this scenario, relict preserved DNA released from dead cells differs between Holocene and Pleistocene samples and bias increases with relict DNA pool size (similar to (Carini *et al.*, 2016). Within the Pleistocene samples, 83% of the enumerated cells were non-viable and Holocene samples had ~8 fold higher viable cells (**Figure 3.1**). Hence, it is possible that relict DNA might be an important factor in epoch-based separation of Holocene and Pleistocene microbial community structure. However, this scenario seems unlikely for two reasons. First, (Burkert *et al.*, 2019) did not find a significant change in microbial community structure after removal of relict DNA preserved within Beringian permafrost. Second, (Lennon *et al.*, 2018) reported a minimal effect of relict DNA on estimates of microbial alpha diversity as long as the species abundance distribution of

the relict and intact DNA pools are equivalent. Hence, since our alpha diversity indices did not indicate any statistically significant variation between epochs (**Supplementary Table 3.3**), the species abundance distribution of the relict and intact DNA are likely equivalent. However, it is not possible to fully exclude this scenario.

3.5. Conclusion

Anthropocene warming in the western Arctic exceeds the dramatic warming associated with the Early Holocene thermal maximum, and arguably represents the warmest temperatures of the last ca. 14,000 years (Porter *et al.*, 2019). As a result fragile cold-adapted systems have been predicted to be near a threshold- similar to the Pleistocene-Holocene transition (Miller *et al.*, 2010). Similar changes observed in this study might occur in modern cold soils, which could alter ecosystem services with unknown consequences. The single core and six samples from this study only represent a snap shot of the effects of dramatic climate change on microbial population dynamics across the Pleistocene-Holocene transition at one location. Future investigations should focus on different types of permafrost-affected regions with different terrain types or different permafrost stratigraphy, both at microbial community and functional levels. It is yet to be seen if our findings are more generally representative of the microbial community dynamics across the Pleistocene-Holocene transition at a pan-Arctic scale. If our threshold hypothesis is supported by more regional studies in diverse settings, it may provide a framework for a better understanding of potential changes in important bacterial functional guilds, which could in turn improve climate models by predicting microbial responses in a warmer world.

Also, we noticed that bacteria entrapped in Pleistocene aged permafrost are distantly related to the known reference sequences, this suggest that the microbial members of the Eastern Beringian permafrost are mainly unknown. Future research demands to isolate these strains and study them at a phylogenetic and genome levels for possible biotechnological applications or for expanding our knowledge regarding bacterial evolution/succession over geologically meaningfully timescales.

3.6. Summary of chapter 3

Despite the presence of well-documented changes in vegetation and faunal communities at the Pleistocene-Holocene transition, it is unclear whether similar shifts occurred in soil microbes. Recent studies do not show a clear connection between soil parameters and community structure, suggesting permafrost microbiome-climate studies may be unreliable. However, the majority of the permafrost microbial ecological studies have been performed only in either Holocene- or Pleistocene-aged sediments and not on permafrost that formed across the dramatic ecosystem reorganization at the Pleistocene-Holocene transition. In this study, I used permafrost recovered in proximity to the Pleistocene-Holocene transition subsampled under strict sterile conditions developed for ancient DNA studies. My ordination analyses of microbial community composition based on 16S RNA genes and chemical composition of the soil samples resulted into two distinct clusters based on whether they were of late Pleistocene or Holocene age, while samples within an epoch were more similar than those across the boundary and did not result in age-based separation. Between epochs, there was a statistically significant correlation between changes in OTU composition and soil chemical properties, but only Ca and Mn were correlated

to OTU composition within Holocene aged samples; furthermore, no chemical parameters were correlated to OTU composition within Pleistocene aged samples. Thus, the results indicate that both soil chemical and microbial parameters are fairly stable until a threshold, driven by climate change in our study, is crossed, after which there is a shift to a new steady state. Modern anthropogenic climate change may lead to similar transitions in state for soil biogeochemical systems and microbial communities in Arctic regions.

Chapter 4

A major shift in activity and composition of methanotrophs in permafrost active layer soil in response to soil disturbance and temperature changes

Chapter 4 of this thesis is in preparation for publication. No specific journal has been selected yet. The potential title for the publication is going to be "Saidi-Mehrabad, A., Strilets, T., Forster, M., Froese, D., Lanoil, B. (2021. A major shift in activity and composition of methanotrophs in permafrost active layer soil in response to soil disturbance and temperature changes".

4.1. Introduction

Permafrost of the northern hemisphere contains a substantial quantity of sequestered organic carbon ranging from ~191 Pg (10^{15} g) to a depth of 30 cm, ~495 Pg to a depth of 100 cm, ~1024 Pg to a depth of 300 cm, and ~241-407 Pg beyond the depth of 300 cm (Jansson & Taş, 2014; Tarnocai *et al.*, 2009). Climate change is causing dramatic changes in permafrost-affected regions of the North, here defined as active layer soil and thawing underlying permafrost (Schuur *et al.*, 2008; Schuur *et al.*, 2015; Vonk *et al.*, 2015). Processes resulting in terrain changes of permafrost landscapes, such as hillslope/active layer detachment and slumping, wetland, and thaw pond formation are collectively known as thermokarst (Vonk *et al.*, 2015). Thermokarst formation may stimulate microbial decomposition and respiration of labile organic matter, by releasing the sequestered labile organic matter from thawing permafrost and allowing easy access to this mass wealth of nutrients, thus promoting carbon flux to the atmosphere and amplification of climate change (Coolen & Orsi, 2015; Coolen *et al.*, 2011; Deng *et al.*, 2015; Feng *et al.*, 2020; Mackelprang *et al.*, 2016). A metatranscriptomic based study of permafrost

obtained from a moist acidic tundra region in Arctic Alaska, demonstrated a major change in transcript sequences before and after thaw over a course of 11 days (Coolen & Orsi, 2015). Although the permafrost was frozen, a great majority of the transcripts were associated with survival strategies, whereases after thaw, enzymes involved in the decomposition of organic matter became dominant, demonstrating a rapid enzymatic response to permafrost thaw and the subsequent increase in organic matter in the surrounding environment (Coolen & Orsi, 2015). In addition, transcripts indicative of methanogenesis (acetate, methanol and methylamine utilization) and acetogenesis (could provide acetate to acetolactic methanogens) also became dominant after permafrost thaw, demonstrating a rapid response by methanogenic archaea and acetogenic bacteria to the permafrost thaw (Coolen & Orsi, 2015).

One major consequence of thermokarst development is the change in hydrology of the permafrost affected regions, which can induce anoxia in disturbed soils (Battin *et al.*, 2009; Vonk & Gustafsson, 2013). The endpoint of the microbial metabolism under anoxic conditions is CH_4 generated by methanogenic archaea (Wei *et al.*, 2018). CH_4 is a potent greenhouse gas with a heat-trapping potential 34 × higher per molecule than CO_2 on a time scale of 100 years (Stocker *et al.*, 2013b). Methanogenesis in Arctic soil has a strong positive linear relationship with temperature (Zheng *et al.*, 2018) and may account for 20-25% (15-50 Tg CH_4 yr^{-1}) (1 Tg = 10^{12} g) of global non-anthropogenic natural CH_4 emissions (Saunois *et al.*, 2016a).

Based on the widely used greenhouse gas trajectory model 8.5, (Representative Concentration Pathway 8.5), adopted by Intergovernmental Panel on Climate Change, ~ 30-99% of near-

surface permafrost will thaw and release ~ 37-174 Pg of carbon in response to a 10 ºC increase in Arctic atmospheric temperature expected by the year 2100 (Koven *et al.*, 2013; Schuur *et al.*, 2015). RCP 8.5 is considered as a very high baseline emission scenario in comparison to other RCP models (RCP 6 and RCP 4.5), which represents the 90th percentile of no climate change policy baseline scenario (Riahi *et al.*, 2011). This scenario predicts that in the absence of an effective climate change policy, greenhouse gas radiative forcing will reach ~8.5 W/m^2 at the end of the century (Riahi *et al.*, 2011). RCP 8.5 has been extensively used in carbon climate feedback modeling, literature and media. Although new scenarios have been recently introduced, for instance the Shared Socioeconomic Pathways, they haven't been fully integrated into the field of permafrost microbiology (Riahi *et al.*, 2017). Increased permafrost thaw could further amplify atmospheric CH_4 concentration due to increased methanogenic activity; however, as much as 20-60% of the CH_4 generated in CH_4 hotspots becomes oxidized to CO_2 before reaching the atmosphere (Singleton *et al.*, 2018). The sink for this permafrost-generated CH_4 is biological oxidation by aerobic CH_4 oxidizing (methanotrophic) bacteria (MOB) (He *et al.*, 2012a, 2012b; Khmelenina *et al.*, 2018; Singleton *et al.*, 2018; Zhang *et al.*, 2020a) and by anaerobic methanotrophic archaea (Cui *et al.*, 2015; Winkel *et al.*, 2019).

Aerobic MOB are a functional guild of microbes that utilize CH_4 as a source of both energy and carbon (Khmelenina *et al.*, 2018). While the Verrucomicrobia phylum includes a group of acidophilic aerobic methanotrophs (Dunfield *et al.*, 2007) and candidate phylum NC10 include a denitrifying methanotrophs (Ettwig *et al.*, 2010), the best characterized and most common MOB are affiliated with the phylum Proteobacteria (Khmelenina *et al.*, 2018). Proteobacterial MOB are broadly classified into two morphologically, physiologically, and phylogenetically distinct

groups: Type I (Gammaproteobacteria) and Type II (Alphaproteobacteria) (Khmelenina *et al.*, 2018). These groups differ in their optimal CH_4 concentrations, oxygen concentrations, pH, and temperature (He *et al.*, 2012a, 2012b; Khmelenina *et al.*, 2018; Mayr *et al.*, 2020a). Hence, changes in these parameters could directly affect the MOB community structure and CH_4 oxidation rates by selecting one type over another (Amaral *et al.*, 1995; Graham *et al.*, 1993).

In addition to their taxonomic classification, Proteobacterial MOB have been broadly divided into two major groups based on their affinity to CH_4 (a^0_s); low-affinity methanotrophs (LAM), which are unable to colonize in the presence of trace CH_4 at atmospheric level, and high-affinity methanotrophs (HAM), which are capable of growing in the presence of trace CH_4 at atmospheric levels (Tveit *et al.*, 2019). HAM are designated as aerobic upland soil clusters (USC), which are either phylogenetically affiliated with Gammaproteobacteria class (USCγ) or Alphaproteobacteria class (USCα) (Tveit *et al.*, 2019). HAM are less known than LAM; currently, there is only one cultivated HAM strain reported (MG08 affiliated to USCα (Tveit *et al.*, 2019)). HAM have been recently found in permafrost affected regions (Martineau *et al.*, 2014; Tveit *et al.*, 2019).

Oxidation of CH_4 as an energy source is only restricted to MOB and methane oxidizing archaea (Amaral *et al.*, 1995), hence, any type of disturbance that causes changes in the methanotrophic community structure could hamper methanotrophy and instead favor methanogenesis, turning an ecosystem into a major CH_4 source. Most studies examining methanotrophic response to disturbance have only considered single events and focused on methanotrophs from non-

cryogenic environments (Bissett *et al.*, 2012; Danilova *et al.*, 2015; Ho *et al.*, 2011; Ho *et al.*, 2016; Kumaresan *et al.*, 2011; Ogram *et al.*, 2006; Singh & Singh, 2013; Tiwari *et al.*, 2018). However, those studies that have investigated the temperature disturbance on methanotrophs demonstrated significant increases in CH_4 oxidation rates in response to increased temperature (e.g. (Börjesson *et al.*, 2004; Zeng *et al.*, 2019). The only comprehensive study regarding the methanotrophic community dynamics in permafrost affected regions, to our knowledge, indicates a significant change in methanotroph community structure and increasing CH_4 oxidation rates with increase rate of thaw (Singleton *et al.*, 2018). However, the combined effects of thermokarst development and increases in temperature on methanotrophs and the entire microbial community structure inhabiting the permafrost affected regions are not known. The frequency of both thermokarst formation and warmer temperatures, which are interconnected, are expected to increase in the future (Coolen & Orsi, 2015; Deng *et al.*, 2015; Koven *et al.*, 2013; Schuur *et al.*, 2015). The capacity of methanotrophs in preventing a large concentration of CH_4 from entering the atmosphere from thawed permafrost is not considered in most permafrost climate feedback models. This gap of knowledge has recently been shown to cause an overestimation of 5-10 Tg yr^{-1} of CH_4 emission in widely used atmospheric CH_4 models (McCalley, 2020; Oh *et al.*, 2020). A recently developed biogeochemical model indicates that HAM methanotrophic activity will increase in parallel with methanogenesis in a warmer world, leading to a net increase of only 18% in CH_4 emissions from thawing permafrost regions (Oh *et al.*, 2020). This discrepancy between CH_4 climate models reflects uncertainty regarding the methanotrophic capacity of the rapidly changing Arctic regions (McCalley, 2020; Oh *et al.*, 2020).

The objectives of this study were to investigate: **1)** methanotrophic and whole bacterial community structure shifts in response to active layer soil disturbance and temperature, **2)** changes in CH_4 oxidizing capacity in response to the active layer soil disturbance and temperature, and **3)** the relationship between CH_4 oxidizing capacity and community structure in permafrost affected soils. To achieve our objectives, we used anthropogenically disturbed active layer samples as an analog to a climate change-induced thermokarst formation.

The geographical settings (see below) of the study site including the potential changes in microbial community structure and changes in soil chemistry with increased thaw was previously characterized (unpublished results). Although the sampling site was not created due to climate change, however, it had all the characteristics of a natural themokarst formation (**Supplementary Figure 4.1 a, b**). Both natural disturbances of the active layer caused by climate change or anthropogenic activities such as road building or surface mining could result in major terrain changes of permafrost landscapes and can ultimately lead to thermokarst formation. For example, human mining activities, especially open-pit mining in permafrost affected regions, can greatly promote permafrost thaw and active layer disturbance over the long term (Booshehrian *et al.*, 2020). The overall goal of our study was to improve our understanding of CH_4 dynamics in a warmer world.

4.2. Material and methods

4.2.1. Sampling location

The samples were obtained from an active placer mining site near Dominion Creek, Yukon, Canada. The regional setting of our study site has been described previously (Froese *et al.*, 2000b). At this site, ~ 35 cm of the thawed layer soil from the surface to the permafrost table was removed (bulldozed) and there were signs of permafrost thaw **(Supplementary Figure 4.1 A, B)**. While drilling, we were cautious not to introduce any soil material or water from the surface layer into the boreholes. In May 2018, active layer soil samples from inside of two boreholes (termed DC 7 and DC 8 in this manuscript), ~26 cm apart from each other, were collected from a disturbed site (N63.712285°, W138.547704°) **(Supplementary Figure 4.1 A, B)**. DC7 and DC 8 were ~126 cm from a 61 cm deep thaw pond (thermokarst pond) **(Supplementary Figure 4.1 A, B)**. Another set of samples from inside of two other boreholes (termed DC5 and DC6 in this manuscript), ~15 cm apart from each other, were collected from a site with no signs of disturbance that contained intact surface vegetation with sphagnum moss and variety of lichens (N63.712331°, W138.547767°). The depth of the thaw layer at time of sampling (May 2018) was ~21 cm **(Supplementary Figure 4.1 A, B)**.

Undisturbed (DC5 and DC6) and disturbed (DC7 and DC8) active layer samples were aseptically collected using 50 ml conical centrifuge tubes by pressing the tubes into the interior walls of ~150 cm deep boreholes created after drilling. Approximately 5 bags per boreholes were collected. The reason for collecting soil samples from the interior walls of the boreholes was to obtain clean and untrampled soil samples.

In addition to peat samples, ~8 L of thermokarst water was collected from 0-10 cm of the thaw pond for making soil slurries to measure methanotrophic activity (see below). Prior to water sampling, sterilized 4 L polycarbonate containers were rinsed several times with the water from the thaw pond. Soil samples in 500 mL Whirl-Pak bags (Nasco, USA) and water samples were stored with ice packs and frozen permafrost core segments in coolers for shipping. Upon arrival at the University of Alberta, some were immediately transferred to a 4 ^{o}C cold room (for subsequent activity measurements) and some were transferred to -80 ^{o}C freezer (for subsequent DNA experiments). Samples were prepared for analysis less than 24 hours after arrival.

4.2.2. Soil edaphic parameters

Basic soil chemical parameters including pH, total organic matter (OM), and gravimetric water content (GW) were measured as described in **chapter 2**. These soil chemical parameters are the main abiotic factors influencing CH_4 dynamics in Arctic soils (Hodgkins *et al.*, 2014; Pokrovsky *et al.*, 2011; Vonk *et al.*, 2015; Zhang *et al.*, 2020b).

4.2.3. Sample preparations for CH_4 gas flux measurements and DNA-SIP

Prior to subsampling from each bag of soil sample, the content of the bag was homogenized by thorough mixing. Thaw pond water was filter-sterilized with gamma-irradiated 0.25 μm PVDF filters (Pall Life Sciences, USA) and autoclaved 3 times with 1-2 h of cooling intervals. A total of 10 g of each soil type (wet weight) was weighed from multiple bags after mixing (n=5,

selected randomly), placed in 125 ml autoclaved Wheaton bottles, and mixed with 10 ml of sterilized thermokarst water to create slurries. Bottles were prepared in triplicate for each of five incubation temperatures (see below). Each microcosm was either given a 9-13% headspace injection of 99% pure $^{12}CH_4$ (vol/vol in the air) or 5-12% headspace injection of 99 atom % $^{13}CH_4$ (vol/vol; Sigma-Aldrich Canada). Microcosms were incubated at 22 °C, 4 °C, 0 °C, -10 °C and -20 °C. These temperatures were in a range above and below the average daily high temperatures recorded in our sampling region. The warmest season of the year in our sampling site is from May 10 to September 7, with an average daily temperature of 13.8 ºC and the coldest season is from November 8 to February 29, with an average daily temperature of -11.1 ºC (Average Weather at Dawson City Airport Canada). The 22 °C, 4 °C, and 0 °C microcosms were shaken at 170 r.p.m. The -10 °C and -20 °C microcosms were not shaken as the bottles were frozen. To maintain a constant temperature of 0 °C, a water bath with a shaker was placed in a 4 °C cold room and was filled with a mixture of crushed ice and cold water. The ice content and temperature were monitored daily. Triplicate autoclaved killed slurries and triplicate blank leakage controls were prepared for each temperature with either ^{12}C or ^{13}C methane in the headspace at the same concentrations as the experimental incubations.

4.2.4. CH_4 consumption measurements

The headspace residual CH_4 in microcosms was monitored by injecting 50 µl of headspace gas into a Hewlett Packard 5890 Series II gas chromatograph (Agilent Technologies, USA), equipped with a thermal conductivity detector (TCD) (set at 180 ºC for the detector, and 180 ºC for the injector), and an 8″1/8″stainless steel HayeSep D metal packed column with a 100/120

Mesh size (125-150 Micron, oven set at 90 ºC) (Chromatographic Specialties, Canada). Helium was used as a carrier gas with a constant flow rate of 30 ml/min. Headspace CH_4 concentrations were measured daily for samples incubated above 0 ºC, and initially every 5 days for samples incubated at 0 °C, -10 °C, and -20 °C. However, after two months no signs of CH_4 oxidation in samples incubated at sub-zero temperatures were observed; thenceforth, the headspace CH_4 was monitored monthly. After 155 days of incubation, no methanotrophic activity was observed in the sub-zero incubations; hence, they were removed from downstream analyses. The CH_4 oxidation rates in the 0 °C, 4 °C, and 22 °C incubations were calculated by linear regression of CH_4 mixing ratios in the bottle headspaces. When the residual CH_4 concentration in microcosms reached ~1%, the experiment was stopped and DNA was extracted (10 g of soil) (see **Appendix 3**) and used to characterize microbial community composition in downstream molecular analyses.

4.2.5. DNA extraction and *pmoA* and *mmoX* gene-based PCR

All DNA extraction steps were performed under strict sterile conditions designed for permafrost microbiology and ancient DNA analysis as described in **chapter 2**. For PCR-based screening of the samples, the DNA was extracted with a modified DNeasy PowerSoil kit protocol (Qiagen Canada) from 1 g of each active layer soil sample after homogenization. The modified DNA extraction protocol, the protocols used for PCR, and the thermocycling steps are available in the **Appendix 3**.

Prior to CH_4 oxidation activity measurements or DNASIP, the presence of methanotrophic bacteria was assessed via PCR amplification of *pmoA* and *mmoX* genes. The *pmoA* gene, which encodes for the alpha subunit of the particulate methane monooxygenase (pMMO) enzyme (which is universal in aerobic methanotrophs except for genera *Methylocella* and *Methyloferula*) and *mmoX* gene (which encodes for the alpha subunit of the soluble methane monooxygenase (sMMO)) enzyme are routinely used for screening for aerobic methanotrophs in culture-independent approaches (Bourne *et al.*, 2001; Dedysh *et al.*, 2000; McDonald *et al.*, 2008; Vorobev *et al.*, 2011).

After detecting PCR products in samples, DNA from 10 g of each soil type stored at -80 ^{o}C were extracted with the same protocol mentioned above and was used as a time zero control.

4.2.6. DNA-SIP

All reagents used in the SIP procedure were prepared as described previously (Neufeld *et al.*, 2007), with the only exception that the average density of the stock CsCl gradient was set to 1.76 g/ml. After samples demonstrated ~5% consumption of headspace ^{13}C methane, microcosms were sacrificed and 10 g of soil was used for DNA extraction with a modified DNeasy PowerSoil kit protocol (Qiagen Canada) (see **Appendix 3**). With each SIP run, tubes of *Methylomicrobium album* BG8 (strain ACM 3308) DNA, mixed from cultures grown under ^{13}C and ^{12}C methane atmospheres, were included as a positive control for assuring gradient formation (**Supplementary Figure 4.2**). Each sample produced in 13 fractions with ~500 µl of the mixture of CsCl/DNA/GB. The DNA was purified from each fraction as previously described (Neufeld *et al.*, 2007), with the only exception that polyethylene glycol 8000 (PEG 8000) was utilized

instead of PEG 6000. The DNA concentration was measured with a Qubit dsDNA HS Assay Kit according to the manufacturer's protocol (Thermofisher Scientific, Canada).

4.2.7. Sequencing and ASV construction

Genomic DNA samples (incubated under $^{12}CH_4$ or $^{13}CH_4$ atmosphere), SIP fractions, a lab constructed mock community (15 strains) (**Supplementary Figure 4.3**), and a series of DNA extraction kit negative controls (n = 4) (**Supplementary Table 4.1**) were sequenced as described in **chapter 3**. 16S rRNA genes were targeted with the aid of the Earth microbiome primers (515F and 806R (Caporaso *et al.*, 2011)) in our sequencing approach since known *pmoA* genes primers are unable to detect some methanotrophic strains such as *Crenothrix, Methylacidiphilum, Methylocella, Methyloferula*, and Ca. *Methylomirabilis oxyfera* (Dedysh *et al.*, 2000; Kip *et al.*, 2011; Luesken *et al.*, 2011; Vorobev *et al.*, 2011).

Amplicon Sequence Variants (ASVs) from the sequences were resolved with the aid of the DADA2 pipeline (version 3.10) in the R studio environment (version 3.6.3) following the default parameters (Callahan *et al.*, 2016). The reason for selecting ASVs instead of OTUs is to improve the taxonomic resolution of our work and allow the study of distinct ecological attributes of MOB between disturbed and undisturbed samples (Callahan *et al.*, 2017). Also, ASV construction is consistent across different datasets, allowing accurate comparison between disturbed and undisturbed data (see below)) (Callahan *et al.*, 2017). In general, ASVs allow us to

gain high-resolution insights into the low-resolution 16S rRNA gene marker used in this study and help address our questions asked above.

The DADA 2 pipeline was selected to construct ASVs because it tends to find more ASVs from the soil in comparison to two other widely used ASV constructing pipelines of UNOISE (Edgar, 2016b) and Deblur (Amir *et al.*, 2017; Nearing *et al.*, 2018). As such, DADA 2 has been recommended for studies that are investigating rare species (e.g. MOB) (Nearing *et al.*, 2018).

At the truncation step, position 240 bp was selected from the forward sequence reads and position 200 bp from the reverse sequence reads, which resulted in the removal of 10 nucleotides from the forward sequences and 50 nucleotides from the reverse sequences. These cut off positions were determined based on the frequency of the quality score at each base position. In the filtering step, no "Ns" were allowed, and the maximum number of expected errors allowed (maxEE) was set to 2 and 5 for forwards and reverse reads, respectively.

105 Mb in 437,681 reads from 13 samples were used to determine the error rate in the forward sequences and 102 Mb in 510,533 reads from 15 samples were used to determine the error rate in the reverse sequences. From the 64 samples, 5661 ASVs were created, of which the majority (92%; 5210 ASVs) were 253 bp in length. 95% of the sequences passed the chimera filtering parameter, resulting in 4920 ASVs. ASVs were assigned to taxonomy via naïve Bayesian classification (Wang *et al.*, 2007) using a Silva trained database (Silva version 132) formatted for the DADA2 pipeline (https://zenodo.org/record/1172783#.Xrt9K2hKhBw). The minimum bootstrap was set to 70%. In addition to the Silva database, the taxonomic identity of the ASVs was checked with the NCBI database (standard nucleotide collection nt/nr) via the basic local

alignment search tool (BLAST) (Altschul *et al.*, 1990). Any BLAST results > 97% identity in 16 rRNA genes to the reference sequences were labeled to the species level (STACKEBRANDT & GOEBEL, 1994); sequences with < 97% sequence identity to reference sequences were labeled "Like" after the species name. Sequences related to Archaea (see **chapter 3**), chloroplasts, mitochondria, and Eukarya (all together referred to as anomalous sequences) were removed from the dataset. Removal of anomalous sequence resulted in a final set of 4822 ASVs (97.78% of ASVs were retained from the original number of the ASVs generated by the DADA2 pipeline) in all samples. Sequences processed in this manuscript are available in NCBI Sequence Read Archive under the ascension number of PRJNA655978, and BioSample accession numbers of SAMN15763028 (DC5 and DC6 samples), and SAMN15763027 (DC7 and DC8 samples).

4.2.8. Community analysis

Unless otherwise noted, all statistical analyses were performed in R studio environment (version 3.6.3). The generated ASV table from DADA2 pipeline was divided into two sets: the overall community, which was not subjected to ultracentrifugation, and the SIP samples (here referred to as the SIP dataset). The overall community was further divided into two separate ASV tables: known methanotrophs only (here referred to as the methanotroph dataset) and the overall community (here referred to as the complete dataset). The overall community includes all ASVs from the non-SIP samples, including the methanotroph ASVs in the methanotroph dataset. The overall community included 2450 ASVs and the methanotroph dataset included 67 ASVs. The remaining ASVs (2305) were related to the SIP dataset. Only abundance analysis was performed on the SIP dataset to demonstrate how changes in temperature and soil disturbance affect the

abundance of the active methanotrophic communities. Also, the SIP dataset only represents the microbial community members that are actively involved in the consumption of the $^{13}CH_4$ as a result this community does not represent the entire community structure to perform diversity analyses. For assessing changes in the relative abundance of active methanotrophs between the SIP dataset and complete dataset, the ASV tables were rarefied to the lowest read count (13,740) based on a random subsampling approach implemented in Mothur (version 1.39.5) (Schloss *et al.*, 2009). To assess the probability value (p-value), a zero-inflated negative binomial regression model was employed (Mwalili *et al.*, 2008). This analysis was performed with the aid of the package pscl (version 1.5.5) (Zeileis *et al.*, 2008). For assessing the abundance of active methanotrophs in the heaviest fractions within each sample, non-rarefied/non-normalized SIP ASVs were used to prevent data waste (McMurdie & Holmes, 2014).

The soil chemical parameters were $\log_{10}(x + 1)$ transformed and used as a variable matrix in the phyloseq object file created by the phyloseq package (version 1.30) (McMurdie & Holmes, 2013). Two separate phyloseq objects were created for the methanotroph dataset and the complete dataset respectively. For alpha diversity (observed ASVs, Shannon Index, Fisher's alpha, and Simpson evenness), the raw reads without rarefaction or normalization were used in phyloseq according to prior recommendation (McMurdie & Holmes, 2014). Venn diagrams were generated from the ASV tables to study the shared or unique ASVs based on the number of observed ASVs with the aid of the Mothur's (version 1.39.5) "venn" function.

For beta diversity, the ASV tables were normalized based on the DESeq2 method by using a variance stabilizing transformation algorithm in R studio (version 3.6.3) (Love *et al.*, 2014). The generated negative values were converted to zero in R studio (version 3.6.3) to allow analysis based on the Bray Curtis dissimilarity matrix (Faith *et al.*, 1987). Bray Curtis dissimilarity matrix was calculated for assessing potential differences in the ASV structure of the methanotroph dataset or the complete dataset between disturbed and undisturbed active layer soil samples with the aid of the vegan package (version 2.5.6) (Oksanen *et al.*, 2007). The results were visualized in non-metric multidimensional scaling (NMDS) biplots (Cox & Cox, 2008) constructed with the vegan package (version 2.5.6). To assess the clustering of the samples based on temperature alone, an unsupervised hierarchical cluster analysis was performed with the aid of the package "stats" (version 3.6.3) on disturbed and undisturbed samples individually. The distance matrix used was Manhattan (Faith *et al.*, 1987) and the clustering was performed with the ward.d2 (minimum variance method) algorithm (Murtagh & Legendre, 2014). The optimal number of clusters was determined based on the "elbow method" and gap statistic (Tibshirani *et al.*, 2001) implemented in the factoextra package (version 1.07) (Kassambara, 2017). The hierarchical trees were cut based on the determined cluster numbers with the cut tree function of the factoextra package (version 1.07).

Prior to relative abundance analysis, the ASV reads from both datasets were rarefied to the lowest read counts per sample via the Mothur's (version 1.39.5) random subsampling function. The lowest read counts per sample were 18,694 and 1468 for the complete and methanotroph datasets, respectively. To assess which taxa were significantly differentially abundant in disturbed and undisturbed soil types, the DESeq2 differential abundance method with $p < 0.01$

using the Benjamini-Hochberg algorithm for controlling the false discovery rate was employed (implemented in Phyloseq 1.30) on the non-rarefied ASV tables. For assessing the probability value of changes in the abundance of the most dominant phyla between different temperatures within each soil type, a zero-inflated negative binomial regression model was used based on the criteria mentioned above.

The influence of each soil parameter on the methanotroph dataset and the complete dataset, including the effect of soil disturbance, was investigated with the "many linear model" function of the mvabund package (version 4.0.1) (Wang *et al.*, 2012) by using the Gaussian distribution (Warton *et al.*, 2012) for analysis and Wald's test for statistical significance of this approach (Warton *et al.*, 2012).

4.3. Results

4.3.1. Effect of active layer disturbance and temperature on CH_4 oxidation rates

Soils incubated at 22 ^{o}C showed the highest CH_4 oxidation rates irrespective of soil type. CH_4 oxidation rates demonstrated a strong positive linear relationship with temperature in both disturbed (R^2=0.99) and undisturbed (R^2=0.99) active layer soils (**Figure 4.1**). Disturbed samples demonstrated a stronger response in CH_4 oxidation rate to shifts in temperature than undisturbed samples (**Figure 4.1**).

Incubation at 4 ^{o}C resulted in 63.5% and 73.8% decrease in oxidation rates ($p < 0.01$) in the composite undisturbed and disturbed samples, respectively, relative to the 22 ^{o}C incubation

(**Supplementary Figure 4.4 A, B**; **Supplementary Table 4.2**). Further decrease in oxidation rates was observed when comparing 22 ºC to 0 ºC incubations ($p < 0.01$). The 0 ºC incubation was 86.6% and 92.1% lower in composite undisturbed and disturbed samples, respectively (**Supplementary Figure 4.4 A, C**; **Supplementary Table 4.2**). Samples also demonstrated statistically significant decrease in oxidation rates ($p < 0.01$) between 4 ºC to 0 ºC incubations, which resulted in 63.2% and 69.8% decrease in composite undisturbed and disturbed samples respectively (**Supplementary Figure 4.4 A, C**; **Supplementary Table 4.2**).

Disturbed samples showed 55.5% and 37.8% higher CH_4 oxidation rates ($p < 0.01$) in 22 ºC and 4 ºC samples, respectively, than the undisturbed samples (**Supplementary Figure 4.4 A, B**; **Supplementary Table 4.2**). However, there was no significant change in oxidation rates at 0 ºC between disturbed and undisturbed samples (**Supplementary Figure 4.4 C**; **Supplementary Table 4.2**).

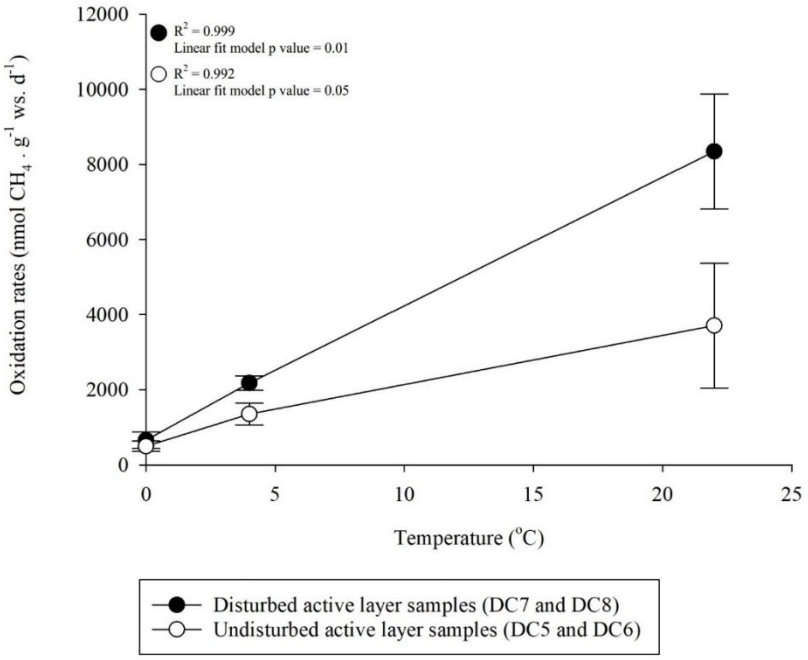

Figure 4.1. Linear relationship between CH_4 oxidation rates and temperature.

4.3.2. The influence of disturbance and temperature on active layer community composition

Simpson evenness was the only measured alpha diversity index that was statistically significantly different between disturbed and undisturbed samples in the complete dataset ($p < 0.01$) (**Supplementary Table 4.3**). No differences were observed in any other alpha diversity metrics at any temperature or between disturbed and undisturbed samples in complete and methanotroph datasets (**Supplementary Figure 4.5 A, B**). Disturbed and undisturbed time zero samples with

no incubation at different temperatures did not demonstrate any significant changes in any alpha diversity index, including Simpson Evenness (**Supplementary Figure 4.5 C**).

For the complete dataset, the microbial communities of the undisturbed samples were clearly different from the disturbed samples, irrespective of the incubation temperature (**Figure 4.2 A**). ASVs associated with samples incubated at 4 ^{o}C and 0 ^{o}C were more similar to each other than ASV samples incubated at 22 ^{o}C, irrespective of the soil type (**Figure 4.2 A**, **Supplementary Figure 4.6 A**, **B** and **Supplementary Figure 4.7 A** and **B**). Bacterial communities were primarily clustered based on disturbance, with secondary structuring based on incubation temperature, indicating that disturbance is a more potent driver of microbial community structure than temperature. The separation of the time zero control samples into disturbed and undisturbed clusters demonstrates that this effect was present prior to and was not an artifact of laboratory incubations (**Supplementary Figure 4.8 A-C**). The duplicate disturbed samples were indistinguishable from each other; however, the duplicate undisturbed samples were clearly distinguishable (**Supplementary Figure 4.8 A-C**).

Similar to the complete bacterial community, the methanotroph communities also were more strongly influenced by disturbance than temperature (**Figure 4.2 B**). Within soil type samples incubated at the same temperature were more similar but between soil type they were drastically dissimilar (**Figure 4.2 B, Supplementary Figure 4.9 A, B, Supplementary Figure 4.10 A, B**).

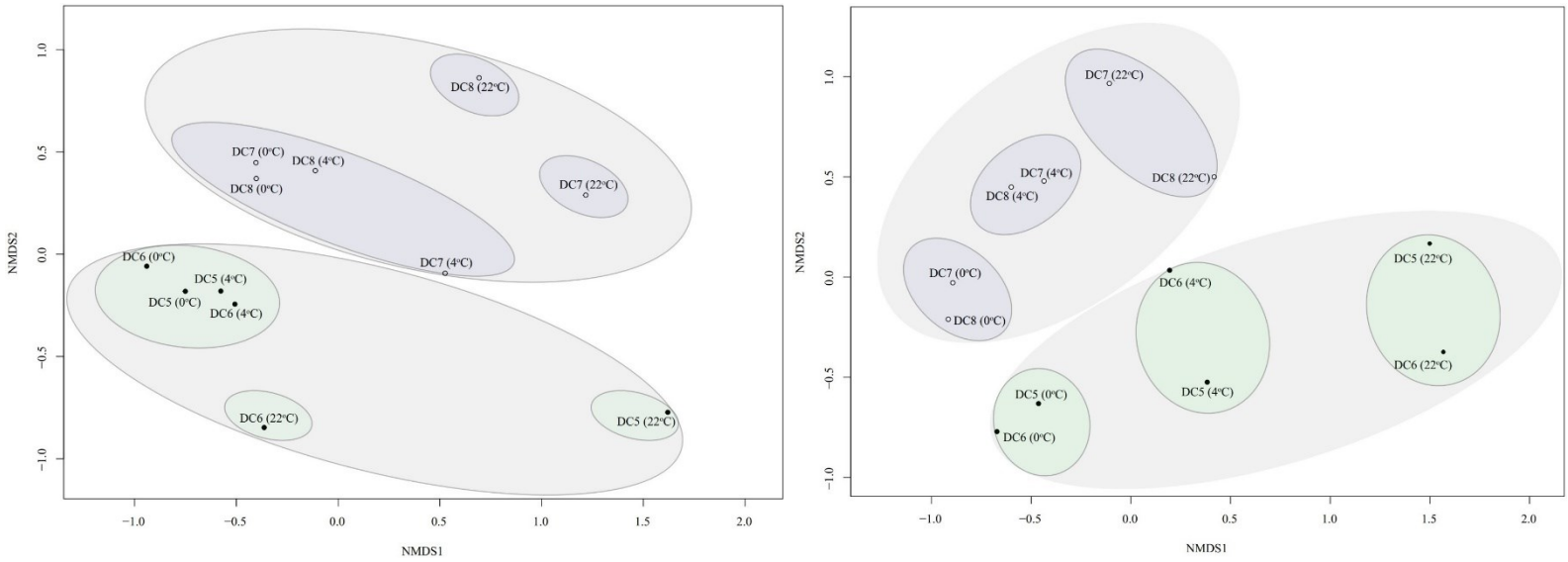

A **B**

Figure 4.2. Non-metric Multidimensional Scaling (NMDS) biplot of (A) the entire dataset and (B) methanotroph dataset. Filled black circles represent undisturbed active layer samples (DC5 and DC6) and open circles represent disturbed samples (DC7 and DC8). Values in parentheses represent the incubated temperatures. The large gray ovals separate the undisturbed (DC5 and DC6) samples (open circles) from disturbed (DC7 and DC8) samples (filled circles) based on Bray-Curtis dissimilarity matrix. Small light green and dark purple clusters separate the samples based on the incubated temperatures. Clusters were designed based on hierarchical trees (see the main text and **Supplementary Figures 4.6 A, B; 4.7 A, B; 4.9 A, B, and 4.10 A, B**).

All active layer soil samples of DC5, DC6, DC7, and DC8 resulted in the amplification of the *pmoA* gene (data not shown). However, none of the samples had PCR amplifiable *mmoX* genes (data not shown). Some methanotrophic ASVs were found only in either the disturbed soils or undisturbed soils, despite incubation at the same temperature and conditions (**Supplementary Figures 4.11 A-C**). Hence, we examined the taxa underlying the observed differences between disturbed and undisturbed samples.

In the complete dataset, 8 phyla (Proteobacteria, Firmicutes, Bacteroidetes, Verrucomicrobia, Actinobacteria, Acidobacteria, Chloroflexi, and Patescibacteria) and 69 genera had significantly different abundance ($p < 0.01$) between soil types (**Supplementary Figures 4.12 A**). The Proteobacteria and Bacteroidetes were the most dominant phyla in composite undisturbed samples and were significantly different in abundance from 0 ºC to 22 ºC, 4 ºC to 22 ºC, and 0 ºC to 4 ºC ($p < 0.01$) (**Supplementary Figures 4.13 A**). The Proteobacteria and Bacteroidetes showed 21.2% and 23.9% reduction in abundance, respectively, from 0 ºC to 22 ºC ($p < 0.01$). Similarly from 4 ºC to 22 ºC phyla Proteobacteria and Bacteroidetes demonstrated a significant decrease in abundance with 2.4% and 37.3% reduction, respectively ($p < 0.01$). However, only Proteobacteria demonstrated a statistically significant decrease in abundance from 0 ºC to 4 ºC with a 19.2% reduction in abundance ($p < 0.01$) (**Supplementary Figures 4.13 A**). In the disturbed samples, Bacteroidetes and Proteobacteria were the most dominant phyla, and their abundance significantly changed from 0 ºC to 22 ºC and from 0 ºC to 4 ºC ($p < 0.01$) (**Supplementary Figures 4.13 B**). However, in contrast to the undisturbed samples, Proteobacteria showed 13.3% increase in abundance from 0 ºC to 22 ºC ($p < 0.01$), while Bacteroidetes showed 26.4% reduction in abundance from 0 ºC to 22 ºC ($p < 0.01$)

(**Supplementary Figures 4.13 B**). From 4 ºC to 22 ºC, only Bacteroidetes showed a significant reduction in abundance (18.72%) ($p < 0.01$). From 0 ºC to 4 ºC, phylum Proteobacteria showed 8.5% increase, while the Bacteroidetes showed 9.4% decrease in abundance ($p < 0.01$) (**Supplementary Figures 4.13 B**).

All ASVs in the methanotroph dataset were associated with Proteobacteria (**Supplementary Figures 4.12 B**) and 11 species were significantly differentially abundant between disturbed and undisturbed soils (**Supplementary Figures 4.12 B**). Gammaproteobacteria (Type I) was the most dominant class at all three incubated temperatures for both disturbed and undisturbed samples (**Supplementary Figures 4.14 A, B**). In the undisturbed samples, Gammaproteobacteria formed 99.3% of the methanotrophs in the 0 ºC incubated; 99.3% of the methanotrophs in the 4 ºC incubated, and 83.6% of methanotrophs in the 22 ºC incubated samples (**Supplementary Figures 4.14 A**). Alphaproteobacteria (Type II) formed 0.61% of the 0 ºC; 0.61% of 4 ºC, and 16.4% of 22 ºC of the methanotroph sequences in undisturbed samples (**Supplementary Figures 4.14 B**). In disturbed samples, Gammaproteobacteria formed 98.2% of the 0 ºC; 98.5% of the 4 ºC, and 96.5% of the 22 ºC of the methanotroph ASVs (**Supplementary Figures 4.14 B**). Alphaproteobacteria formed 1.7% of the 0 ºC; 1.4% of the 4 ºC, and 3.4% of the 22 ºC methanotrophic sequences in disturbed samples (**Supplementary Figures 4.14 B**).

Within the methanotroph dataset, *Methylobacter* (64.5%) was the most dominant methanotrophic species in the undisturbed samples, forming 98.6% of the 0 ºC; 79.3% of the 4 ºC, and 53% of the 22 ºC incubated sequences (**Supplementary Figures 4.15 A**). No statistically significant

shift in abundance of the genus *Methylobacter* was observed from 0 ºC to 22 ºC samples. In the disturbed samples, *Methylobacter* was the most dominant methanotroph in 0 ºC and 4 ºC samples, forming 93.1% and 47.7% of the methanotrophic sequences, while in 22 ºC samples, *Methylovulum* formed 55.5% of the methanotrophic sequences and *Methylobacter* formed 20.1% of the methanotrophic sequences in 22 ºC samples (**Supplementary Figure 4.15 B**). The lower relative abundance of genus *Methylobacter* was significant between 0 ºC and 22 ºC (40.4%) ($p < 0.05$) and 4 ºC and 22 ºC (57.8%) ($p < 0.01$) samples (**Supplementary Figure 4.15 B**). There was no significant change in the abundance of *Methylobacter* between 0 ºC and 4 ºC samples. *Methylovulum* was significantly more abundant ($p < 0.05$) in 22 ºC than in 0 ºC samples, while there was no significant difference in abundance between 4 ºC and 22 ºC. However, there was a significant difference in the abundance of genus *Methylovulum* between 0 ºC and 4 ºC ($p < 0.01$) (**Supplementary Figure 4.15 B**).

4.3.3. DNA-SIP

Although the methanotroph dataset indicated a dominance of Gammaproteobacteria, in our samples, it is not clear that these known methanotrophs are the main active consumers of CH_4 in our system. Therefore, we performed stable isotope probing (SIP) to determine the identity of the primary CH_4 consumers. All of the dominant active methanotrophs in our $^{13}CH_4$ incubations were associated with the Proteobacterial Type I group; those associated with Type II methanotrophs were less than 1% of the ASVs (**Supplementary Figure 4.16 A-F**).

Our composite heavy fractions demonstrated some level of cross-feeding irrespective of the soil type or incubation temperature (**Supplementary Figure 4.16 A-F**). The main species that is not

a known methanotroph was *Methylotenera*, whose nearest relatives are methylotrophs (i.e. use methyl groups, but not CH_4). *Methylotenera* formed 18% and 20% of the 0 ºC; 14% and 15% of the 4 ºC; 0.01% and 5% of the 22 ºC ASVs in composite heavy fractions of the undisturbed and disturbed samples, respectively. This genus decreased 22% from 0 ºC to 4 ºC; 99% from 0 ºC to 22 ºC, and 99% from 4 ºC to 22 ºC in composite heavy fractions of the undisturbed samples. In composite heavy fractions of the disturbed samples, *Methylotenera* decreased 25% from 0 ºC to 4 ºC; 71% from 0 ºC to 22 ºC, and 61% from 4 ºC to 22 ºC. However, due to a major zero inflation effect (presence of a large number of zeros in the data), we were unable to estimate the p-value of the differences in the relative abundance of genus *Methylotenera* between soil type and temperatures. The presence of a large number of zeros in the ASV table could be due to either technological limitation of current sequencing platforms or pipelines in detecting microbial strains with low frequency (rare biosphere) (also known as the technical zero). Alternatively, some strains may actually be absent in the samples used for sequencing (known as the sampling zero) (Warton, 2005; Xu *et al.*, 2015). Zero inflation could lead to type I error inflation and smaller standard error by affecting the statistical methods of choice (Brill *et al.*, 2019; Warton *et al.*, 2012). Hence, it could increase the chance of false-positive findings.

Despite isolates being unable to utilize CH_4, *Methylotenera* seems to be commonly labeled in SIP experiments along with methanotrophs (He *et al.*, 2012b; Oshkin *et al.*, 2015). However, irrespective of temperature or soil type, methanotrophic ASVs were the most dominant in the isotopically labeled DNA, demonstrating that the cross labeling did not affect our effort to distinguish the active methanotrophs. Active known methanotrophs together formed 80.2% of the ASVs (81.6% including the potential active methanotrophs with the suffix “like”) in

undisturbed and 35.7% of the ASVs (40.9% including the potential active methanotrophs) in disturbed samples (**Supplementary Figure 4.16 A-F**). The statistical analysis of the abundance of dominant active methanotrophs between the SIP dataset and the complete dataset are presented in **the supporting materials**.

In composite undisturbed samples, the most dominant active methanotroph at 0 ºC was *Methylobacter* (63.6%); at 4 ºC *Methylosoma* (33%); and at 22 ºC *Methylomicrobium* (99%) (**Figure 4.3 A-C**). *Methylobacter* showed 57% decrease in relative abundance from 0 ºC to 4 ºC; 99% decrease from 0 ºC to 22 ºC, and 99% decrease from 4 ºC to 22 ºC. *Methylosoma* increased 95% in relative abundance from 0 ºC to 4 ºC and was absent in 22 ºC samples. *Methylomicrobium* increased 68% in relative abundance from 0 ºC to 4 ºC; 97% from 0 ºC to 22 ºC, and 66% from 4 ºC to 22 ºC (**Figure 4.3 A-C**).

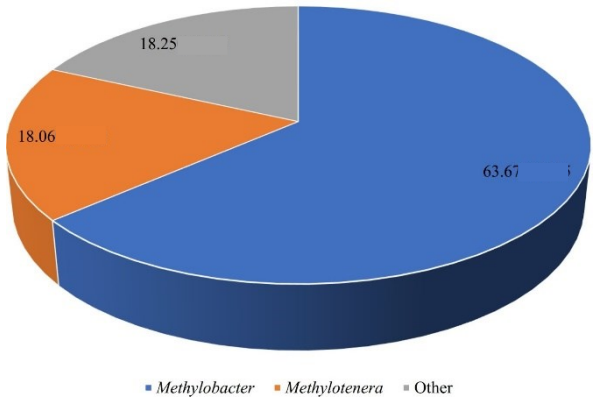

A

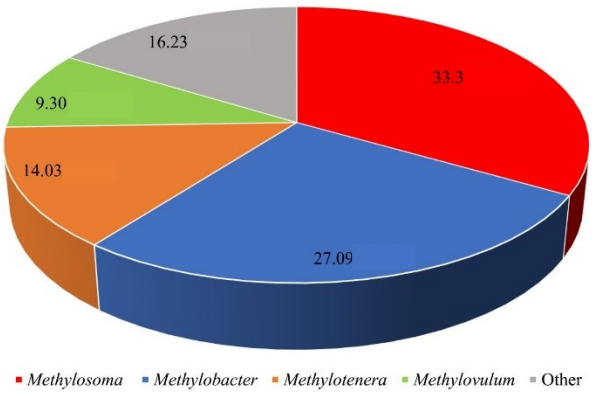

B

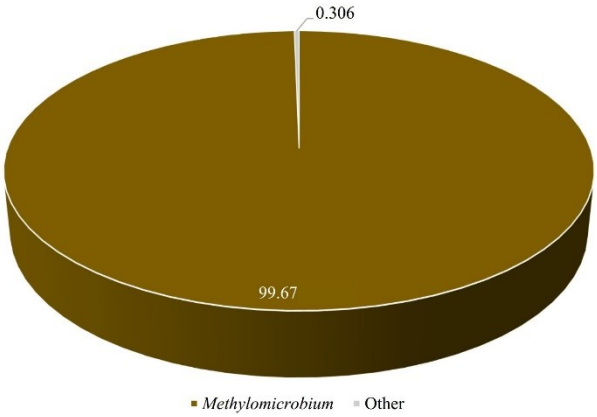

C

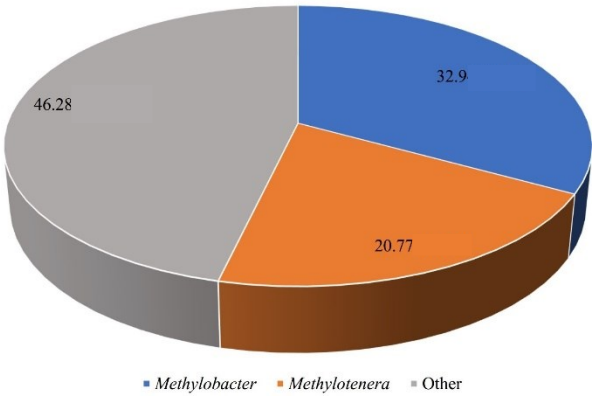

D

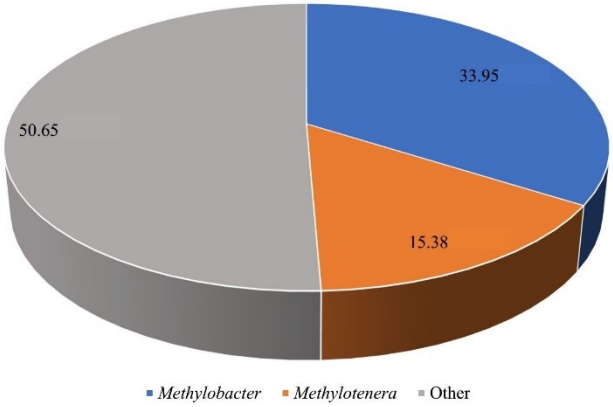

E

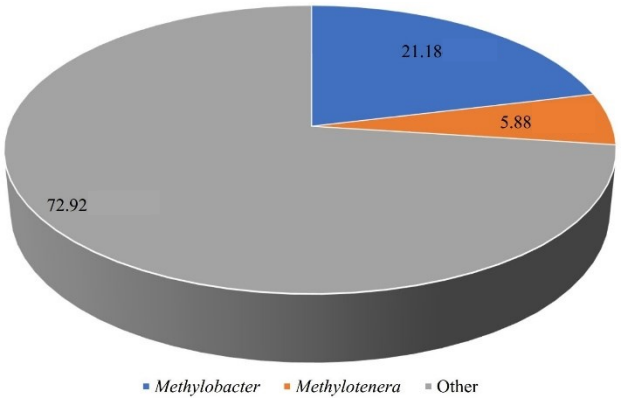

F

Figure 4.3. The relative abundance of active strains detected in the heaviest ^{13}C fractions of the composite undisturbed (DC5 and DC6) (A-C) and composite disturbed (DC7 and DC8) (D-F) samples incubated at 0 ºC (A and D), 4 ºC (B and E) and 22 ºC (C and F). The pie charts only represent the top two ASVs with the highest percent relative abundance, the rest are grouped in "Other".

In the composite disturbed samples, *Methylobacter* was the most dominant active methanotroph irrespective of the incubation temperature, forming 32.9%, 33.9%, and 21.1% of the 0 ºC, 4 ºC and 22 ºC of the sequences in the heaviest fractions respectively (**Figure 4.3 D-F**). However, due to a major zero inflation effect, we were unable to estimate the p-value of the differences in the relative abundance of active methanotrophs between soil type and temperatures. It is also important to mention that at 0 ºC, the heavy DNA did not separate very well from the light DNA in comparison to 4 ºC and 22 ºC incubated samples, which could be due to a reduction in the number of active methanotrophs or low CH_4 oxidation activity (**Supplementary Figure 4.17 A**). However, there was a very low abundance of other active methanotrophs in comparison to the genus *Methylobacter* in these samples; therefore, we tentatively label the detected *Methylobacter* as the active methanotrophs in the 0 ºC incubations (**Figure 4.3 D-F**).

The only detected active Type II methanotroph was a *Methylocapsa palsarum*-like strain in the undisturbed 0 ºC (0.04%) and 4 ºC (0.04%) samples and disturbed 22 ºC (0.4%) sample. *Methylocapsa palsarum* was originally isolated from sub-Arctic discontinuous permafrost and it is capable of growing at a wide range of temperatures (6 ºC – 32 ºC) (Dedysh *et al.*, 2015). No known methanotrophic species affiliated with the candidate division NC10 or Verrucomicrobia phylum were detected, although because the known Verrucomicrobial CH_4 oxidizers are autotrophs and are not detectable by the use of a conventional SIP method, we cannot exclude their presence (Sharp *et al.*, 2012). Nonetheless, since no ASV related to known Verrucomicrobial CH_4 oxidizers were present in the overall community or known methanotroph datasets, we think it is unlikely that they play a major role in CH_4 consumption in permafrost.

4.3.4. Soil edaphic parameters

There were no statistically significant differences in organic matter (OM) and gravimetric water content (GW) between or within samples (**Supplementary Table 4.3**). However, pH was significantly lower ($p < 0.01$) in composite disturbed samples (n=6, 6.34 (±0.36)) relative to composite undisturbed samples (n=6, 7.06 (±0.21)) (**Supplementary Table 4.3**).

Soil disturbance ($p < 0.05$) and temperature ($p < 0.01$) were the only variables that significantly affected the ASV composition of the entire dataset (**Supplementary Table 4.4**). In contrast, disturbance, temperature, and pH all showed statistically significant ($p < 0.05$) effects on the methanotrophic ASV structure (**Supplementary Table 4.4**).

4.4. Discussion

Methanotrophic response to thermokarst formation and temperature are factors that are not well understood in changing Arctic. This gap of knowledge has resulted in an overestimation of carbon feedback to the atmosphere by the widely used greenhouse gas trajectory models (McCalley, 2020; Oh *et al.*, 2020). Limited studies have been conducted on Arctic methanotrophs and their response to abrupt disturbance such as thermokarst formation; those studies are mainly based on gradual thawing of permafrost (Singleton *et al.*, 2018; Turetsky *et al.*, 2020). It is important to help fill these gaps of knowledge because changes in the CH_4 oxidation capacity and community structure of methanotrophs could have major implications on the CH_4 cycle in the Arctic and subsequently on a global scale.

We found a strong linear relationship between temperature and CH_4 oxidation rates (**Figure 4.1**). Studies of active layer soils from the Canadian High Arctic showed CH_4 oxidation rates of samples incubated at 4 °C and room temperature (not specified) were all ≤ 20 nmol $CH_4 \cdot g$ (dry weight)$^{-1} \cdot day^{-1}$ (Martineau *et al.*, 2010). These rates are several orders of magnitude less than ours at 22 °C (8354.8 nmol $CH_4 \cdot g$ (wet soil)$^{-1} \cdot day^{-1}$) and 4 °C (**Supplementary Figure 4.4 A, B**; **Supplementary Table 4.2**). Studies of upper and lower active layer soils from Lena Delta, Siberia showed the highest CH_4 oxidation rates in upper active layer samples at 21°C of 50 nmol $CH_4 \cdot g^{-1}$ (dry weight)$\cdot d^{-1}$ (Liebner & Wagner, 2007). Similar to our results, the lowest overall CH_4 oxidation rates for active layer soils from Lena Delta, Siberia were at 0 °C for all active layer depths (< 23 nmol$\cdot g^{-1}$ (dry weight) $\cdot d^{-1}$) (Liebner & Wagner, 2007). Our lowest recorded CH_4 oxidation rates were for undisturbed active layer samples at 0 °C, at 496.8 nmol $CH_4 \cdot g$ wet soil$^{-1} \cdot day^{-1}$ (**Supplementary Figure 4.4 C**; **Supplementary Table 4.2**). This CH_4 oxidation rate is ~22 × higher than the observed rate obtained in (Liebner & Wagner, 2007). One possible reason for this difference is that our sampling site is located in the Canadian sub-Arctic region at the 63rd parallel, while the other studies were at much higher latitude. The sampling site for the Canadian High Arctic active layers was at the 80th parallel north, and for Lena Delta, Siberia was at the 73rd parallel north (Christiansen *et al.*, 2015; Liebner & Wagner, 2007). This difference in latitudes also corresponds to different environments (Canadian High Arctic, Siberian Arctic) whose soils have different physicochemical properties (Singh *et al.*, 2007). Thus, we note a difference that may indicate a much higher level of variability than previously assumed for CH_4 oxidation rates in Northern, permafrost-affected soils.

We found that active layer soil disturbance restructured the entire microbial community, including the methanotrophs, irrespective of the incubation temperature and resulted in the formation of a community structure that was dramatically different from the undisturbed samples (**Figure 4.2 A, B**). These findings reflect those of other studies that found a distinct temporal shift in methanotrophic community structure and rapid population growth and greatly increased activity after disturbance (Ho *et al.*, 2011; Ho *et al.*, 2016; Singh & Singh, 2013; Zhang *et al.*, 2020a). However, most previous studies that demonstrated increased activity after disturbance also noted a significant shift from type I to type II (e.g. (Ho *et al.*, 2011) or type II to type I methanotrophs (e.g. (Ho *et al.*, 2016). It seems that the nature of disturbance and the system of the study are important in selecting certain types of methanotrophs. For example, Type I methanotrophs were selected after physical disturbance of soil (sieved and ground soil) (Kumaresan *et al.*, 2011), prolonged drought (Ho *et al.*, 2016), deforestation (pasture soil) (Singh *et al.*, 2007), or major change in temperature imposed on the soil obtained from cold environments (Zhang *et al.*, 2020a). After moderate and severe die-offs of the microbial community in soil due to γ-irradiation, the methanotrophic community shifted from Type I to Type II methanotrophs (Ho *et al.*, 2011). Furthermore, Type II methanotrophs are able to recover over time after disturbance (Ho *et al.*, 2016). However, in our study we did not observe a shift between type I and type II methanotrophs under any conditions, and Type II methanotrophs remained unchanged in abundance (**Supplementary Figures 4.14 A, B** and **4.15 A, B**).

Similar to previous observations from other cold environments such as Siberian and high Canadian sub-Arctic soils, Type I methanotrophs dominated and Type II methanotrophs formed a negligible percentage of the methanotrophic community (**Supplementary Figures 4.14 A, B**

and **4.15 A, B**) (Crevecoeur *et al.*, 2017; Khmelenina *et al.*, 2002). One explanation for the absence of the Type II methanotrophs is that they prefer non-permafrost affected habitats with higher temperatures (e.g. (Börjesson *et al.*, 2004; He *et al.*, 2012b). In addition, Type II has a lower CH_4 threshold for growth in comparison to Type I methanotrophs. As a result, environments that emit high concentrations of CH_4, such as thermokarst, may not be ecologically suitable for Type II methanotrophs to proliferate.

Studies that have particularly focused on physical disturbance of soil and its impact on the methanotrophic community structure demonstrated the dominance of Type I over the Type II methanotrophs (Abell *et al.*, 2009; He *et al.*, 2012b; Kumaresan *et al.*, 2011; Singh *et al.*, 2007). Physical disturbance of the soil structure appears to select for Type I methanotrophs since this clade of proteobacterial methanotrophs are known to respond much faster to disturbance compared to Type II methanotrophs and outcompete this class (Buckling *et al.*, 2000; Graham *et al.*, 1993; Henckel *et al.*, 2000).

One potential explanation regarding our findings is the compaction of the soil due to the heavy equipment used at the site (bulldozing effect). Compacted soil has a small pore size and a smaller volume; this reduced space could result in reduction of available air in the soil matrix (Frey *et al.*, 2011; Rachor *et al.*, 2011). Limited oxygen and possibly increased concentration of CH_4 in compacted soils (Frey *et al.*, 2011) could select Type I methanotrophs over Type II. Compacted aerated forest soils have been seen to shift from a net CH_4 sink to a net CH_4 source after compaction caused by heavy harvesting machines (Frey *et al.*, 2011). Although, increase in the

moisture content of the soil due to thawing of the underlain permafrost could induce anoxia (Battin *et al.*, 2009; Vonk & Gustafsson, 2013), however, we did not observe a statistically significant change in gravimetric water content between disturbed and undisturbed samples (**Supplementary Tables 4.3** and **4.4**). Hence, possibly the water content did not play an important role in causing a shift in the methanotrophic or the entire microbial community structures. Type I methanotrophs possess a highly efficient carbon fixation pathway of RuMP in comparison to Type II methanotrophs, which complete methanotrophy via the serine cycle (Stein *et al.*, 2012). Higher concentrations of CH_4 in compacted soil could help Type I to grow faster and outcompete Type II (Stein *et al.*, 2012). In general Type II methanotrophs require less CH_4 for proliferation in comparison to Type I class (Stein *et al.*, 2012).

Methylobacter was the only dominant methanotroph in our distributed SIP samples irrespective of the incubation temperature (**Figure 4.3 D-F**). Cultivated members of this genus are able to remain metabolically active under suboxic conditions by relying on dissimilatory nitrate reduction (Smith *et al.*, 2018), utilizing nitrite in the electron transport chain, diverting oxygen for methanotrophy (Smith *et al.*, 2018). This mode of survival occurs extensively in disturbed permafrost affected regions such as wetlands (Smith *et al.*, 2018). In addition, some species of *Methylobacter*, such as *M. tundripaludum*, are psychrotolerant (Wartiainen *et al.*, 2006) and some, such as *M. psychrophilus*, are true psychrophilic methanotrophs, allowing them to remain metabolically active in cold near-zero temperatures (Berestovskaya *et al.*, 2002).

In our study, in the absence of disturbance, the dominant methanotrophs shifted in response to temperature. A similar shift was seen in a SIP-based study conducted on Arctic lake sediments, where 4 ºC microcosms were dominated by *Methylobacter*, at 10 ºC by *Methylosoma*, and at 21 ºC by *Methylomonas* (He *et al.*, 2012b). In the absence of disturbance, the methanotrophic community appears to be primarily structured by temperature. Changes in temperature can strongly affect soil parameters such as pH; however, the effect was not strong enough to reshape the methanotrophic and the entire microbial community structures in our study. pH is the most important parameter affecting the relative influences of stochastic and deterministic processes that govern the assembly of microbial communities in successional soils (Tripathi *et al.*, 2018). Hence, we can not fully exclude the influence of pH on shaping the active layer methanotrophs and the entire microbial community structures.

Methylobacter was the only dominant active methanotroph in the disturbed samples (**Figure 4.3 D-F**). Other Type I methanotrophs were possibly not favored by the disturbed conditions due to anoxia caused by compaction. However, the methanotrophic activity was ~2 × higher with increase in temperature in disturbed samples in comparison to the undisturbed samples ($p < 0.05$) (**Figure 4.1**). One possible explanation for this increased activity is direct changes in the soil aggregates and structure, which resulted in increase in the oxidation activity of the *Methylobacter* strains (Kumaresan *et al.*, 2011). Another possible explanation for the increase in methanotrophic activity of the *Methylobacter* strain in disturbed samples is due to partnership with non-methanotrophic species such as genus *Methylotenera* (Hernandez *et al.*, 2015). Most studies have attributed the increase in the abundance of the genus *Methylotenera* as a result of the cross-feeding of ^{13}C phenomenon in SIP experiments (e.g. (He *et al.*, 2012b), but recent

studies are showing the possibility of some type of a syntrophic relation between genera *Methylobacter* and *Methylotenera* under suboxic conditions (Hernandez *et al.*, 2015; Oshkin *et al.*, 2015). At a higher oxygen concentrations of 150-225 μM the partners involved in a syntrophic methanotrophy is between genera *Methylosarcina* and *Methylophilus* while under oxygen-limited conditions (15-75 μM) these partners shift to genera *Methylobacter* and *Methylotenera*, suggesting that oxygen is a major parameter that could select for certain methanotrophs and their non-methanotrophic partners under disturbed conditions (Hernandez *et al.*, 2015). Additionally, a study considered a possibility of direct methanotrophy (direct fixation of CH_4) by methylotrophs through an unknown pathway (Martineau *et al.*, 2010). In conclusion, changes in oxygen level and creation or loss of ecological niches with possible syntrophic association with genus *Methylotenera* could have all played an important role in significant increase in CH_4 oxidation activity of the genus *Methylobacter* in disturbed samples.

All in all, based on our observed oxidation rates from disturbed and undisturbed active layer soils, we predict that low CH_4 affinity methanotrophs, specifically Gammaproteobacterial Type I methanotrophs, will show increased CH_4 oxidation under increased atmospheric temperature and that this increase will be even greater in disturbed soils. Similar to the other Arctic and sub-Arctic sites, the main persistent active methanotroph was *Methylobacter* in both disturbed and undisturbed soils at low temperatures and in disturbed soils at all temperatures. This observation highlights its ecological importance in permafrost affected ecosystems. In addition, our findings highlight that disturbance acts as a primary factor in reorganizing both the methanotrophic and the entire microbial community structures in the active layer and temperature changes act as a

secondary factor. Hence, it is important to consider types of disturbance in addition to changes in temperature in climate feedback models.

4.5. Conclusion

Studies such as ours provide a baseline for improving and closing the gap between different climate-carbon feedback models by elucidating methanotrophic and microbial communities' response to a thermokarst formation and increase in temperature, which has been predicted to increase in a warmer world. Most soil microbial ecology studies only focus on soil parameters such as temperature and pH in explaining variations in microbial community dynamics with changing environments; however, we demonstrate that disturbance is the primary factor in reshaping the microbial community structure of the active layer and temperature is the secondary factor. Hence, it is important to characterize and understand functionally important microorganisms, such as methanotrophs, response to disturbance prior to implementing methanotrophy in the climate feedback models. We showed that changes in CH_4 oxidation capacity of methanotrophs are directly linked to changes in their community structure, and activity increased in disturbed soils, possibly indicating that sites that are disturbed due to thermokarst formation may have stronger capacity to consume locally produced CH_4. This finding shows that these species are important in the CH_4 balance in a warmer Arctic and that abrupt thermokarst formation, such as those resulting from anthropogenic disturbances or major thaw events, should be accounted for in CH_4 flux and climate change models.

4.6. Summary of chapter 4

The combined effects of thermokarst formation and temperature on the methanotrophic capacity of permafrost affected regions are not well understood. The frequency of abrupt thermokarst formation is expected to increase in a warmer world. Because of this gap of knowledge, greenhouse gas trajectory models may have overestimated the amount of CH_4 feedback to the atmosphere from the northern permafrost. In this study, I subjected disturbed and undisturbed permafrost active layer microcosms to below and above zero temperatures (-20 ºC to +22 ºC) to investigate the methanotroph and the total bacterial community dynamics. There was a strong linear relationship between increases in methanotrophic activity and increases in temperature; however, disturbed samples at 4 ºC and 22 ºC demonstrated significantly (~ 2 ×) higher CH_4 oxidation activity compared to the undisturbed samples. Disturbance resulted in the restructuring of the entire microbial community, including the methanotrophs, irrespective of the incubation temperature. Temperature acted as a secondary factor in restructuring both methanotroph and total bacterial communities. SIP of the undisturbed samples demonstrated that at 0 ºC *Methylobacter*, at 4 ºC *Methylosoma*, and at 22 ºC *Methylomicrobium* were the most dominant active methanotrophs. In contrast, SIP of the disturbed samples showed that *Methylobacter* was the most dominant active methanotroph, irrespective of the incubation temperature. I predict that Gammaproteobacterial (Type I) methanotrophs in permafrost-affected regions of the North will show increased CH_4 oxidation under increased atmospheric temperature and that this increase will be even greater in disturbed active layer soils. This finding shows that Type I methanotrophs and especially *Methylobacter* are very important in the CH_4 balance in a warmer Arctic. In the context of climate change, more emphasis should be placed on the active layer soil disturbance in parallel with temperature in studies of permafrost ecology and carbon climate-feedback models.

Chapter 5

5.1. Conclusion and future directions

The link between terrestrial biodiversity loss and climate change is undeniable; however, little is known regarding the effect of climate change on soil microorganisms, which are vital for ecosystem functioning (e.g. (Cavicchioli *et al.*, 2019). Our limited knowledge of microbial response to climate change has been further obscured by contradictory results obtained from soil warming experiments. Some of these experiments demonstrated a lag or inertia in microbial activity and composition, while others demonstrated a rapid shift in microbial community structure in a short period of time (e.g. (Waldrop & Firestone, 2006).

This is not the first time the terrestrial biosphere is experiencing rapid climate change. The most recent global climate change occurred at the Pleistocene-Holocene transition, which was very rapid (Guthrie, 2006). This geological epoch transition is as a major tipping point event in the Earth's climate system, leading to a rapid change in all ecosystem components, including the soil chemistry (Boers *et al.*, 2018). The remnants of the past and present biosphere are preserved in the permafrost of Eastern Beringia, which was not subjected to destructive glaciation (e.g. (Zazula *et al.*, 2003a). A glacier's movement can drastically reshape the landscape, hence changing soil properties and destroying the signals of the past climatic oscillations (DiPietro, 2018). Fossils and ancient DNA preserved in the Eastern Beringian permafrost have been used to reconstruct both the ancient ecosystem that once thrived in Beringia, and the natural variation and the evolution of the current climatic conditions of this region (e.g. (Zazula *et al.*, 2007).

Since the soil microbial community structure is influenced by climatic and edaphic parameters, I hypothesized that I can understand how microbial communities were shaped in response to the climatic conditions that occurred across the Pleistocene-Holocene boundary by using the Eastern Beringian permafrost as a model. Although some papers demonstrated the presence of microbial cells in Eastern Beringian permafrost close to the geographical region where my samples were acquired, e.g. (D'Costa *et al.*, 2011; Johnson *et al.*, 2007; Porter *et al.*, 2013), prior to my Ph.D. research, it was not known if the Eastern Beringian permafrost had the capacity to preserve viable, dead and the entire microbial community structure across the Pleistocene-Holocene boundary. In order to test my hypothesis, I accessed the indigenous microbes in permafrost, which required stringent methods that allow distinguishing contaminant DNA from endogenous DNA.

In this thesis, I introduced highly effective decontamination and DNA extraction methods to allow permafrost microbiologists to acquire contaminant-free DNA from permafrost with low biomass. To my knowledge, this is the first study that systemically compared the widely used DNA extraction and decontamination protocols in permafrost microbiology. For this comparison, I used a molecular contamination marker pBAD/His B plasmid harboring mNeonGreen gene to trace microbial contamination at a very low level via PCR or macrophotography of the mNeon Green protein under UV light (Guzman *et al.*, 1995; Hostettler *et al.*, 2017). My results strongly show that contamination monitoring is very important in permafrost microbiology. For example, by systematically studying the best decontamination approach and using ideas from aDNA in my studies, I have made it more rigorous and cast at least some doubt on other studies that mainly used the dry shaving method and to some extent disk-based subsampling approaches in the field

of permafrost microbiology. Studies that have solely relied on these methods or did not address contamination tracing and decontamination may still have been affected by contamination. The recommendation made in my studies to the community could help overcome both some issues with the work and some skepticism about the findings.

In addition, for the first time I demonstrated that permafrost chemical parameters, age, and soil texture did not influence the decontamination procedure, however, the permafrost type influenced the DNA extraction. The microbial and genomic section of the new Permafrost Archives Science Laboratory facility at the University of Alberta was designed in part based on my Ph.D. research.

My decontamination method allowed me to investigate the microbial community structure of permafrost that formed at the time of the Pleistocene-Holocene transition. I selected samples from across the Pleistocene-Holocene transition zone because they reflect drastically different climates and edaphic parameters, enabling me to compare how these parameters may affect the structure of the microbial community. My results showed that both the microbial communities and the chemical parameters were stable within each era until they crossed a threshold, which was driven by climate change during the Pleistocene-Holocene transition. After that threshold, there was an abrupt switch to a new microbial community and new soil chemistry. In addition, each era contained a unique microbiome, which was phylogenetically separate from the other, despite a very short spatial distance, possibly selected for by the harsh conditions of the permafrost and not the soil chemistry.

My results help us to understand microbial dynamics over a long geological timescale, a topic that many scientists have tried with a large variety of methods, which have generated conflicting results. Such discrepancies have hindered our ability in designing accurate carbon-climate feedback models, which are necessary for generating effective strategies to combat large-scale species extinction and better management of novel ecosystems. In addition, my findings helped explain the reason for the discrepancies created in soil warming experiments and opened a new avenue for scientists to explore further. Under the current climate change regime, the thawing of ice-rich Pleistocene permafrost has resulted in the deepening of the active layer soil and the formation of anoxic thermokarst systems suitable for the methanogenic activity (e.g. (Strauss *et al.*, 2017; Wei *et al.*, 2018). Methanogens are the only known biological source of CH_4, which is a potent greenhouse gas (Lyu *et al.*, 2018).

Most of the traditional carbon-climate feedback models do not consider the influence of increased temperature on methanotrophs, which are the only known biogenic sink of CH_4 (Hanson & Hanson, 1996; Oh *et al.*, 2020). Most climate models predict that with increased atmospheric temperatures in the Arctic due to anthropogenic climate change and the associated thermokarst formation, methanogenic activity will increase (e.g. (Oh *et al.*, 2020). However, the methanotrophic response is somewhat unclear (Oh *et al.*, 2020). Changes in the balance of methanogenic and methanotrophic activities could turn a system into either a CH_4 source or sink. Most of the studies that looked into the changes in aerobic methanotrophic bacterial community structure or their CH_4 oxidation capacity in response to disturbance have only considered one type of disturbance, mainly natural permafrost thaw gradient (Singleton *et al.*, 2018), changes in temperature (Zhang *et al.*, 2020a) or soil water content (Ho *et al.*, 2016). Hence, changes in the

methanotrophic capacity of the disturbed soil in response to increased temperature is not well understood.

By using an anthropogenically disturbed active layer site as an analog for climate change-induced thermokarst formation, I demonstrated that the methanotroph as well as the entire microbial community was primarily structured based on soil disturbance and only secondarily by temperature. CH_4 oxidation activity increased in parallel with an increase in temperature (0-22 ^oC), however, soil disturbance resulted in a 2 × increase in oxidation rate at 22 ^oC. DNA-SIP results showed that the soil disturbance mainly selected for genus *Methylobacter* (mainly *M. tundrapaludum*) over other methanotrophic strains. In the absence of disturbance, genera *Methylomicrobium* at 22 ^oC, *Methylosoma* at 4 ^oC, and *Methylobacter* at 0 ^oC were the most dominant methanotrophs. Type I (Gammaproteobacteria) methanotrophs were the most active CH_4 oxidizers in all samples combined. Disturbance of the soil and temperature significantly affected the composition of the entire microbial community in comparison to other measured basic soil parameters. Soil disturbance, temperature, and pH showed a statistically significant effect on the methanotrophic community structure. Among these parameters, the disturbance was shown to have the most influence on methanotrophs.

My results show that in a warmer world, methanotrophs in a thermokarst system such as a disturbed active layer have the potential to oxidize generated CH_4 at a faster rate than the undisturbed active layer methanotrophs. By studying the changes in the methanotrophic capacity of thermokarst systems at increased temperature, we may be able to tell when a particular region

in the circumpolar Arctic will become a CH_4 source or sink. In turn, this will help us to have a better understanding of the overall carbon cycle in fragile Arctic ecosystems under the current climate change regime or in a warmer world.

Overall, the first part of my project paved the path for accessing the true endogenous permafrost microbial community structure. The second part of the project elucidated microbial community dynamics across two completely different climatic and ecosystem conditions. The third part of the project demonstrated how microbial community structure, including methanotrophs, respond to a tipping point event such as thermokarst formation and increase in temperature: two main components of Anthropocene climate change. My projects will help fulfill one of the major goals of environmental microbiology, which is investigating and predicting microbial populations and community dynamics in complex environments. My findings could pave the path for other researchers to answer the bigger question of "what is the effect of climate change on soil microbes".

There are still questions that remain unanswered and need to be addressed in the future. These include: **i)** how stable are the microbial communities from the functional perspective across the Pleistocene-Holocene boundary? Drastic changes in the soil chemistry have been seen to drastically alter the microbial functional capacity (Coolen & Orsi, 2015), as a result, it is important to understand how drastic changes in the soil chemistry such as the Pleistocene-Holocene transition could change the microbial function. This question could be answered by relying on "Omic" technologies such as metagenomics or proteomics.

ii) Are the changes I observed across the Pleistocene-Holocene transition the same across the Arctic, or are they limited to eastern Beringia? The Pleistocene-Holocene transition was a global phenomenon, which drastically changed the global systems. In addition, it will be interesting to see if the changes in the microbial community structure have any link to the geographical location. Furthermore, it will be interesting to investigate the phylogeny of the Pleistocene and Holocene aged permafrost communities to see if the same dominant strains (Proteobacteria or Actinobacteria) detected in this study are still dominant at a pan-arctic scale. Repeating the same experimental designs of chapters 2 and 3 on a large variety of samples from different geographical locations across Beringia and the Canadian High Arctic might help to answer this question.

iii) Is there a link between plant community and microbial community dynamics across the Pleistocene-Holocene? Plants, like microbes, remained stable until the Pleistocene terminus (Zazula *et al.*, 2003b). Holocene-aged permafrost samples contained a large quantity of partially degraded plant material, whereas fibrous plant remains were rare in Pleistocene-aged permafrost samples. To answering this question *trnL* intron from chloroplast DNA (cp DNA) (Porter *et al.*, 2013) could be sequenced across the Pleistocene-Holocene transition zone preserved in Eastern Beringian permafrost and models such as MGLM could be used to assess the relationship between changes in the microbial community (16S rRNA genes) and plants across the epoch transition zone.

iv) Horizontal gene transfer (HGT) is commonplace in extreme environments such as permafrost and is considered necessary for microbial fitness and evolution (Douglas & Langille, 2019; Fuchsman *et al.*, 2017). What is the role of HGT in the stability of the microbial community structure and function across the Pleistocene-Holocene transition? In addition, how does the HGT intensity change across the Pleistocene-Holocene transition? Could changes in HGT intensity influence carbon utilization? To answer this question, metagenomics should be conducted across the preserved Pleistocene-Holocene transition zone in Eastern Beringian permafrost. Later the metagenome-assembled genomes (MAGS) constructed from the metagenome could be investigated for the HGT signatures. Some examples of HGT signatures include genes involved in the uptake of extracellular DNA such as type IV pili (shows potential for transformation), a high number of genes involved in the expression of tra proteins (involved in cell-cell junction), or genes involved in the expression of proteins involved in the formation of relaxosome complex, presence of a large number of reference plasmid sequences involved in HGT and presence of a large number of phage genomic material (Douglas & Langille, 2019).

v) How did the archaeal community structures shift across the Pleistocene-Holocene transition? I was able to demonstrate changes in the bacterial community structure but not the archaeal community structure. Pleistocene-Holocene transition coincided with extensive increase in global atmospheric CO_2 and CH_4. Some scientists believe thermokarst formation and increase in the activity of methanogens is the most plausible explanation, however no laboratory based analysis have been conducted on methanogenic community dynamics a cross Pleistocene-Holocene transition (Kanevskiy *et al.*, 2014; Köhler *et al.*, 2014). This question could be answered via metagenomics or by direct sequencing of the Archaeal genes.

vi) What is the effect of active layer disturbance on Type II methanotrophs? Type II methanotrophs seem to be resilient to major environmental changes (Ho *et al.*, 2011) and some members are able to form spores in response to stressors (Bowman, 2006). Why they are rare in disturbed active layer soils? Type II and Type I strains present in permafrost should be further tested in a laboratory setting by manipulating the soil physical and chemical parameters and CH_4 concentration in parallel with DNA-SIP, to see how drastic changes in the mentioned variables are affecting the active type I and Type II strains.

viii) What is the role of the abundant, non-methanotrophic species detected in my SIP samples? Maybe under certain scenarios methanotrophs and non-methanotrophic strains can carry out methanotrophy through a syntrophic association? And finally, why are *Methylobacter* strains more abundant in disturbed active layer systems? Soil chemical parameters, CH_4 concentration and oxygen levels should be manipulated in a laboratory setting to see how changes in these parameters are promoting syntrophy between MOB, such as genus *Methylobacter* with non-methanotrophs. DNA-SIP alone or combined with proteomics or metatranscriptomics could be used to monitor the community dynamics and evolution of the $^{13}CH_4$ used in response to changes in tested variables.

References

Abbott, B. W., Larouche, J. R., Jones Jr, J. B., Bowden, W. B., & Balser, A. W. (2014). Elevated dissolved organic carbon biodegradability from thawing and collapsing permafrost. *Journal of Geophysical Research: Biogeosciences, 119*(10), 2049-2063.

Abe, Y. S., & Sasaki, S. (2016). DNA cleavage at the AP site via β-elimination mediated by the AP site-binding ligands. *Bioorganic & Medicinal Chemistry, 24*(4), 910-914.

Abell, G. C., Stralis-Pavese, N., Sessitsch, A., & Bodrossy, L. (2009). Grazing affects methanotroph activity and diversity in an alpine meadow soil. *Environmental microbiology reports, 1*(5), 457-465.

Aduayom, I., Denizeau, F., & Jumarie, C. (2005). Multiple effects of mercury on cell volume regulation, plasma membrane permeability, and thiol content in the human intestinal cell line Caco-2. *Cell biology and Toxicology, 21*(3-4), 163-179.

Aghajari, N., Van Petegem, F., Villeret, V., Chessa, J. P., Gerday, C., Haser, R., & Van Beeumen, J. (2003). Crystal structures of a psychrophilic metalloprotease reveal new insights into catalysis by cold-adapted proteases. *Proteins: Structure, Function, and Bioinformatics, 50*(4), 636-647.

Ågren, G. I. (2010). Microbial mitigation. *Nature Geoscience, 3*(5), 303-304.

Aguilar, P. S., Hernandez-Arriaga, A. M., Cybulski, L. E., Erazo, A. C., & de Mendoza, D. (2001). Molecular basis of thermosensing: a two-component signal transduction thermometer in Bacillus subtilis. *The EMBO journal, 20*(7), 1681-1691.

Ajsuvakova, O. P., Tinkov, A. A., Aschner, M., Rocha, J. B., Michalke, B., Skalnaya, M. G., . . . Sarac, I. (2020). Sulfhydryl groups as targets of mercury toxicity. *Coordination Chemistry Reviews, 417*, 213343.

Åkerman, H. J., & Johansson, M. (2008). Thawing permafrost and thicker active layers in sub-arctic Sweden. *Permafrost and Periglacial Processes, 19*(3), 279-292.

Allan, J., Ronholm, J., Mykytczuk, N., Greer, C., Onstott, T. C., & Whyte, L. (2014). Methanogen community composition and rates of methane consumption in C anadian H igh A rctic permafrost soils. *Environmental microbiology reports, 6*(2), 136-144.

Alley, R. B. (2000). Ice-core evidence of abrupt climate changes. *Proceedings of the National Academy of Sciences, 97*(4), 1331-1334.

Alley, R. B., Marotzke, J., Nordhaus, W. D., Overpeck, J. T., Peteet, D. M., Pielke, R. A., . . . Talley, L. D. (2003). Abrupt climate change. *Science, 299*(5615), 2005-2010.

Allison, S. D., & Martiny, J. B. (2008). Resistance, resilience, and redundancy in microbial communities. *Proceedings of the National Academy of Sciences, 105*(Supplement 1), 11512-11519.

Altschul, S. F., Gish, W., Miller, W., Myers, E. W., & Lipman, D. J. (1990). Basic local alignment search tool. *Journal of Molecular Biology, 215*(3), 403-410.

Altshuler, I., Goordial, J., & Whyte, L. G. (2017). Microbial life in permafrost *Psychrophiles: from biodiversity to biotechnology* (pp. 153-179): Springer.

Amaral, J., Archambault, C., Richards, S., & Knowles, R. (1995). Denitrification associated with groups I and II methanotrophs in a gradient enrichment system. *FEMS microbiology ecology, 18*(4), 289-298.

Amir, A., McDonald, D., Navas-Molina, J. A., Kopylova, E., Morton, J. T., Xu, Z. Z., . . . Gonzalez, A. (2017). Deblur rapidly resolves single-nucleotide community sequence patterns. *Msystems, 2*(2).

Anderson, D. M. (1967). Ice nucleation and the substrate-ice interface. *Nature, 216*(5115), 563-566.

Angert, A., Biraud, S., Bonfils, C., Henning, C., Buermann, W., Pinzon, J., . . . Fung, I. (2005). Drier summers cancel out the CO2 uptake enhancement induced by warmer springs. *Proceedings of the National Academy of Sciences, 102*(31), 10823-10827.

Anthony, K. W., Zimov, S., Grosse, G., Jones, M. C., Anthony, P., Chapin III, F. S., . . . Frenzel, P. (2014). A shift of thermokarst lakes from carbon sources to sinks during the Holocene epoch. *Nature, 511*(7510), 452-456.

Anuchin, A. M., Mulyukin, A. L., Suzina, N. E., Duda, V. I., El-Registan, G. I., & Kaprelyants, A. S. (2009). Dormant forms of Mycobacterium smegmatis with distinct morphology. *Microbiology, 155*(4), 1071-1079.

Asakura, H., Ishiwa, A., Arakawa, E., Makino, S. i., Okada, Y., Yamamoto, S., & Igimi, S. (2007). Gene expression profile of Vibrio cholerae in the cold stress-induced viable but non-culturable state. *Environmental microbiology, 9*(4), 869-879.

Assessment, A. C. I. (2004). *Impacts of a warming Arctic-Arctic climate impact assessment.* Paper presented at the iwaa.

Baani, M., & Liesack, W. (2008). Two isozymes of particulate methane monooxygenase with different methane oxidation kinetics are found in Methylocystis sp. strain SC2. *Proceedings of the National Academy of Sciences, 105*(29), 10203-10208.

Bai, Y., Yang, D., Wang, J., Xu, S., Wang, X., & An, L. (2006). Phylogenetic diversity of culturable bacteria from alpine permafrost in the Tianshan Mountains, northwestern China. *Research in microbiology, 157*(8), 741-751.

Baker, P. W., Futamata, H., Harayama, S., & Watanabe, K. (2001). Molecular diversity of pMMO and sMMO in a TCE-contaminated aquifer during bioremediation. *FEMS microbiology ecology, 38*(2-3), 161-167.

Bakermans, C., Ayala-del-Río, H. L., Ponder, M. A., Vishnivetskaya, T., Gilichinsky, D., Thomashow, M. F., & Tiedje, J. M. (2006). Psychrobacter cryohalolentis sp. nov. and Psychrobacter arcticus sp. nov., isolated from Siberian permafrost. *International Journal of Systematic and Evolutionary Microbiology, 56*(6), 1285-1291.

Bakermans, C., Skidmore, M. L., Douglas, S., & McKay, C. P. (2014). Molecular characterization of bacteria from permafrost of the Taylor Valley, Antarctica. *FEMS microbiology ecology, 89*(2), 331-346.

Bakermans, C., Tsapin, A. I., Souza-Egipsy, V., Gilichinsky, D. A., & Nealson, K. H. (2003). Reproduction and metabolism at− 10 C of bacteria isolated from Siberian permafrost. *Environmental microbiology, 5*(4), 321-326.

Baldrian, P., Kolařík, M., Štursová, M., Kopecký, J., Valášková, V., Větrovský, T., . . . Vlček, Č. (2012). Active and total microbial communities in forest soil are largely different and highly stratified during decomposition. *The ISME journal, 6*(2), 248-258.

Ballhausen, M.-B., Hewitt, R., & Rillig, M. C. (2020). Mimicking climate warming effects on Alaskan soil microbial communities via gradual temperature increase. *Scientific Reports, 10*(1), 1-10.

Balser, T. C., & Firestone, M. K. (2005). Linking microbial community composition and soil processes in a California annual grassland and mixed-conifer forest. *Biogeochemistry, 73*(2), 395-415.

Bang-Andreasen, T., Schostag, M., Priemé, A., Elberling, B., & Jacobsen, C. S. (2017). Potential microbial contamination during sampling of permafrost soil assessed by tracers. *Scientific Reports, 7*(1), 1-11.

Barbato, R. A., Garcia-Reyero, N., Foley, K., Jones, R., Courville, Z., Douglas, T., . . . Reynolds, C. M. (2016). Removal of Exogenous Materials from the Outer Portion of Frozen Cores to Investigate the Ancient Biological Communities Harbored Inside. *JoVE (Journal of Visualized Experiments)*(113), e54091.

Barbier, B. A., Dziduch, I., Liebner, S., Ganzert, L., Lantuit, H., Pollard, W., & Wagner, D. (2012). Methane-cycling communities in a permafrost-affected soil on Herschel Island, Western Canadian Arctic: active layer profiling of mcrA and pmoA genes. *FEMS microbiology ecology, 82*(2), 287-302.

Barnes, I., Matheus, P., Shapiro, B., Jensen, D., & Cooper, A. (2002). Dynamics of Pleistocene population extinctions in Beringian brown bears. *Science, 295*(5563), 2267-2270.

Barnosky, A. D., Koch, P. L., Feranec, R. S., Wing, S. L., & Shabel, A. B. (2004). Assessing the causes of late Pleistocene extinctions on the continents. *Science, 306*(5693), 70-75.

Barnosky, A. D., Matzke, N., Tomiya, S., Wogan, G. O., Swartz, B., Quental, T. B., . . . Maguire, K. C. (2011). Has the Earth's sixth mass extinction already arrived? *Nature, 471*(7336), 51-57.

Battin, T. J., Luyssaert, S., Kaplan, L. A., Aufdenkampe, A. K., Richter, A., & Tranvik, L. J. (2009). The boundless carbon cycle. *Nature Geoscience, 2*(9), 598-600.

Beal, E. J., House, C. H., & Orphan, V. J. (2009). Manganese-and iron-dependent marine methane oxidation. *Science, 325*(5937), 184-187.

Bellemain, E., Davey, M. L., Kauserud, H., Epp, L. S., Boessenkool, S., Coissac, E., . . . Gussarova, G. (2013). Fungal palaeodiversity revealed using high-throughput metabarcoding of ancient DNA from arctic permafrost. *Environmental microbiology, 15*(4), 1176-1189.

Bennett, K. (1990). Milankovitch cycles and their effects on species in ecological and evolutionary time. *Paleobiology*, 11-21.

Benstead, J., King, G., & Williams, H. (1998). Methanol promotes atmospheric methane oxidation by methanotrophic cultures and soils. *Applied and environmental Microbiology, 64*(3), 1091-1098.

Berestovskaya, Y. Y., Vasil'eva, L., Chestnykh, O., & Zavarzin, G. (2002). Methanotrophs of the psychrophilic microbial community of the Russian arctic tundra. *Microbiology, 71*(4), 460-466.

Berhe, A. A., Harte, J., Harden, J. W., & Torn, M. S. (2007). The significance of the erosion-induced terrestrial carbon sink. *Bioscience, 57*(4), 337-346.

Berner, R. A. (2003). The long-term carbon cycle, fossil fuels and atmospheric composition. *Nature, 426*(6964), 323-326.

Biasi, C., Meyer, H., Rusalimova, O., Hämmerle, R., Kaiser, C., Baranyi, C., . . . Richter, A. (2008). Initial effects of experimental warming on carbon exchange rates, plant growth and microbial dynamics of a lichen-rich dwarf shrub tundra in Siberia. *Plant and Soil, 307*(1-2), 191-205.

Binu, M., Lee, Y. K., Adams, J., Ke, D., Kim, M., & Stegen, J. (2018). Soil pH mediates the balance between stochastic and deterministic assembly of bacteria.

Biosca, E. G., Amaro, C., Marco-Noales, E., & Oliver, J. D. (1996). Effect of low temperature on starvation-survival of the eel pathogen Vibrio vulnificus biotype 2. *Applied and environmental Microbiology, 62*(2), 450-455.
Birks, H. J. B., & Birks, H. H. (2016). How have studies of ancient DNA from sediments contributed to the reconstruction of Quaternary floras? *New Phytologist, 209*(2), 499-506.
Bischoff, J., Mangelsdorf, K., Gattinger, A., Schloter, M., Kurchatova, A. N., Herzschuh, U., & Wagner, D. (2013). Response of methanogenic archaea to Late Pleistocene and Holocene climate changes in the Siberian Arctic. *Global Biogeochemical Cycles, 27*(2), 305-317.
Bissett, A., Abell, G. C., Bodrossy, L., Richardson, A. E., & Thrall, P. H. (2012). Methanotrophic communities in Australian woodland soils of varying salinity. *FEMS microbiology ecology, 80*(3), 685-695.
Bittelli, M. (2011). Measuring soil water content: A review. *HortTechnology, 21*(3), 293-300.
Black, T., Chen, W., Barr, A., Arain, M., Chen, Z., Nesic, Z., . . . Yang, P. (2000). Increased carbon sequestration by a boreal deciduous forest in years with a warm spring. *Geophysical Research Letters, 27*(9), 1271-1274.
Boch, J., Kempf, B., & Bremer, E. (1994). Osmoregulation in Bacillus subtilis: synthesis of the osmoprotectant glycine betaine from exogenously provided choline. *Journal of bacteriology, 176*(17), 5364-5371.
Boers, N., Ghil, M., & Rousseau, D.-D. (2018). Ocean circulation, ice shelf, and sea ice interactions explain Dansgaard–Oeschger cycles. *Proceedings of the National Academy of Sciences, 115*(47), E11005-E11014.
Bollongino, R., Tresset, A., & Vigne, J.-D. (2008). Environment and excavation: Pre-lab impacts on ancient DNA analyses. *Comptes Rendus Palevol, 7*(2-3), 91-98.
Bond, G., Broecker, W., Johnsen, S., McManus, J., Labeyrie, L., Jouzel, J., & Bonani, G. (1993). Correlations between climate records from North Atlantic sediments and Greenland ice. *Nature, 365*(6442), 143-147.
Booshehrian, A., Wan, R., & Su, X. (2020). Hydraulic variations in permafrost due to open-pit mining and climate change: a case study in the Canadian Arctic. *Acta Geotechnica, 15*(4), 883-905.
Börjesson, G., Sundh, I., & Svensson, B. (2004). Microbial oxidation of CH4 at different temperatures in landfill cover soils. *FEMS microbiology ecology, 48*(3), 305-312.
Bottos, E. M., Kennedy, D. W., Romero, E. B., Fansler, S. J., Brown, J. M., Bramer, L. M., . . . Stegen, J. C. (2018). Dispersal limitation and thermodynamic constraints govern spatial structure of permafrost microbial communities. *FEMS microbiology ecology, 94*(8), fiy110.
Bourne, D. G., McDonald, I. R., & Murrell, J. C. (2001). Comparison of pmoA PCR primer sets as tools for investigating methanotroph diversity in three Danish soils. *Applied and environmental Microbiology, 67*(9), 3802-3809.
Bouskill, N. J., Wood, T. E., Baran, R., Ye, Z., Bowen, B. P., Lim, H., . . . Northen, T. R. (2016). Belowground response to drought in a tropical forest soil. I. Changes in microbial functional potential and metabolism. *Frontiers in microbiology, 7*, 525.
Bowman, J. (2006). The methanotrophs—the families Methylococcaceae and Methylocystaceae. *The prokaryotes, 5*, 266-289.
Bradford, M. A., Davies, C. A., Frey, S. D., Maddox, T. R., Melillo, J. M., Mohan, J. E., . . . Wallenstein, M. D. (2008). Thermal adaptation of soil microbial respiration to elevated temperature. *Ecology letters, 11*(12), 1316-1327.

Bradley, R. S. (1999). *Paleoclimatology: reconstructing climates of the Quaternary*: Elsevier.
Brady, N. C., Weil, R. R., & Weil, R. R. (2008). *The nature and properties of soils* (Vol. 13): Prentice Hall Upper Saddle River, NJ.
Braid, M. D., Daniels, L. M., & Kitts, C. L. (2003). Removal of PCR inhibitors from soil DNA by chemical flocculation. *Journal of microbiological methods, 52*(3), 389-393.
BREMER, E. (2000). Coping with osmotic challenges: osmoregulation through accumulation and release of compatible solutes in bacteria. *Bacterial stress responses*, 79-97.
Briggs, A. W., Stenzel, U., Johnson, P. L., Green, R. E., Kelso, J., Prüfer, K., . . . Lachmann, M. (2007). Patterns of damage in genomic DNA sequences from a Neandertal. *Proceedings of the National Academy of Sciences, 104*(37), 14616-14621.
Brigulla, M., Hoffmann, T., Krisp, A., Völker, A., Bremer, E., & Völker, U. (2003). Chill induction of the SigB-dependent general stress response in Bacillus subtilis and its contribution to low-temperature adaptation. *Journal of bacteriology, 185*(15), 4305-4314.
Brill, B., Amir, A., & Heller, R. (2019). Testing for differential abundance in compositional counts data, with application to microbiome studies. *arXiv preprint arXiv:1904.08937*.
Broadgate, W., Riebesell, U., Armstrong, C., Brewer, P., Denman, K., Feely, R., . . . Kleypas, J. (2013). Ocean acidification: summary for policymakers.
Brouchkov, A., Griva, G., Fursova, O., Fursova, N., Ignatov, S., & Pogorelko, G. (2016). Is the ancient permafrost bacteria able to keep DNA stable? *Journal of genetics, 95*(4), 1003-1007.
Brown, J., Ferrians Jr, O., Heginbottom, J., & Melnikov, E. (1997). *Circum-Arctic map of permafrost and ground-ice conditions*: US Geological Survey Reston, VA.
Buckling, A., Kassen, R., Bell, G., & Rainey, P. B. (2000). Disturbance and diversity in experimental microcosms. *Nature, 408*(6815), 961-964.
Burkert, A., Douglas, T. A., Waldrop, M. P., & Mackelprang, R. (2019). Changes in the active, dead, and dormant microbial community structure across a Pleistocene permafrost chronosequence. *Applied and environmental Microbiology, 85*(7).
Burney, D. A., & Flannery, T. F. (2005). Fifty millennia of catastrophic extinctions after human contact. *Trends in Ecology & Evolution, 20*(7), 395-401.
Burt, R. (2004). Soil survey laboratory methods manual.
Cadet, J., & Davies, K. J. (2017). Oxidative DNA damage & repair: an introduction. *Free Radical Biology and Medicine, 107*, 2-12.
Callahan, B. J., McMurdie, P. J., & Holmes, S. P. (2017). Exact sequence variants should replace operational taxonomic units in marker-gene data analysis. *The ISME journal, 11*(12), 2639-2643.
Callahan, B. J., McMurdie, P. J., Rosen, M. J., Han, A. W., Johnson, A. J. A., & Holmes, S. P. (2016). DADA2: high-resolution sample inference from Illumina amplicon data. *Nature methods, 13*(7), 581-583.
Canfield, D. E., Glazer, A. N., & Falkowski, P. G. (2010). The evolution and future of Earth's nitrogen cycle. *Science, 330*(6001), 192-196.
Cannariato, K. G., & Stott, L. D. (2004). Evidence against clathrate-derived methane release to Santa Barbara Basin surface waters? *Geochemistry, Geophysics, Geosystems, 5*(5).
Cao, X. (2003). Climate change and energy development: implications for developing countries. *Resources policy, 29*(1-2), 61-67.
Caporaso, J. G., Lauber, C. L., Walters, W. A., Berg-Lyons, D., Lozupone, C. A., Turnbaugh, P. J., . . . Knight, R. (2011). Global patterns of 16S rRNA diversity at a depth of millions of

sequences per sample. *Proceedings of the National Academy of Sciences, 108*(Supplement 1), 4516-4522.
Carini, P., Marsden, P. J., Leff, J. W., Morgan, E. E., Strickland, M. S., & Fierer, N. (2016). Relic DNA is abundant in soil and obscures estimates of soil microbial diversity. *Nature microbiology, 2*(3), 1-6.
Carpenter, E. J., Lin, S., & Capone, D. G. (2000). Bacterial activity in South Pole snow. *Applied and environmental Microbiology, 66*(10), 4514-4517.
Carr, M. H. (2007). *The surface of Mars* (Vol. 6): Cambridge University Press.
Castro, H. F., Classen, A. T., Austin, E. E., Norby, R. J., & Schadt, C. W. (2010). Soil microbial community responses to multiple experimental climate change drivers. *Applied and environmental Microbiology, 76*(4), 999-1007.
Cavicchioli, R., Ripple, W. J., Timmis, K. N., Azam, F., Bakken, L. R., Baylis, M., . . . Classen, A. T. (2019). Scientists' warning to humanity: microorganisms and climate change. *Nature Reviews Microbiology, 17*(9), 569-586.
Cavigelli, M. A., & Robertson, G. P. (2000). The functional significance of denitrifier community composition in a terrestrial ecosystem. *Ecology, 81*(5), 1402-1414.
Chadwick, O. A., & Chorover, J. (2001). The chemistry of pedogenic thresholds. *Geoderma, 100*(3-4), 321-353.
Chappellaz, J., Bluniert, T., Raynaud, D., Barnola, J., Schwander, J., & Stauffert, B. (1993). Synchronous changes in atmospheric CH4 and Greenland climate between 40 and 8 kyr BP. *Nature, 366*(6454), 443-445.
Chase, J. M., & Myers, J. A. (2011). Disentangling the importance of ecological niches from stochastic processes across scales. *Philosophical transactions of the Royal Society B: Biological sciences, 366*(1576), 2351-2363.
Chave, J. (2004). Neutral theory and community ecology. *Ecology letters, 7*(3), 241-253.
Chen, D., Lei, L., Lu, C., Galaleldeen, A., Hart, P. J., & Zhong, G. (2010). Characterization of Pgp3, a Chlamydia trachomatis plasmid-encoded immunodominant antigen. *Journal of bacteriology, 192*(22), 6017-6024.
Chen, L., Liang, J., Qin, S., Liu, L., Fang, K., Xu, Y., . . . Yang, Y. (2016). Determinants of carbon release from the active layer and permafrost deposits on the Tibetan Plateau. *Nature communications, 7*(1), 1-12.
Chisholm, R. A., & Pacala, S. W. (2011). Theory predicts a rapid transition from niche-structured to neutral biodiversity patterns across a speciation-rate gradient. *Theoretical Ecology, 4*(2), 195-200.
Chistoserdova, L., Kalyuzhnaya, M. G., & Lidstrom, M. E. (2009). The expanding world of methylotrophic metabolism. *Annual review of microbiology, 63*, 477-499.
Chowdhury, T. R., Lee, J.-Y., Bottos, E. M., Brislawn, C. J., White, R. A., Bramer, L. M., . . . Jumpponen, A. (2019). Metaphenomic responses of a native prairie soil microbiome to moisture perturbations. *Msystems, 4*(4).
Christiansen, J. R., Romero, A. J. B., Jørgensen, N. O., Glaring, M. A., Jørgensen, C. J., Berg, L. K., & Elberling, B. (2015). Methane fluxes and the functional groups of methanotrophs and methanogens in a young Arctic landscape on Disko Island, West Greenland. *Biogeochemistry, 122*(1), 15-33.
Christner, B. C. (2002). Incorporation of DNA and Protein Precursors into Macromolecules by Bacteria at− 15oC. *Applied and environmental Microbiology, 68*(12), 6435-6438.

Clark, P., Clague, J., Curry, B. B., Dreimanis, A., Hicock, S., Miller, G., . . . Miller, B. (1993). Initiation and development of the Laurentide and Cordilleran ice sheets following the last interglaciation. *Quaternary Science Reviews, 12*(2), 79-114.

Classen, A. T., Sundqvist, M. K., Henning, J. A., Newman, G. S., Moore, J. A., Cregger, M. A., . . . Patterson, C. M. (2015). Direct and indirect effects of climate change on soil microbial and soil microbial-plant interactions: What lies ahead? *Ecosphere, 6*(8), 1-21.

Cody, M. L. (2002). Hubbell, SP: The Unified Neutral Theory of Biodiversity and Biogeography. *Plant Systematics and Evolution*.

Cole, J. R., Wang, Q., Fish, J. A., Chai, B., McGarrell, D. M., Sun, Y., . . . Tiedje, J. M. (2014). Ribosomal Database Project: data and tools for high throughput rRNA analysis. *Nucleic acids research, 42*(D1), D633-D642.

Colwell, F., Pryfogle, P., Lee, B., & Bishop, C. (1994). Use of a cyanobacterium as a particulate tracer for terrestrial subsurface applications. *Journal of microbiological methods, 20*(2), 93-101.

Conant, R. T., Ryan, M. G., Ågren, G. I., Birge, H. E., Davidson, E. A., Eliasson, P. E., . . . Hopkins, F. M. (2011). Temperature and soil organic matter decomposition rates–synthesis of current knowledge and a way forward. *Global Change Biology, 17*(11), 3392-3404.

Connon, R., Devoie, É., Hayashi, M., Veness, T., & Quinton, W. (2018). The influence of shallow taliks on permafrost thaw and active layer dynamics in subarctic Canada. *Journal of Geophysical Research: Earth Surface, 123*(2), 281-297.

Cook, K., & Bolster, C. (2007). Survival of Campylobacter jejuni and Escherichia coli in groundwater during prolonged starvation at low temperatures. *Journal of applied microbiology, 103*(3), 573-583.

Coolen, M. J., & Orsi, W. D. (2015). The transcriptional response of microbial communities in thawing Alaskan permafrost soils. *Frontiers in microbiology, 6*, 197.

Coolen, M. J., van de Giessen, J., Zhu, E. Y., & Wuchter, C. (2011). Bioavailability of soil organic matter and microbial community dynamics upon permafrost thaw. *Environmental microbiology, 13*(8), 2299-2314.

Cooper, A., & Poinar, H. N. (2000). Ancient DNA: do it right or not at all. *Science, 289*(5482), 1139-1139.

Costa, C., Dijkema, C., Friedrich, M., Garcia-Encina, P., Fernandez-Polanco, F., & Stams, A. (2000). Denitrification with methane as electron donor in oxygen-limited bioreactors. *Applied microbiology and biotechnology, 53*(6), 754-762.

Costello, A. M., Auman, A. J., Macalady, J. L., Scow, K. M., & Lidstrom, M. E. (2002). Estimation of methanotroph abundance in a freshwater lake sediment. *Environmental microbiology, 4*(8), 443-450.

Cowan, D. A., Russell, N. J., Mamais, A., & Sheppard, D. M. (2002). Antarctic Dry Valley mineral soils contain unexpectedly high levels of microbial biomass. *Extremophiles, 6*(5), 431-436.

Cox, M. A., & Cox, T. F. (2008). Multidimensional scaling *Handbook of data visualization* (pp. 315-347): Springer.

Craft, C. B., & Richardson, C. J. (2008). Soil characteristics of the Everglades peatland *Everglades experiments* (pp. 59-72): Springer.

Crevecoeur, S., Vincent, W. F., Comte, J., Matveev, A., & Lovejoy, C. (2017). Diversity and potential activity of methanotrophs in high methane-emitting permafrost thaw ponds. *PloS one, 12*(11), e0188223.

Crowther, T. W., & Bradford, M. A. (2013). Thermal acclimation in widespread heterotrophic soil microbes. *Ecology letters, 16*(4), 469-477.

Cuffey, K. M., & Clow, G. D. (1997). Temperature, accumulation, and ice sheet elevation in central Greenland through the last deglacial transition. *Journal of Geophysical Research: Oceans, 102*(C12), 26383-26396.

Cui, M., Ma, A., Qi, H., Zhuang, X., & Zhuang, G. (2015). Anaerobic oxidation of methane: an "active" microbial process. *Microbiologyopen, 4*(1), 1-11.

D'Costa, V. M., King, C. E., Kalan, L., Morar, M., Sung, W. W., Schwarz, C., . . . Debruyne, R. (2011). Antibiotic resistance is ancient. *Nature, 477*(7365), 457-461.

Dabney, J., Meyer, M., & Pääbo, S. (2013). Ancient DNA damage. *Cold Spring Harbor perspectives in biology, 5*(7), a012567.

Dalluge, J. J., Hamamoto, T., Horikoshi, K., Morita, R. Y., Stetter, K. O., & McCloskey, J. A. (1997). Posttranscriptional modification of tRNA in psychrophilic bacteria. *Journal of bacteriology, 179*(6), 1918-1923.

Danilova, O., Belova, S., Kulichevskaya, I., & Dedysh, S. (2015). Decline of activity and shifts in the methanotrophic community structure of an ombrotrophic peat bog after wildfire. *Microbiology, 84*(5), 624-629.

Dansgaard, W., Johnsen, S. J., Clausen, H. B., Dahl-Jensen, D., Gundestrup, N., Hammer, C., . . . Jouzel, J. (1993). Evidence for general instability of past climate from a 250-kyr ice-core record. *Nature, 364*(6434), 218-220.

Davidson, E., & Trumbore, S. u. AMUNDSON, R.(2000): Soil warming and organic carbon content. *Nature, 408*, 788-789.

Davidson, E. A., & Janssens, I. A. (2006). Temperature sensitivity of soil carbon decomposition and feedbacks to climate change. *Nature, 440*(7081), 165-173.

DavidsonEA, J. (2006). Temperaturesensitivityofsoilcarbondecompositionandfeedbackstoclimatechange. *Nature, 440*(7081), 165r173.

Davies, L. J., Appleby, P., Jensen, B. J., Magnan, G., Mullan-Boudreau, G., Noernberg, T., . . . Zaccone, C. (2018). High-resolution age modelling of peat bogs from northern Alberta, Canada, using pre-and post-bomb 14C, 210Pb and historical cryptotephra. *Quaternary Geochronology, 47*, 138-162.

De Vos, D., Collins, T., Nerinckx, W., Savvides, S., Claeyssens, M., Gerday, C., . . . Van Beeumen, J. (2006). Oligosaccharide binding in family 8 glycosidases: crystal structures of active-site mutants of the β-1, 4-xylanase pXyl from Pseudoaltermonas haloplanktis TAH3a in complex with substrate and product. *Biochemistry, 45*(15), 4797-4807.

De Vries, F. T., & Shade, A. (2013). Controls on soil microbial community stability under climate change. *Frontiers in microbiology, 4*, 265.

DeAngelis, K. M., Pold, G., Topçuoğlu, B. D., van Diepen, L. T., Varney, R. M., Blanchard, J. L., . . . Frey, S. D. (2015). Long-term forest soil warming alters microbial communities in temperate forest soils. *Frontiers in microbiology, 6*, 104.

Dedysh, S. N., Didriksen, A., Danilova, O. V., Belova, S. E., Liebner, S., & Svenning, M. M. (2015). Methylocapsa palsarum sp. nov., a methanotroph isolated from a subArctic

discontinuous permafrost ecosystem. *International Journal of Systematic and Evolutionary Microbiology, 65*(10), 3618-3624.
Dedysh, S. N., Liesack, W., Khmelenina, V. N., Suzina, N. E., Trotsenko, Y. A., Semrau, J. D., . . . Tiedje, J. M. (2000). Methylocella palustris gen. nov., sp. nov., a new methane-oxidizing acidophilic bacterium from peat bogs, representing a novel subtype of serine-pathway methanotrophs. *International Journal of Systematic and Evolutionary Microbiology, 50*(3), 955-969.
del Mar Lleò, M., Benedetti, D., Tafi, M. C., Signoretto, C., & Canepari, P. (2007). Inhibition of the resuscitation from the viable but non-culturable state in Enterococcus faecalis. *Environmental microbiology, 9*(9), 2313-2320.
Deng, J., Gu, Y., Zhang, J., Xue, K., Qin, Y., Yuan, M., . . . Schuur, E. A. (2015). Shifts of tundra bacterial and archaeal communities along a permafrost thaw gradient in A laska. *Molecular ecology, 24*(1), 222-234.
Dini-Andreote, F., Stegen, J. C., Van Elsas, J. D., & Salles, J. F. (2015). Disentangling mechanisms that mediate the balance between stochastic and deterministic processes in microbial succession. *Proceedings of the National Academy of Sciences, 112*(11), E1326-E1332.
DiPietro, J. A. (2018). *Geology and Landscape Evolution: General Principles Applied to the United States*: Elsevier.
Docherty, K. M., Borton, H. M., Espinosa, N., Gebhardt, M., Gil-Loaiza, J., Gutknecht, J. L., . . . Purdy, G. (2015). Key edaphic properties largely explain temporal and geographic variation in soil microbial communities across four biomes. *PloS one, 10*(11), e0135352.
Doelle, H. W. (2014). *Bacterial metabolism*: Academic Press.
Dokken, T. M., Nisancioglu, K. H., Li, C., Battisti, D. S., & Kissel, C. (2013). Dansgaard-Oeschger cycles: Interactions between ocean and sea ice intrinsic to the Nordic seas. *Paleoceanography, 28*(3), 491-502.
Douglas, G. M., & Langille, M. G. (2019). Current and promising approaches to identify horizontal gene transfer events in metagenomes. *Genome biology and evolution, 11*(10), 2750-2766.
Downie, D. E., & Taskey, R. D. (1997). *Soil characteristics of blue oak and coast live oak ecosystems.* Paper presented at the In: Pillsbury, Norman H.; Verner, Jared; Tietje, William D., technical coordinators. 1997. Proceedings of a symposium on oak woodlands: ecology, management, and urban interface issues; 19–22 March 1996; San Luis Obispo, CA. Gen. Tech. Rep. PSW-GTR-160. Albany, CA: Pacific Southwest Research Station, Forest Service, US Department of Agriculture; p. 65-74.
Drotz, S. H., Sparrman, T., Nilsson, M. B., Schleucher, J., & Öquist, M. G. (2010). Both catabolic and anabolic heterotrophic microbial activity proceed in frozen soils. *Proceedings of the National Academy of Sciences, 107*(49), 21046-21051.
Du, M., Chen, J., Zhang, X., Li, A., Li, Y., & Wang, Y. (2007). Retention of virulence in a viable but nonculturable Edwardsiella tarda isolate. *Applied and environmental Microbiology, 73*(4), 1349-1354.
Dunfield, P. F. (2007). 10 The soil methane sink. *Greenhouse gas sinks*, 152.
Dunfield, P. F., & Dedysh, S. N. (2014). Methylocella: a gourmand among methanotrophs. *Trends in microbiology, 22*(7), 368-369.

Dunfield, P. F., Yuryev, A., Senin, P., Smirnova, A. V., Stott, M. B., Hou, S., . . . Ren, Y. (2007). Methane oxidation by an extremely acidophilic bacterium of the phylum Verrucomicrobia. *Nature, 450*(7171), 879-882.

Durfee, T., Nelson, R., Baldwin, S., Plunkett, G., Burland, V., Mau, B., . . . Ayele, M. (2008). The complete genome sequence of Escherichia coli DH10B: insights into the biology of a laboratory workhorse. *Journal of bacteriology, 190*(7), 2597-2606.

Edgar, R. C. (2010). Search and clustering orders of magnitude faster than BLAST. *Bioinformatics, 26*(19), 2460-2461.

Edgar, R. C. (2013). UPARSE: highly accurate OTU sequences from microbial amplicon reads. *Nature methods, 10*(10), 996-998.

Edgar, R. C. (2016a). SINTAX: a simple non-Bayesian taxonomy classifier for 16S and ITS sequences. *bioRxiv*, 074161.

Edgar, R. C. (2016b). UNOISE2: improved error-correction for Illumina 16S and ITS amplicon sequencing. *bioRxiv*, 081257.

Ehn, M., Thornton, J. A., Kleist, E., Sipilä, M., Junninen, H., Pullinen, I., . . . Lee, B. (2014). A large source of low-volatility secondary organic aerosol. *Nature, 506*(7489), 476-479.

Eisenhofer, R., Minich, J. J., Marotz, C., Cooper, A., Knight, R., & Weyrich, L. S. (2019). Contamination in low microbial biomass microbiome studies: issues and recommendations. *Trends in microbiology, 27*(2), 105-117.

Elberling, B., & Brandt, K. K. (2003). Uncoupling of microbial CO2 production and release in frozen soil and its implications for field studies of arctic C cycling. *Soil Biology and Biochemistry, 35*(2), 263-272.

Elberling, B., Christiansen, H. H., & Hansen, B. U. (2010). High nitrous oxide production from thawing permafrost. *Nature Geoscience, 3*(5), 332-335.

Eliasson, P. E., McMurtrie, R. E., Pepper, D. A., Strömgren, M., Linder, S., & Ågren, G. I. (2005). The response of heterotrophic CO2 flux to soil warming. *Global Change Biology, 11*(1), 167-181.

Eller, G., Känel, L., & Krüger, M. (2005). Cooccurrence of aerobic and anaerobic methane oxidation in the water column of Lake Plußsee. *Applied and environmental Microbiology, 71*(12), 8925-8928.

Elsig, J., Schmitt, J., Leuenberger, D., Schneider, R., Eyer, M., Leuenberger, M., . . . Stocker, T. F. (2009). Stable isotope constraints on Holocene carbon cycle changes from an Antarctic ice core. *Nature, 461*(7263), 507-510.

Emmerton, C., St Louis, V., Lehnherr, I., Humphreys, E., Rydz, E., & Kosolofski, H. (2014). The net exchange of methane with high Arctic landscapes during the summer growing season. *Biogeosciences, 11*(12), 3095-3106.

Erimban, S., & Daschakraborty, S. (2020). Cryostablization of the Cell Membrane of a Psychrotolerant Bacteria via Homeoviscous Adaptation. *The Journal of Physical Chemistry Letters*.

Ernakovich, J. G., Wallenstein, M. D., & Calderón, F. (2015). Chemical indicators of cryoturbation and microbial processing throughout an Alaskan permafrost soil depth profile. *Soil Science Society of America Journal, 79*(3), 783-793.

Ernst, R., Ejsing, C. S., & Antonny, B. (2016). Homeoviscous adaptation and the regulation of membrane lipids. *Journal of Molecular Biology, 428*(24), 4776-4791.

Ettema, C. H., & Wardle, D. A. (2002). Spatial soil ecology. *Trends in Ecology & Evolution, 17*(4), 177-183.

Ettwig, K. F., Butler, M. K., Le Paslier, D., Pelletier, E., Mangenot, S., Kuypers, M. M., . . . de Beer, D. (2010). Nitrite-driven anaerobic methane oxidation by oxygenic bacteria. *Nature, 464*(7288), 543-548.

Ettwig, K. F., Shima, S., Van De Pas-Schoonen, K. T., Kahnt, J., Medema, M. H., Op Den Camp, H. J., . . . Strous, M. (2008). Denitrifying bacteria anaerobically oxidize methane in the absence of Archaea. *Environmental microbiology, 10*(11), 3164-3173.

Evans, S., Martiny, J. B., & Allison, S. D. (2017). Effects of dispersal and selection on stochastic assembly in microbial communities. *The ISME journal, 11*(1), 176-185.

Fabian, C., Reimann, C., Fabian, K., Birke, M., Baritz, R., Haslinger, E., & Team, T. G. P. (2014). GEMAS: Spatial distribution of the pH of European agricultural and grazing land soil. *Applied Geochemistry, 48*, 207-216.

Faith, D. P., Minchin, P. R., & Belbin, L. (1987). Compositional dissimilarity as a robust measure of ecological distance. *Vegetatio, 69*(1-3), 57-68.

Falge, E., Baldocchi, D., Tenhunen, J., Aubinet, M., Bakwin, P., Berbigier, P., . . . Davis, K. J. (2002). Seasonality of ecosystem respiration and gross primary production as derived from FLUXNET measurements. *Agricultural and Forest Meteorology, 113*(1-4), 53-74.

Fatima, F., Pathak, N., & Rastogi Verma, S. (2014). An improved method for soil DNA extraction to study the microbial assortment within rhizospheric region. *Molecular biology international, 2014*.

Feller, G. (2013). Psychrophilic enzymes: from folding to function and biotechnology. *Scientifica, 2013*.

Feller, G., Narinx, E., Arpigny, J. L., Aittaleb, M., Baise, E., Genicot, S., & Gerday, C. (1996). Enzymes from psychrophilic organisms. *FEMS microbiology reviews, 18*(2-3), 189-202.

Fenchel, T., & Finlay, B. J. (2004). The ubiquity of small species: patterns of local and global diversity. *Bioscience, 54*(8), 777-784.

Feng, J., Wang, C., Lei, J., Yang, Y., Yan, Q., Zhou, X., . . . Qin, Y. (2020). Warming-induced permafrost thaw exacerbates tundra soil carbon decomposition mediated by microbial community. *Microbiome, 8*(1), 1-12.

Fierer, N., McCain, C. M., Meir, P., Zimmermann, M., Rapp, J. M., Silman, M. R., & Knight, R. (2011). Microbes do not follow the elevational diversity patterns of plants and animals. *Ecology, 92*(4), 797-804.

Fierer, N., & Schimel, J. P. (2002). Effects of drying–rewetting frequency on soil carbon and nitrogen transformations. *Soil Biology and Biochemistry, 34*(6), 777-787.

Firestone, R. B., West, A., Kennett, J. P., Becker, L., Bunch, T. E., Revay, Z. S., . . . Erlandson, J. (2007). Evidence for an extraterrestrial impact 12,900 years ago that contributed to the megafaunal extinctions and the Younger Dryas cooling. *Proceedings of the National Academy of Sciences, 104*(41), 16016-16021.

Fisher, R. A. (1936). The use of multiple measurements in taxonomic problems. *Annals of eugenics, 7*(2), 179-188.

Fox-Dobbs, K., Leonard, J. A., & Koch, P. L. (2008). Pleistocene megafauna from eastern Beringia: Paleoecological and paleoenvironmental interpretations of stable carbon and nitrogen isotope and radiocarbon records. *Palaeogeography, Palaeoclimatology, Palaeoecology, 261*(1-2), 30-46.

Frank-Fahle, B. A., Yergeau, É., Greer, C. W., Lantuit, H., & Wagner, D. (2014). Microbial functional potential and community composition in permafrost-affected soils of the NW Canadian Arctic. *PloS one, 9*(1), e84761.

Fraser, T., & Burn, C. R. (1997). On the nature and origin of" muck" deposits in the Klondike area, Yukon Territory. *Canadian Journal of Earth Sciences, 34*(10), 1333-1344.
Freedman, Z., & Zak, D. R. (2015). Soil bacterial communities are shaped by temporal and environmental filtering: evidence from a long-term chronosequence. *Environmental microbiology, 17*(9), 3208-3218.
Frey, B., Niklaus, P. A., Kremer, J., Lüscher, P., & Zimmermann, S. (2011). Heavy-machinery traffic impacts methane emissions as well as methanogen abundance and community structure in oxic forest soils. *Applied and environmental Microbiology, 77*(17), 6060-6068.
Frey, B., Rime, T., Phillips, M., Stierli, B., Hajdas, I., Widmer, F., & Hartmann, M. (2016). Microbial diversity in European alpine permafrost and active layers. *FEMS microbiology ecology, 92*(3), fiw018.
Frey, S., Drijber, R., Smith, H., & Melillo, J. (2008). Microbial biomass, functional capacity, and community structure after 12 years of soil warming. *Soil Biology and Biochemistry, 40*(11), 2904-2907.
Frey, S. D., Lee, J., Melillo, J. M., & Six, J. (2013). The temperature response of soil microbial efficiency and its feedback to climate. *Nature climate change, 3*(4), 395-398.
Friend, A. D., Lucht, W., Rademacher, T. T., Keribin, R., Betts, R., Cadule, P., . . . Falloon, P. D. (2014). Carbon residence time dominates uncertainty in terrestrial vegetation responses to future climate and atmospheric CO2. *Proceedings of the National Academy of Sciences, 111*(9), 3280-3285.
Friese, A., Kallmeyer, J., Axel Kitte, J., Montaño Martínez, I., Bijaksana, S., Wagner, D., . . . Team, t. I. T. D. S. (2017). A simple and inexpensive technique for assessing contamination during drilling operations. *Limnology and Oceanography: Methods, 15*(2), 200-211. doi: https://doi.org/10.1002/lom3.10159
Froese, D., Barendregt, R., Enkin, R., & Baker, J. (2000a). Paleomagnetic evidence for multiple late Pliocene-early Pleistocene glaciations in the Klondike area, Yukon Territory. *Canadian Journal of Earth Sciences, 37*(6), 863-877.
Froese, D., Reyes, A., Westgate, J., Preece, S., & Jensen, B. (2009a). Ancient permafrost and a future, warmer Arctic. *AGUSM, 2009*, B31A-01.
Froese, D., Westgate, J., Preece, S., & Storer, J. (2002). Age and significance of the late Pleistocene Dawson tephra in eastern Beringia. *Quaternary Science Reviews, 21*(20-22), 2137-2142.
Froese, D. G., Enkin, R., Smith, D., Edmond, D., & Weston, L. (2000b). Placer depositional settings and their ages along Dominion Creek, Klondike area, Yukon. *Yukon exploration and geology*, 159-169.
Froese, D. G., Westgate, J. A., Reyes, A. V., Enkin, R. J., & Preece, S. J. (2008). Ancient permafrost and a future, warmer Arctic. *Science, 321*(5896), 1648-1648.
Froese, D. G., Zazula, G. D., Westgate, J. A., Preece, S. J., Sanborn, P. T., Reyes, A. V., & Pearce, N. J. (2009b). The Klondike goldfields and Pleistocene environments of Beringia. *GSA Today, 19*(8), 4-10.
Fuchsman, C. A., Collins, R. E., Rocap, G., & Brazelton, W. J. (2017). Effect of the environment on horizontal gene transfer between bacteria and archaea. *PeerJ, 5*, e3865.
Gaglioti, B. V., Mann, D. H., Jones, B. M., Wooller, M. J., & Finney, B. P. (2016). High-resolution records detect human-caused changes to the boreal forest wildfire regime in interior Alaska. *The Holocene, 26*(7), 1064-1074.

Ganzert, L., Jurgens, G., Münster, U., & Wagner, D. (2007). Methanogenic communities in permafrost-affected soils of the Laptev Sea coast, Siberian Arctic, characterized by 16S rRNA gene fingerprints. *FEMS microbiology ecology, 59*(2), 476-488.

Gargaud, M., Martin, H., López-García, P., Montmerle, T., & Pascal, R. (2013). *Young sun, early earth and the origins of life: lessons for astrobiology*: Springer Science & Business Media.

Gilbert, M. T. P., Bandelt, H.-J., Hofreiter, M., & Barnes, I. (2005). Assessing ancient DNA studies. *Trends in Ecology & Evolution, 20*(10), 541-544.

Gilichinsky, D. (2002). Encyclopedia of environmental microbiology: Bitton, G., Ed.

Gilichinsky, D., Rivkina, E., Bakermans, C., Shcherbakova, V., Petrovskaya, L., Ozerskaya, S., . . . Pecheritsina, S. (2005). Biodiversity of cryopegs in permafrost. *FEMS microbiology ecology, 53*(1), 117-128.

Gilichinsky, D., Rivkina, E., Shcherbakova, V., Laurinavichuis, K., & Tiedje, J. (2003). Supercooled water brines within permafrost—an unknown ecological niche for microorganisms: a model for astrobiology. *Astrobiology, 3*(2), 331-341.

Gilichinsky, D., Soina, V., & Petrova, M. (1993). Cryoprotective properties of water in the Earth cryolithosphere and its role in exobiology. *Origins of Life and Evolution of the Biosphere, 23*(1), 65-75.

Gilichinsky, D., Vishnivetskaya, T., Petrova, M., Spirina, E., Mamykin, V., & Rivkina, E. (2008). Bacteria in permafrost *Psychrophiles: from biodiversity to biotechnology* (pp. 83-102): Springer.

Gilichinsky, D., Wilson, G., Friedmann, E., McKay, C., Sletten, R., Rivkina, E., . . . Kochkina, G. (2007). Microbial populations in Antarctic permafrost: biodiversity, state, age, and implication for astrobiology. *Astrobiology, 7*(2), 275-311.

Girguis, P. R., Orphan, V. J., Hallam, S. J., & DeLong, E. F. (2003). Growth and methane oxidation rates of anaerobic methanotrophic archaea in a continuous-flow bioreactor. *Applied and environmental Microbiology, 69*(9), 5472-5482.

Gittel, A., Bárta, J., Kohoutová, I., Mikutta, R., Owens, S., Gilbert, J., . . . Maerz, J. (2014). Distinct microbial communities associated with buried soils in the Siberian tundra. *The ISME journal, 8*(4), 841-853.

Godin, E., & Fortier, D. (2012). Geomorphology of a thermo-erosion gully, Bylot Island, Nunavut, Canada. *Canadian Journal of Earth Sciences, 49*(8), 979-986.

Goebel, M.-O., Woche, S. K., & Bachmann, J. (2009). Do soil aggregates really protect encapsulated organic matter against microbial decomposition? *Biologia, 64*(3), 443-448.

Goldfarb, K. C., Karaoz, U., Hanson, C. A., Santee, C. A., Bradford, M. A., Treseder, K. K., . . . Brodie, E. L. (2011). Differential growth responses of soil bacterial taxa to carbon substrates of varying chemical recalcitrance. *Frontiers in microbiology, 2*, 94.

González-Pastor, J. E., Hobbs, E. C., & Losick, R. (2003). Cannibalism by sporulating bacteria. *Science, 301*(5632), 510-513.

González-Oliver, A., Márquez-Morfín, L., Jiménez, J. C., & Torre-Blanco, A. (2001). Founding amerindian mitochondrial DNA lineages in ancient Maya from Xcaret, Quintana Roo. *American Journal of Physical Anthropology: The Official Publication of the American Association of Physical Anthropologists, 116*(3), 230-235.

Graham, D. W., Chaudhary, J. A., Hanson, R. S., & Arnold, R. G. (1993). Factors affecting competition between type I and type II methanotrophs in two-organism, continuous-flow reactors. *Microbial ecology, 25*(1), 1-17.

Grandcolas, P., Nattier, R., & Trewick, S. (2014). Relict species: a relict concept? *Trends in Ecology & Evolution, 29*(12), 655-663.
Grannas, A. M., Bogdal, C., Hageman, K. J., & Wania, F. (2013). The Role of the Global Cryosphere on the Fate of Organic Contaminants. *Atmospheric Chemistry and Physics, 13*(6), 3271.
Griffiths, B. S., & Philippot, L. (2013). Insights into the resistance and resilience of the soil microbial community. *FEMS microbiology reviews, 37*(2), 112-129.
Griffiths, R., & Whiteley, A. (2000). O′ Donnell, AG and Bailey, MJ (2000) Rapid method for coextraction of DNA and RNA from natural environments for analysis of ribosomal DNA-and rRNA-based microbial community composition. *Applied and environmental Microbiology, 66*, 5488-5491.
Grosse, G., Jones, B. M., & Arp, C. D. (2013). Thermokarst lakes, drainage, and drained basins.
Guérin, C. (1983). Paleoecology of Beringia, DM Hopkins, JV Matthews Jr., CE Schweger, SB Young (Eds.), Academic Press, Moscou (1982), ISBN: 0-12-355860-3: Elsevier Masson.
Gulledge, J., & Schimel, J. P. (1998). Moisture control over atmospheric CH4 consumption and CO2 production in diverse Alaskan soils. *Soil Biology and Biochemistry, 30*(8-9), 1127-1132.
Guo, D., & Sun, J. (2015). Permafrost thaw and associated settlement hazard onset timing over the Qinghai-Tibet engineering corridor. *International Journal of Disaster Risk Science, 6*(4), 347-358.
Guthrie, R. D. (2006). New carbon dates link climatic change with human colonization and Pleistocene extinctions. *Nature, 441*(7090), 207-209.
Guzman, L. M., Belin, D., Carson, M. J., & Beckwith, J. (1995). Tight regulation, modulation, and high-level expression by vectors containing the arabinose PBAD promoter. *Journal of bacteriology, 177*(14), 4121-4130. doi: 10.1128/jb.177.14.4121-4130.1995
Hackl, E., Zechmeister-Boltenstern, S., Bodrossy, L., & Sessitsch, A. (2004). Comparison of diversities and compositions of bacterial populations inhabiting natural forest soils. *Applied and environmental Microbiology, 70*(9), 5057-5065.
Hagelberg, E., Thomas, M. G., Cook, C. E., Sher, A. V., Baryshnikov, G. F., & Lister, A. M. (1994). DNA from ancient mammoth bones. *Nature, 370*(6488), 333-334.
Haile, J., Froese, D. G., MacPhee, R. D., Roberts, R. G., Arnold, L. J., Reyes, A. V., . . . Robinson, S. (2009). Ancient DNA reveals late survival of mammoth and horse in interior Alaska. *Proceedings of the National Academy of Sciences, 106*(52), 22352-22357.
Hajdas, I. (2008). Radiocarbon dating and its applications in Quaternary studies. *Eiszeitalter und Gegenwart Quaternary Science Journal, 57*(2), 24.
Halliwell, B., & Gutteridge, J. M. (2015). *Free radicals in biology and medicine*: Oxford University Press, USA.
Hansen, A. A., Herbert, R. A., Mikkelsen, K., Jensen, L. L., Kristoffersen, T., Tiedje, J. M., . . . Finster, K. W. (2007). Viability, diversity and composition of the bacterial community in a high Arctic permafrost soil from Spitsbergen, Northern Norway. *Environmental microbiology, 9*(11), 2870-2884.
Hanson, R. S., & Hanson, T. E. (1996). Methanotrophic bacteria. *Microbiological reviews, 60*(2), 439-471.
Hardie, M., & Doyle, R. (2012). Measuring soil salinity *Plant salt tolerance* (pp. 415-425): Springer.

Haroon, M. F., Hu, S., Shi, Y., Imelfort, M., Keller, J., Hugenholtz, P., . . . Tyson, G. W. (2013). Anaerobic oxidation of methane coupled to nitrate reduction in a novel archaeal lineage. *Nature, 500*(7464), 567-570.

Hartley, I. P., Hopkins, D. W., Garnett, M. H., Sommerkorn, M., & Wookey, P. A. (2008). Soil microbial respiration in arctic soil does not acclimate to temperature. *Ecology letters, 11*(10), 1092-1100.

Hartley, I. P., & Ineson, P. (2008). Substrate quality and the temperature sensitivity of soil organic matter decomposition. *Soil Biology and Biochemistry, 40*(7), 1567-1574.

Hawkes, C. V., & Keitt, T. H. (2015). Resilience vs. historical contingency in microbial responses to environmental change. *Ecology letters, 18*(7), 612-625.

Hazen, T. C., Rocha, A. M., & Techtmann, S. M. (2013). Advances in monitoring environmental microbes. *Current opinion in biotechnology, 24*(3), 526-533.

He, R., Wooller, M. J., Pohlman, J. W., Quensen, J., Tiedje, J. M., & Leigh, M. B. (2012a). Diversity of active aerobic methanotrophs along depth profiles of arctic and subarctic lake water column and sediments. *The ISME journal, 6*(10), 1937-1948.

He, R., Wooller, M. J., Pohlman, J. W., Quensen, J., Tiedje, J. M., & Leigh, M. B. (2012b). Shifts in identity and activity of methanotrophs in arctic lake sediments in response to temperature changes. *Applied and environmental Microbiology, 78*(13), 4715-4723.

Hébraud, M., & Potier, P. (1999). Cold shock response and low temperature adaptation in psychrotrophic bacteria. *Journal of molecular microbiology and biotechnology, 1*(2), 211-219.

Heilig, G. K. (1994). The greenhouse gas methane (CH 4): Sources and sinks, the impact of population growth, possible interventions. *Population and environment, 16*(2), 109-137.

Heimann, M., & Reichstein, M. (2008). Terrestrial ecosystem carbon dynamics and climate feedbacks. *Nature, 451*(7176), 289-292.

Henckel, T., Roslev, P., & Conrad, R. (2000). Effects of O2 and CH4 on presence and activity of the indigenous methanotrophic community in rice field soil. *Environmental microbiology, 2*(6), 666-679.

Hernandez, M. E., Beck, D. A., Lidstrom, M. E., & Chistoserdova, L. (2015). Oxygen availability is a major factor in determining the composition of microbial communities involved in methane oxidation. *PeerJ, 3*, e801.

Hicks Pries, C. E., Schuur, E. A., & Crummer, K. G. (2013). Thawing permafrost increases old soil and autotrophic respiration in tundra: Partitioning ecosystem respiration using δ13C andΔ 14C. *Global Change Biology, 19*(2), 649-661.

Higuchi, R., Bowman, B., Freiberger, M., Ryder, O. A., & Wilson, A. C. (1984). DNA sequences from the quagga, an extinct member of the horse family. *Nature, 312*(5991), 282-284.

Hinojosa, M. B., Parra, A., Laudicina, V. A., & Moreno, J. M. (2016). Post-fire soil functionality and microbial community structure in a Mediterranean shrubland subjected to experimental drought. *Science of the Total Environment, 573*, 1178-1189.

Hinzman, L., Kane, D., Gieck, R., & Everett, K. (1991). Hydrologic and thermal properties of the active layer in the Alaskan Arctic. *Cold Regions Science and Technology, 19*(2), 95-110.

Ho, A., Lüke, C., & Frenzel, P. (2011). Recovery of methanotrophs from disturbance: population dynamics, evenness and functioning. *The ISME journal, 5*(4), 750-758.

Ho, A., van den Brink, E., Reim, A., Krause, S., & Bodelier, P. L. (2016). Recurrence and frequency of disturbance have cumulative effect on methanotrophic activity, abundance, and community structure. *Frontiers in microbiology, 6*, 1493.
Ho, J. (2010). The implications of Arctic sea ice decline on shipping. *Marine Policy, 34*(3), 713-715.
Hodgkins, S. B., Tfaily, M. M., McCalley, C. K., Logan, T. A., Crill, P. M., Saleska, S. R., . . . Chanton, J. P. (2014). Changes in peat chemistry associated with permafrost thaw increase greenhouse gas production. *Proceedings of the National Academy of Sciences, 111*(16), 5819-5824.
Hoffecker, J. F., Elias, S. A., & O'Rourke, D. H. (2014). Out of Beringia? *Science, 343*(6174), 979-980.
Hoffmann, T., & Bremer, E. (2011). Protection of Bacillus subtilis against cold stress via compatible-solute acquisition. *Journal of bacteriology, 193*(7), 1552-1562.
Hofreiter, M., Serre, D., Poinar, H. N., Kuch, M., & Pääbo, S. (2001). ancient DNA. *Nature Reviews Genetics, 2*(5), 353-359.
Høj, L., Rusten, M., Haugen, L. E., Olsen, R. A., & Torsvik, V. L. (2006). Effects of water regime on archaeal community composition in Arctic soils. *Environmental microbiology, 8*(6), 984-996.
Holmes, A. J., Owens, N. J., & Murrell, J. C. (1995). Detection of novel marine methanotrophs using phylogenetic and functional gene probes after methane enrichment. *Microbiology, 141*(8), 1947-1955.
Holtmann, G., & Bremer, E. (2004). Thermoprotection of Bacillus subtilis by exogenously provided glycine betaine and structurally related compatible solutes: involvement of Opu transporters. *Journal of bacteriology, 186*(6), 1683-1693.
Hope, C., & Schaefer, K. (2016). Economic impacts of carbon dioxide and methane released from thawing permafrost. *Nature climate change, 6*(1), 56-59.
Horowitz, N., Cameron, R. E., & Hubbard, J. S. (1972). Microbiology of the dry valleys of Antarctica. *Science, 176*(4032), 242-245.
Hoss, M., Paabo, S., & Vereshchagin, N. (1994). Mammoth DNA sequences. *Nature, 370*(6488), 333-333.
Hostettler, L., Grundy, L., Käser-Pébernard, S., Wicky, C., Schafer, W. R., & Glauser, D. A. (2017). The bright fluorescent protein mNeonGreen facilitates protein expression analysis in vivo. *G3: Genes, Genomes, Genetics, 7*(2), 607-615.
Hu, G., Zhao, L., Li, R., Wu, X., Wu, T., Zhu, X., . . . Zou, D. (2019). Simulation of land surface heat fluxes in permafrost regions on the Qinghai-Tibetan Plateau using CMIP5 models. *Atmospheric Research, 220*, 155-168.
Hugelius, G., & Kuhry, P. (2009). Landscape partitioning and environmental gradient analyses of soil organic carbon in a permafrost environment. *Global Biogeochemical Cycles, 23*(3).
Hultman, J., Waldrop, M. P., Mackelprang, R., David, M. M., McFarland, J., Blazewicz, S. J., . . . Shah, M. B. (2015). Multi-omics of permafrost, active layer and thermokarst bog soil microbiomes. *Nature, 521*(7551), 208-212.
Hutchins, D. A., Jansson, J. K., Remais, J. V., Rich, V. I., Singh, B. K., & Trivedi, P. (2019). Climate change microbiology—problems and perspectives. *Nature Reviews Microbiology, 17*(6), 391-396.

Isenring, P., & Forbush, B. (2001). Ion transport and ligand binding by the Na–K–Cl cotransporter, structure–function studies. *Comparative Biochemistry and Physiology Part A: Molecular & Integrative Physiology, 130*(3), 487-497.
Islam, T., Jensen, S., Reigstad, L. J., Larsen, Ø., & Birkeland, N.-K. (2008). Methane oxidation at 55 C and pH 2 by a thermoacidophilic bacterium belonging to the Verrucomicrobia phylum. *Proceedings of the National Academy of Sciences, 105*(1), 300-304.
Itcus, C., Pascu, M. D., Lavin, P., Perşoiu, A., Iancu, L., & Purcarea, C. (2018). Bacterial and archaeal community structures in perennial cave ice. *Scientific Reports, 8*(1), 1-14.
Jackson, B. E., & McInerney, M. J. (2002). Anaerobic microbial metabolism can proceed close to thermodynamic limits. *Nature, 415*(6870), 454-456.
Janssen, P. H. (2006). Identifying the dominant soil bacterial taxa in libraries of 16S rRNA and 16S rRNA genes. *Applied and environmental Microbiology, 72*(3), 1719-1728.
Jansson, J. K., & Taş, N. (2014). The microbial ecology of permafrost. *Nature Reviews Microbiology, 12*(6), 414-425.
Jenny, H. (1994). *Factors of soil formation: a system of quantitative pedology*: Courier Corporation.
Johnson, C. J. (2013). Identifying ecological thresholds for regulating human activity: Effective conservation or wishful thinking? *Biological Conservation, 168*, 57-65.
Johnson, S. S., Hebsgaard, M. B., Christensen, T. R., Mastepanov, M., Nielsen, R., Munch, K., . . . Bunce, M. (2007). Ancient bacteria show evidence of DNA repair. *Proceedings of the National Academy of Sciences, 104*(36), 14401-14405.
Jorgenson, M. T., Racine, C. H., Walters, J. C., & Osterkamp, T. E. (2001). Permafrost degradation and ecological changes associated with a warmingclimate in central Alaska. *Climatic Change, 48*(4), 551-579.
Juck, D., Whissell, G., Steven, B., Pollard, W., McKay, C., Greer, C., & Whyte, L. (2005). Utilization of fluorescent microspheres and a green fluorescent protein-marked strain for assessment of microbiological contamination of permafrost and ground ice core samples from the Canadian High Arctic. *Applied and environmental Microbiology, 71*(2), 1035-1041.
Jung, G., & Kunstmann, H. (2007). High-resolution regional climate modeling for the Volta region of West Africa. *Journal of Geophysical Research: Atmospheres, 112*(D23).
Junge, K., Eicken, H., Swanson, B. D., & Deming, J. W. (2006). Bacterial incorporation of leucine into protein down to− 20 C with evidence for potential activity in sub-eutectic saline ice formations. *Cryobiology, 52*(3), 417-429.
Kallmeyer, J. (2017). Contamination control for scientific drilling operations *Advances in Applied Microbiology* (Vol. 98, pp. 61-91): Elsevier.
Kallmeyer, J., Mangelsdorf, K., Cragg, B., & Horsfield, B. (2006). Techniques for contamination assessment during drilling for terrestrial subsurface sediments. *Geomicrobiology Journal, 23*(3-4), 227-239.
Kallmeyer, J., Pockalny, R., Adhikari, R. R., Smith, D. C., & D'Hondt, S. (2012). Global distribution of microbial abundance and biomass in subseafloor sediment. *Proceedings of the National Academy of Sciences, 109*(40), 16213-16216. doi: 10.1073/pnas.1203849109
Kalmár, T., Bachrati, C. Z., Marcsik, A., & Raskó, I. (2000). A simple and efficient method for PCR amplifiable DNA extraction from ancient bones. *Nucleic acids research, 28*(12), e67-e67.

Kampichler, C., Kandeler, E., Bardgett, R. D., Jones, T. H., & Thompson, L. J. (1998). Impact of elevated atmospheric CO2 concentration on soil microbial biomass and activity in a complex, weedy field model ecosystem. *Global Change Biology, 4*(3), 335-346.

Kandeler, E., Tscherko, D., Bardgett, R., Hobbs, P., Kampichler, C., & Jones, T. (1998). The response of soil microorganisms and roots to elevated CO2 and temperature in a terrestrial model ecosystem. *Plant and Soil, 202*(2), 251-262.

Kanevskiy, M., Jorgenson, T., Shur, Y., O'Donnell, J. A., Harden, J. W., Zhuang, Q., & Fortier, D. (2014). Cryostratigraphy and permafrost evolution in the lacustrine lowlands of west-central Alaska. *Permafrost and Periglacial Processes, 25*(1), 14-34.

Kaplan, L., & Cory, R. (2016). Dissolved organic matter in stream ecosystems: forms, functions, and fluxes of watershed Tea *Stream ecosystems in a changing environment* (pp. 241-320): Elsevier.

Kappen, L. (1993). Lichens in the Antarctic region. *Antarctic microbiology*, 433-490.

Kasprzak, J. M., Czerwoniec, A., & Bujnicki, J. M. (2012). Molecular evolution of dihydrouridine synthases. *BMC bioinformatics, 13*(1), 153.

Kassambara, A. (2017). *Practical guide to principal component methods in R: PCA, M (CA), FAMD, MFA, HCPC, factoextra* (Vol. 2): STHDA.

Kaufman, D. S., Ager, T. A., Anderson, N. J., Anderson, P. M., Andrews, J. T., Bartlein, P. J., . . . Duvall, M. L. (2004). Holocene thermal maximum in the western Arctic (0–180 W). *Quaternary Science Reviews, 23*(5-6), 529-560.

Kemp, B. M., & Smith, D. G. (2005). Use of bleach to eliminate contaminating DNA from the surface of bones and teeth. *Forensic science international, 154*(1), 53-61.

Kempf, B., & Bremer, E. (1998). Uptake and synthesis of compatible solutes as microbial stress responses to high-osmolality environments. *Archives of microbiology, 170*(5), 319-330.

Kennett, D. J., Kennett, J. P., West, A., Mercer, C., Hee, S. Q., Bement, L., . . . Wolbach, W. S. (2009). Nanodiamonds in the Younger Dryas boundary sediment layer. *Science, 323*(5910), 94-94.

Kennett, J. P., Cannariato, K. G., Hendy, I. L., & Behl, R. J. (2000). Carbon isotopic evidence for methane hydrate instability during Quaternary interstadials. *Science, 288*(5463), 128-133.

Khachane, A. N., Timmis, K. N., & dos Santos, V. A. M. (2005). Uracil content of 16S rRNA of thermophilic and psychrophilic prokaryotes correlates inversely with their optimal growth temperatures. *Nucleic acids research, 33*(13), 4016-4022.

Khadem, A. F., Pol, A., Wieczorek, A., Mohammadi, S. S., Francoijs, K.-J., Stunnenberg, H. G., . . . den Camp, H. J. O. (2011). Autotrophic methanotrophy in Verrucomicrobia: Methylacidiphilum fumariolicumSolV uses the Calvin-Benson-Bassham cycle for carbon dioxide fixation. *Journal of bacteriology, 193*(17), 4438-4446.

Khmelenina, V., Makutina, V., Kalyuzhnaya, M., Rivkina, E., Gilichinsky, D., & Trotsenko, Y. A. (2002). *Discovery of viable methanotrophic bacteria in permafrost sediments of northeast Siberia.* Paper presented at the Doklady Biological Sciences.

Khmelenina, V. N., Murrell, J. C., Smith, T. J., & Trotsenko, Y. A. (2018). Physiology and biochemistry of the aerobic methanotrophs.

Kieft, T. L., Amy, P. S., Brockman, F. J., Fredrickson, J. K., Bjornstad, B. N., & Rosacker, L. L. (1993). Microbial abundance and activities in relation to water potential in the vadose zones of arid and semiarid sites. *Microbial ecology, 26*(1), 59-78.

King, A. J., Freeman, K. R., McCormick, K. F., Lynch, R. C., Lozupone, C., Knight, R., & Schmidt, S. K. (2010). Biogeography and habitat modelling of high-alpine bacteria. *Nature communications, 1*(1), 1-6.
Kip, N., Ouyang, W., van Winden, J., Raghoebarsing, A., van Niftrik, L., Pol, A., . . . Reichart, G.-J. (2011). Detection, isolation, and characterization of acidophilic methanotrophs from Sphagnum mosses. *Applied and environmental Microbiology, 77*(16), 5643-5654.
Knapp, M., Clarke, A. C., Horsburgh, K. A., & Matisoo-Smith, E. A. (2012). Setting the stage–Building and working in an ancient DNA laboratory. *Annals of Anatomy-Anatomischer Anzeiger, 194*(1), 3-6.
Knief, C. (2015). Diversity and habitat preferences of cultivated and uncultivated aerobic methanotrophic bacteria evaluated based on pmoA as molecular marker. *Frontiers in microbiology, 6*, 1346.
Knief, C., Lipski, A., & Dunfield, P. F. (2003). Diversity and activity of methanotrophic bacteria in different upland soils. *Applied and environmental Microbiology, 69*(11), 6703-6714.
Knoblauch, C., Beer, C., Liebner, S., Grigoriev, M. N., & Pfeiffer, E.-M. (2018). Methane production as key to the greenhouse gas budget of thawing permafrost. *Nature climate change, 8*(4), 309-312.
Knoblauch, C., Beer, C., Sosnin, A., Wagner, D., & Pfeiffer, E. M. (2013). Predicting long-term carbon mineralization and trace gas production from thawing permafrost of N ortheast S iberia. *Global Change Biology, 19*(4), 1160-1172.
Koch, P. L., & Barnosky, A. D. (2006). Late Quaternary extinctions: state of the debate. *Annual Review of Ecology, Evolution, and Systematics, 37*.
Koh, H. Y., Park, H., Lee, J. H., Han, S. J., Sohn, Y. C., & Lee, S. G. (2017). Proteomic and transcriptomic investigations on cold-responsive properties of the psychrophilic A ntarctic bacterium P sychrobacter sp. PAMC 21119 at subzero temperatures. *Environmental microbiology, 19*(2), 628-644.
Köhler, P., Knorr, G., & Bard, E. (2014). Permafrost thawing as a possible source of abrupt carbon release at the onset of the Bølling/Allerød. *Nature communications, 5*(1), 1-10.
Kolb, S. (2009). The quest for atmospheric methane oxidizers in forest soils. *Environmental microbiology reports, 1*(5), 336-346.
Konings, W. N., Albers, S.-V., Koning, S., & Driessen, A. J. (2002). The cell membrane plays a crucial role in survival of bacteria and archaea in extreme environments. *Antonie Van Leeuwenhoek, 81*(1-4), 61-72.
Korlević, P., Gerber, T., Gansauge, M.-T., Hajdinjak, M., Nagel, S., Aximu-Petri, A., & Meyer, M. (2015). Reducing microbial and human contamination in DNA extractions from ancient bones and teeth. *Biotechniques, 59*(2), 87-93.
Kotler, E., & Burn, C. R. (2000). Cryostratigraphy of the Klondike" muck" deposits, west-central Yukon Territory. *Canadian Journal of Earth Sciences, 37*(6), 849-861.
Koven, C. D., Riley, W. J., & Stern, A. (2013). Analysis of permafrost thermal dynamics and response to climate change in the CMIP5 Earth System Models. *Journal of climate, 26*(6), 1877-1900.
Kowalchuk, G. A., Buma, D. S., de Boer, W., Klinkhamer, P. G., & van Veen, J. A. (2002). Effects of above-ground plant species composition and diversity on the diversity of soil-borne microorganisms. *Antonie Van Leeuwenhoek, 81*(1-4), 509.

Kraft, N. J., Adler, P. B., Godoy, O., James, E. C., Fuller, S., & Levine, J. M. (2015a). Community assembly, coexistence and the environmental filtering metaphor. *Functional Ecology, 29*(5), 592-599.

Kraft, N. J. B., Adler, P. B., Godoy, O., James, E. C., Fuller, S., & Levine, J. M. (2015b). Community assembly, coexistence and the environmental filtering metaphor. *Functional Ecology, 29*(5), 592-599. doi: https://doi.org/10.1111/1365-2435.12345

Krivushin, K., Kondrashov, F., Shmakova, L., Tutukina, M., Petrovskaya, L., & Rivkina, E. (2015). Two metagenomes from Late Pleistocene northeast Siberian permafrost. *Genome announcements, 3*(1).

Kuffner, M., Hai, B., Rattei, T., Melodelima, C., Schloter, M., Zechmeister-Boltenstern, S., . . . Sessitsch, A. (2012). Effects of season and experimental warming on the bacterial community in a temperate mountain forest soil assessed by 16S rRNA gene pyrosequencing. *FEMS microbiology ecology, 82*(3), 551-562.

Kulakova, L., Galkin, A., Nakayama, T., Nishino, T., & Esaki, N. (2004). Cold-active esterase from Psychrobacter sp. Ant300: gene cloning, characterization, and the effects of Gly→ Pro substitution near the active site on its catalytic activity and stability. *Biochimica et Biophysica Acta (BBA)-Proteins and Proteomics, 1696*(1), 59-65.

Kumaresan, D., Stralis-Pavese, N., Abell, G. C., Bodrossy, L., & Murrell, J. C. (2011). Physical disturbance to ecological niches created by soil structure alters community composition of methanotrophs. *Environmental microbiology reports, 3*(5), 613-621.

Kunin, V., Engelbrektson, A., Ochman, H., & Hugenholtz, P. (2010). Wrinkles in the rare biosphere: pyrosequencing errors can lead to artificial inflation of diversity estimates. *Environmental microbiology, 12*(1), 118-123.

Kuria, D. N. (2012). Climate Change-Realities, Impacts Over Ice Cap, Sea Level and Risks: Intech Open.

Lacelle, D., Fontaine, M., Pellerin, A., Kokelj, S. V., & Clark, I. D. (2019). Legacy of Holocene landscape changes on soil biogeochemistry: a perspective from paleo-active layers in northwestern Canada. *Journal of Geophysical Research: Biogeosciences, 124*(9), 2662-2679.

Lacelle, D., Radtke, K., Clark, I. D., Fisher, D., Lauriol, B., Utting, N., & Whyte, L. G. (2011). Geomicrobiology and occluded O2–CO2–Ar gas analyses provide evidence of microbial respiration in ancient terrestrial ground ice. *Earth and Planetary Science Letters, 306*(1-2), 46-54.

Lamb, E. G., Han, S., Lanoil, B. D., Henry, G. H., Brummell, M. E., Banerjee, S., & Siciliano, S. D. (2011). A High Arctic soil ecosystem resists long-term environmental manipulations. *Global Change Biology, 17*(10), 3187-3194.

Langenheder, S., & Székely, A. J. (2011). Species sorting and neutral processes are both important during the initial assembly of bacterial communities. *The ISME journal, 5*(7), 1086-1094.

Lantuit, H., & Pollard, W. (2008). Fifty years of coastal erosion and retrogressive thaw slump activity on Herschel Island, southern Beaufort Sea, Yukon Territory, Canada. *Geomorphology, 95*(1-2), 84-102.

Lau, M. C., Stackhouse, B., Layton, A. C., Chauhan, A., Vishnivetskaya, T., Chourey, K., . . . Lamarche-Gagnon, G. (2015). An active atmospheric methane sink in high Arctic mineral cryosols. *The ISME journal, 9*(8), 1880-1891.

Lauber, C. L., Hamady, M., Knight, R., & Fierer, N. (2009a). Pyrosequencing-based assessment of soil pH as a predictor of soil bacterial community structure at the continental scale. *Applied and environmental Microbiology, 75*(15), 5111-5120.
Lauber, C. L., Hamady, M., Knight, R., & Fierer, N. (2009b). Soil pH as a predictor of soil bacterial community structure at the continental scale: a pyrosequencing-based assessment. *Applied and environmental Microbiology*.
Lawrence, D. M., & Slater, A. G. (2005). A projection of severe near-surface permafrost degradation during the 21st century. *Geophysical Research Letters, 32*(24).
Lawrence, J. E., & Hornberger, G. M. (2007). Soil moisture variability across climate zones. *Geophysical Research Letters, 34*(20).
Lawton, T. J., & Rosenzweig, A. C. (2016). Methane-oxidizing enzymes: an upstream problem in biological gas-to-liquids conversion. *Journal of the American Chemical Society, 138*(30), 9327-9340.
Leadley, P. (2010). *Biodiversity scenarios: projections of 21st century change in biodiversity, and associated ecosystem services: a technical report for the global biodiversity outlook 3*: UNEP/Earthprint.
Lennon, J., Muscarella, M., Placella, S., & Lehmkuhl, B. (2018). How, when, and where relic DNA affects microbial diversity. *MBio, 9*(3).
Lennon, J. T., & Jones, S. E. (2011). Microbial seed banks: the ecological and evolutionary implications of dormancy. *Nature Reviews Microbiology, 9*(2), 119-130.
Lenton, T. M. (2012). Arctic climate tipping points. *Ambio, 41*(1), 10-22.
Levy, M., & Miller, S. L. (1998). The stability of the RNA bases: implications for the origin of life. *Proceedings of the National Academy of Sciences, 95*(14), 7933-7938.
Lewis, S. L., & Maslin, M. A. (2015). Defining the anthropocene. *Nature, 519*(7542), 171-180.
Lewkowicz, A. G., & Harris, C. (2005). Morphology and geotechnique of active-layer detachment failures in discontinuous and continuous permafrost, northern Canada. *Geomorphology, 69*(1-4), 275-297.
Li, C., & Born, A. (2019). Coupled atmosphere-ice-ocean dynamics in Dansgaard-Oeschger events. *Quaternary Science Reviews, 203*, 1-20.
Li, D., Sharp, J. O., Saikaly, P. E., Ali, S., Alidina, M., Alarawi, M. S., . . . Drewes, J. E. (2012). Dissolved organic carbon influences microbial community composition and diversity in managed aquifer recharge systems. *Applied and environmental Microbiology, 78*(19), 6819-6828.
Li, L., Mendis, N., Trigui, H., Oliver, J. D., & Faucher, S. P. (2014). The importance of the viable but non-culturable state in human bacterial pathogens. *Frontiers in microbiology, 5*, 258.
Liang, R., Lau, M., Vishnivetskaya, T., Lloyd, K. G., Wang, W., Wiggins, J., . . . Onstott, T. C. (2019). Predominance of anaerobic, spore-forming bacteria in metabolically active microbial communities from ancient Siberian permafrost. *Applied and environmental Microbiology, 85*(15), e00560-00519.
Liebner, S., Rublack, K., Stuehrmann, T., & Wagner, D. (2009). Diversity of aerobic methanotrophic bacteria in a permafrost active layer soil of the Lena Delta, Siberia. *Microbial ecology, 57*(1), 25-35.
Liebner, S., & Wagner, D. (2007). Abundance, distribution and potential activity of methane oxidizing bacteria in permafrost soils from the Lena Delta, Siberia. *Environmental microbiology, 9*(1), 107-117.

Lim, C., & Jackson, M. (1982). In methods of soil analysis. Part 2. *Chemical and microbiological properties, 2nd ed. SSSA, Madison, WI*, 1-12.
Lindahl, T. (1993). Instability and decay of the primary structure of DNA. *Nature, 362*(6422), 709-715.
Lindquist, J. A., & Mertens, P. R. (2018). Cold shock proteins: from cellular mechanisms to pathophysiology and disease. *Cell Communication and Signaling, 16*(1), 63.
Llamas, B., Valverde, G., Fehren-Schmitz, L., Weyrich, L. S., Cooper, A., & Haak, W. (2017). From the field to the laboratory: Controlling DNA contamination in human ancient DNA research in the high-throughput sequencing era. *STAR: Science & Technology of Archaeological Research, 3*(1), 1-14.
Logan, S. (1982). The origin and status of the Arrhenius equation. *Journal of Chemical Education, 59*(4), 279.
Lorenzen, E. D., Nogués-Bravo, D., Orlando, L., Weinstock, J., Binladen, J., Marske, K. A., . . . Nielsen, R. (2011). Species-specific responses of Late Quaternary megafauna to climate and humans. *Nature, 479*(7373), 359-364.
Love, M. I., Huber, W., & Anders, S. (2014). Moderated estimation of fold change and dispersion for RNA-seq data with DESeq2. *Genome biology, 15*(12), 550.
Lu, P., Liu, T., Ni, B.-J., Guo, J., Yuan, Z., & Hu, S. (2019). Growth kinetics of Candidatus 'Methanoperedens nitroreducens' enriched in a laboratory reactor. *Science of the Total Environment, 659*, 442-450.
Luesken, F. A., Zhu, B., van Alen, T. A., Butler, M. K., Diaz, M. R., Song, B., . . . Ettwig, K. F. (2011). pmoA primers for detection of anaerobic methanotrophs. *Applied and environmental Microbiology, 77*(11), 3877-3880.
Lundquist, E., Scow, K., Jackson, L., Uesugi, S., & Johnson, C. (1999). Rapid response of soil microbial communities from conventional, low input, and organic farming systems to a wet/dry cycle. *Soil Biology and Biochemistry, 31*(12), 1661-1675.
Luo, Y. (2007). Terrestrial carbon–cycle feedback to climate warming. *Annu. Rev. Ecol. Evol. Syst., 38*, 683-712.
Luo, Y., Wan, S., Hui, D., & Wallace, L. L. (2001). Acclimatization of soil respiration to warming in a tall grass prairie. *Nature, 413*(6856), 622-625.
Lydolph, M. C., Jacobsen, J., Arctander, P., Gilbert, M. T. P., Gilichinsky, D. A., Hansen, A. J., . . . Lange, L. (2005). Beringian paleoecology inferred from permafrost-preserved fungal DNA. *Applied and environmental Microbiology, 71*(2), 1012-1017.
Lyu, Z., Shao, N., Akinyemi, T., & Whitman, W. B. (2018). Methanogenesis. *Current Biology, 28*(13), R727-R732.
Macdonald, F. A., Schmitz, M. D., Crowley, J. L., Roots, C. F., Jones, D. S., Maloof, A. C., . . . Schrag, D. P. (2010). Calibrating the cryogenian. *Science, 327*(5970), 1241-1243.
MacDonald, G. M., Beilman, D. W., Kremenetski, K. V., Sheng, Y., Smith, L. C., & Velichko, A. A. (2006). Rapid early development of circumarctic peatlands and atmospheric CH4 and CO2 variations. *Science, 314*(5797), 285-288.
Mackelprang, R., Burkert, A., Haw, M., Mahendrarajah, T., Conaway, C. H., Douglas, T. A., & Waldrop, M. P. (2017). Microbial survival strategies in ancient permafrost: insights from metagenomics. *The ISME journal, 11*(10), 2305-2318.
Mackelprang, R., Saleska, S. R., Jacobsen, C. S., Jansson, J. K., & Taş, N. (2016). Permafrost meta-omics and climate change. *Annual Review of Earth and Planetary Sciences, 44*, 439-462.

Mackelprang, R., Waldrop, M. P., DeAngelis, K. M., David, M. M., Chavarria, K. L., Blazewicz, S. J., . . . Jansson, J. K. (2011). Metagenomic analysis of a permafrost microbial community reveals a rapid response to thaw. *Nature, 480*(7377), 368-371.

Mandakovic, D., Rojas, C., Maldonado, J., Latorre, M., Travisany, D., Delage, E., . . . Fernández-Gómez, B. (2018). Structure and co-occurrence patterns in microbial communities under acute environmental stress reveal ecological factors fostering resilience. *Scientific Reports, 8*(1), 5875.

Mann, P. J., Spencer, R. G., Hernes, P. J., Six, J., Aiken, G. R., Tank, S. E., . . . Holmes, R. M. (2016). Pan-Arctic trends in terrestrial dissolved organic matter from optical measurements. *Frontiers in Earth Science, 4*, 25.

Margesin, R. (2008). *Permafrost soils* (Vol. 16): Springer Science & Business Media.

Margesin, R., Schinner, F., Marx, J.-C., & Gerday, C. (2008). *Psychrophiles: from biodiversity to biotechnology*: Springer.

Marques, V. S. (2012). Thoughts and Considerations. CLIMATE CHANGE AS THE DEFINING CRISIS FOR THE 21st CENTURY. *JANUS. NET, e-journal of International Relations, 3*(2), 165-168.

Martineau, C., Pan, Y., Bodrossy, L., Yergeau, E., Whyte, L. G., & Greer, C. W. (2014). Atmospheric methane oxidizers are present and active in Canadian high Arctic soils. *FEMS microbiology ecology, 89*(2), 257-269.

Martineau, C., Whyte, L. G., & Greer, C. W. (2010). Stable isotope probing analysis of the diversity and activity of methanotrophic bacteria in soils from the Canadian high Arctic. *Applied and environmental Microbiology, 76*(17), 5773-5784.

Martínez-Meyer, E., Townsend Peterson, A., & Hargrove, W. W. (2004). Ecological niches as stable distributional constraints on mammal species, with implications for Pleistocene extinctions and climate change projections for biodiversity. *Global Ecology and Biogeography, 13*(4), 305-314.

Mascarelli, A. (2009). A sleeping giant? *Nature climate change, 1*(904), 46-49.

Masini, J. C., Abate, G., Lima, E. C., Hahn, L. C., Nakamura, M. S., Lichtig, J., & Nagatomy, H. R. (1998). Comparison of methodologies for determination of carboxylic and phenolic groups in humic acids. *Analytica Chimica Acta, 364*(1-3), 223-233.

Maslin, M., Owen, M., Betts, R., Day, S., Dunkley Jones, T., & Ridgwell, A. (2010). Gas hydrates: past and future geohazard? *Philosophical Transactions of the Royal Society A: Mathematical, Physical and Engineering Sciences, 368*(1919), 2369-2393.

Maslin, M., Owen, M., Day, S., & Long, D. (2004). Linking continental-slope failures and climate change: testing the clathrate gun hypothesis. *Geology, 32*(1), 53-56.

Matheson, C. D., Gurney, C., Esau, N., & Lehto, R. (2010). Assessing PCR inhibition from humic substances. *The Open Enzyme Inhibition Journal, 3*(1), 38-45.

Maynard, D., Kalra, Y., & Crumbaugh, J. (1993). Nitrate and exchangeable ammonium nitrogen. *Soil sampling and methods of analysis, 1*.

Mayr, M. J., Zimmermann, M., Dey, J., Brand, A., Wehrli, B., & Bürgmann, H. (2020a). Growth and rapid succession of methanotrophs effectively limit methane release during lake overturn. *Communications biology, 3*(1), 1-9.

Mayr, M. J., Zimmermann, M., Guggenheim, C., Brand, A., & Bürgmann, H. (2020b). Niche partitioning of methane-oxidizing bacteria along the oxygen–methane counter gradient of stratified lakes. *The ISME journal, 14*(1), 274-287.

McCalley, C. K. (2020). Methane-eating microbes. *Nature climate change, 10*(4), 275-276.

McCalley, C. K., Woodcroft, B. J., Hodgkins, S. B., Wehr, R. A., Kim, E.-H., Mondav, R., . . . Tyson, G. W. (2014). Methane dynamics regulated by microbial community response to permafrost thaw. *Nature, 514*(7523), 478-481.

McDonald, I., Kenna, E., & Murrell, J. (1995). Detection of methanotrophic bacteria in environmental samples with the PCR. *Applied and environmental Microbiology, 61*(1), 116-121.

McDonald, I. R., Bodrossy, L., Chen, Y., & Murrell, J. C. (2008). Molecular ecology techniques for the study of aerobic methanotrophs. *Applied and environmental Microbiology, 74*(5), 1305-1315.

McGuire, A., Joyce, L., Kicklighter, D., Melillo, J., Esser, G., & Vorosmarty, C. (1993). Productivity response of climax temperate forests to elevated temperature and carbon dioxide: a North American comparison between two global models. *Climatic Change, 24*(4), 287-310.

McGuire, A. D., Anderson, L. G., Christensen, T. R., Dallimore, S., Guo, L., Hayes, D. J., . . . Roulet, N. (2009). Sensitivity of the carbon cycle in the Arctic to climate change. *Ecological Monographs, 79*(4), 523-555.

McGuire, A. D., Macdonald, R. W., Schuur, E. A., Harden, J. W., Kuhry, P., Hayes, D. J., . . . Heimann, M. (2010). The carbon budget of the northern cryosphere region. *Current Opinion in Environmental Sustainability, 2*(4), 231-236.

McHale, G., Newton, M., & Shirtcliffe, N. (2005). Water-repellent soil and its relationship to granularity, surface roughness and hydrophobicity: a materials science view. *European Journal of Soil Science, 56*(4), 445-452.

McKew, B. A., Taylor, J. D., McGenity, T. J., & Underwood, G. J. (2011). Resistance and resilience of benthic biofilm communities from a temperate saltmarsh to desiccation and rewetting. *The ISME journal, 5*(1), 30-41.

McMahon, S. K., Wallenstein, M. D., & Schimel, J. P. (2009). Microbial growth in Arctic tundra soil at− 2 C. *Environmental microbiology reports, 1*(2), 162-166.

McMurdie, P. J., & Holmes, S. (2013). phyloseq: an R package for reproducible interactive analysis and graphics of microbiome census data. *PloS one, 8*(4), e61217.

McMurdie, P. J., & Holmes, S. (2014). Waste not, want not: why rarefying microbiome data is inadmissible. *PLoS Comput Biol, 10*(4), e1003531.

Megonigal, J. P., Hines, M., & Visscher, P. (2004). Anaerobic metabolism: linkages to trace gases and aerobic processes. *Biogeochemistry*.

Mehta, A., & Haber, J. E. (2014). Sources of DNA double-strand breaks and models of recombinational DNA repair. *Cold Spring Harbor perspectives in biology, 6*(9), a016428.

Melillo, J., Steudler, P., Aber, J., Newkirk, K., Lux, H., Bowles, F., . . . Morrisseau, S. (2002). Soil warming and carbon-cycle feedbacks to the climate system. *Science, 298*(5601), 2173-2176.

Melillo, J. M., Frey, S. D., DeAngelis, K. M., Werner, W. J., Bernard, M. J., Bowles, F. P., . . . Grandy, A. S. (2017). Long-term pattern and magnitude of soil carbon feedback to the climate system in a warming world. *Science, 358*(6359), 101-105.

Melvin, A. M., Larsen, P., Boehlert, B., Neumann, J. E., Chinowsky, P., Espinet, X., . . . Bothner, A. (2017). Climate change damages to Alaska public infrastructure and the economics of proactive adaptation. *Proceedings of the National Academy of Sciences, 114*(2), E122-E131.

Metcalfe, D. B. (2017). Microbial change in warming soils. *Science, 358*(6359), 41-42.

Michel, B. (2005). After 30 years of study, the bacterial SOS response still surprises us. *PLoS Biol, 3*(7), e255.
Mielke Jr, P. W., Berry, K. J., & Johnson, E. S. (1976). Multi-response permutation procedures for a priori classifications. *Communications in Statistics-Theory and Methods, 5*(14), 1409-1424.
Mikkelson, K. M., Lozupone, C. A., & Sharp, J. O. (2016). Altered edaphic parameters couple to shifts in terrestrial bacterial community structure associated with insect-induced tree mortality. *Soil Biology and Biochemistry, 95*, 19-29.
Millar, C. D., & Lambert, D. M. (2013). Towards a million-year-old genome. *Nature, 499*(7456), 34-36.
Miller, G. H., Alley, R. B., Brigham-Grette, J., Fitzpatrick, J. J., Polyak, L., Serreze, M. C., & White, J. W. (2010). Arctic amplification: can the past constrain the future? *Quaternary Science Reviews, 29*(15-16), 1779-1790.
Mondav, R., Woodcroft, B. J., Kim, E.-H., McCalley, C. K., Hodgkins, S. B., Crill, P. M., . . . Saleska, S. R. (2014). Discovery of a novel methanogen prevalent in thawing permafrost. *Nature communications, 5*(1), 1-7.
Monnin, E., Indermühle, A., Dällenbach, A., Flückiger, J., Stauffer, B., Stocker, T. F., . . . Barnola, J.-M. (2001). Atmospheric CO2 concentrations over the last glacial termination. *Science, 291*(5501), 112-114.
Montañez, I. P., & Poulsen, C. J. (2013). The Late Paleozoic ice age: an evolving paradigm. *Annual Review of Earth and Planetary Sciences, 41*, 629-656.
Monteux, S., Weedon, J. T., Blume-Werry, G., Gavazov, K., Jassey, V. E., Johansson, M., . . . Dorrepaal, E. (2018). Long-term in situ permafrost thaw effects on bacterial communities and potential aerobic respiration. *The ISME journal, 12*(9), 2129-2141.
Moyer, C. L., & Morita, R. Y. (2007). Psychrophiles and psychrotrophs. *eLS*.
Mu, C., Zhang, T., Zhang, X., Li, L., Guo, H., Zhao, Q., . . . Cheng, G. (2016). Carbon loss and chemical changes from permafrost collapse in the northern Tibetan Plateau. *Journal of Geophysical Research: Biogeosciences, 121*(7), 1781-1791.
Murtagh, F., & Legendre, P. (2014). Ward's hierarchical agglomerative clustering method: which algorithms implement Ward's criterion? *Journal of classification, 31*(3), 274-295.
Murton, J. B., Goslar, T., Edwards, M. E., Bateman, M. D., Danilov, P. P., Savvinov, G. N., . . . Kanevskiy, M. (2015). Palaeoenvironmental interpretation of Yedoma Silt (ice complex) deposition as cold-climate loess, Duvanny Yar, Northeast Siberia. *Permafrost and Periglacial Processes, 26*(3), 208-288.
Mwalili, S. M., Lesaffre, E., & Declerck, D. (2008). The zero-inflated negative binomial regression model with correction for misclassification: an example in caries research. *Statistical methods in medical research, 17*(2), 123-139.
Mykytczuk, N. C., Foote, S. J., Omelon, C. R., Southam, G., Greer, C. W., & Whyte, L. G. (2013). Bacterial growth at− 15 C; molecular insights from the permafrost bacterium Planococcus halocryophilus Or1. *The ISME journal, 7*(6), 1211-1226.
Nearing, J. T., Douglas, G. M., Comeau, A. M., & Langille, M. G. (2018). Denoising the Denoisers: an independent evaluation of microbiome sequence error-correction approaches. *PeerJ, 6*, e5364.
Negandhi, K., Laurion, I., & Lovejoy, C. (2014). Bacterial communities and greenhouse gas emissions of shallow ponds in the High Arctic. *Polar biology, 37*(11), 1669-1683.

Neufeld, J. D., Vohra, J., Dumont, M. G., Lueders, T., Manefield, M., Friedrich, M. W., & Murrell, J. C. (2007). DNA stable-isotope probing. *Nature protocols, 2*(4), 860-866.
Newman, E. A. (2019). Disturbance ecology in the Anthropocene. *Frontiers in Ecology and Evolution, 7*, 147.
Nicholson, W., Munakata, N., Horneck, G., Melosh, H., & Setlow, P. (2000). Resistance of Bacillus endospores to extreme terrestrial and extraterrestrial environments. Microbiol Mol Biol Rev64: 548–572.
Nikrad, M. P., Kerkhof, L. J., & Häggblom, M. M. (2016). The subzero microbiome: microbial activity in frozen and thawing soils. *FEMS microbiology ecology, 92*(6), fiw081.
Nocker, A., Sossa-Fernandez, P., Burr, M. D., & Camper, A. K. (2007). Use of propidium monoazide for live/dead distinction in microbial ecology. *Applied and environmental Microbiology, 73*(16), 5111-5117.
Nowakowska, J., & Oliver, J. D. (2013). Resistance to environmental stresses by Vibrio vulnificus in the viable but nonculturable state. *FEMS microbiology ecology, 84*(1), 213-222.
Nunez, S., Arets, E., Alkemade, R., Verwer, C., & Leemans, R. (2019). Assessing the impacts of climate change on biodiversity: is below 2° C enough? *Climatic Change, 154*(3-4), 351-365.
Oechel, W. C., Cowles, S., Grulke, N., Hastings, S. J., Lawrence, B., Prudhomme, T., . . . Vourlitis, G. (1994). Transient nature of CO 2 fertilization in Arctic tundra. *Nature, 371*(6497), 500-503.
Ogram, A., Castro, H., Stanley, E., Chen, W., & Prenger, J. (2006). Distribution of methanotrophs in managed and highly disturbed watersheds. *Ecological Indicators, 6*(4), 631-643.
Oh, Y., Zhuang, Q., Liu, L., Welp, L. R., Lau, M. C., Onstott, T. C., . . . Hugelius, G. (2020). Reduced net methane emissions due to microbial methane oxidation in a warmer Arctic. *Nature climate change, 10*(4), 317-321.
Oksanen, J., Kindt, R., Legendre, P., O'Hara, B., Stevens, M. H. H., Oksanen, M. J., & Suggests, M. (2007). The vegan package. *Community ecology package, 10*(631-637), 719.
Oliva, M., & Fritz, M. (2018). Permafrost degradation on a warmer Earth: Challenges and perspectives. *Current Opinion in Environmental Science & Health, 5*, 14-18.
Opel, T., Meyer, H., Wetterich, S., Laepple, T., Dereviagin, A., & Murton, J. (2018). Ice wedges as archives of winter paleoclimate: A review. *Permafrost and Periglacial Processes, 29*(3), 199-209.
Orlando, L., Ginolhac, A., Zhang, G., Froese, D., Albrechtsen, A., Stiller, M., . . . Moltke, I. (2013). Recalibrating Equus evolution using the genome sequence of an early Middle Pleistocene horse. *Nature, 499*(7456), 74-78.
Orphan, V. J., House, C. H., Hinrichs, K.-U., McKeegan, K. D., & DeLong, E. F. (2002). Multiple archaeal groups mediate methane oxidation in anoxic cold seep sediments. *Proceedings of the National Academy of Sciences, 99*(11), 7663-7668.
Oshkin, I. Y., Beck, D. A., Lamb, A. E., Tchesnokova, V., Benuska, G., McTaggart, T. L., . . . Chistoserdova, L. (2015). Methane-fed microbial microcosms show differential community dynamics and pinpoint taxa involved in communal response. *The ISME journal, 9*(5), 1119-1129.
Osterkamp, T. (2007). Characteristics of the recent warming of permafrost in Alaska. *Journal of Geophysical Research: Earth Surface, 112*(F2).

Pääbo, S. (1985). Molecular cloning of ancient Egyptian mummy DNA. *Nature, 314*(6012), 644-645.
Pääbo, S., Higuchi, R. G., & Wilson, A. C. (1989). Ancient DNA and the polymerase chain reaction: the emerging field of molecular archaeology (Minireview). *The Journal of biological chemistry, 264*(17), 9709-9712.
Pääbo, S., Irwin, D. M., & Wilson, A. C. (1990). DNA damage promotes jumping between templates during enzymatic amplification. *Journal of Biological Chemistry, 265*(8), 4718-4721.
Paillard, D. (2001). Glacial cycles: toward a new paradigm. *Reviews of geophysics, 39*(3), 325-346.
Palmirotta, R., Verginelli, F., Di Tota, G., Battista, P., Cama, A., Caramiello, S., . . . Mariani-Costantini, R. (1997). Use of a multiplex polymerase chain reaction assay in the sex typing of DNA extracted from archaeological bone. *International Journal of Osteoarchaeology, 7*(6), 605-609.
Palumbi, S. R. (2001). Humans as the world's greatest evolutionary force. *Science, 293*(5536), 1786-1790.
Panikov, N. S., & Dedysh, S. (2000). Cold season CH4 and CO2 emission from boreal peat bogs (West Siberia): Winter fluxes and thaw activation dynamics. *Global Biogeochemical Cycles, 14*(4), 1071-1080.
Papke, R. T., & Ward, D. M. (2004). The importance of physical isolation to microbial diversification. *FEMS microbiology ecology, 48*(3), 293-303.
Paredes, D. I., Watters, K., Pitman, D. J., Bystroff, C., & Dordick, J. S. (2011). Comparative void-volume analysis of psychrophilic and mesophilic enzymes: structural bioinformatics of psychrophilic enzymes reveals sources of core flexibility. *BMC Structural Biology, 11*(1), 42.
Parton, W., Schimel, D. S., Cole, C., & Ojima, D. (1987). Analysis of factors controlling soil organic matter levels in Great Plains grasslands. *Soil Science Society of America Journal, 51*(5), 1173-1179.
Pecl, G. T., Araújo, M. B., Bell, J. D., Blanchard, J., Bonebrake, T. C., Chen, I.-C., . . . Evengård, B. (2017). Biodiversity redistribution under climate change: Impacts on ecosystems and human well-being. *Science, 355*(6332).
Penton, C. R., StLouis, D., Cole, J. R., Luo, Y., Wu, L., Schuur, E. G., . . . Tiedje, J. M. (2013). Fungal diversity in permafrost and tallgrass prairie soils under experimental warming conditions. *Applied and environmental Microbiology, 79*(22), 7063-7072.
Peteet, D. (2000). Sensitivity and rapidity of vegetational response to abrupt climate change. *Proceedings of the National Academy of Sciences, 97*(4), 1359-1361.
Phadtare, S. (2004). Recent developments in bacterial cold-shock response. *Current issues in molecular biology, 6*(2), 125-136.
Piette, F., Struvay, C., & Feller, G. (2011). The protein folding challenge in psychrophiles: facts and current issues. *Environmental microbiology, 13*(8), 1924-1933.
Pikuta, E. V., Marsic, D., Bej, A., Tang, J., Krader, P., & Hoover, R. B. (2005). Carnobacterium pleistocenium sp. nov., a novel psychrotolerant, facultative anaerobe isolated from permafrost of the Fox Tunnel in Alaska. *International Journal of Systematic and Evolutionary Microbiology, 55*(1), 473-478.
Ping, C., Jastrow, J., Jorgenson, M., Michaelson, G., & Shur, Y. (2015). Permafrost soils and carbon cycling. *Soil, 1*(1), 147.

Pingoud, A., Fuxreiter, M., Pingoud, V., & Wende, W. (2005). Type II restriction endonucleases: structure and mechanism. *Cellular and molecular life sciences, 62*(6), 685.
Poinar, H. N., Höss, M., Bada, J. L., & Pääbo, S. (1996). Amino acid racemization and the preservation of ancient DNA. *Science, 272*(5263), 864-866.
Poinar, H. N., Schwarz, C., Qi, J., Shapiro, B., MacPhee, R. D., Buigues, B., . . . Auch, A. (2006). Metagenomics to paleogenomics: large-scale sequencing of mammoth DNA. *Science, 311*(5759), 392-394.
Pokrovsky, O., Shirokova, L., Kirpotin, S., Audry, S., Viers, J., & Dupré, B. (2011). Effect of permafrost thawing on organic carbon and trace element colloidal speciation in the thermokarst lakes of western Siberia. *Biogeosciences, 8*(3), 565.
Ponder, M., Vishnivetskaya, T., McGrath, J., & Tiedje, J. (2004). Microbial life in permafrost: extended times in extreme conditions *Life in the Frozen State* (pp. 177-196): CRC Press.
Ponder, M. A., Gilmour, S. J., Bergholz, P. W., Mindock, C. A., Hollingsworth, R., Thomashow, M. F., & Tiedje, J. M. (2005). Characterization of potential stress responses in ancient Siberian permafrost psychroactive bacteria. *FEMS microbiology ecology, 53*(1), 103-115.
Porrini, L., Cybulski, L. E., Altabe, S. G., Mansilla, M. C., & de Mendoza, D. (2014). Cerulenin inhibits unsaturated fatty acids synthesis in Bacillus subtilis by modifying the input signal of DesK thermosensor. *Microbiologyopen, 3*(2), 213-224.
Porter, T. J., Schoenemann, S. W., Davies, L. J., Steig, E. J., Bandara, S., & Froese, D. G. (2019). Recent summer warming in northwestern Canada exceeds the Holocene thermal maximum. *Nature communications, 10*(1), 1-10.
Porter, T. M., Golding, G. B., King, C., Froese, D., Zazula, G., & Poinar, H. N. (2013). Amplicon pyrosequencing late Pleistocene permafrost: the removal of putative contaminant sequences and small-scale reproducibility. *Molecular Ecology Resources, 13*(5), 798-810.
Potts, M. (1994). Desiccation tolerance of prokaryotes. Microbiol. storage. *Soil Biol. Biochem, 23*, 313-322.
Prevost-Boure, N. C., Dequiedt, S., Thioulouse, J., Lelievre, M., Saby, N. P., Jolivet, C., . . . Ranjard, L. (2014). Similar processes but different environmental filters for soil bacterial and fungal community composition turnover on a broad spatial scale. *PloS one, 9*(11), e111667.
Puspita, I. D., Kitagawa, W., Kamagata, Y., Tanaka, M., & Nakatsu, C. H. (2015). Increase in bacterial colony formation from a permafrost ice wedge dosed with a Tomitella biformata recombinant resuscitation-promoting factor protein. *Microbes and environments*, ME14119.
Rachor, I., Gebert, J., Gröngröft, A., & Pfeiffer, E.-M. (2011). Assessment of the methane oxidation capacity of compacted soils intended for use as landfill cover materials. *Waste management, 31*(5), 833-842.
Raghoebarsing, A. A., Pol, A., Van de Pas-Schoonen, K. T., Smolders, A. J., Ettwig, K. F., Rijpstra, W. I. C., . . . Jetten, M. S. (2006). A microbial consortium couples anaerobic methane oxidation to denitrification. *Nature, 440*(7086), 918-921.
Rahmstorf, S. (2002). Ocean circulation and climate during the past 120,000 years. *Nature, 419*(6903), 207-214.
Ramanathan, V., & Feng, Y. (2009). Air pollution, greenhouse gases and climate change: Global and regional perspectives. *Atmospheric environment, 43*(1), 37-50.

Rampelotto, P. H. (2014). Polar microbiology: Recent advances and future perspectives: Multidisciplinary Digital Publishing Institute.
Rasmussen, S. O., Andersen, K. K., Svensson, A., Steffensen, J. P., Vinther, B. M., Clausen, H. B., . . . Dahl-Jensen, D. (2006). A new Greenland ice core chronology for the last glacial termination. *Journal of Geophysical Research: Atmospheres, 111*(D6).
Rastetter, E. B., Ågren, G. I., & Shaver, G. R. (1997). Responses of N-limited ecosystems to increased CO2: A balanced-nutrition, coupled-element-cycles model. *Ecological Applications, 7*(2), 444-460.
Rastogi, R. P., Kumar, A., Tyagi, M. B., & Sinha, R. P. (2010). Molecular mechanisms of ultraviolet radiation-induced DNA damage and repair. *Journal of nucleic acids, 2010*.
Razanamalala, K., Razafimbelo, T., Maron, P.-A., Ranjard, L., Chemidlin, N., Lelièvre, M., . . . Becquer, T. (2018). Soil microbial diversity drives the priming effect along climate gradients: a case study in Madagascar. *The ISME journal, 12*(2), 451-462.
Repenning, C. A., & Brouwers, E. M. (1992). *Late Pliocene-early Pleistocene ecologic changes in the Arctic Ocean borderland*: US Government Printing Office.
Reuter, H. I., Lado, L. R., Hengl, T., & Montanarella, L. (2008). Continental-scale digital soil mapping using European soil profile data: soil pH. *Hamburger Beiträge zur Physischen Geographie und Landschaftsökologie, 19*, 91-102.
Riahi, K., Rao, S., Krey, V., Cho, C., Chirkov, V., Fischer, G., . . . Rafaj, P. (2011). RCP 8.5—A scenario of comparatively high greenhouse gas emissions. *Climatic Change, 109*(1-2), 33.
Riahi, K., Van Vuuren, D. P., Kriegler, E., Edmonds, J., O'neill, B. C., Fujimori, S., . . . Fricko, O. (2017). The shared socioeconomic pathways and their energy, land use, and greenhouse gas emissions implications: an overview. *Global Environmental Change, 42*, 153-168.
Rice, K. M., Walker Jr, E. M., Wu, M., Gillette, C., & Blough, E. R. (2014). Environmental mercury and its toxic effects. *Journal of preventive medicine and public health, 47*(2), 74.
Ringelberg, D. B., Stair, J. O., Almeida, J., Norby, R. J., O'Neill, E. G., & White, D. C. (1997). Consequences of rising atmospheric carbon dioxide levels for the belowground microbiota associated with white oak. *Journal of Environmental Quality, 26*(2), 495-503.
Rinnan, R., Michelsen, A., Bååth, E., & Jonasson, S. (2007). Fifteen years of climate change manipulations alter soil microbial communities in a subarctic heath ecosystem. *Global Change Biology, 13*(1), 28-39.
Rivkina, E., Abramov, A., Spirina, E., Petrovskaya, L., Shatilovich, A., Shmakova, L., . . . Vishnivetskaya, T. (2018). Earth's perennially frozen environments as a model of cryogenic planet ecosystems. *Permafrost and Periglacial Processes, 29*(4), 246-256.
Rivkina, E., Friedmann, E., McKay, C., & Gilichinsky, D. (2000). Metabolic activity of permafrost bacteria below the freezing point. *Applied and environmental Microbiology, 66*(8), 3230-3233.
Rivkina, E., Gilichinsky, D., Wagener, S., Tiedje, J., & McGrath, J. (1998). Biogeochemical activity of anaerobic microorganisms from buried permafrost sediments. *Geomicrobiology Journal, 15*(3), 187-193.
Rivkina, E., Petrovskaya, L., Vishnivetskaya, T., Krivushin, K., Shmakova, L., Tutukina, M., . . . Kondrashov, F. (2016). Metagenomic analyses of the late Pleistocene permafrost–additional tools for reconstruction of environmental conditions. *Biogeosciences, 13*(7).

Rivkina, E., Shcherbakova, V., Laurinavichius, K., Petrovskaya, L., Krivushin, K., Kraev, G., . . . Gilichinsky, D. (2007). Biogeochemistry of methane and methanogenic archaea in permafrost. *FEMS microbiology ecology, 61*(1), 1-15.

Rogers, S. O., Theraisnathan, V., Ma, L., Zhao, Y., Zhang, G., Shin, S.-G., . . . Starmer, W. (2004a). Comparisons of protocols for decontamination of environmental ice samples for biological and molecular examinations. *Applied and environmental Microbiology, 70*(4), 2540-2544.

Rogers, S. O., Theraisnathan, V., Ma, L. J., Zhao, Y., Zhang, G., Shin, S.-G., . . . Starmer, W. T. (2004b). Comparisons of Protocols for Decontamination of Environmental Ice Samples for Biological and Molecular Examinations. *Applied and environmental Microbiology, 70*(4), 2540-2544. doi: 10.1128/aem.70.4.2540-2544.2004

Romanovskii, N., Hubberten, H. W., Gavrilov, A., Tumskoy, V., Tipenko, G., Grigoriev, M., & Siegert, C. (2000). Thermokarst and land–ocean interactions, Laptev Sea region, Russia. *Permafrost and Periglacial Processes, 11*(2), 137-152.

Romanovsky, V. E., Drozdov, D., Oberman, N. G., Malkova, G., Kholodov, A. L., Marchenko, S., . . . Abramov, A. (2010). Thermal state of permafrost in Russia. *Permafrost and Periglacial Processes, 21*(2), 136-155.

Rousk, J., Bååth, E., Brookes, P. C., Lauber, C. L., Lozupone, C., Caporaso, J. G., . . . Fierer, N. (2010). Soil bacterial and fungal communities across a pH gradient in an arable soil. *The ISME journal, 4*(10), 1340-1351.

Rousk, J., Frey, S. D., & Bååth, E. (2012). Temperature adaptation of bacterial communities in experimentally warmed forest soils. *Global Change Biology, 18*(10), 3252-3258.

Rowe, M., Dunstall, G., Kirk, R., Loughney, C., Cooke, J., & Brown, S. (1998). Development of an image system for the study of viable but non-culturable forms ofCampylobacter jejuniand its use to determine their resistance to disinfectants. *Food microbiology, 15*(5), 491-498.

Russell, N. J. (2000). Toward a molecular understanding of cold activity of enzymes from psychrophiles. *Extremophiles, 4*(2), 83-90.

Saita, E., Albanesi, D., & de Mendoza, D. (2016). Sensing membrane thickness: Lessons learned from cold stress. *Biochimica et Biophysica Acta (BBA)-Molecular and Cell Biology of Lipids, 1861*(8), 837-846.

Sakaguchi, M., Matsuzaki, M., Niimiya, K., Seino, J., Sugahara, Y., & Kawakita, M. (2007). Role of proline residues in conferring thermostability on aqualysin I. *The Journal of Biochemistry, 141*(2), 213-220.

Salamon, M., Tuross, N., Arensburg, B., & Weiner, S. (2005). Relatively well preserved DNA is present in the crystal aggregates of fossil bones. *Proceedings of the National Academy of Sciences, 102*(39), 13783-13788.

Salter, S. J., Cox, M. J., Turek, E. M., Calus, S. T., Cookson, W. O., Moffatt, M. F., . . . Walker, A. W. (2014). Reagent and laboratory contamination can critically impact sequence-based microbiome analyses. *BMC biology, 12*(1), 87.

Sandle, T., & Skinner, K. (2013). Study of psychrophilic and psychrotolerant micro-organisms isolated in cold rooms used for pharmaceutical processing. *Journal of applied microbiology, 114*(4), 1166-1174.

Sandom, C., Faurby, S., Sandel, B., & Svenning, J.-C. (2014). Global late Quaternary megafauna extinctions linked to humans, not climate change. *Proceedings of the Royal Society B: Biological Sciences, 281*(1787), 20133254.

Sattler, B., Puxbaum, H., & Psenner, R. (2001). Bacterial growth in supercooled cloud droplets. *Geophysical Research Letters, 28*(2), 239-242.
Saunois, M., Bousquet, P., Poulter, B., Peregon, A., Ciais, P., Canadell, J., . . . Houweling, S. (2016a). The Global Methane Budget 2000-2012. Earth System Science Data, 8, 697-751.
Saunois, M., Bousquet, P., Poulter, B., Peregon, A., Ciais, P., Canadell, J. G., . . . Houweling, S. (2016b). The global methane budget 2000–2012. *Earth System Science Data, 8*(2), 697-751.
Schädel, C., Schuur, E. A., Bracho, R., Elberling, B., Knoblauch, C., Lee, H., . . . Turetsky, M. R. (2014). Circumpolar assessment of permafrost C quality and its vulnerability over time using long-term incubation data. *Global Change Biology, 20*(2), 641-652.
Schaefer, K., Elshorbany, Y., Jafarov, E., Schuster, P. F., Striegl, R. G., Wickland, K. P., & Sunderland, E. M. (2020). Potential impacts of mercury released from thawing permafrost. *Nature communications, 11*(1), 1-6.
Schaefer, K., Zhang, T., Bruhwiler, L., & Barrett, A. P. (2011). Amount and timing of permafrost carbon release in response to climate warming. *Tellus B: Chemical and Physical Meteorology, 63*(2), 168-180.
Scheffer, M., Carpenter, S., Foley, J. A., Folke, C., & Walker, B. (2001). Catastrophic shifts in ecosystems. *Nature, 413*(6856), 591-596.
Scheller, S., Ermler, U., & Shima, S. (2020). Catabolic pathways and enzymes involved in anaerobic methane oxidation. *Anaerobic Utilization of Hydrocarbons, Oils, and Lipids*, 31-59.
Schimel, J. P., Gulledge, J. M., Clein-Curley, J. S., Lindstrom, J. E., & Braddock, J. F. (1999). Moisture effects on microbial activity and community structure in decomposing birch litter in the Alaskan taiga. *Soil Biology and Biochemistry, 31*(6), 831-838.
Schirrmeister, L., Froese, D., Tumskoy, V., Grosse, G., & Wetterich, S. (2013). Yedoma: Late Pleistocene ice-rich syngenetic permafrost of Beringia *Encyclopedia of Quaternary Science. 2nd edition* (pp. 542-552): Elsevier.
Schloss, P. D., Westcott, S. L., Ryabin, T., Hall, J. R., Hartmann, M., Hollister, E. B., . . . Robinson, C. J. (2009). Introducing mothur: open-source, platform-independent, community-supported software for describing and comparing microbial communities. *Applied and environmental Microbiology, 75*(23), 7537-7541.
Schmidt, M. W., Torn, M. S., Abiven, S., Dittmar, T., Guggenberger, G., Janssens, I. A., . . . Manning, D. A. (2011). Persistence of soil organic matter as an ecosystem property. *Nature, 478*(7367), 49-56.
Schneegurt, M. A., Dore, S. Y., & Kulpa Jr, C. F. (2003). Direct extraction of DNA from soils for studies in microbial ecology. *Current issues in molecular biology, 5*(1), 1-8.
Schneider, P., & Hook, S. J. (2010). Space observations of inland water bodies show rapid surface warming since 1985. *Geophysical Research Letters, 37*(22).
Schostag, M., Priemé, A., Jacquiod, S., Russel, J., Ekelund, F., & Jacobsen, C. S. (2019). Bacterial and protozoan dynamics upon thawing and freezing of an active layer permafrost soil. *The ISME journal, 13*(5), 1345-1359.
Schostag, M., Stibal, M., Jacobsen, C. S., Bælum, J., Taş, N., Elberling, B., . . . Priemé, A. (2015). Distinct summer and winter bacterial communities in the active layer of Svalbard permafrost revealed by DNA-and RNA-based analyses. *Frontiers in microbiology, 6*, 399.

Schuster, P. F., Schaefer, K. M., Aiken, G. R., Antweiler, R. C., Dewild, J. F., Gryziec, J. D., . . . Krabbenhoft, D. P. (2018). Permafrost stores a globally significant amount of mercury. *Geophysical Research Letters, 45*(3), 1463-1471.

Schuur, E. A., Bockheim, J., Canadell, J. G., Euskirchen, E., Field, C. B., Goryachkin, S. V., . . . Lee, H. (2008). Vulnerability of permafrost carbon to climate change: Implications for the global carbon cycle. *Bioscience, 58*(8), 701-714.

Schuur, E. A., McGuire, A. D., Schädel, C., Grosse, G., Harden, J., Hayes, D. J., . . . Lawrence, D. M. (2015). Climate change and the permafrost carbon feedback. *Nature, 520*(7546), 171-179.

Semrau, J. D., DiSpirito, A. A., & Vuilleumier, S. (2011). Facultative methanotrophy: false leads, true results, and suggestions for future research. *FEMS microbiology letters, 323*(1), 1-12.

Shackleton, N. J., Sánchez-Goñi, M. F., Pailler, D., & Lancelot, Y. (2003). Marine isotope substage 5e and the Eemian interglacial. *Global and Planetary Change, 36*(3), 151-155.

Shade, A., Caporaso, J. G., Handelsman, J., Knight, R., & Fierer, N. (2013). A meta-analysis of changes in bacterial and archaeal communities with time. *The ISME journal, 7*(8), 1493-1506.

Shade, A., Peter, H., Allison, S., Baho, D., Berga, M., Buergmann, H., . . . Handelsman, J. (2012). Fundamentals of Microbial Community Resistance and Resilience. *Frontiers in microbiology, 3*(417). doi: 10.3389/fmicb.2012.00417

Shaner, N. C., Lambert, G. G., Chammas, A., Ni, Y., Cranfill, P. J., Baird, M. A., . . . Wang, J. (2013). A bright monomeric green fluorescent protein derived from Branchiostoma lanceolatum. *Nature methods, 10*(5), 407-409. doi: 10.1038/nmeth.2413

Shapiro, B., & Cooper, A. (2003). Beringia as an Ice Age genetic museum. *Quaternary Research, 60*(1), 94-100.

Shapiro, B., Drummond, A., Rambaut, A., Pybus, O., Gilbert, M., Wilson, M., . . . Willerslev, E. (2004). The impact of large-scale climate change on genetic diversity in large mammal populations. *Science.(In the press.)*.

Sharp, C., Stott, M., & Dunfield, P. (2012). Detection of autotrophic verrucomicrobial methanotrophs in a geothermal environment using stable isotope probing. *Frontiers in microbiology, 3*, 303.

Shcherbakova, V., Chuvilskaya, N., Rivkina, E., Pecheritsyna, S., Laurinavichius, K., Suzina, N., . . . Akimenko, V. (2005). Novel psychrophilic anaerobic spore-forming bacterium from the overcooled water brine in permafrost: description Clostridium algoriphilum sp. nov. *Extremophiles, 9*(3), 239-246.

Shcherbakova, V., Yoshimura, Y., Ryzhmanova, Y., Taguchi, Y., Segawa, T., Oshurkova, V., & Rivkina, E. (2016). Archaeal communities of Arctic methane-containing permafrost. *FEMS microbiology ecology, 92*(10).

Shendure, J., Balasubramanian, S., Church, G. M., Gilbert, W., Rogers, J., Schloss, J. A., & Waterston, R. H. (2017). DNA sequencing at 40: past, present and future. *Nature, 550*(7676), 345-353.

Shleeva, M., Mukamolova, G. V., Young, M., Williams, H. D., & Kaprelyants, A. S. (2004). Formation of 'non-culturable'cells of Mycobacterium smegmatis in stationary phase in response to growth under suboptimal conditions and their Rpf-mediated resuscitation. *Microbiology, 150*(6), 1687-1697.

Siddiqui, K. S., Poljak, A., Guilhaus, M., De Francisci, D., Curmi, P. M., Feller, G., . . . Cavicchioli, R. (2006). Role of lysine versus arginine in enzyme cold-adaptation: Modifying lysine to homo-arginine stabilizes the cold-adapted α-amylase from Pseudoalteramonas haloplanktis. *Proteins: Structure, Function, and Bioinformatics, 64*(2), 486-501.

Sierra, C. A. (2012). Temperature sensitivity of organic matter decomposition in the Arrhenius equation: some theoretical considerations. *Biogeochemistry, 108*(1-3), 1-15.

Signoretto, C., del Mar Lleò, M., Tafi, M. C., & Canepari, P. (2000). Cell Wall Chemical Composition ofEnterococcus faecalis in the Viable but Nonculturable State. *Applied and environmental Microbiology, 66*(5), 1953-1959.

Sikes, E. L., Samson, C. R., Guilderson, T. P., & Howard, W. R. (2000). Old radiocarbon ages in the southwest Pacific Ocean during the last glacial period and deglaciation. *Nature, 405*(6786), 555-559.

Sinensky, M. (1974). Homeoviscous adaptation—a homeostatic process that regulates the viscosity of membrane lipids in Escherichia coli. *Proceedings of the National Academy of Sciences, 71*(2), 522-525.

Singh, B. K., Tate, K. R., Kolipaka, G., Hedley, C. B., Macdonald, C. A., Millard, P., & Murrell, J. C. (2007). Effect of afforestation and reforestation of pastures on the activity and population dynamics of methanotrophic bacteria. *Applied and environmental Microbiology, 73*(16), 5153-5161.

Singh, S., & Singh, D. (2013). Impact of anthropogenic disturbances on methanotrophs abundance in dry tropical forest ecosystems, India. *Expert Opin Environ Biol 2, 3*, 2.

Singleton, C. M., McCalley, C. K., Woodcroft, B. J., Boyd, J. A., Evans, P. N., Hodgkins, S. B., . . . Saleska, S. R. (2018). Methanotrophy across a natural permafrost thaw environment. *The ISME journal, 12*(10), 2544-2558.

Sjögersten, S., Caul, S., Daniell, T., Jurd, A., O'Sullivan, O., Stapleton, C., & Titman, J. J. (2016). Organic matter chemistry controls greenhouse gas emissions from permafrost peatlands. *Soil Biology and Biochemistry, 98*, 42-53.

Skalova, T., Dohnálek, J., Spiwok, V., Lipovová, P., Vondráčková, E., Petroková, H., . . . Hašek, J. (2005). Cold-active β-galactosidase from Arthrobacter sp. C2-2 forms compact 660 kDa hexamers: crystal structure at 1.9 Å resolution. *Journal of Molecular Biology, 353*(2), 282-294.

Skoglund, P., Northoff, B. H., Shunkov, M. V., Derevianko, A. P., Pääbo, S., Krause, J., & Jakobsson, M. (2014). Separating endogenous ancient DNA from modern day contamination in a Siberian Neandertal. *Proceedings of the National Academy of Sciences, 111*(6), 2229-2234.

Skoog, D. A., Holler, F. J., & Crouch, S. R. (2017). *Principles of instrumental analysis*: Cengage learning.

Slessarev, E., Lin, Y., Bingham, N., Johnson, J., Dai, Y., Schimel, J., & Chadwick, O. (2016). Water balance creates a threshold in soil pH at the global scale. *Nature, 540*(7634), 567-569.

Smalla, K., Cresswell, N., Mendonca-Hagler, L. C., Wolters, A., & Elsas, J. v. (1993). Rapid DNA extraction protocol from soil for polymerase chain reaction-mediated amplification. *Journal of Applied Bacteriology, 74*(1), 78-85.

Smith, D. C., Spivack, A. J., Fisk, M. R., Haveman, S. A., & Staudigel, H. (2000). Tracer-based estimates of drilling-induced microbial contamination of deep sea crust. *Geomicrobiology Journal, 17*(3), 207-219.

Smith, G. J., Angle, J. C., Solden, L. M., Borton, M. A., Morin, T. H., Daly, R. A., . . . Gil, B. (2018). Members of the genus Methylobacter are inferred to account for the majority of aerobic methane oxidation in oxic soils from a freshwater wetland. *MBio, 9*(6).

Smith, L., MacDonald, G., Velichko, A., Beilman, D., Borisova, O., Frey, K., . . . Sheng, Y. (2004). Siberian peatlands a net carbon sink and global methane source since the early Holocene. *Science, 303*(5656), 353-356.

Smith, L. C., Sheng, Y., & MacDonald, G. M. (2007). A first pan-Arctic assessment of the influence of glaciation, permafrost, topography and peatlands on northern hemisphere lake distribution. *Permafrost and Periglacial Processes, 18*(2), 201-208.

Song, C., Wang, X., Miao, Y., Wang, J., Mao, R., & Song, Y. (2014). Effects of permafrost thaw on carbon emissions under aerobic and anaerobic environments in the Great Hing'an Mountains, China. *Science of the Total Environment, 487*, 604-610.

Sparks, D. L., Page, A., Helmke, P., & Loeppert, R. H. (2020). *Methods of soil analysis, part 3: Chemical methods* (Vol. 14): John Wiley & Sons.

Spiegel, D. S., Raymond, S. N., Dressing, C. D., Scharf, C. A., & Mitchell, J. L. (2010). Generalized Milankovitch cycles and long-term climatic habitability. *The Astrophysical Journal, 721*(2), 1308.

Spiegelhalter, F., & Bremer, E. (1998). Osmoregulation of the opuE proline transport gene from Bacillus subtilis: contributions of the sigma A-and sigma B-dependent stress-responsive promoters. *Molecular microbiology, 29*(1), 285-296.

STACKEBRANDT, E., & GOEBEL, B. M. (1994). Taxonomic Note: A Place for DNA-DNA Reassociation and 16S rRNA Sequence Analysis in the Present Species Definition in Bacteriology. *International Journal of Systematic and Evolutionary Microbiology, 44*(4), 846-849. doi: https://doi.org/10.1099/00207713-44-4-846

Stackhouse, B. T., Vishnivetskaya, T. A., Layton, A., Chauhan, A., Pfiffner, S., Mykytczuk, N. C., . . . Saad, N. (2015). Effects of simulated spring thaw of permafrost from mineral cryosol on CO2 emissions and atmospheric CH4 uptake. *Journal of Geophysical Research: Biogeosciences, 120*(9), 1764-1784.

Stark, S., Männistö, M. K., & Eskelinen, A. (2014). Nutrient availability and pH jointly constrain microbial extracellular enzyme activities in nutrient-poor tundra soils. *Plant and Soil, 383*(1-2), 373-385.

Steffen, W., Rockström, J., Richardson, K., Lenton, T. M., Folke, C., Liverman, D., . . . Crucifix, M. (2018). Trajectories of the Earth System in the Anthropocene. *Proceedings of the National Academy of Sciences, 115*(33), 8252-8259.

Stegen, J. C., Bottos, E. M., & Jansson, J. K. (2018). A unified conceptual framework for prediction and control of microbiomes. *Current opinion in microbiology, 44*, 20-27.

Stegen, J. C., Lin, X., Fredrickson, J. K., Chen, X., Kennedy, D. W., Murray, C. J., . . . Konopka, A. (2013). Quantifying community assembly processes and identifying features that impose them. *The ISME journal, 7*(11), 2069-2079.

Stein, L. Y., Roy, R., & Dunfield, P. F. (2012). Aerobic methanotrophy and nitrification: processes and connections. *eLS*.

Steven, B., Briggs, G., McKay, C. P., Pollard, W. H., Greer, C. W., & Whyte, L. G. (2007). Characterization of the microbial diversity in a permafrost sample from the Canadian

high Arctic using culture-dependent and culture-independent methods. *FEMS microbiology ecology, 59*(2), 513-523.
Steven, B., Leveille, R., Pollard, W. H., & Whyte, L. G. (2006). Microbial ecology and biodiversity in permafrost. *Extremophiles, 10*(4), 259-267.
Stocker, T. F. (2000). Past and future reorganizations in the climate system. *Quaternary Science Reviews, 19*(1-5), 301-319.
Stocker, T. F., Qin, D., Plattner, G.-K., Tignor, M., Allen, S. K., Boschung, J., . . . Midgley, P. M. (2013a). Climate Change 2013. The Physical Science Basis. Working Group I Contribution to the Fifth Assessment Report of the Intergovernmental Panel on Climate Change-Abstract for decision-makers; Changements climatiques 2013. Les elements scientifiques. Contribution du groupe de travail I au cinquieme rapport d'evaluation du groupe d'experts intergouvernemental sur l'evolution du CLIMAT-Resume a l'intention des decideurs.
Stocker, T. F., Qin, D., Plattner, G.-K., Tignor, M., Allen, S. K., Boschung, J., . . . Midgley, P. M. (2013b). Climate change 2013: The physical science basis. *Contribution of working group I to the fifth assessment report of the intergovernmental panel on climate change, 1535*.
Strauss, J., Schirrmeister, L., Grosse, G., Fortier, D., Hugelius, G., Knoblauch, C., . . . Schuur, E. A. (2017). Deep Yedoma permafrost: A synthesis of depositional characteristics and carbon vulnerability. *Earth-Science Reviews, 172*, 75-86.
Strauss, J., Schirrmeister, L., Grosse, G., Wetterich, S., Ulrich, M., Herzschuh, U., & Hubberten, H. W. (2013). The deep permafrost carbon pool of the Yedoma region in Siberia and Alaska. *Geophysical Research Letters, 40*(23), 6165-6170.
Streletskiy, D. A., Suter, L. J., Shiklomanov, N. I., Porfiriev, B. N., & Eliseev, D. O. (2019). Assessment of climate change impacts on buildings, structures and infrastructure in the Russian regions on permafrost. *Environmental Research Letters, 14*(2), 025003.
Strocchi, M., Ferrer, M., Timmis, K. N., & Golyshin, P. N. (2006). Low temperature-induced systems failure in Escherichia coli: insights from rescue by cold-adapted chaperones. *Proteomics, 6*(1), 193-206.
Strous, M. (2010). Global consequences of anaerobic methane oxidation *Handbook of Hydrocarbon and Lipid Microbiology*.
Sun, L., Perdue, E., Meyer, J., & Weis, J. (1997). Use of elemental composition to predict bioavailability of dissolved organic matter in a Georgia river. *Limnology and Oceanography, 42*(4), 714-721.
T. Weedon, J., A. Kowalchuk, G., Aerts, R., van Hal, J., van Logtestijn, R., Taş, N., . . . M. van Bodegom, P. (2012). Summer warming accelerates sub-arctic peatland nitrogen cycling without changing enzyme pools or microbial community structure. *Global Change Biology, 18*(1), 138-150.
Tang, H., & Chen, Y. (2013). Global glaciations and atmospheric change at ca. 2.3 Ga. *Geoscience Frontiers, 4*(5), 583-596.
Tank, S. E., Mann, P. J., Hoering, K., Bulygina, E., Spencer, R. G., Wang, Z., . . . Holmes, R. M. (2012). Rapid photo-mineralization of dissolved organic carbon flowing from large Arctic rivers to the Arctic Ocean. *AGUFM, 2012*, B41D-0320.
Tanski, G., Lantuit, H., Ruttor, S., Knoblauch, C., Radosavljevic, B., Strauss, J., . . . Fritz, M. (2017). Transformation of terrestrial organic matter along thermokarst-affected permafrost coasts in the Arctic. *Science of the Total Environment, 581*, 434-447.

Tarnocai, C. (2009). The impact of climate change on Canadian peatlands. *Canadian Water Resources Journal, 34*(4), 453-466.
Tarnocai, C., Canadell, J., Schuur, E. A., Kuhry, P., Mazhitova, G., & Zimov, S. (2009). Soil organic carbon pools in the northern circumpolar permafrost region. *Global Biogeochemical Cycles, 23*(2).
Taş, N., Prestat, E., McFarland, J. W., Wickland, K. P., Knight, R., Berhe, A. A., . . . Jansson, J. K. (2014). Impact of fire on active layer and permafrost microbial communities and metagenomes in an upland Alaskan boreal forest. *The ISME journal, 8*(9), 1904-1919.
Teichmann, L., Kümmel, H., Warmbold, B., & Bremer, E. (2018). OpuF, a new Bacillus compatible solute ABC transporter with a substrate-binding protein fused to the transmembrane domain. *Applied and environmental Microbiology, 84*(20).
Thiagarajan, N., Subhas, A. V., Southon, J. R., Eiler, J. M., & Adkins, J. F. (2014). Abrupt pre-Bølling–Allerød warming and circulation changes in the deep ocean. *Nature, 511*(7507), 75-78.
Thomas, R. H., Schaffner, W., Wilson, A. C., & Pääbo, S. (1989). DNA phylogeny of the extinct marsupial wolf. *Nature, 340*(6233), 465-467.
Thomson, D. J. (1995). The seasons, global temperature, and precession. *Science, 268*(5207), 59-68.
Tibshirani, R., Walther, G., & Hastie, T. (2001). Estimating the number of clusters in a data set via the gap statistic. *Journal of the Royal Statistical Society: Series B (Statistical Methodology), 63*(2), 411-423.
Tillotson, J., & Tillotson, G. S. (2010). ABC transporters in microorganisms. *Expert Review of Anti-infective Therapy, 8*(4), 375-377.
Tiwari, S., Singh, C., & Singh, J. S. (2018). Land use changes: a key ecological driver regulating methanotrophs abundance in upland soils. *Energy, Ecology and Environment, 3*(6), 355-371.
Toggweiler, J. R., & Russell, J. (2008). Ocean circulation in a warming climate. *Nature, 451*(7176), 286-288.
Treat, C. C., & Frolking, S. (2013). Carbon Storage: A permafrost carbon bomb? *Nature climate change, 3*(10), 865-867.
Treat, C. C., Wollheim, W. M., Varner, R. K., Grandy, A. S., Talbot, J., & Frolking, S. (2014). Temperature and peat type control CO 2 and CH 4 production in Alaskan permafrost peats. *Global Change Biology, 20*(8), 2674-2686.
Tripathi, B. M., Stegen, J. C., Kim, M., Dong, K., Adams, J. M., & Lee, Y. K. (2018). Soil pH mediates the balance between stochastic and deterministic assembly of bacteria. *The ISME journal, 12*(4), 1072-1083.
Trisos, C. H., Merow, C., & Pigot, A. L. (2020). The projected timing of abrupt ecological disruption from climate change. *Nature, 580*(7804), 496-501.
Trotsenko, Y. A., & Khmelenina, V. N. (2005). Aerobic methanotrophic bacteria of cold ecosystems. *FEMS microbiology ecology, 53*(1), 15-26.
Tsai, Y.-L., & Olson, B. H. (1992). Rapid method for separation of bacterial DNA from humic substances in sediments for polymerase chain reaction. *Applied and environmental Microbiology, 58*(7), 2292-2295.
Tuorto, S. J., Darias, P., McGuinness, L. R., Panikov, N., Zhang, T., Häggblom, M. M., & Kerkhof, L. J. (2014). Bacterial genome replication at subzero temperatures in permafrost. *The ISME journal, 8*(1), 139-149.

Turetsky, M. R., Abbott, B. W., Jones, M. C., Anthony, K. W., Olefeldt, D., Schuur, E. A., . . . Koven, C. (2020). Carbon release through abrupt permafrost thaw. *Nature Geoscience, 13*(2), 138-143.

Tveit, A. T., Hestnes, A. G., Robinson, S. L., Schintlmeister, A., Dedysh, S. N., Jehmlich, N., . . . Richter, A. (2019). Widespread soil bacterium that oxidizes atmospheric methane. *Proceedings of the National Academy of Sciences, 116*(17), 8515-8524.

Valko, M., Rhodes, C., Moncol, J., Izakovic, M., & Mazur, M. (2006). Free radicals, metals and antioxidants in oxidative stress-induced cancer. *Chemico-biological interactions, 160*(1), 1-40.

Vallino, J., Hopkinson, C., & Hobbie, J. (1996). Modeling bacterial utilization of dissolved organic matter: optimization replaces Monod growth kinetics. *Limnology and Oceanography, 41*(8), 1591-1609.

Van Breemen, N., Mulder, J., & Driscoll, C. (1983). Acidification and alkalinization of soils. *Plant and Soil, 75*(3), 283-308.

Van der Putten, W. H. (2012). Climate change, aboveground-belowground interactions, and species' range shifts. *Annual Review of Ecology, Evolution, and Systematics, 43*.

Van Everdingen, R. O., & Association, I. P. (1998). *Multi-language glossary of permafrost and related ground-ice terms in chinese, english, french, german*: Arctic Inst. of North America University of Calgary.

Van Huissteden, J., & Dolman, A. (2012). Soil carbon in the Arctic and the permafrost carbon feedback. *Current Opinion in Environmental Sustainability, 4*(5), 545-551.

Van Schmus, W. (1995). Natural radioactivity of the crust and mantle *Global earth physics: A handbook of physical constants* (Vol. 1, pp. 283-291): Wiley Online Library.

van Teeseling, M. C., Pol, A., Harhangi, H. R., van der Zwart, S., Jetten, M. S., den Camp, H. J. O., & van Niftrik, L. (2014). Expanding the verrucomicrobial methanotrophic world: description of three novel species of Methylacidimicrobium gen. nov. *Applied and environmental Microbiology, 80*(21), 6782-6791.

Vinther, B. M., Buchardt, S. L., Clausen, H. B., Dahl-Jensen, D., Johnsen, S. J., Fisher, D., . . . Andersen, K. K. (2009). Holocene thinning of the Greenland ice sheet. *Nature, 461*(7262), 385-388.

Vishnivetskaya, T., Kathariou, S., McGrath, J., Gilichinsky, D., & Tiedje, J. M. (2000). Low-temperature recovery strategies for the isolation of bacteria from ancient permafrost sediments. *Extremophiles, 4*(3), 165-173.

Vishnivetskaya, T. A., Erokhina, L. G., Spirina, E. V., Shatilovich, A., Vorobyova, E., & Gilichinsky, D. (2001). Ancient viable phototrophs within the permafrost. *Nova Hedwigia Beiheft, 123*, 427-442.

Vishnivetskaya, T. A., Layton, A. C., Lau, M. C., Chauhan, A., Cheng, K. R., Meyers, A. J., . . . Williams, D. E. (2014). Commercial DNA extraction kits impact observed microbial community composition in permafrost samples. *FEMS microbiology ecology, 87*(1), 217-230.

Vishnivetskaya, T. A., Petrova, M. A., Urbance, J., Ponder, M., Moyer, C. L., Gilichinsky, D. A., & Tiedje, J. M. (2006). Bacterial community in ancient Siberian permafrost as characterized by culture and culture-independent methods. *Astrobiology, 6*(3), 400-414.

Visnes, T., Doseth, B., Pettersen, H. S., Hagen, L., Sousa, M. M., Akbari, M., . . . Krokan, H. E. (2009). Uracil in DNA and its processing by different DNA glycosylases. *Philosophical transactions of the Royal Society B: Biological sciences, 364*(1517), 563-568.

Vitousek, P. M., Ladefoged, T. N., Kirch, P. V., Hartshorn, A. S., Graves, M. W., Hotchkiss, S. C., . . . Chadwick, O. A. (2004). Soils, agriculture, and society in precontact Hawaii. *Science, 304*(5677), 1665-1669.

Volossiouk, T., Robb, E. J., & Nazar, R. N. (1995). Direct DNA extraction for PCR-mediated assays of soil organisms. *Applied and environmental Microbiology, 61*(11), 3972-3976.

Von Blohn, C., Kempf, B., Kappes, R. M., & Bremer, E. (1997). Osmostress response in Bacillus subtilis: characterization of a proline uptake system (OpuE) regulated by high osmolarity and the alternative transcription factor sigma B. *Molecular microbiology, 25*(1), 175-187.

Vonk, J. E., & Gustafsson, Ö. (2013). Permafrost-carbon complexities. *Nature Geoscience, 6*(9), 675-676.

Vonk, J. E., Tank, S. E., Bowden, W. B., Laurion, I., Vincent, W. F., Alekseychik, P., . . . Cory, R. M. (2015). Reviews and syntheses: Effects of permafrost thaw on Arctic aquatic ecosystems. *Biogeosciences, 12*(23), 7129-7167.

Vorobev, A. V., Baani, M., Doronina, N. V., Brady, A. L., Liesack, W., Dunfield, P. F., & Dedysh, S. N. (2011). Methyloferula stellata gen. nov., sp. nov., an acidophilic, obligately methanotrophic bacterium that possesses only a soluble methane monooxygenase. *International Journal of Systematic and Evolutionary Microbiology, 61*(10), 2456-2463.

Vorobyova, E., Soina, V., Gorlenko, M., Minkovskaya, N., Zalinova, N., Mamukelashvili, A., . . . Vishnivetskaya, T. (1997). The deep cold biosphere: facts and hypothesis. *FEMS microbiology reviews, 20*(3-4), 277-290.

Wagner, D. (2017). Effect of varying soil water potentials on methanogenesis in aerated marshland soils. *Scientific Reports, 7*(1), 1-9.

Wagner, D., Gattinger, A., Embacher, A., PFEIFFER, E. M., Schloter, M., & Lipski, A. (2007). Methanogenic activity and biomass in Holocene permafrost deposits of the Lena Delta, Siberian Arctic and its implication for the global methane budget. *Global Change Biology, 13*(5), 1089-1099.

Waldrop, M., & Firestone, M. (2004). Altered utilization patterns of young and old soil C by microorganisms caused by temperature shifts and N additions. *Biogeochemistry, 67*(2), 235-248.

Waldrop, M., & Firestone, M. (2006). Response of microbial community composition and function to soil climate change. *Microbial ecology, 52*(4), 716-724.

Waldrop, M. P., Wickland, K. P., White Iii, R., Berhe, A. A., Harden, J. W., & Romanovsky, V. E. (2010). Molecular investigations into a globally important carbon pool: Permafrost-protected carbon in Alaskan soils. *Global Change Biology, 16*(9), 2543-2554.

Walter, K. M., Edwards, M. E., Grosse, G., Zimov, S., & Chapin, F. (2007). Thermokarst lakes as a source of atmospheric CH4 during the last deglaciation. *Science, 318*(5850), 633-636.

Walter, K. M., Zimov, S., Chanton, J. P., Verbyla, D., & Chapin, F. S. (2006). Methane bubbling from Siberian thaw lakes as a positive feedback to climate warming. *Nature, 443*(7107), 71-75.

Walther, G.-R., Post, E., Convey, P., Menzel, A., Parmesan, C., Beebee, T. J., . . . Bairlein, F. (2002). Ecological responses to recent climate change. *Nature, 416*(6879), 389-395.

Wang, H., Hu, X., Wetz, M. S., Hayes, K. C., & Lu, K. (2020). Photomineralization of organic carbon in a eutrophic, semiarid estuary. *Limnology and Oceanography Letters, 5*(3), 246-253.

Wang, J., Shen, J., Wu, Y., Tu, C., Soininen, J., Stegen, J. C., . . . Zhang, E. (2013). Phylogenetic beta diversity in bacterial assemblages across ecosystems: deterministic versus stochastic processes. *The ISME journal, 7*(7), 1310-1321.

Wang, Q., Garrity, G. M., Tiedje, J. M., & Cole, J. R. (2007). Naive Bayesian classifier for rapid assignment of rRNA sequences into the new bacterial taxonomy. *Applied and environmental Microbiology, 73*(16), 5261-5267.

Wang, W., Wang, H., Zu, Y., Li, X., & Koike, T. (2006). Characteristics of the temperature coefficient, Q 10, for the respiration of non-photosynthetic organs and soils of forest ecosystems. *Frontiers of Forestry in China, 1*(2), 125-135.

Wang, X., Li, X., Hu, Y., Lv, J., Sun, J., Li, Z., & Wu, Z. (2010). Effect of temperature and moisture on soil organic carbon mineralization of predominantly permafrost peatland in the Great Hing'an Mountains, Northeastern China. *Journal of Environmental Sciences, 22*(7), 1057-1066.

Wang, Y., Naumann, U., Wright, S. T., & Warton, D. I. (2012). mvabund–an R package for model-based analysis of multivariate abundance data. *Methods in Ecology and Evolution, 3*(3), 471-474.

Wanner, H., Solomina, O., Grosjean, M., Ritz, S. P., & Jetel, M. (2011). Structure and origin of Holocene cold events. *Quaternary Science Reviews, 30*(21-22), 3109-3123.

Ward, C. P., & Cory, R. M. (2015). Chemical composition of dissolved organic matter draining permafrost soils. *Geochimica et Cosmochimica Acta, 167*, 63-79.

Wartiainen, I., Hestnes, A. G., McDonald, I. R., & Svenning, M. M. (2006). Methylobacter tundripaludum sp. nov., a methane-oxidizing bacterium from Arctic wetland soil on the Svalbard islands, Norway (78 N). *International Journal of Systematic and Evolutionary Microbiology, 56*(1), 109-113.

Warton, D. I. (2005). Many zeros does not mean zero inflation: comparing the goodness-of-fit of parametric models to multivariate abundance data. *Environmetrics: The official journal of the International Environmetrics Society, 16*(3), 275-289.

Warton, D. I. (2011). Regularized sandwich estimators for analysis of high-dimensional data using generalized estimating equations. *Biometrics, 67*(1), 116-123.

Warton, D. I., Wright, S. T., & Wang, Y. (2012). Distance-based multivariate analyses confound location and dispersion effects. *Methods in Ecology and Evolution, 3*(1), 89-101.

Waters, M. R., & Stafford, T. W. (2007). Redefining the age of Clovis: implications for the peopling of the Americas. *Science, 315*(5815), 1122-1126.

Wear, E. K., Wilbanks, E. G., Nelson, C. E., & Carlson, C. A. (2018). Primer selection impacts specific population abundances but not community dynamics in a monthly time-series 16S rRNA gene amplicon analysis of coastal marine bacterioplankton. *Environmental microbiology, 20*(8), 2709-2726.

Wegener, G., Niemann, H., Elvert, M., Hinrichs, K. U., & Boetius, A. (2008). Assimilation of methane and inorganic carbon by microbial communities mediating the anaerobic oxidation of methane. *Environmental microbiology, 10*(9), 2287-2298.

Wei, H., Guenet, B., Vicca, S., Nunan, N., AbdElgawad, H., Pouteau, V., . . . Janssens, I. A. (2014). Thermal acclimation of organic matter decomposition in an artificial forest soil is

related to shifts in microbial community structure. *Soil Biology and Biochemistry, 71*, 1-12.
Wei, S., Cui, H., Zhu, Y., Lu, Z., Pang, S., Zhang, S., . . . Su, X. (2018). Shifts of methanogenic communities in response to permafrost thaw results in rising methane emissions and soil property changes. *Extremophiles, 22*(3), 447-459.
Weichart, D., & Kjelleberg, S. (1996). Stress resistance and recovery potential of culturable and viable but nonculturable cells of Vibrio vulnificus. *Microbiology, 142*(4), 845-853.
Welsh, D. T. (2000). Ecological significance of compatible solute accumulation by micro-organisms: from single cells to global climate. *FEMS microbiology reviews, 24*(3), 263-290.
West, T. S. (1981). Soil as the source of trace elements. *Philosophical Transactions of the Royal Society of London. B, Biological Sciences, 294*(1071), 19-39.
Weyrich, L. S., Farrer, A. G., Eisenhofer, R., Arriola, L. A., Young, J., Selway, C. A., . . . Cooper, A. (2019). Laboratory contamination over time during low-biomass sample analysis. *Molecular Ecology Resources, 19*(4), 982-996.
Whalen, S., & Reeburgh, W. (1990). Consumption of atmospheric methane by tundra soils. *Nature, 346*(6280), 160-162.
Whatmore, A. M., Chudek, J. A., & Reed, R. H. (1990). The effects of osmotic upshock on the intracellular solute pools of Bacillus subtilis. *Microbiology, 136*(12), 2527-2535.
White, J., Ager, T., Adam, D., Leopold, E., Liu, G., Jette, H., & Schweger, C. (1997). An 18 million year record of vegetation and climate change in northwestern Canada and Alaska: tectonic and global climatic correlates. *Palaeogeography, Palaeoclimatology, Palaeoecology, 130*(1-4), 293-306.
Whitehouse, C. A., & Hottel, H. E. (2007). Comparison of five commercial DNA extraction kits for the recovery of Francisella tularensis DNA from spiked soil samples. *Molecular and cellular probes, 21*(2), 92-96.
Wielicki, B. A., Wong, T., Loeb, N., Minnis, P., Priestley, K., & Kandel, R. (2005). Changes in Earth's albedo measured by satellite. *Science, 308*(5723), 825-825.
Wilhelm, R. C., Niederberger, T. D., Greer, C., & Whyte, L. G. (2011). Microbial diversity of active layer and permafrost in an acidic wetland from the Canadian High Arctic. *Canadian Journal of Microbiology, 57*(4), 303-315.
Willerslev, E., & Cooper, A. (2005). Ancient dna. *Proceedings of the Royal Society B: Biological Sciences, 272*(1558), 3-16.
Willerslev, E., Davison, J., Moora, M., Zobel, M., Coissac, E., Edwards, M. E., . . . Haile, J. (2014). Fifty thousand years of Arctic vegetation and megafaunal diet. *Nature, 506*(7486), 47-51.
Willerslev, E., Hansen, A. J., Binladen, J., Brand, T. B., Gilbert, M. T. P., Shapiro, B., . . . Cooper, A. (2003). Diverse plant and animal genetic records from Holocene and Pleistocene sediments. *Science, 300*(5620), 791-795.
Willerslev, E., Hansen, A. J., & Poinar, H. N. (2004a). Isolation of nucleic acids and cultures from fossil ice and permafrost. *Trends in Ecology & Evolution, 19*(3), 141-147.
Willerslev, E., Hansen, A. J., Rønn, R., Brand, T. B., Barnes, I., Wiuf, C., . . . Cooper, A. (2004b). Long-term persistence of bacterial DNA. *Current Biology, 14*(1), R9-R10.
Williams, J. W., & Jackson, S. T. (2007). Novel climates, no-analog communities, and ecological surprises. *Frontiers in Ecology and the Environment, 5*(9), 475-482.

Williams, P. J., & Smith, M. W. (1989). *The frozen earth: fundamentals of geocryology*: Cambridge University Press.
Winkel, M., Sepulveda-Jauregui, A., Martinez-Cruz, K., Heslop, J., Rijkers, R., Horn, F., . . . Anthony, K. W. (2019). First evidence for cold-adapted anaerobic oxidation of methane in deep sediments of thermokarst lakes. *Environmental Research Communications, 1*(2), 021002.
Wright, G. D., & Poinar, H. (2012). Antibiotic resistance is ancient: implications for drug discovery. *Trends in microbiology, 20*(4), 157-159.
Wu, X., Zhang, W., Liu, G., Yang, X., Hu, P., Chen, T., . . . Li, Z. (2012). Bacterial diversity in the foreland of the Tianshan No. 1 glacier, China. *Environmental Research Letters, 7*(1), 014038.
Xu, L., Paterson, A. D., Turpin, W., & Xu, W. (2015). Assessment and selection of competing models for zero-inflated microbiome data. *PloS one, 10*(7), e0129606.
Yan, F., Schubert, S., & Mengel, K. (1996). Soil pH increase due to biological decarboxylation of organic anions. *Soil Biology and Biochemistry, 28*(4-5), 617-624.
Yanagawa, K., Nunoura, T., McAllister, S., Hirai, M., Breuker, A., Brandt, L., . . . Aoike, K. (2013). The first microbiological contamination assessment by deep-sea drilling and coring by the D/V Chikyu at the Iheya North hydrothermal field in the Mid-Okinawa Trough (IODP Expedition 331). *Frontiers in microbiology, 4*, 327.
Yang, D. Y., & Watt, K. (2005). Contamination controls when preparing archaeological remains for ancient DNA analysis. *Journal of Archaeological Science, 32*(3), 331-336.
Yergeau, E., Bezemer, T. M., Hedlund, K., Mortimer, S. R., Kowalchuk, G. A., & Van Der Putten, W. H. (2010a). Influences of space, soil, nematodes and plants on microbial community composition of chalk grassland soils. *Environmental microbiology, 12*(8), 2096-2106.
Yergeau, E., Bokhorst, S., Kang, S., Zhou, J., Greer, C. W., Aerts, R., & Kowalchuk, G. A. (2012). Shifts in soil microorganisms in response to warming are consistent across a range of Antarctic environments. *The ISME journal, 6*(3), 692-702.
Yergeau, E., Hogues, H., Whyte, L. G., & Greer, C. W. (2010b). The functional potential of high Arctic permafrost revealed by metagenomic sequencing, qPCR and microarray analyses. *The ISME journal, 4*(9), 1206-1214.
Yu, F., Tanaka, Y., Yamashita, K., Suzuki, T., Nakamura, A., Hirano, N., . . . Tanaka, I. (2011). Molecular basis of dihydrouridine formation on tRNA. *Proceedings of the National Academy of Sciences, 108*(49), 19593-19598.
Yun, J., Ju, Y., Deng, Y., & Zhang, H. (2014). Bacterial community structure in two permafrost wetlands on the Tibetan Plateau and Sanjiang Plain, China. *Microbial ecology, 68*(2), 360-369.
Zalasiewicz, J., & Freedman, K. (2009). *The earth after us: What legacy will humans leave in the rocks?* : Oxford University Press.
Zazula, G., Froese, D., Schweger, C., Mathewes, R., Beaudoin, A., Telka, A., . . . Westgate, J. (2003a). Late Pleistocene steppe macrofossils in east Beringia. *Nature, 423*, 603.
Zazula, G. D., Froese, D. G., Elias, S. A., Kuzmina, S., & Mathewes, R. W. (2007). Arctic ground squirrels of the mammoth-steppe: paleoecology of Late Pleistocene middens (~ 24 000–29 450 14C yr BP), Yukon Territory, Canada. *Quaternary Science Reviews, 26*(7-8), 979-1003.

Zazula, G. D., Froese, D. G., Schweger, C. E., Mathewes, R. W., Beaudoin, A. B., Telka, A. M., . . . Westgate, J. A. (2003b). Ice-age steppe vegetation in east Beringia. *Nature, 423*(6940), 603-603.

Zeileis, A., Kleiber, C., & Jackman, S. (2008). Regression models for count data in R. *Journal of statistical software, 27*(8), 1-25.

Zeng, L., Tian, J., Chen, H., Wu, N., Yan, Z., Du, L., . . . Wang, X. (2019). Changes in methane oxidation ability and methanotrophic community composition across different climatic zones. *Journal of Soils and Sediments, 19*(2), 533-543.

Zhang, B., Chen, S., He, X., Liu, W., Zhao, Q., Zhao, L., & Tian, C. (2014). Responses of soil microbial communities to experimental warming in alpine grasslands on the Qinghai-Tibet Plateau. *PloS one, 9*(8), e103859.

Zhang, B., Wu, X., Zhang, G., Li, S., Zhang, W., Chen, X., . . . Chen, T. (2016). The diversity and biogeography of the communities of Actinobacteria in the forelands of glaciers at a continental scale. *Environmental Research Letters, 11*(5), 054012.

Zhang, L.-M., Wang, M., Prosser, J. I., Zheng, Y.-M., & He, J.-Z. (2009). Altitude ammonia-oxidizing bacteria and archaea in soils of Mount Everest. *FEMS microbiology ecology, 70*(2), 208-217.

Zhang, L., Dumont, M. G., Bodelier, P. L., Adams, J. M., He, D., & Chu, H. (2020a). DNA stable-isotope probing highlights the effects of temperature on functionally active methanotrophs in natural wetlands. *Soil Biology and Biochemistry, 149*, 107954.

Zhang, L., Liu, X., Duddleston, K., & Hines, M. E. (2020b). The Effects of pH, Temperature, and Humic-Like Substances on Anaerobic Carbon Degradation and Methanogenesis in Ombrotrophic and Minerotrophic Alaskan Peatlands. *Aquatic Geochemistry*, 1-24.

Zhang, Y.-Y., Wu, W., & Liu, H. (2019). Factors affecting variations of soil pH in different horizons in hilly regions. *PloS one, 14*(6), e0218563.

Zhang, Y., Chen, W., & Riseborough, D. W. (2008a). Disequilibrium response of permafrost thaw to climate warming in Canada over 1850–2100. *Geophysical Research Letters, 35*(2).

Zhang, Y., Chen, W., & Riseborough, D. W. (2008b). Transient projections of permafrost distribution in Canada during the 21st century under scenarios of climate change. *Global and Planetary Change, 60*(3-4), 443-456.

Zheng, J., RoyChowdhury, T., Yang, Z., Gu, B., Wullschleger, S. D., & Graham, D. E. (2018). Impacts of temperature and soil characteristics on methane production and oxidation in Arctic tundra. *Biogeosciences (Online), 15*(21).

Zhou, J., Deng, Y., Zhang, P., Xue, K., Liang, Y., Van Nostrand, J. D., . . . Stahl, D. A. (2014). Stochasticity, succession, and environmental perturbations in a fluidic ecosystem. *Proceedings of the National Academy of Sciences, 111*(9), E836-E845.

Zhou, J., Xia, B., Treves, D. S., Wu, L.-Y., Marsh, T. L., O'Neill, R. V., . . . Tiedje, J. M. (2002). Spatial and resource factors influencing high microbial diversity in soil. *Applied and environmental Microbiology, 68*(1), 326-334.

Ziegler, C., Bremer, E., & Krämer, R. (2010). The BCCT family of carriers: from physiology to crystal structure. *Molecular microbiology, 78*(1), 13-34.

Zimmermann, H., Epp, L., Overduin, P., Schwamborn, G., Schirrmeister, L., & Herzschuh, U. (2016). *Late Quaternary vegetation history of North-Eastern Siberia inferred from ancient DNA analyses of permafrost sediment cores*.

Zimov, S. A., Schuur, E. A., & Chapin III, F. S. (2006). Permafrost and the global carbon budget. *Science(Washington), 312*(5780), 1612-1613.

Zimov, S. A. e., Voropaev, Y. V., Semiletov, I., Davidov, S., Prosiannikov, S., Chapin, F., . . . Tyler, S. (1997). North Siberian lakes: a methane source fueled by Pleistocene carbon. *Science, 277*(5327), 800-802.

Appendix 1

Supplementary figures and tables for chapter 2

Supplementary Table 1.1. Previously published permafrost decontamination, DNA extraction and sample handling protocols.

Decontamination protocol	DNA extraction protocol	Spike	Sample handling[g]	Year	Reference
Scraping	CTAB	BE[b]	C, E	2006	(Vishnivetskaya *et al.*, 2006)
	N/A[a]	-[c]	N/A	2006	(Bai *et al.*, 2006)
	Marmur	AE[d]	N/A	2007	(Rivkina *et al.*, 2007)
	Chloroform: octanol	BE	A, C, D	2007	(Johnson *et al.*, 2007)
	PowerSoil	-	N/A	2010	(Waldrop *et al.*, 2010)
	CTAB	-	N/A	2011	(Mackelprang *et al.*, 2011)
	PowerSoil	-	N/A	2013	(Bischoff *et al.*, 2013)
	PowerSoil	-	E	2014	(Frank-Fahle *et al.*, 2014)

	CTAB/phenol: chloroform	AC[e]	N/A	2015	(Hultman *et al.*, 2015)
	PowerSoi	BE	B	2016	(Rivkina *et al.*, 2016)
	PowerSoil	-	E	2018	(Bottos *et al.*, 2018)
Disk sampling	Chloroform: isoamyl alcohol	BE	N/A	2000	(Rivkina *et al.*, 2000)
	PowerMax	AE	N/A	2010	(Yergeau *et al.*, 2010b)
	TCEP	BC[f]	A, C	2011	(D'Costa *et al.*, 2011)
	N/A	BE	N/A	2012	(Wright & Poinar, 2012)
	N/A	-	N/A	2013	(Porter *et al.*, 2013)
	Phenol: chloroform	-	N/A	2014	(Tuorto *et al.*, 2014)
Scraping and disk sampling	Chloroform: octanol	BE	A, C, D	2005	(Lydolph *et al.*, 2005)
	PowerSoil	-	N/A	2011	(Coolen *et al.*, 2011)
	PowerSoil	BE	N/A	2015	(Krivushin *et al.*, 2015)
	PowerSoil	-	N/A	2015	(Coolen & Orsi, 2015)

	Fast DNA	AC	N/A	2017	(Mackelprang *et al.*, 2017)
Not determined	Marmur	-	N/A	2005	(Gilichinsky *et al.*, 2005)
	Fast DNA	-	N/A	2007	(Hansen *et al.*, 2007)
	PowerSoil	-	N/A	2009	(Liebner *et al.*, 2009)
	PowerMax	-	A	2013	(Bellemain *et al.*, 2013)
	Freeze grinding mechanical lysis	-	N/A	2013	(Penton *et al.*, 2013)
	Chloroform fumigation and K_2SO	-	C	2014	(Treat *et al.*, 2014)
	PowerMax	-	N/A	2014	(Mondav *et al.*, 2014)
	PowerMax	-	N/A	2015	(Deng *et al.*, 2015)
	Freeze drying and chemical lysis	-	C	2015	(Schostag *et al.*, 2015)
	PowerSoil	-	C	2018	(Monteux *et al.*, 2018)
	Fast DNA	-	E	2018	(Wei *et al.*, 2018)
	PowerSoil	-	N/A	2018	(Knoblauch *et al.*, 2018)

[a]N/A = not mentioned.
[b]BE = A biological spike applied to coring equipment.
[c]- = Not used.
[d]AE = An artificial spike applied to coring equipment.
[e]AC = An artificial spike directly applied to the permafrost cores.
[f]BC = A biological spike directly applied to the permafrost cores.
[g] A = A clean lab was used, B = Sterile tools were used, C = Clean reagents with controls were used, D = The experiment was replicated in another university, E = Other (Use of a mobile hood, anaerobic glove box or a soil press).

Sterilization procedure of the tools and the work stations

All decontamination methods were performed in a class 1000 clean laboratory separate from the DNA extraction and PCR labs, and with no prior history of DNA work (Cooper & Poinar, 2000). The surface of the working area was washed with 100% concentrated bleach (Clorox, USA) followed by 70% ethanol (Cooper & Poinar, 2000). Later the clean area was covered with bleach (Clorox, USA) and 70% ethanol treated heavy duty aluminum foil (AlCAN Plus, Canada). During decontamination protocol testing, full Tyvek body suits with elasticized hood (Bennett, Canada), standard polypropylene shoe covers (WorkHorse, USA), N95 standard face masks (3M, USA), powder free Sterling nitrile gloves (Kimberly-Clark, USA), and standard safety goggles were worn. 70% ethanol treated gloves were changed regularly during the decontamination process. All the metal objects and glassware were muffle furnace baked at 450 ^{o}C for 5 h. Chisels were burnt with 70% ethanol with a hand torch prior to contact with the samples. Milli Q water used for washing core segments was pre-filtered through Millex-GS 0.22 μm syringe filters (Millipore Canada) and autoclaved twice for 30 min prior to use. Metal rulers and hand saw were cleaned with 70% ethanol and the working area in the walk in 4 ^{o}C cold room was surface cleaned with 100% concentrated bleach (Clorox, USA) followed by 70% ethanol.

Half strength and full strength Luria Bertani (LB, BD Difco manual) and nutrient agar (NA, Thermo Fisher Scientific, Canada) plates without lids were employed to test for the presence of the aerosolized bacteria before, during and after the decontamination procedures (modified from (D'Costa *et al.*, 2011; Porter *et al.*, 2013). All DNA extractions were performed in an EdgeGARD Horizontal Laminar-Flow Clean Bench (model EG6220, Baker, USA) decontaminated with 100% concentrated bleach (Clorox, USA) followed by 70% ethanol. All forceps and spatula were soaked in 70% ethanol and flame sterilized for ~5 s. All the plastic racks for holding the tubes were washed and kept in 10% bleach (Clorox, USA) for 24 h prior to DNA extraction. Certified RNase/DNase and pyrogen safe Filter pipet tips (Axygen Scientific, USA) were used in every step of the extraction procedure and all the hand pipettes were cleaned with 70% ethanol prior to any experiment.

Basic chemical parameter analyses of the core segments

Gravimetric water content was measured by oven drying at 100 ºC for 48 h (Bittelli, 2011), organic matter content was determined based on loss on ignition at 450 ºC for 5 h in a standard muffle furnace (Lim & Jackson, 1982). pH was measured with the aid of an AB15 pH meter (Fisher Scientific, Canada) by buffering the samples with 0.01 M $CaCl_2.2H_2O$ at a 1:2 soil: water ratio (Burt, 2004).

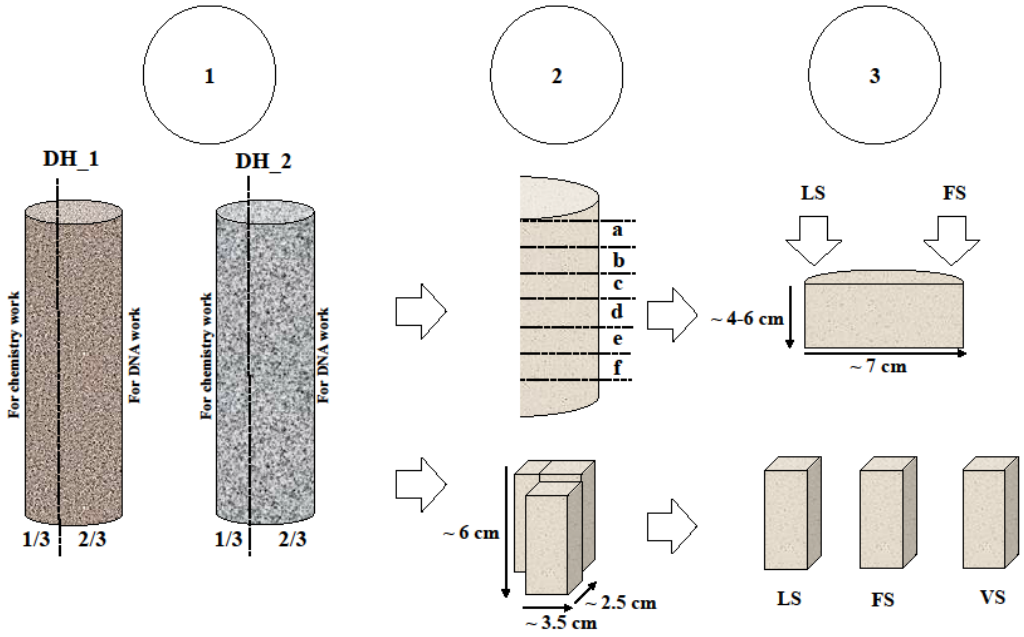

Supplementary Figure 2.1. Sample preparation for decontamination protocols (a-g). Step 1: Initial dry cut. DH-1 and DH-2 cores cut into 1/3 and 2/3 sections. Step 2: Cutting into subsections. The upper portion of the 2/3 section cut horizontally for decontamination protocols (a-f). For protocol (g), the 2/3 section was cut into three rectangular pieces. Step 3: Intentional contamination of the samples. For protocols (a-f), one side of the sample was painted with the spike in the lab (LS) and the other side only contained the sprayed field spike (FS). For protocol g, one rectangular piece only contained the sprayed field spike (FS); one piece was painted with the spike in the lab (LS), and one piece was painted with pure vector (VS).

Modified DNA extraction protocols

Protocol 2: FastDNA SPIN Kit for Soil

Samples were homogenized for 45 s at 2000 × g twice. After adding the Binding Matrix suspension, the samples were placed on a rotor to allow DNA to bind for 15 min and later centrifuged for 1 min at 13,000 × g to remove the silica matrix. The washing solution in the spin filter was evaporated by incubating the tubes in a heat block at 70 °C for 15 min. 50 µl of water was used instead of 100 µl for the final elution step. After confirming that the DNA concentrations were below the detection limit of the Qubit, eluted DNA samples were pooled and mixed for a second time with 4 ml Binding Matrix. The conical tubes were inverted by hand for 2 min to allow binding of DNA and later placed in a rack for 20 min to allow settling of the silica matrix. 600 µl of the mixture was added to new set of spin filters and centrifuged at 13,000 × g for 20 min, which was repeated until all samples passed through into the catch tubes. Then we followed the remaining steps as described by the manufacturer's protocol. The final eluted DNA samples were subjected to Zymo Genomic DNA Clean & Concentrator-10 (Zymo Research, USA) kit by following the manufacturer's instructions.

Protocol 5: PowerSoil DNA Isolation Kit

At step 14, solution C4 was added in a total of 4 ml instead of 1200 µl and the vortexing step was 20 s. The samples were incubated for 30 min prior to step 15. At step 20 instead of 100 µl, the DNA was eluted in 50 µl of solution C6.

Protocol 7: ZymoBIOMICS DNA Microprep Kit

During the DNA extraction, we did not use the Zymo-Spin IV Spin Filters. All the supernatants after the bead beating and centrifugation steps were pooled into a single 50 ml conical tube. For optimal performance, 0.5% beta-mercaptoethanol (vol/vol) was added to the ZymoBIOMICS DNA Binding Buffer prior to use. Three times the volume of ZymoBIOMICS DNA Binding Buffer was used to maintain the ratios. The samples were incubated for 30 min at room temperature with vigorous shaking. The entire DNA binding buffer was passed through 3-4 Zymo-Spin IC-Z columns. After each washing step, samples were centrifuged for extra 3 min to remove the excess ethanol. After adding 10 µl of ZymoBIOMICS DNase/RNase free water the samples were allowed to incubate for 5 min. The final centrifugation step was for 5 min.

Contamination detection

The presence of the tracer was tested with pBAD-forward (5′-ATG-CCA-TAG-CAT-TTT-TAT-CC-3′) and pBAD-reverse (5′-GAT-TTA-ATC-TGT-ATC-AGG-3′) primers (Invitrogen/ThermoFisher, Canada). The 50 µl PCR reaction included: 1× PCR buffer (Invitrogen/ThermoFisher, Canada); 200 µM dNTP mixture (Invitrogen/ThermoFisher, Canada); 0.5 µM each primer; 1.5 mM $MgCl_2$ (Invitrogen/ThermoFisher, Canada); 1.25 U Platinum Taq DNA polymerase (Invitrogen/ThermoFisher, Canada); 36.25 µl of H_2O (Integrated DNA Technologies, Iowa, USA); and 1-2 µl of 1:2, 1:10 or 1:100 diluted DNA template. The program for amplification included: 95 ^oC for 50 s, followed by 33 cycles of 94 ^oC for 20 s, 44 ^oC for 30 s, and 72 ^oC for 1 min, with a holding temperature of 4 ^oC.

16S rRNA gene-targeted PCR protocol

The 16S rRNA gene PCR reactions were performed in a Veriti 96 well thermal cycler (Applied Biosystems, Thermo Fisher Scientific, Canada) using primers targeting the V3 region of the 16S rRNA gene: 341F (5′-CCT-ACG-GGA-GGC-AGC-AG-3′) and 518R (5′-GTA-TTA-CCG-CGG-CTG-CTG-G-3′) (0.25 µM each) (Monteux et al., 2018). The 25 µl reaction for each sample was based on the Q5 high-fidelity DNA polymerase kit instruction provided by the manufacturer (NEB Labs INC, Canada) with the exception that 1-2 µl of the 1:2, 1:5 and 1:10 diluted DNA was used as the template. The touchdown thermocycling program used was: 94 ºC for 3 min, followed by 10 cycles of 94 ºC for 30 s, 65-55 ºC for 40 s, 72 ºC for 1 min, followed by 20 cycles of 94 ºC for 30 s, 55 ºC for 40 s, 72 ºC for 1 min; 53 ºC for 40 s with a final elongation step at 72 ºC for 10 min and a holding temperature at 4 ºC. This PCR protocol was used for 16S rRNA gene amplification throughout this manuscript unless otherwise noted.

A

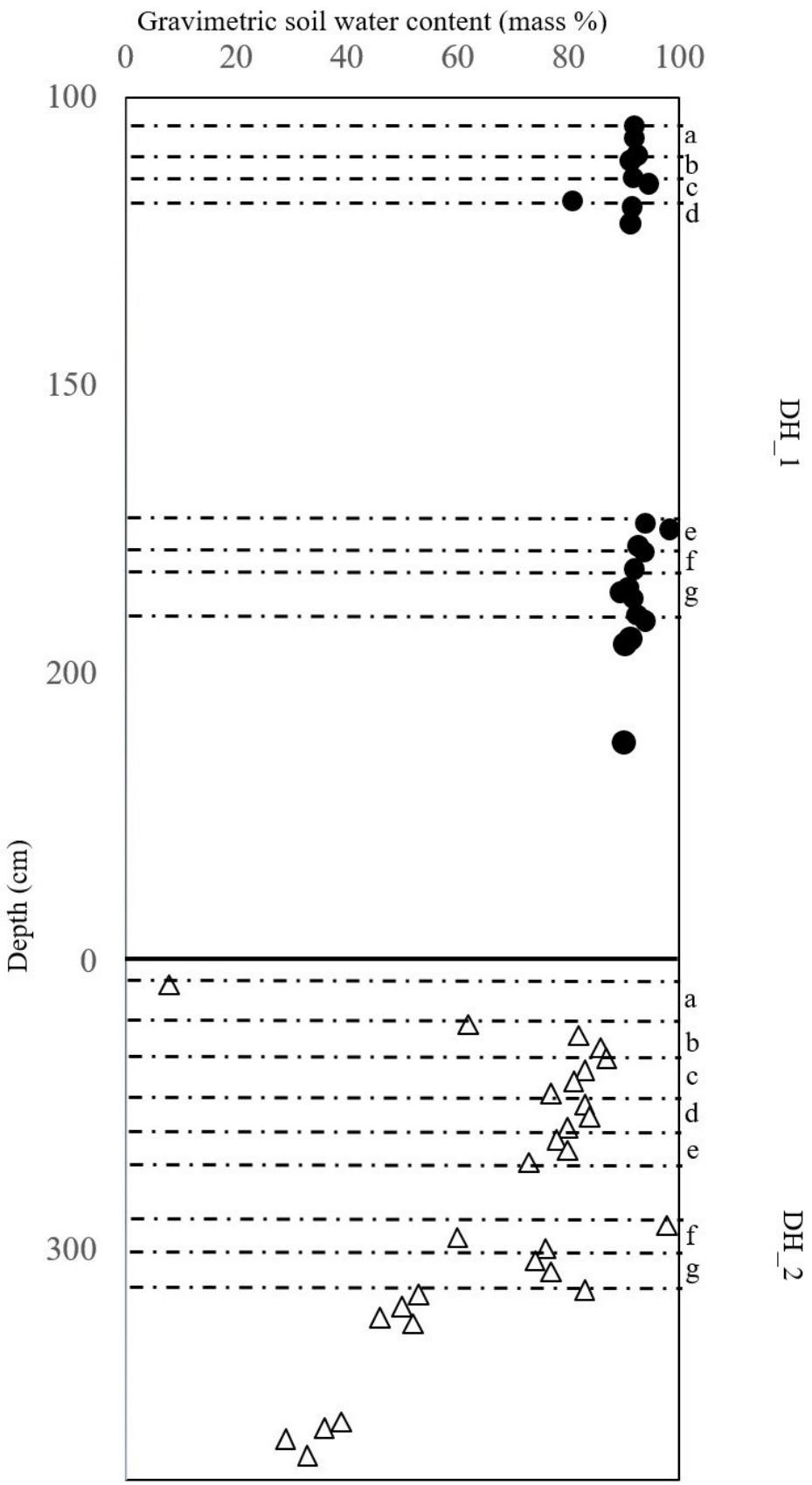
Gravimetric soil water content (mass %)
0
20
40
60
80
100
100
150
200
0
300
Depth (cm)
a
b
c
d
e
f
g
DH_1
a
b
c
d
e
f
g
DH_2

B

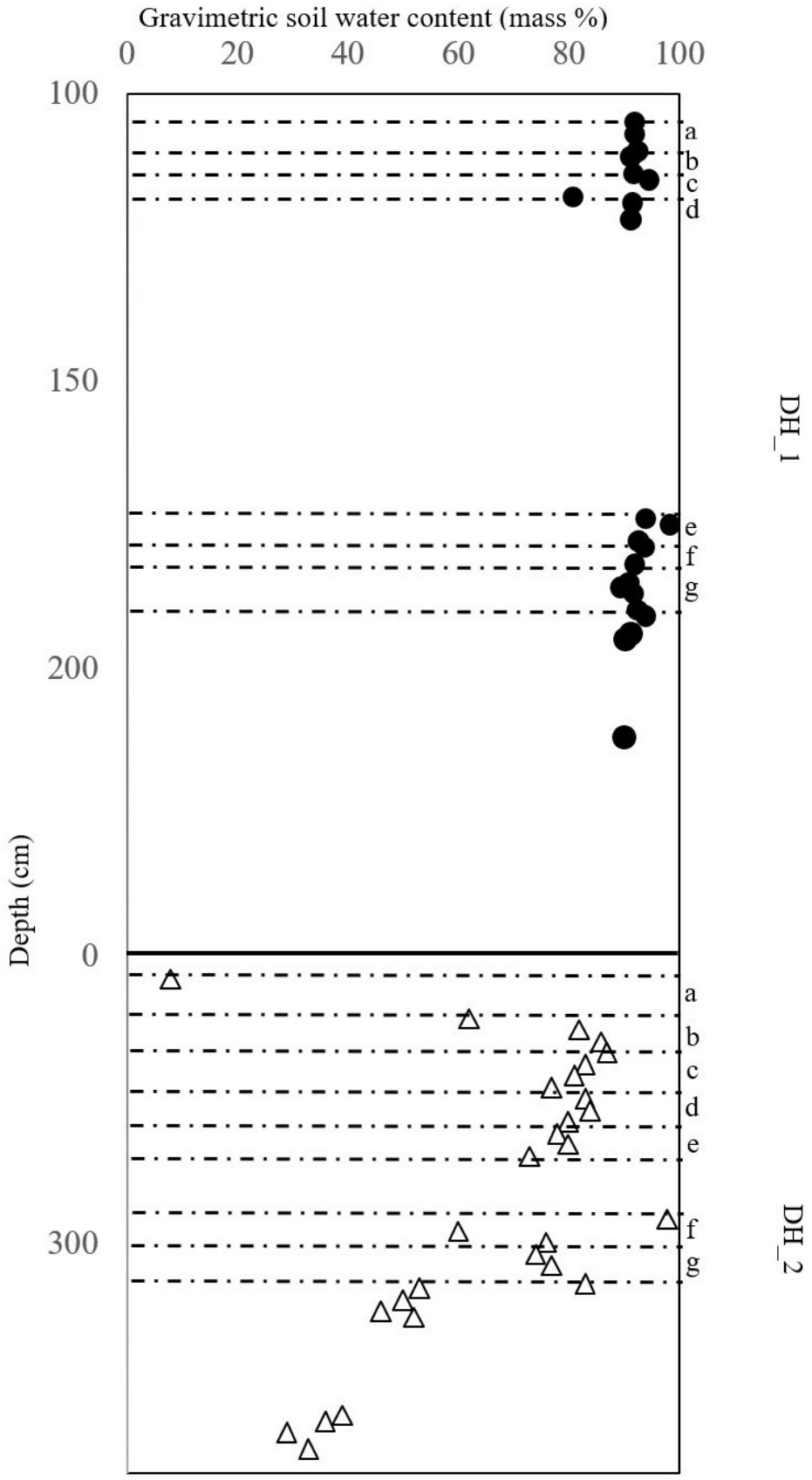
Gravimetric soil water content (mass %)
0
20
40
60
80
100
100
150
200
0
300
Depth (cm)
a
b
c
d
e
f
g
DH_1
a
b
c
d
e
f
g
DH_2

C

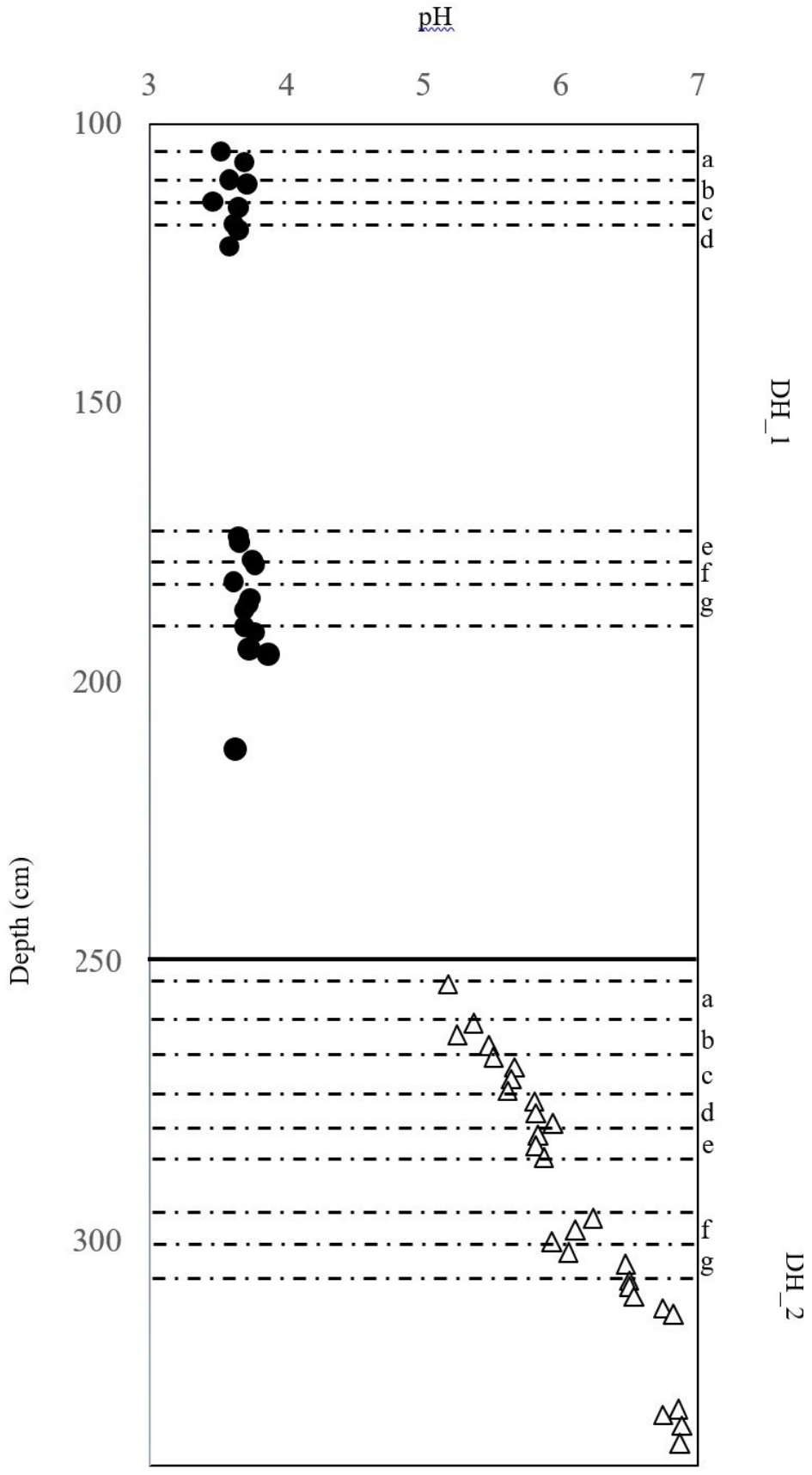

Supplementary Figure 2.2. Chemical profiles of DH_1 and DH_2 permafrost samples in relation to depth. Depth (cm) is relative to the permafrost table. Dashed lines indicate depth of sample used for noted decontamination protocol labeled as in Table 2.1. The solid line depicts the boundary between permafrost with high peat (DH_1, filled dots) and high silt content (DH_2, hollow triangles). A. Organic matter content (mass %), B. Gravimetric water content (mass %), C. pH. The observed gap between sample d and sample e for DH_1 is due to the presence of ice pockets or not measured.

Appendix 2

Supplementary figures and tables for chapter 3

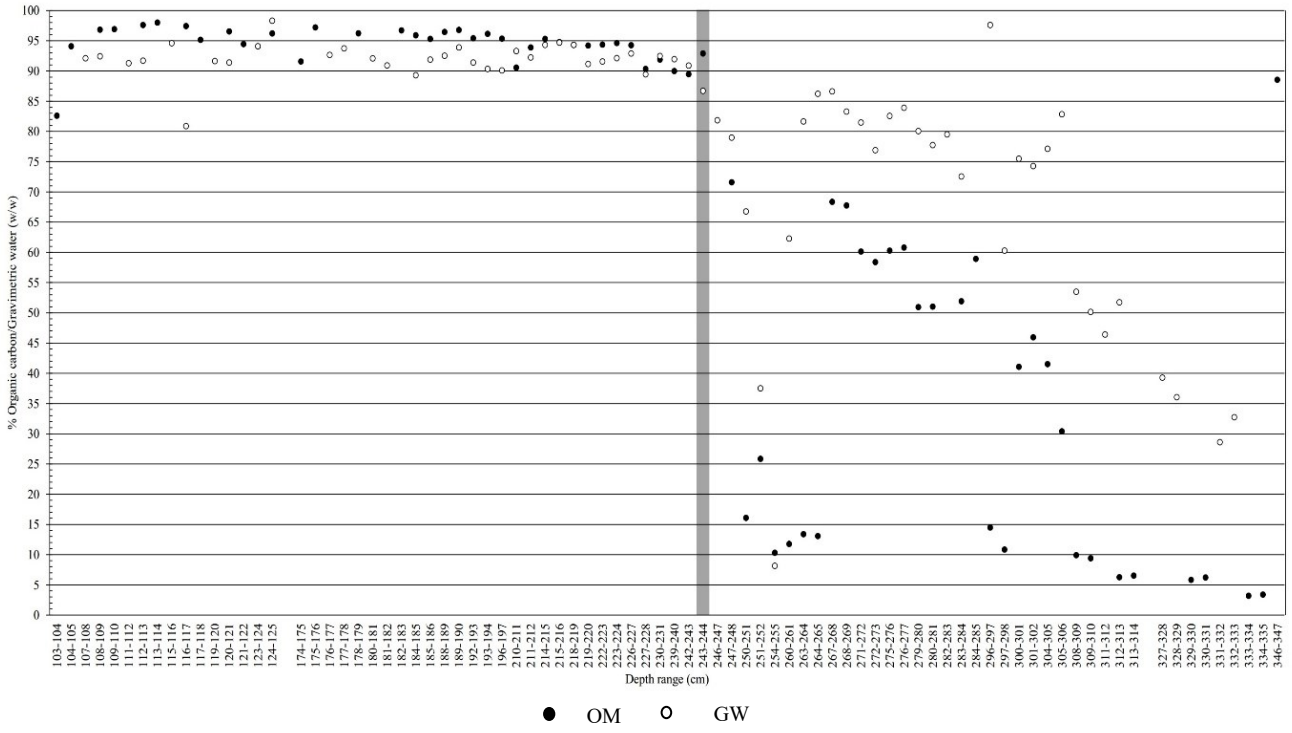

A

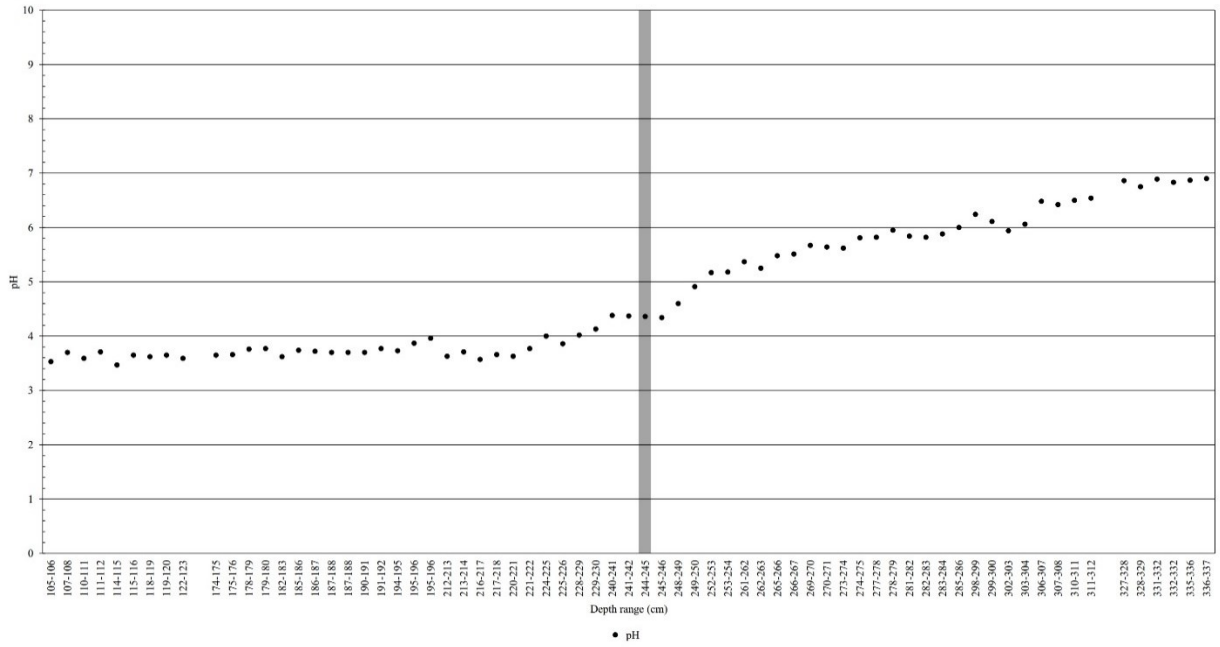
pH
Depth range (cm)
pH

B

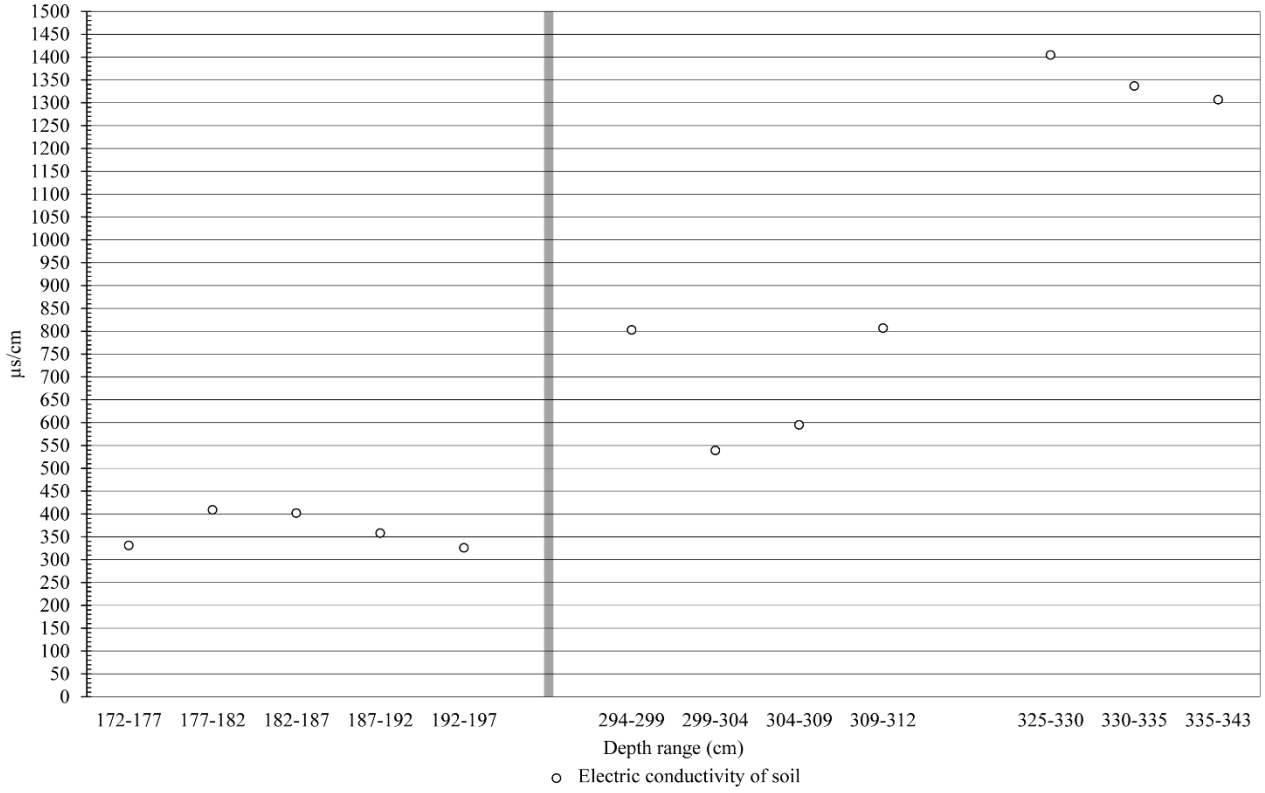
µs/cm
172-177
177-182
182-187
187-192
192-197
294-299
299-304
304-309
309-312
325-330
330-335
335-343
Depth range (cm)
Electric conductivity of soil

C

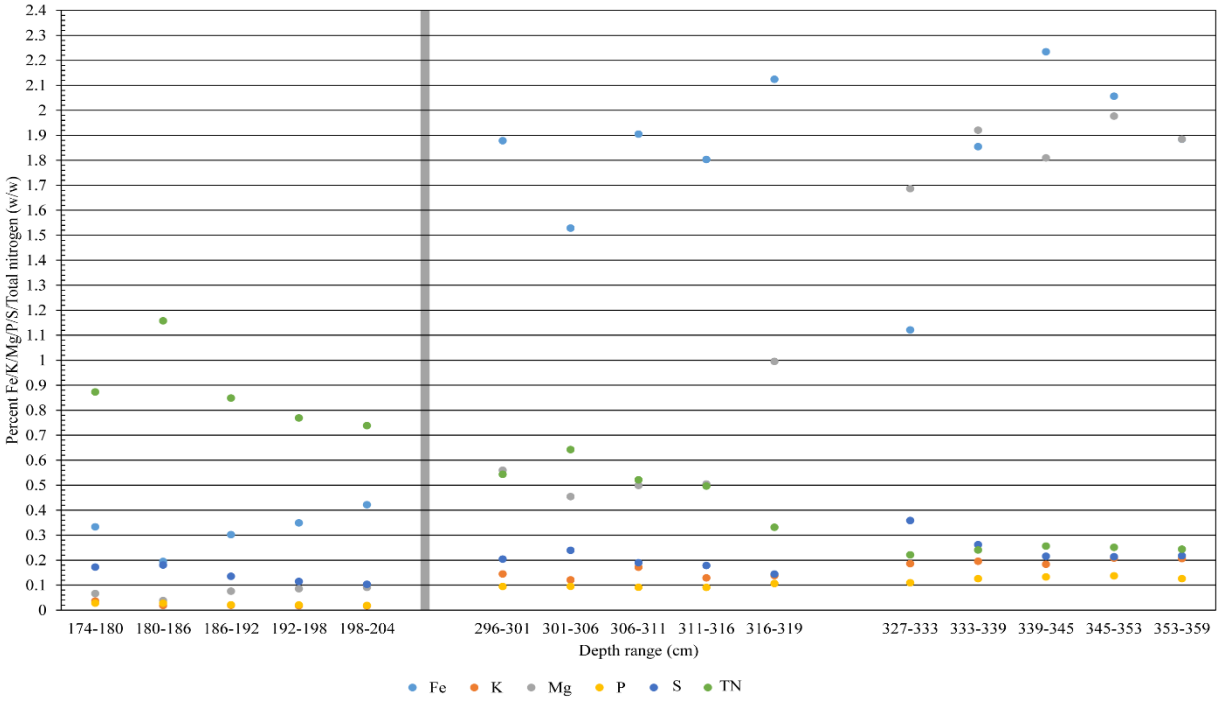
Percent Fe/K/Mg/P/S/Total nitrogen (w/w)
Depth range (cm)
174-180
180-186
186-192
192-198
198-204
296-301
301-306
306-311
311-316
316-319
327-333
333-339
339-345
345-353
353-359
Fe
K
Mg
P
S
TN

D

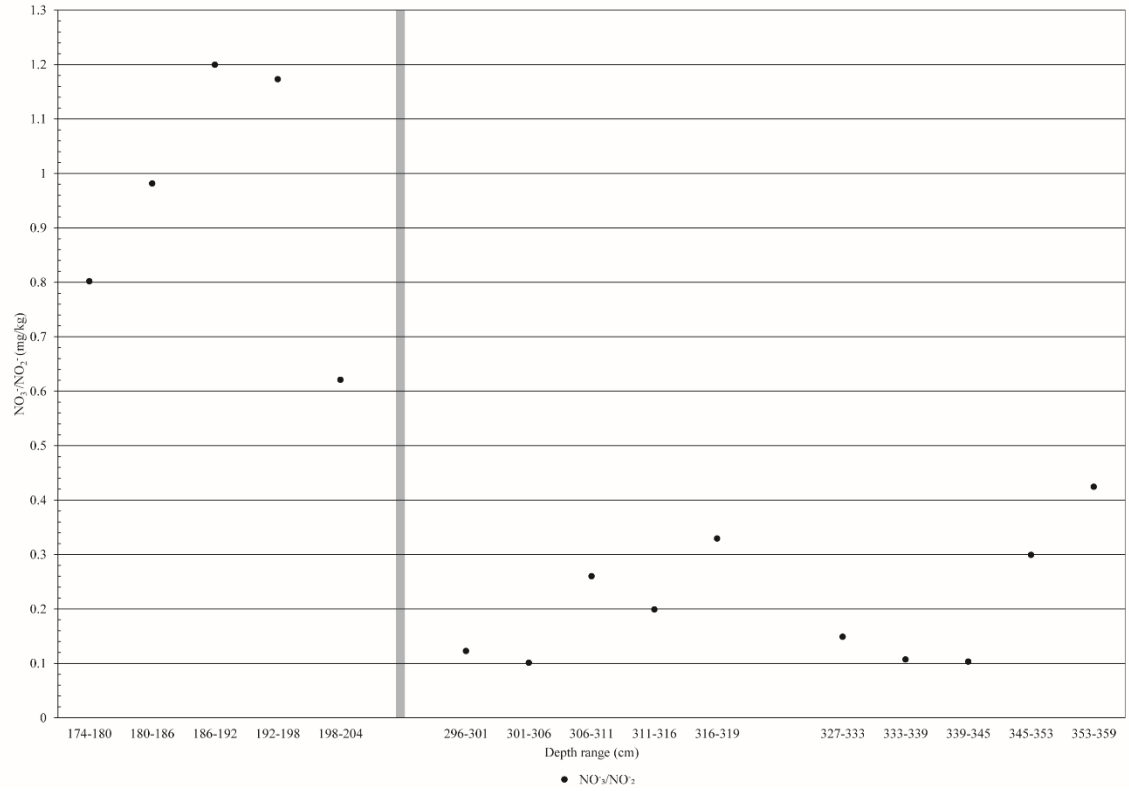
NO3-/NO2- (mg/kg)
Depth range (cm)
174-180
180-186
186-192
192-198
198-204
296-301
301-306
306-311
311-316
316-319
327-333
333-339
339-345
345-353
353-359
NO3-/NO2-

E

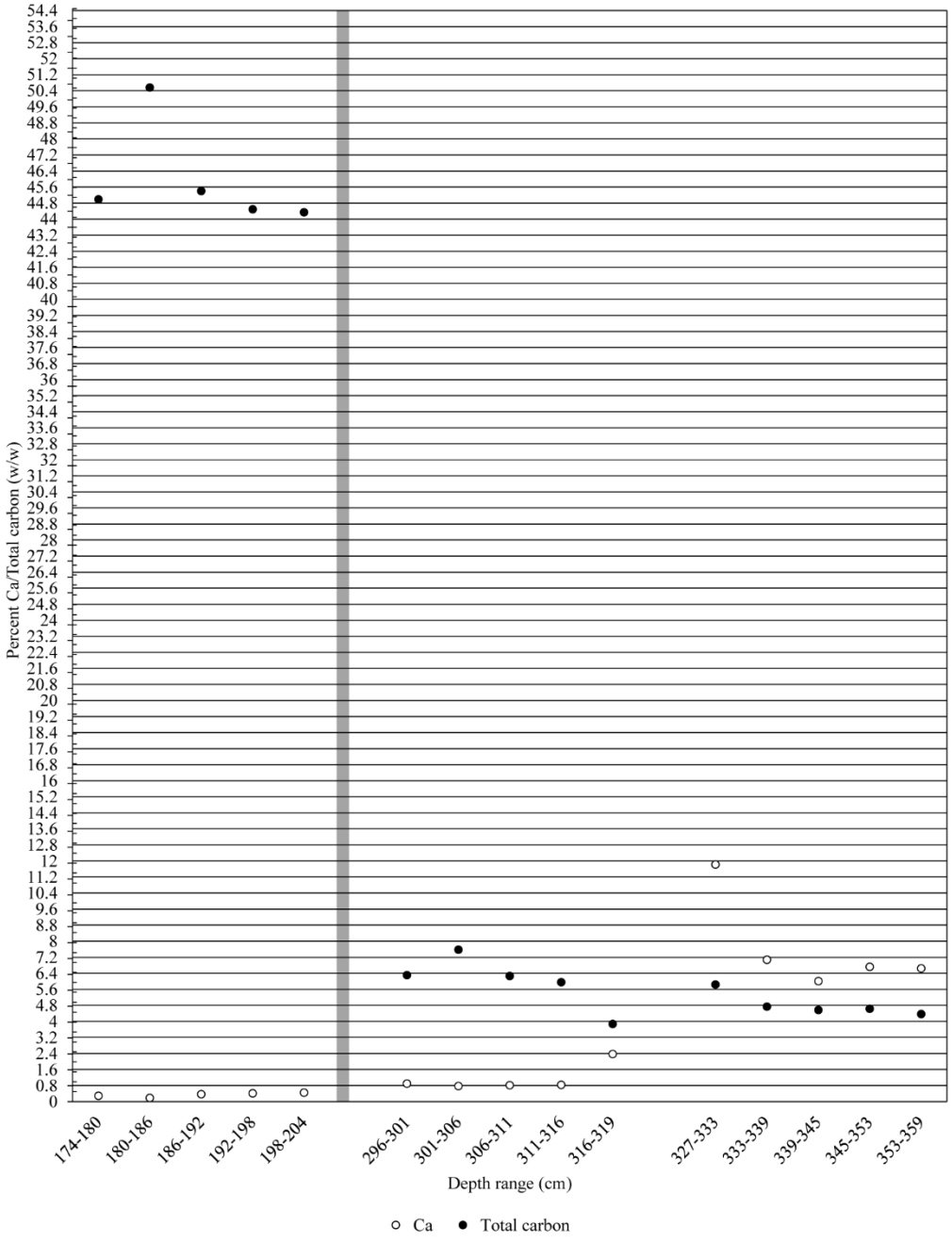
Percent Ca/Total carbon (w/w)
54.4
53.6
52.8
52
51.2
50.4
49.6
48.8
48
47.2
46.4
45.6
44.8
44
43.2
42.4
41.6
40.8
40
39.2
38.4
37.6
36.8
36
35.2
34.4
33.6
32.8
32
31.2
30.4
29.6
28.8
28
27.2
26.4
25.6
24.8
24
23.2
22.4
21.6
20.8
20
19.2
18.4
17.6
16.8
16
15.2
14.4
13.6
12.8
12
11.2
10.4
9.6
8.8
8
7.2
6.4
5.6
4.8
4
3.2
2.4
1.6
0.8
0
174-180
180-186
186-192
192-198
198-204
296-301
301-306
306-311
311-316
316-319
327-333
333-339
339-345
345-353
353-359
Depth range (cm)
Ca
Total carbon

F

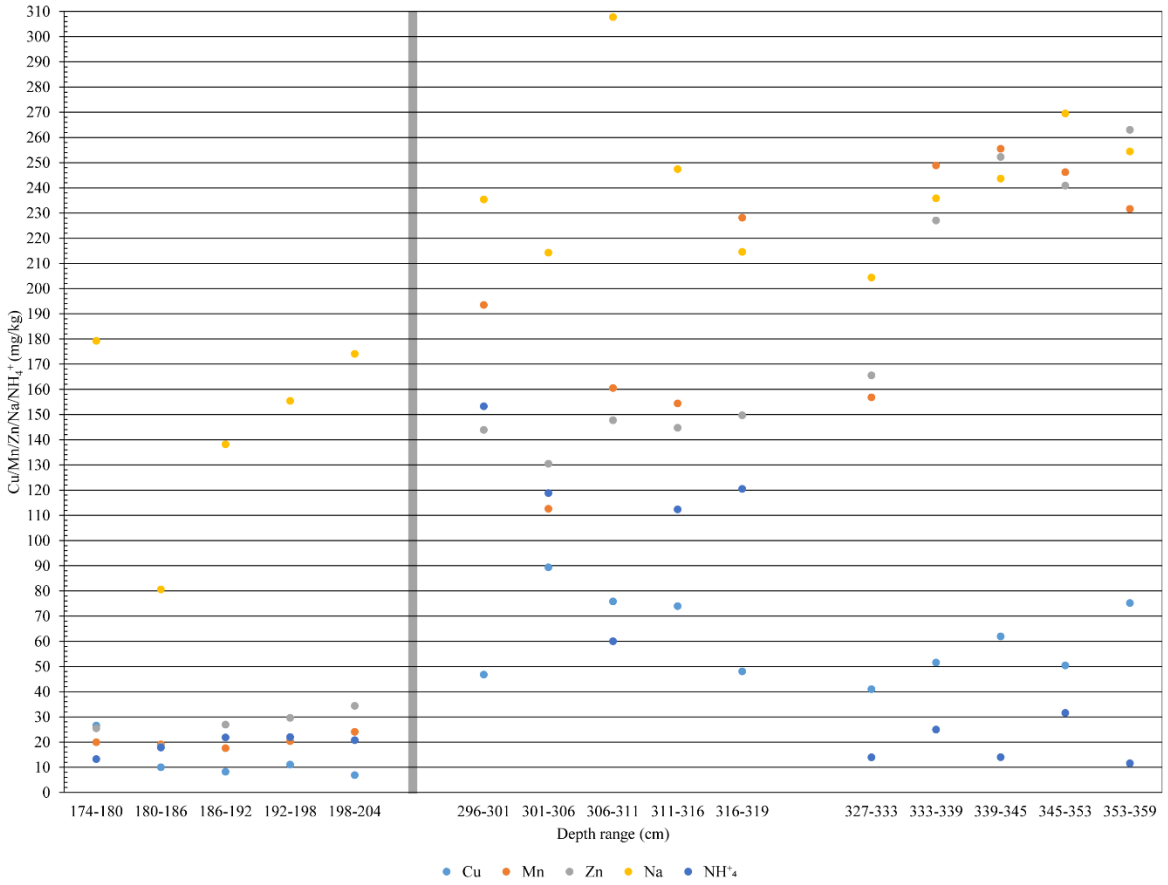

G

Supplementary Figure 3.1. Chemical parameters in DHL16-1 (Holocene-aged) and DHL16-2 and DHL16-3 (Pleistocene-aged). The gray bar is the Pleistocene-Holocene boundary that started at a depth of 244 cm. (A) Organic matter (OM) and gravimetric water content. (B) pH. (C) Electrical Conductivity. (D) Nutrients, including Fe, K, Mg, P, S, and total nitrogen (TN). (E) NO_3^-/NO_2^-. (F) Ca and total carbon. (G) Cations, including Cu, Mn, Zn, Na, and NH_4^+. All measured chemical parameters demonstrated a statistically significant change ($P<0.001$-0.05) from Holocene to Pleistocene soils except NH_4^+ ($p=0.16$).

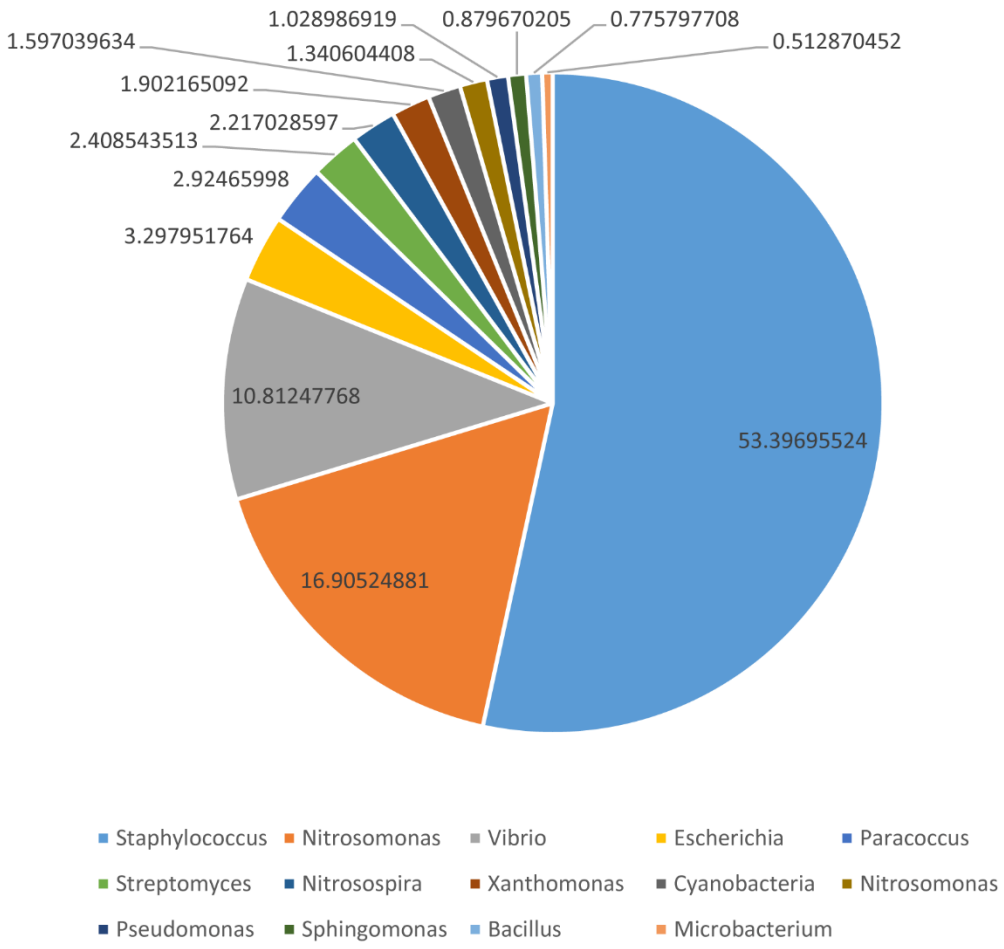

Supplementary Figure 3.2. Relative abundance analysis of the 14 lab strains (lab constructed mock community) used as a positive sequencing control. The strains are shown at the genus level only.

Supplementary Table 3.1. List of the strains detected in the blank sequencing controls via SINTAX algorithm and a V4 16S rRNA RDP (v16; 13k sequences) database.

*d:Bacteria,p:"Proteobacteria",c:Gammaproteobacteria
d:Bacteria,p:Firmicutes,c:Bacilli,o:Bacillales,f:Staphylococcaceae,g:*Staphylococcus*
d:Bacteria,p:"Proteobacteria",c:Gammaproteobacteria,o:"Enterobacteriales",f:Enterobacteriaceae
d:Bacteria,p:"Bacteroidetes",c:"Bacteroidia",o:"Bacteroidales",f:"Porphyromonadaceae"
d:Bacteria,p:"Proteobacteria",c:Gammaproteobacteria,o:"Enterobacteriales",f:Enterobacteriaceae,g:*Escherichia/Shigella,s:Escherichia_fergusonii*
d:Bacteria,p:Firmicutes,c:Bacilli,o:Lactobacillales,f:Streptococcaceae,g:*Streptococcus,s:Streptococcus_gallolyticus_subsp._pasteurianus*
d:Bacteria,p:"Proteobacteria",c:Gammaproteobacteria,o:Pseudomonadales,f:Moraxellaceae,g:*Acinetobacter*
d:Bacteria,p:Firmicutes,c:Clostridia,o:Clostridiales,f:Ruminococcaceae,g:Faecalibacterium,s:Faecalibacterium_prausnitzii
d:Bacteria,p:"Bacteroidetes",c:"Bacteroidia",o:"Bacteroidales",f:"Prevotellaceae"
d:Bacteria,p:"Proteobacteria",c:Betaproteobacteria,o:Burkholderiales,f:Burkholderiaceae,g:*Ralstonia*
d:Bacteria,p:"Actinobacteria",c:Actinobacteria,o:Actinomycetales,f:Corynebacteriaceae,g:*Corynebacterium,s:Corynebacterium_tuberculostearicum*
d:Bacteria,p:Firmicutes,c:Clostridia,o:Clostridiales,f:Clostridiaceae_1,g:Clostridium_sensu_stricto
d:Bacteria,p:"Proteobacteria",c:Gammaproteobacteria,o:"Vibrionales",f:Vibrionaceae,g:*Vibrio,s:Vibrio_cholerae*
d:Bacteria,p:"Bacteroidetes",c:"Bacteroidia",o:"Bacteroidales",f:"Porphyromonadaceae"
d:Archaea,p:"Euryarchaeota",c:Methanobacteria,o:Methanobacteriales,f:Methanobacteriaceae,g:*Methanobrevibacter,s:Methanobrevibacter_smithii*
d:Bacteria,p:"Proteobacteria",c:Gammaproteobacteria,o:Pseudomonadales,f:Pseudomonadaceae,g:*Pseudomonas*
d:Bacteria,p:"Verrucomicrobia",c:Verrucomicrobiae,o:Verrucomicrobiales,f:Verrucomicrobia

ceae,g:*Akkermansia,s:Akkermansia_muciniphila*

d:Bacteria,p:Firmicutes,c:Bacilli,o:Lactobacillales,f:Lactobacillaceae,g:*Lactobacillus,s:Lactobacillus_amylovorus*

d:Bacteria,p:"Proteobacteria",c:Alphaproteobacteria,o:Rhodobacterales,f:Rhodobacteraceae,g:*Paracoccus*

d:Bacteria,p:"Proteobacteria",c:Alphaproteobacteria,o:Sphingomonadales,f:Sphingomonadaceae,g:*Sphingomonas*

d:Bacteria,p:Firmicutes,c:Bacilli,o:Bacillales,f:Bacillaceae_1,g:*Bacillus*

d:Bacteria,p:"Actinobacteria",c:Actinobacteria,o:Actinomycetales,f:Microbacteriaceae,g:*Microbacterium*

d:Bacteria,p:Firmicutes,c:Bacilli,o:Bacillales,f:Bacillaceae_1,g:*Bacillus*

d:Bacteria,p:"Proteobacteria",c:Betaproteobacteria,o:Nitrosomonadales,f:Nitrosomonadaceae,g:*Nitrosomonas*

d:Bacteria,p:"Proteobacteria",c:Betaproteobacteria,o:Nitrosomonadales,f:Nitrosomonadaceae,g:Nitrosomonas,s:*Nitrosomonas_europaea*

d:Bacteria,p:"Bacteroidetes",c:"Bacteroidia",o:"Bacteroidales",f:"Prevotellaceae",g:*Prevotella*

d:Bacteria,p:Firmicutes,c:Clostridia,o:Clostridiales

d:Bacteria

d:Bacteria,p:"Actinobacteria",c:Actinobacteria,o:Actinomycetales,f:Streptomycetaceae,g:*Streptomyces*

d:Bacteria,p:"Proteobacteria",c:Betaproteobacteria,o:Nitrosomonadales,f:Nitrosomonadaceae,g:Nitrosospira,s:*Nitrosospira_multiformis*

d:Bacteria,p:Cyanobacteria/Chloroplast,c:Cyanobacteria

d:Bacteria,p:"Proteobacteria",c:Gammaproteobacteria,o:Xanthomonadales,f:Xanthomonadaceae,g:*Xanthomonas*,s:*Xanthomonas_bromi*

* In the list d: domain, p: phylum, c: class, o: order, f: family, g: genus, and s: species.

Supplementary Table 3.2. The effect of the sequence cleaning process on reads before and after removal of the anomalous sequences detected in blank controls.

Sample (Epoch)	174-179 cm (H)[a]	179-184 cm (H)	189-194 cm (H)	296-301 cm (P)[b]	305-310 cm (P)	314-319 cm (P)
Total number of Reads	2146	3773	32107	15744	13435	19914
Percent contaminant reads*	1.16	8.45	0.14	1.54	3.1	1.74
Total reads after removal of the contaminant strains	2121	3454	32062	15500	13018	19567
Percent reads after removal of the contaminant strains	98.83	91.54	99.85	98.45	96.89	98.25

a = Holocene aged samples, b = Pleistocene aged samples. * These reads have been selected from Supplementary **Table 3.1**.

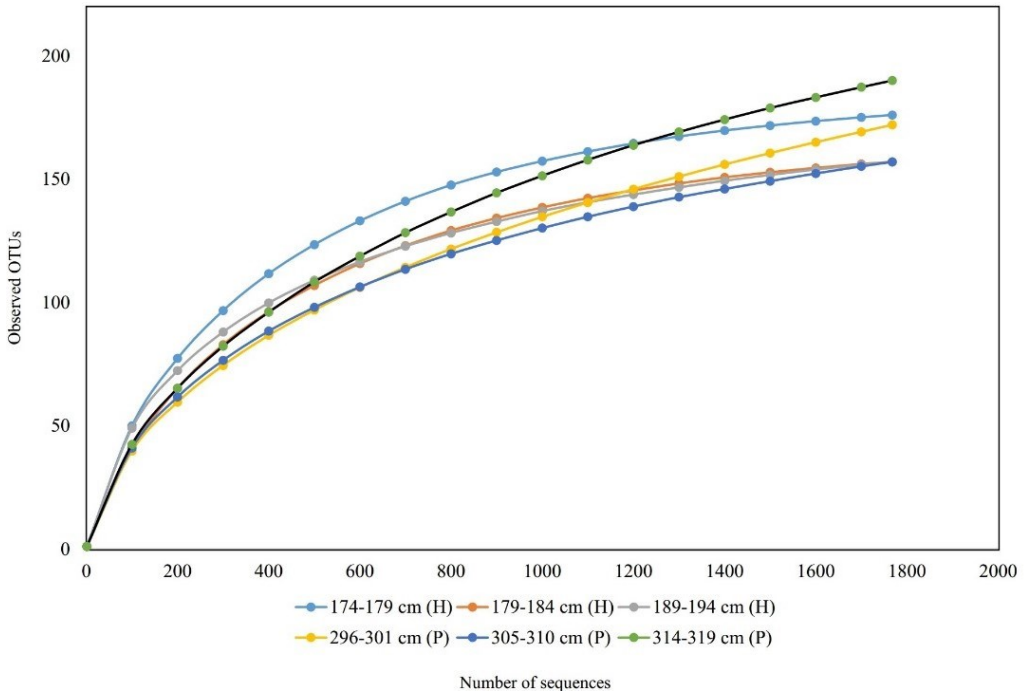

Supplementary Figure 3.3. Rarefaction curve based on the observed OTUs (OTU richness) at 97% cutoff value. Samples were rarefied to 1768 sequences per samples. In parenthesis H = Holocene aged and P= Pleistocene aged samples.

Live/dead microscopy assay protocol

1:100 dilution of homogenized Holocene aged (depth of 174-210 cm from the total core length) and Pleistocene aged (depth of 296-319 cm from the total core length) permafrost samples in 10 mM of tetrasodium pyrophosphate (TSPP) were prepared and sonicated in the presence of sterilized 5 mm borosilicate beads. Later the samples were further diluted in TSPP (1:100 dilution) and filtered twice through a 5 μm and a 0.22 μm blackened polycarbonate filters respectively. After vacuum drying of the 0.22 μm filters, 200 μl of the prepared Live/Dead BacLight staining solution (Invitrogen Thermo Fisher, Canada) was added to the membranes (prepared according to the Manufacturer's protocol). Filters were incubated for 1 h at 4 ºC in dark. The excess stain was removed with 0.85% NaCl and upon mounting on the glass slides the filters were covered with ProLong Gold antifade reagent (Thermo Fisher, Canada).

A **B**

C **D**

Supplementary Figure 3.4. A-D Micrograph of a Pleistocene (~14-15 k cal yr BP) and Holocene (~8-10 k cal yr BP) aged Eastern Beringian permafrost soil samples after 48 h of drying at 70 ^{o}C. Image A depicts a silty Pleistocene aged soil with no traces of organic material, selected from the depth of 296 cm under 4.5 × magnification. Image B depicts a peaty Holocene aged soil sample from a depth of 210 cm under 4.5 × magnification. Image C and D depict the same soil samples shown in images A and B under 67 × magnification respectively.

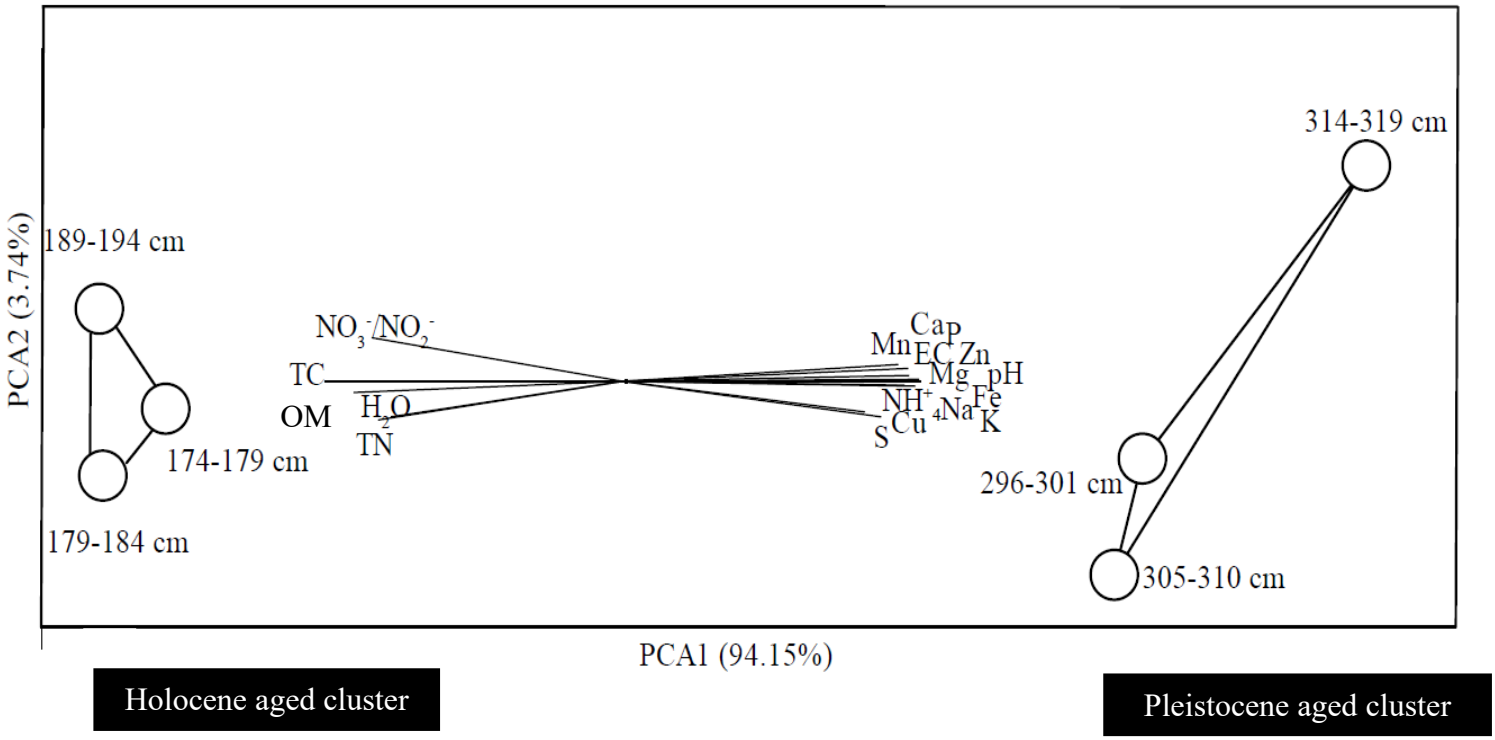

Supplementary Figure 3.5. PCA biplot of the measured soil chemistry from segments associated to Holocene aged DHL-16_1 core (n=3) and Pleistocene aged DHL-16_2 core (n=3). Clustering was based on epoch ($p = 0.021$) and PCA1 and 2 components were able to explain 97.89% of the variation in the system. R^2 of each vector: OM: 0.88, TC: 0.96, TN: 0.79, H_2O: 0.66, pH: 0.97, Ca: 0.88, Cu: 0.84, Fe: 0.97, K: 0.97, Mg: 0.94, Mn: 0.84, Zn: 0.96, Na: 0.96, P: 0.97, S: 0.96, NO^-_3/NO^-_2: 0.88, EC: 0.91, and NH_4^+: 0.99. In the biplot: large white circles represent the samples, TC = total carbon, TN = total nitrogen, and EC = electrical conductivity.

Supplementary Table 3.3. Biodiversity matrices measured between composite Holocene (n=3) and Pleistocene samples (n=3).

Epoch/age	Depth (cm)	Observed OTUs [a]	Chao1 [b]	Shannon [c]	Simpson Evenness [d]	Fisher's Alpha [e]
H*	174-179	176	185.73	4.092	0.0341	48.605
H	179-184	157	163.41	3.321	0.0108	41.619
H	189-194	157	174.22	4.122	0.0507	41.619
P**	296-301	172	267.57	3.552	0.0176	47.103
P	305-310	157	206.13	3.510	0.0147	41.619
P	314-319	190	249.94	3.599	0.0149	53.996

[*] Holocene, **Pleistocene.

[a] Holocene vs Pleistocene (p=0.4867), [b] Holocene vs Pleistocene (p=0.0495), [c] Holocene vs Pleistocene (p=0.4867), [d] Holocene vs Pleistocene (p=0.5127), [e] Holocene vs Pleistocene (p=0.5127). The mean normality of data distribution was investigated with the Shapiro-Wilk test and the nonparametric test of the null hypothesis of the mean measured alpha diversity matric was performed with Mann-Whitney U test.

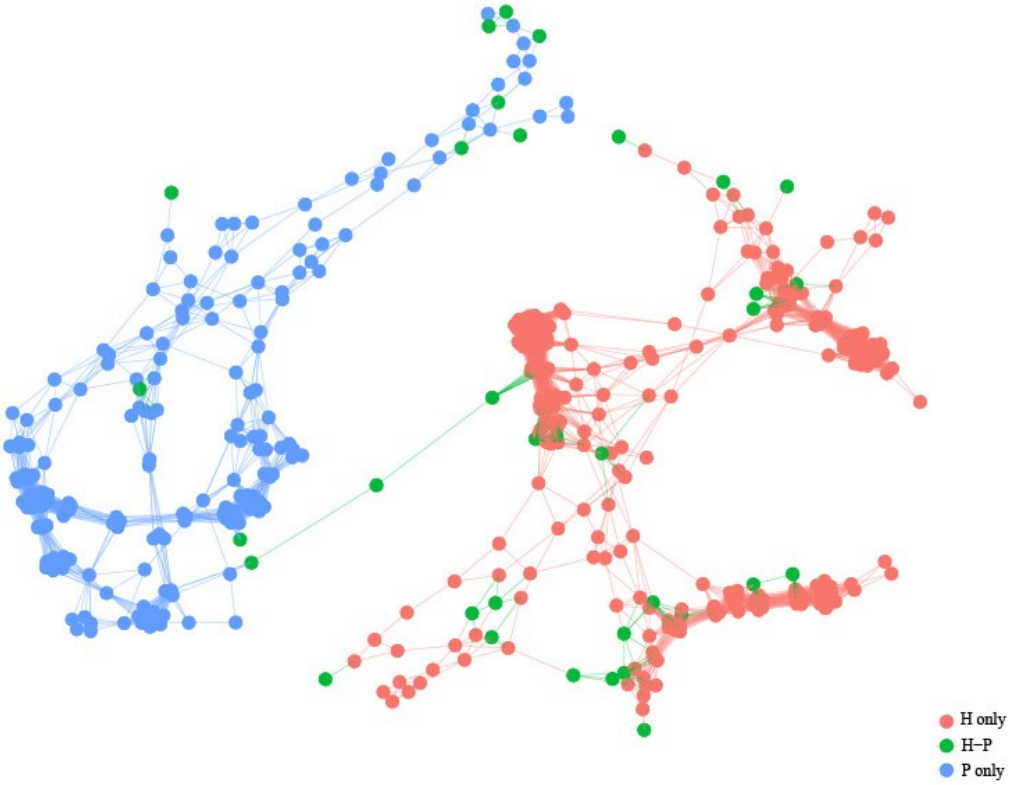

Supplementary Figure 3.6. Co-occurrence net connectivity analysis of shared OTU and core OTUs between and within composite Holocene and Pleistocene samples. Core H OTUs (unique to Holocene aged samples) are shown with red circles (n=284). Core P OTUs (unique to Pleistocene aged samples) are shown with blue circles (n=276). Shared OTUs (n=52) are shown with green circles. H = Holocene, P = Pleistocene, and P-H = shared between Holocene and Pleistocene.

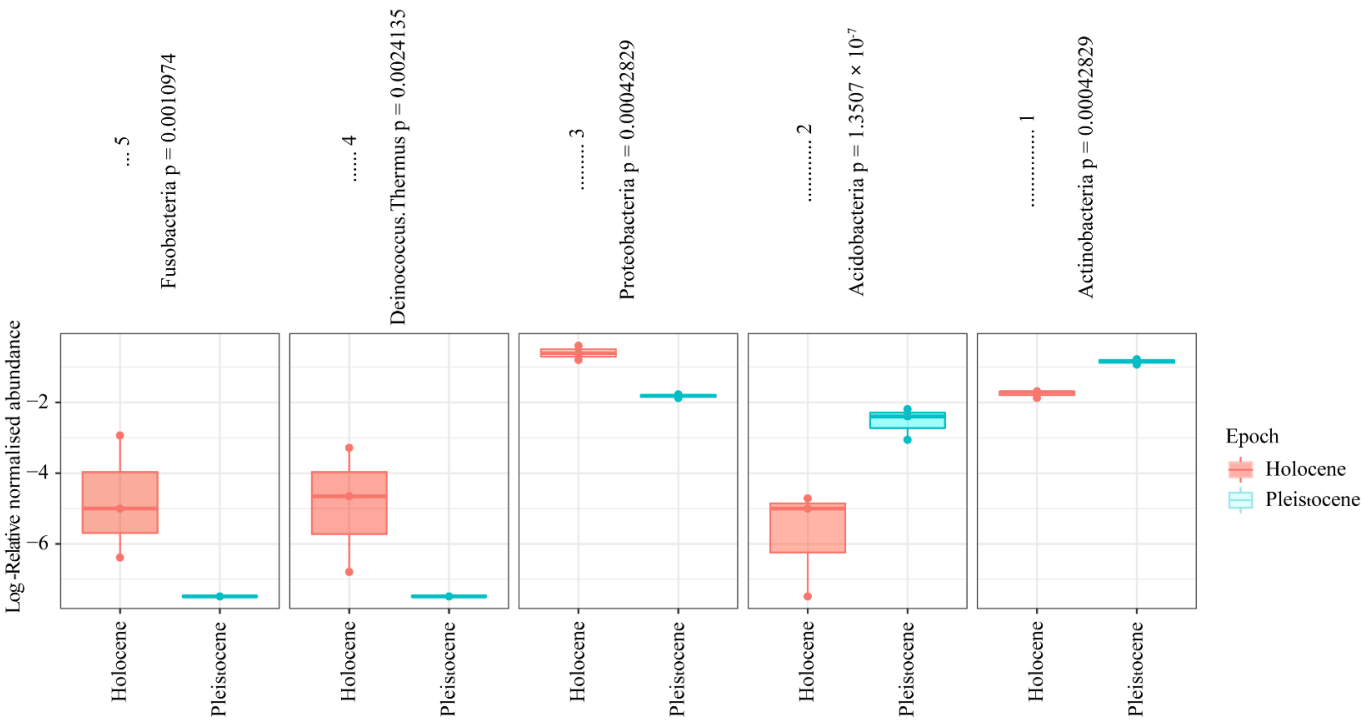

Supplementary Figure 3.7. Differential abundance analysis of the top 10 dominant phyla that were statistically significantly driving the taxonomic difference in abundance between the composite Holocene and Pleistocene samples. Differential abundance was calculated with DEseq2 method.

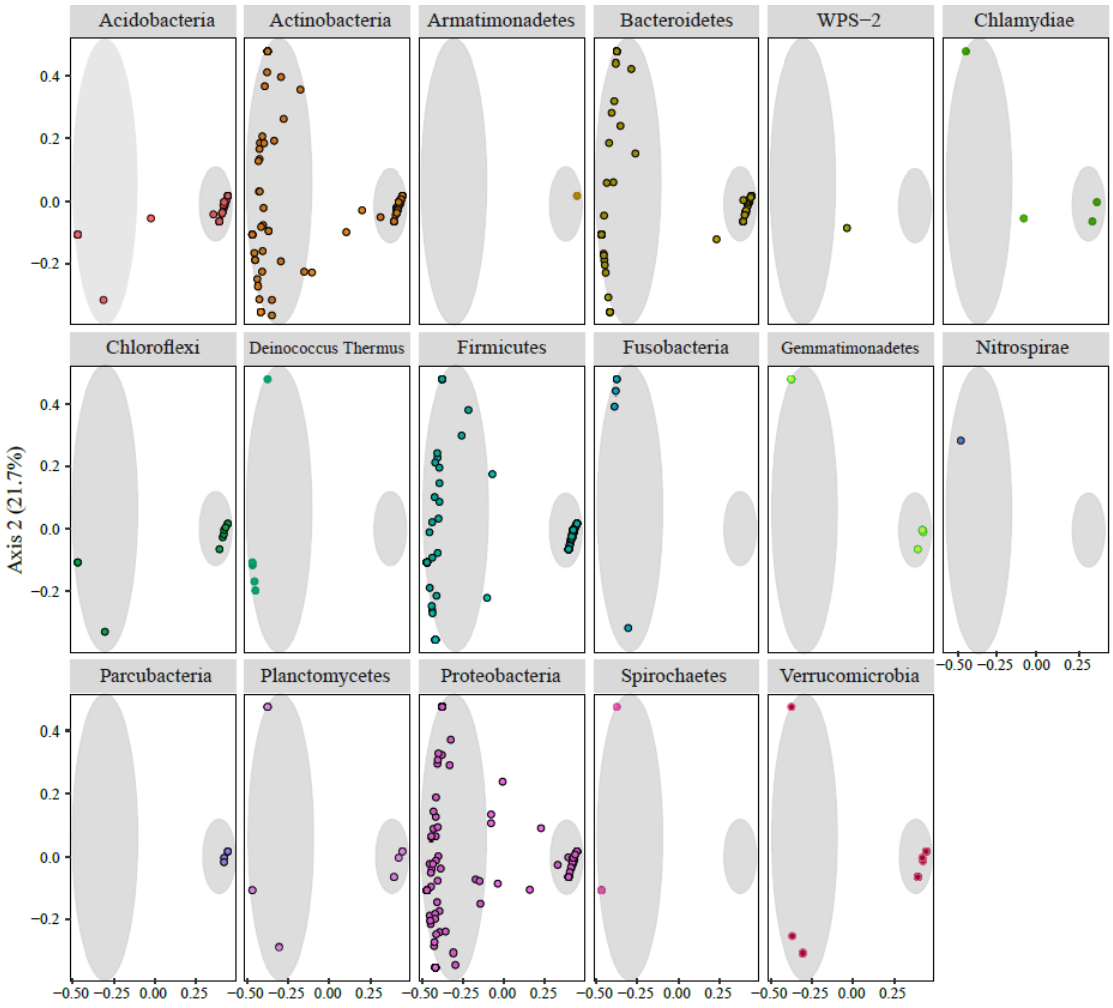

Supplementary Figure 3.8. Difference in taxonomic composition between Pleistocene aged cluster (small gray oval on the right) and Holocene aged cluster (large gray oval on the left) at phylum level. Samples 174-179, 179-184,189-194 cm formed the Holocene cluster (8-10 k cal yr BP) and 296-301, 305-310, 314-319 cm formed the Pleistocene aged cluster (14-15 k cal yr BP). Each small circle represents a taxon. Axis 1 and Axis 2 combined explained 84.7% of the variation in the system (p = 0.022).

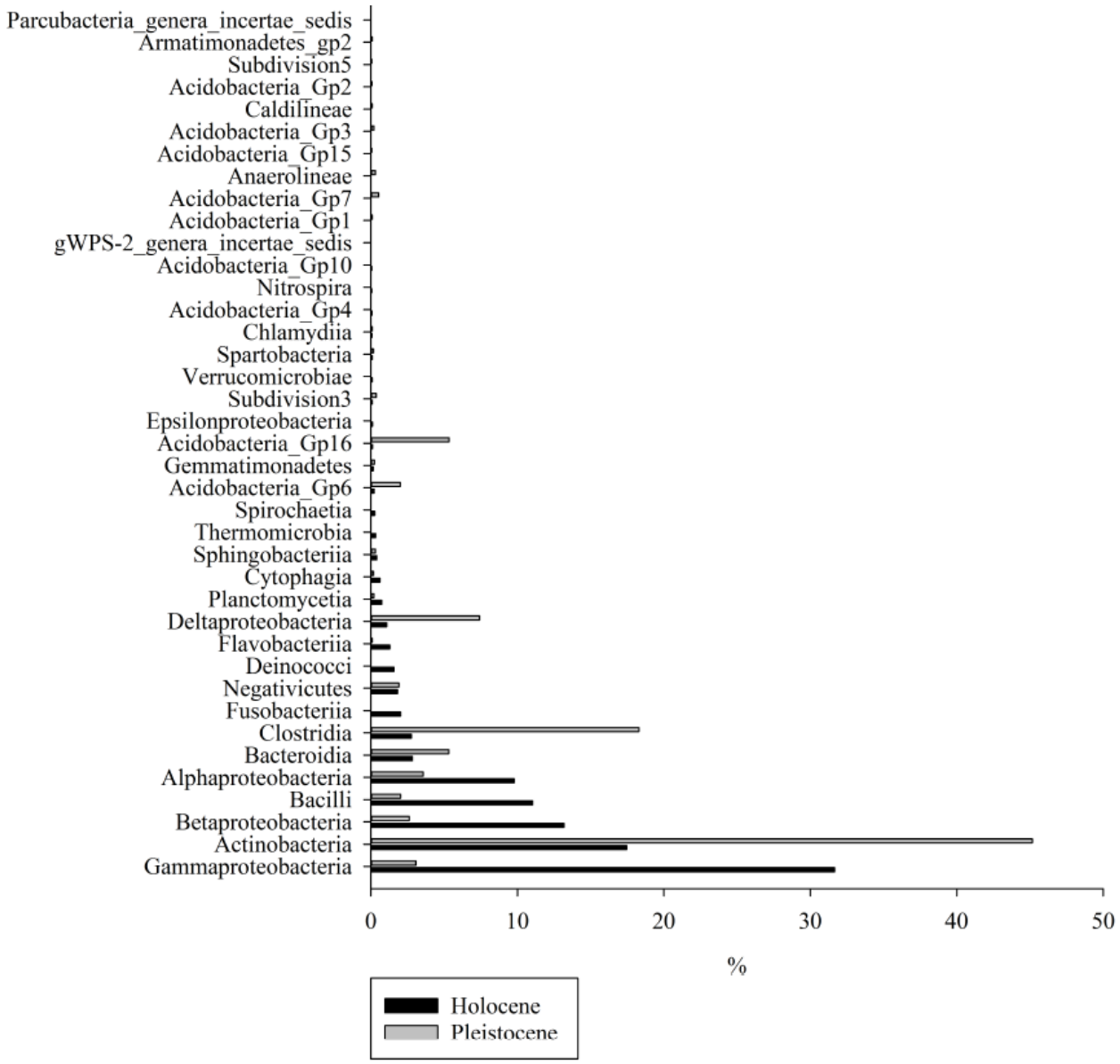

Supplementary Figure 3.9. Relative abundance analysis of composite Holocene and Pleistocene permafrost samples at taxonomic level of class.

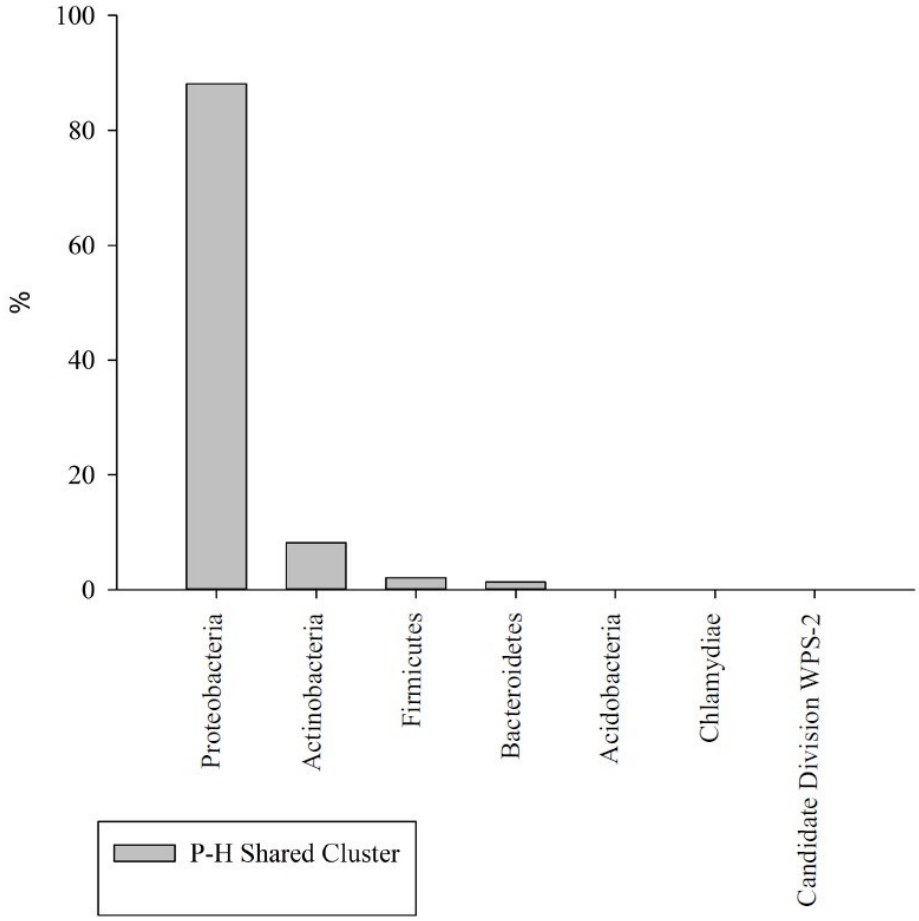

Supplementary Figure 3.10a. Rank abundance analysis of P-H shared group at taxonomic level of phylum. P-H shared = Pleistocene-Holocene shared.

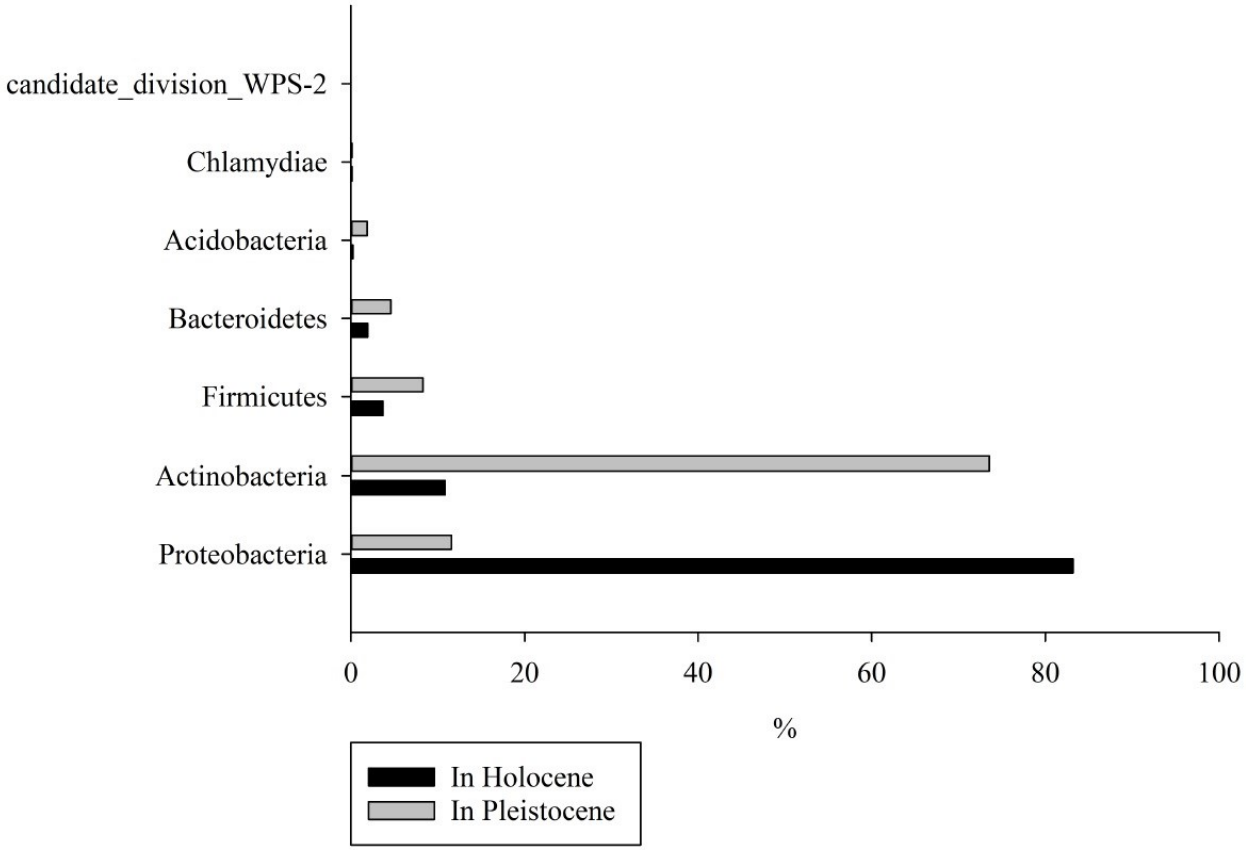

Supplementary Figure 3.10b. Relative abundance analysis of P-H shared group at taxonomic level of phylum. P-H shared = Pleistocene-Holocene shared.

Appendix 3

Supplementary figures and tables for chapter 4

Modified DNA extraction protocol:

The modifications were as follows: 1 g of soil was included in PowerBead tubes. Instead of step 4 of the manufacturer's protocol, samples were subjected to a Precellys 24 bead beader (Bertin Instruments, France) twice at a speed of 5000 r.p.m for 30 s. At step 9 all of the supernatants were utilized. At step 13, 2 ml of C4 solution was used and samples were vortexed for 30 s followed by a 10-20 min incubation period at room temperature. All the optional 5 min incubations at 4 ^{o}C were performed. All 1 min centrifugation steps were extended to 3-5 min. DNA was eluted in 50 µl of C6 solution and prior to final centrifugation step samples were incubated for 5 min at room temperature.

***pmoA* and *mmoX* PCR and the thermocycling steps**

Unless otherwise noted, each 25 µl PCR master mix reaction contained per sample 5 × Q5 Reaction Buffer (New England Biolabs, Canada), 10 mM dNTPs, 10 µM forward and reverse primers, and 0.25 µl of Q5 DNA Polymerase (New England Biolabs, Canada). All PCR reactions were carried out in a Verit 96-Well Thermal Cycler (Applied Biosystem, Thermofisher Canada).

For amplifying the *pmoA* gene, 1-2 µl of a 1/100 diluted template DNA from each active layer sample in triplicates and 1/100 diluted purified *pmoA* gene as a positive control (isolated from

Methylomicrobium album BG8 (strain ACM 3308)) were used in the PCR reaction. Primers 189f (3'-GGN-GAC-TGG-GAC-TTC-TGG-5') (Costello *et al.*, 2002) and 661b (3'-CCG GCG CAA CGT CCT TAC C-5') (Holmes *et al.*, 1995) were selected for the amplification of ~510 bp product size. The touchdown PCR protocol used was as follows: 98 ºC for 30 s, 20 touch down cycles of 94 ºC for 1 min, 65 ºC for 30 s, 72 ºC for 45 s. 15 cycles of 94 ºC for 1 min, 52 ºC for 30 s, 72 ºC for 45 s. One final elongation was carried out at 72 ºC for 5 min.

For amplifying the *mmoX* gene, two sets of primers were utilized to increase the efficiency of our detection. The first set of primers used were mmoX f882 (3'-GGC-TCC-AAG-TTC-AAG-GTC-GAC-5') and mmoX r1403 (3'-TGG-CAC-TCG-TAG-CGC-TCC-GGC-TCG-5') (McDonald *et al.*, 1995), which are able to amplify ~535 pb product. 1-2 µl of 1/100 dilution from each soil type was used as a DNA template in triplicates, and l µl of 1/100 dilution of pure *mmoX* gene extracted from *Methylosinus trichosporium* OB3b was used as a positive control. The PCR protocol used was as follows: 94 °C for 5 min; Q5 DNA polymerase added; 55 °C for 1 min; 72 °C for 1 min; 30 cycles consisting of 94 °C for 1 min, 55 °C for 1 min, and 72 °C for 1 min; and a final cycle consisting of 94 °C for 1 min, 55 °C for 1 min, and 72 °C for 5 min.

The second primer set used for *mmoX* gene amplification were met1 (3'-ACC-AAG-GAG-CAG-TTC-5') and met4 (3'-TCC-AGA-AGG-GTT-GTT-5') (Baker *et al.*, 2001). The PCR protocol was as follows: 98 ºC for 30 s, 94 ºC for 10 min, then 40 cycles at 94 ºC for 1 min, 50 ºC for 1 min, and 72 ºC for 2 min, and a final cycle at 94 ºC for 1 min, 50 ºC 1 min and 72 ºC for 10 min.

Supplementary Figure 4.1. Active layer sampling sites. A. Undisturbed site (DC5 and DC6). B. Disturbed site (DC7 and DC8).

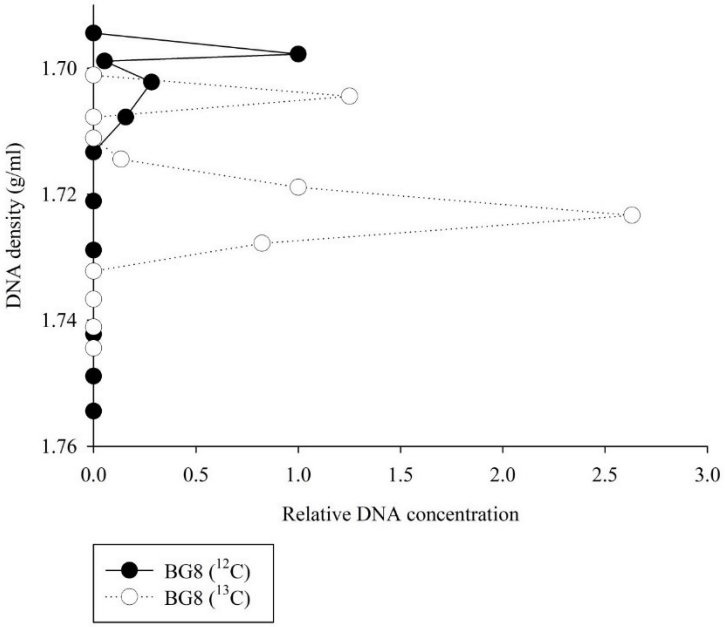

A

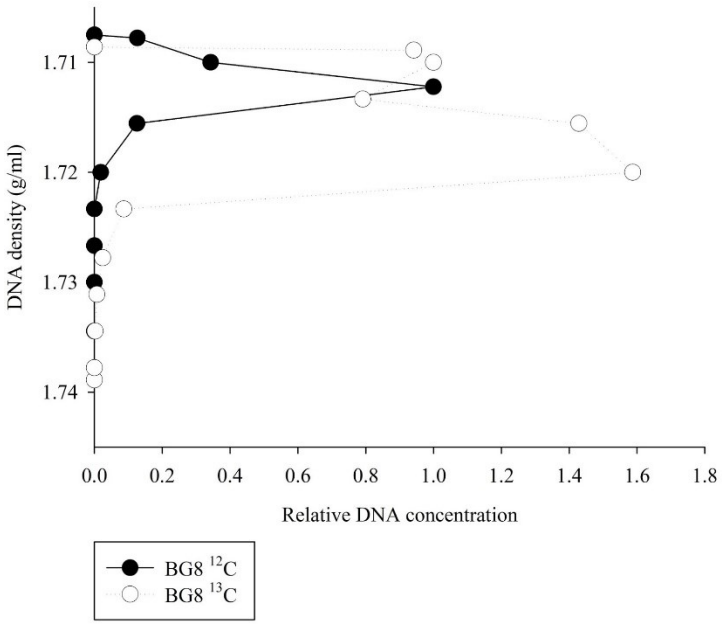

B

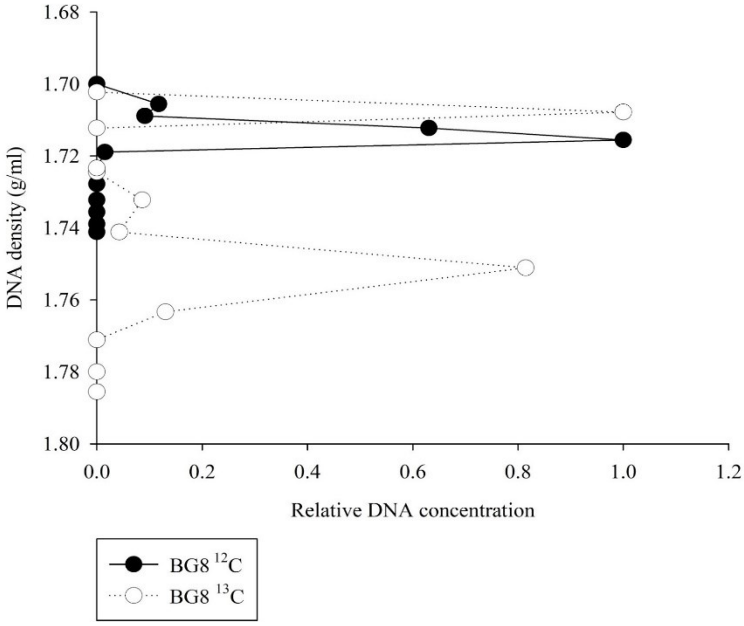

C

Supplementary Figure 4.2. DNA density gradients of control samples prepared from pure cultures of *Methylomicrobium album* BG8 (strain ACM 3308) grown under ^{13}C (black circles)

and ^{12}C (open circles) CH_4 atmosphere. A. Control sample included at 0 ºC SIP run. B. Control sample included at 4 ºC SIP run, C. Control sample included at 22 ºC SIP run.

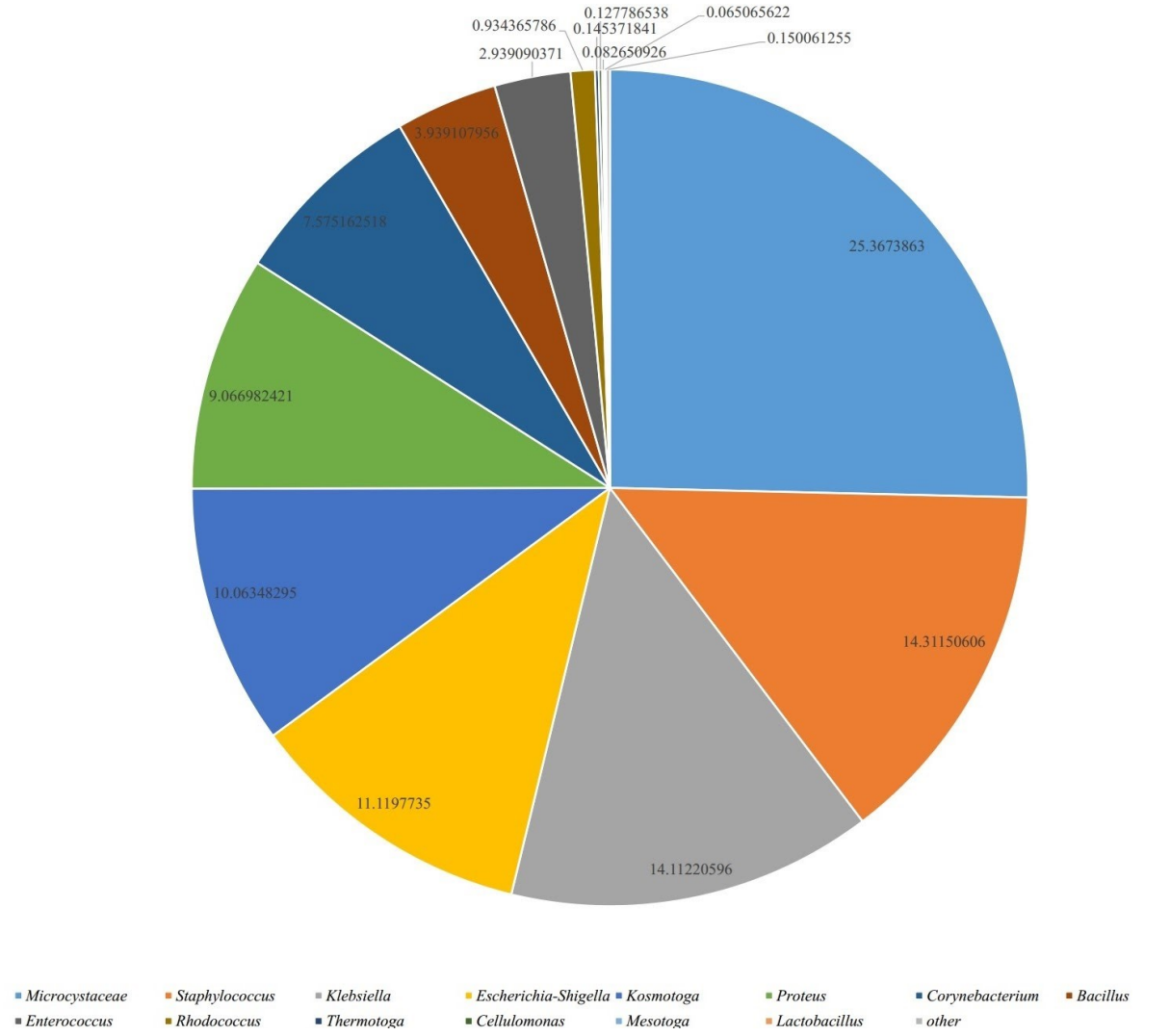

Supplementary Figure 4.3. 15 known bacterial strains used as a positive control in 16S rRNA sequencing.

Analysis of the sequences detected in kit negative controls

The blank controls resulted in 54 ASVs with a total of 672 reads, which constituted ~1% of the ASVs in the dataset. The taxonomic identity of the ASVs in the blank controls was determined based on BLAST with the same criteria mentioned in **chapter 4**. Since these ASVs were rare and it is not possible to differentiate cross contamination (ASVs derived from other samples on the plate) from external contamination (ASVs derived from contamination during pre-sequencing processing steps), we did not remove them from the analysis. These ASVs and their taxonomic identity are reported in **Supplementary Table 4.1**.

Supplementary Table 4.1. The taxonomic identity of the ASVs detected in the blank controls from the DNeasy PowerSoil Kit (Qiagen Canada) used in 16S rRNA genes sequencing.

ASV ID	Blank 1	Blank 2	Blank 3	Blank 4	Taxonomic identity
1	36	35	0	0	*Enterobacter cloacae*
2	36	13	0	0	*Pedobacter insulae*
3	24	13	0	0	*Arthrobacter dokdonellae*
4	20	6	8	0	*Flavobacterium soyangense*
5	0	0	13	18	*Staphylococcus aureus*
6	20	0	5	0	*Sedimenticola thiotaurini* Like
7	13	8	0	0	*Sphingomonas echinoides*

8	12	9	0	0	*Helicobacter typhlonius*
9	0	0	21	0	*Methylobacter tundripaludum*
10	18	0	0	0	*Rhodopseudomonas rhenobacensis*
11	0	0	18	0	*Methylotenera versatilis*
12	12	5	0	0	*Lentimicrobium saccharophilum* Like
13	15	0	0	0	*Novosphingobium lentum*
14	0	14	0	0	*Pseudoxanthomonas yeongjuenesis*
15	0	0	13	0	*Lactobacillus salivarius*
16	12	0	0	0	*Chryseobacterium haifense*
17	0	12	0	0	*Massilia suwonensis*
18	0	12	0	0	*Flavobacterium terrigena*
19	11	0	0	0	*Vicinamibacter silvestris* Like
20	11	0	0	0	*Fluviicola hefeinensis* Like
21	0	0	10	0	*Klebsiella aerogenes*
22	9	0	0	0	*Sphingomonas rhizophila*
23	9	0	0	0	*Lactobacillus intestinalis*
24	9	0	0	0	*Prevotella stercorea* Like
25	0	9	0	0	*Rhizobium daejeonense*

26	0	0	9	0	*Akkermansia muciniphila*
27	0	0	9	0	*Bacteroides rodentium*
28	8	0	0	0	*Arenimonas daechungensis*
29	0	8	0	0	*Acinetobacter baylyi*
30	0	8	0	0	*Pseudomonas sesami*
31	0	0	8	0	*Chthoniobacter flavus Ellin428* Like
32	7	0	0	0	*Acinetobacter lactucae*
33	0	7	0	0	*Sphingomonas sediminicola*
34	0	0	0	7	*Muribaculum intestinale* Like
35	0	0	0	7	*Sphingomonas hengshuiensis*
36	6	0	0	0	*Pseudobacter ginsenosidimutans* Like
37	6	0	0	0	*Flavobacterium cheniae* Like
38	6	0	0	0	*Brevitalea aridisoli* Like
39	6	0	0	0	*Flavobacterium aquatile*
40	0	6	0	0	*Novosphingobium lentum*
41	0	0	5	0	*Luteitalea pratensis* Like
42	0	0	0	5	*Brevitalea deliciosa* Like
43	0	0	0	5	*Lactobacillus crispatus*

44	0	0	0	5	*Eubacterium siraeum* Like
45	0	0	0	5	*Methylobacter psychrophilus*
46	4	0	0	0	*Methylobacter tundripaludum*
47	0	4	0	0	*Fluviicola hefeinensis*
48	0	4	0	0	*Acinetobacter lactucae* Like
49	0	0	0	4	*Corynebacterium efficiens*
50	3	0	0	0	*Rurimicrobium arvi* Like
51	3	0	0	0	*Lacunisphaera parvula*
52	0	0	3	0	*Arthrospira platensis* Like
53	0	0	3	0	*Culturomica massiliensis* Like
54	0	0	0	2	*Prevotella copri*

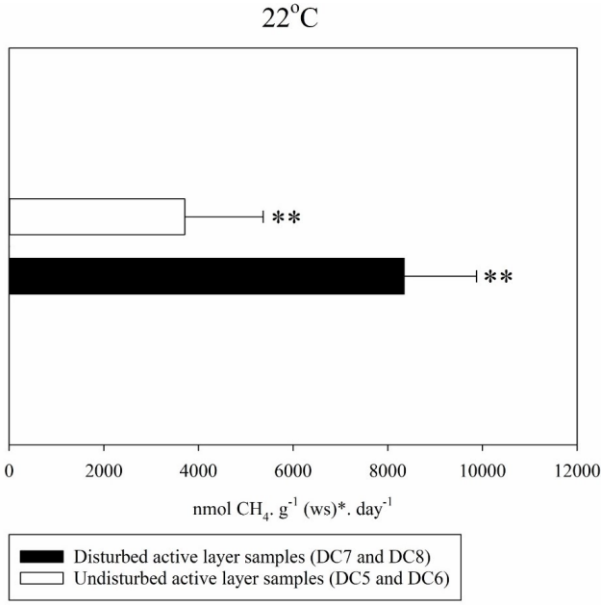

A

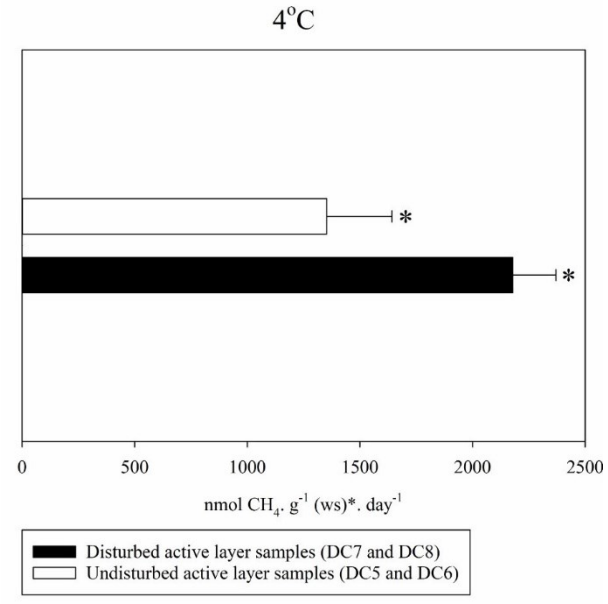

B

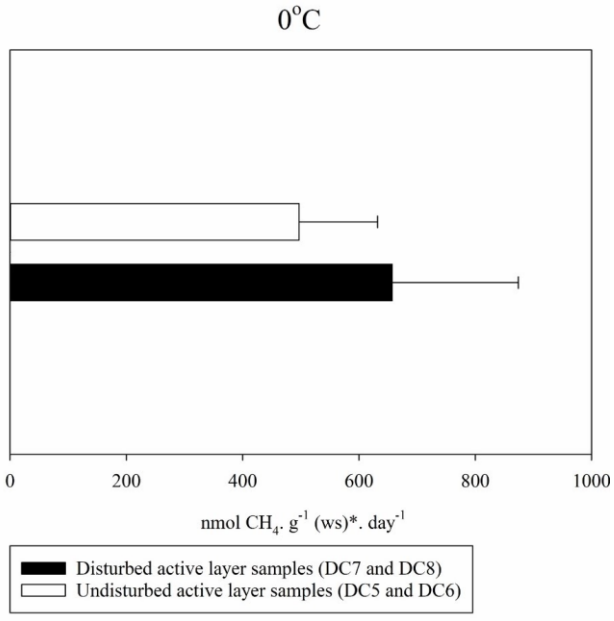

C

Supplementary Figure 4.4. CH_4 oxidation rates in composite undisturbed (DC5 and DC6) and composite disturbed (DC7 and DC8) samples incubated at 22 °C (A), 4 °C (B) and 0 °C (C). *$p < 0.05$ and **$p < 0.01$.

Supplementary Table 4.2. CH_4 oxidation rates under the influence of differing temperatures and soil type.

Temperature (ºC)	CH_4 oxidation rate ($nmolCH_4.ml^{-1}.g$ of wet $soil^{-1}.day^{-1}$)	
	Undisturbed soil (DC5 and DC6)*	disturbed soil (DC7 and DC8)*
22	3708.35 (±1658.6)**	8345.8 (±1532.9)**
4	1353.31 (±289.56)***	2178.8 (±191.35)***
0	496.8 (±135.32)	657.3 (±216.92)

*p<0.01 (DC5, 6 vs DC7, 8), **p < 0.01 (22 ºC DC5,6 vs 22 ºC DC7, 8), ***p < 0.01 (4 ºC DC5,6 vs 4 ºC DC7, 8) measured based on Mann-Whitney U test.

Supplementary Table 4.3. Simpson evenness values for the entire dataset and the methanotroph dataset between undisturbed (DC5 and DC6) and disturbed (DC7 and DC8) active layer samples.

Samples	The entire community*	The methanotrophs only
DC5 0 ºC (D)[a]	0.177	0.534
DC5 4 ºC (D)	0.154	0.340
DC5 22 ºC (D)	0.269	0.34
DC6 0 ºC (D)	0.148	0.423
DC6 4 ºC (D)	0.236	0.334
DC6 22 ºC (D)	0.171	0.734
DC7 0 ºC (UD)[b]	0.061	0.126
DC7 4 ºC (UD)	0.06	0.347
DC7 22 ºC (UD)	0.132	0.430
DC8 0 ºC (UD)	0.05	0.129
DC8 4 ºC (UD)	0.056	0.357
DC8 22 ºC (UD)	0.05	0.6

[a]D = Disturbed active layer samples, [b]UD = Undisturbed active layer samples, *$p < 0.01$ (DC5,6 vs DC7,8).

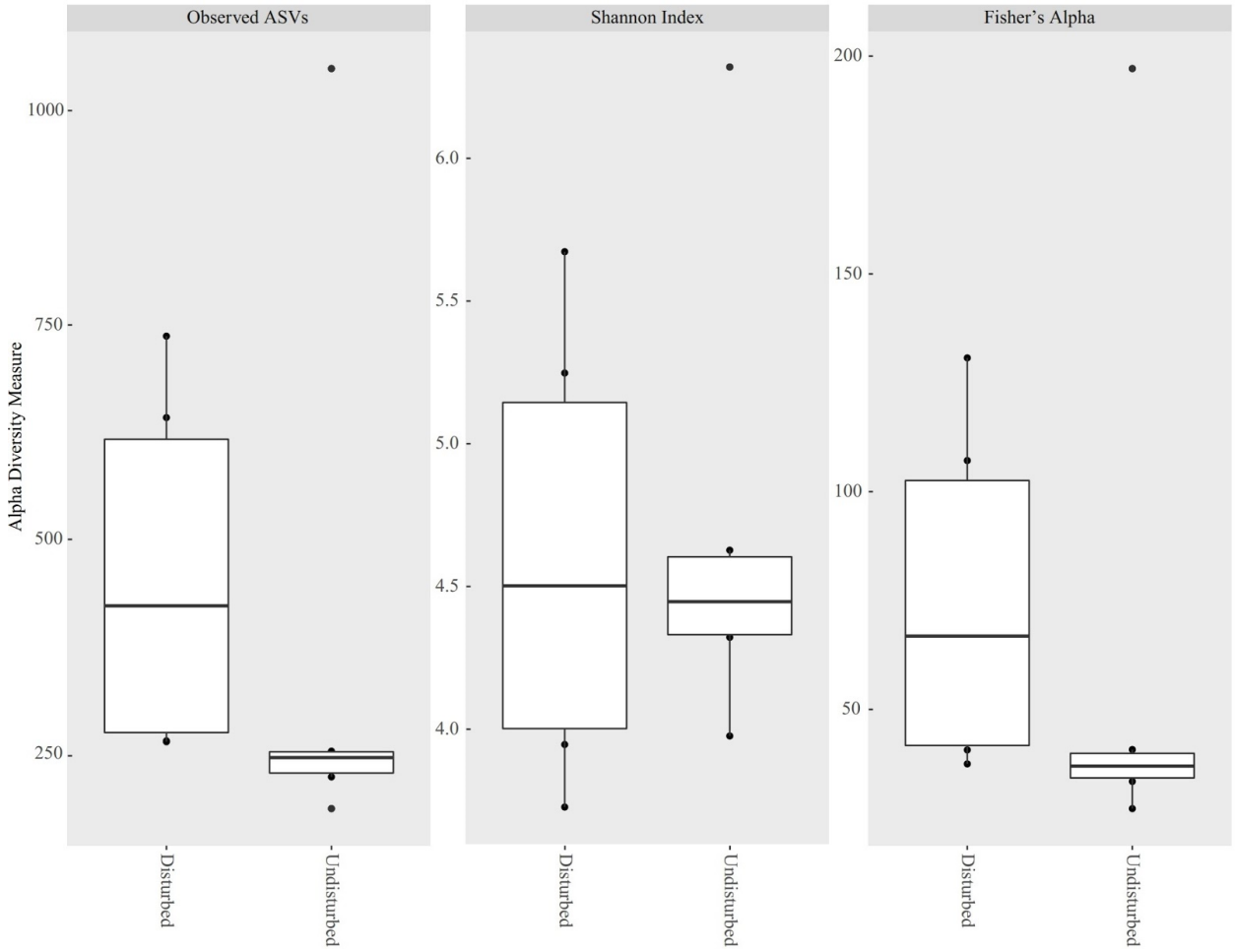
Observed ASVs
Shannon Index
Fisher's Alpha
Alpha Diversity Measure
1000
750
500
250
6.0
5.5
5.0
4.5
4.0
200
150
100
50
Disturbed
Undisturbed
Disturbed
Undisturbed
Disturbed
Undisturbed

A

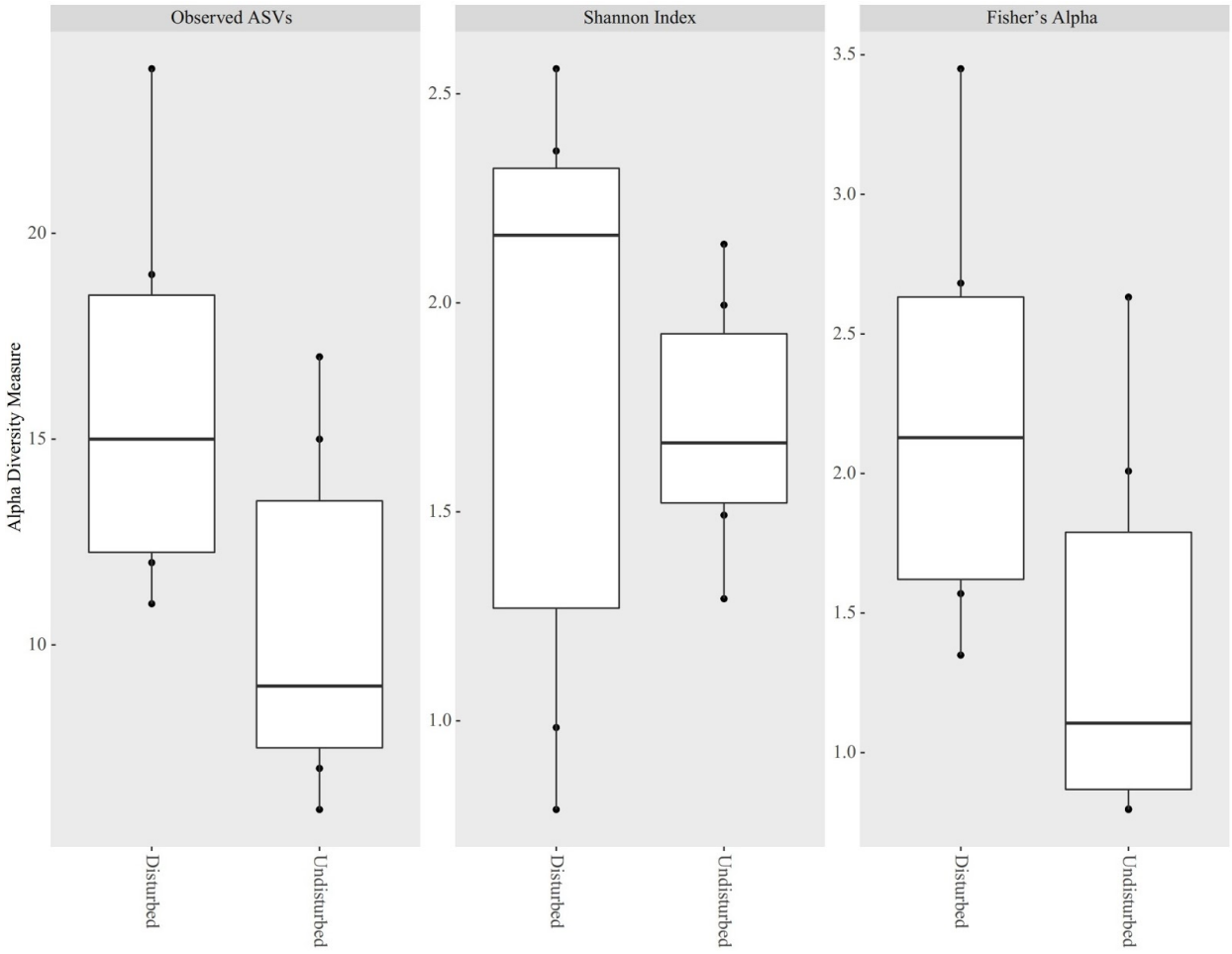
Observed ASVs
Shannon Index
Fisher's Alpha
Alpha Diversity Measure
20
15
10
2.5
2.0
1.5
1.0
3.5
3.0
2.5
2.0
1.5
1.0
Disturbed
Undisturbed
Disturbed
Undisturbed
Disturbed
Undisturbed

B

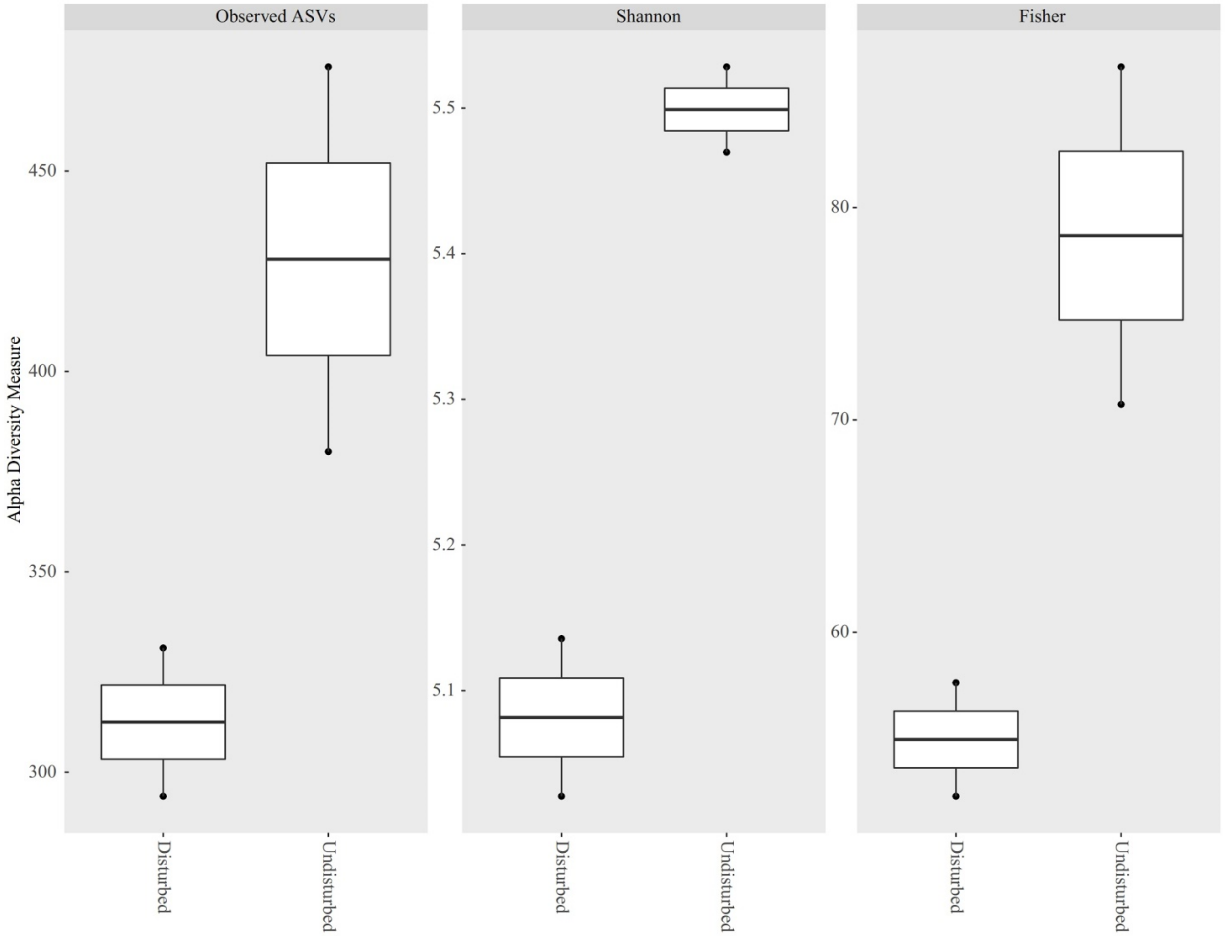

C

Supplementary Figure 4.5. Measured alpha diversity indices between composite disturbed (DC7 and DC8) and undisturbed (DC5 and DC6) active layer soils, A. for complete dataset, B. for the methanotroph dataset and C. time zero samples with no history of laboratory incubation. Probability values were measured with Mann Whitney U-test between and within samples.

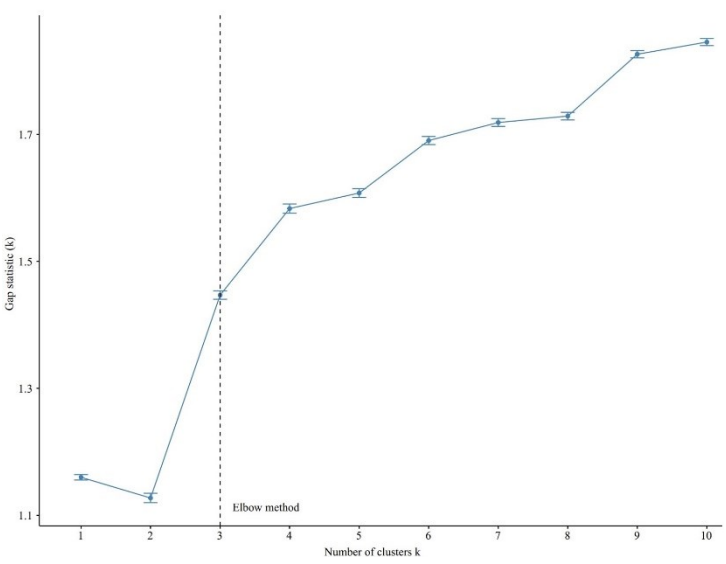

A

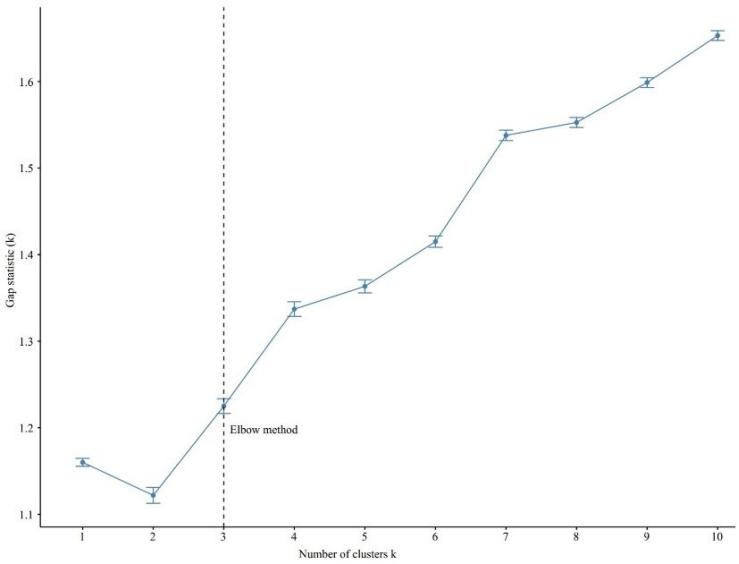

B

Supplementary Figure 4.6. Optimal number of clusters for the complete dataset was determined based on the "elbow method" by the aid of Gap statistics. A. Optimal number of clusters determined in undisturbed samples (DC5 and DC6) from the entire dataset and B. Optimal number of clusters determined in disturbed samples (DC 7 and DC8) from the entire dataset. The dash lines depict the optimum number of clusters.

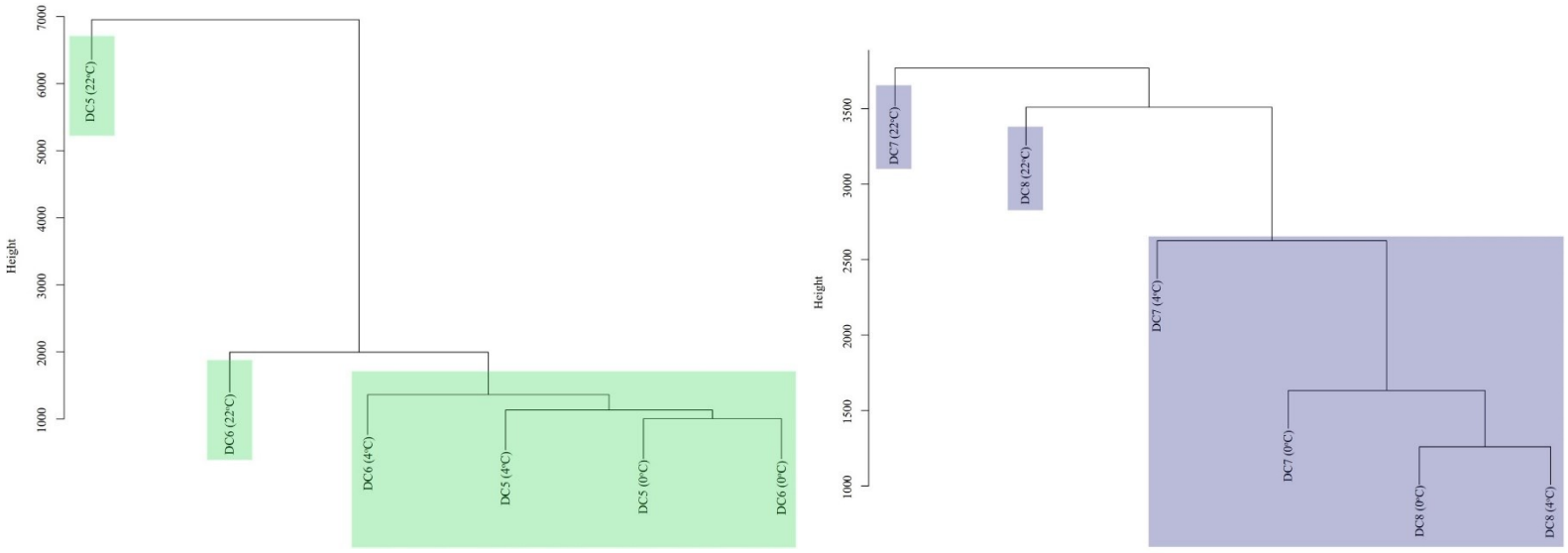

A **B**

Supplementary Figure 4.7. Hierarchical trees of the undisturbed (DC5 and DC6) (A) and disturbed (DC7 and DC8) (B) active layer samples from the entire dataset. The distance matrix used was Manhattan, and the clustering was performed with the ward.d2 algorithm. The optimum number of clusters (in green for undisturbed samples and purple in disturbed samples) were determined based on the "elbow method" by the aid of Gap statistics (see **Supplementary Figure 4.5 A, B**).

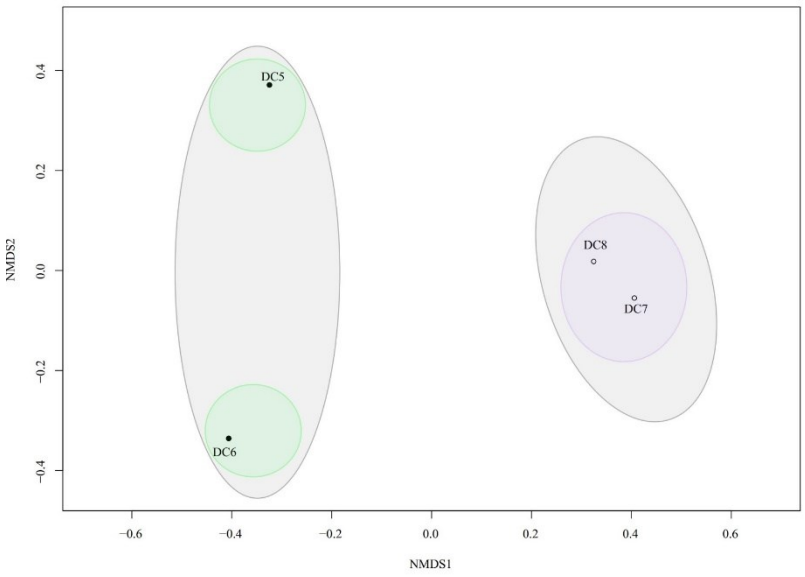

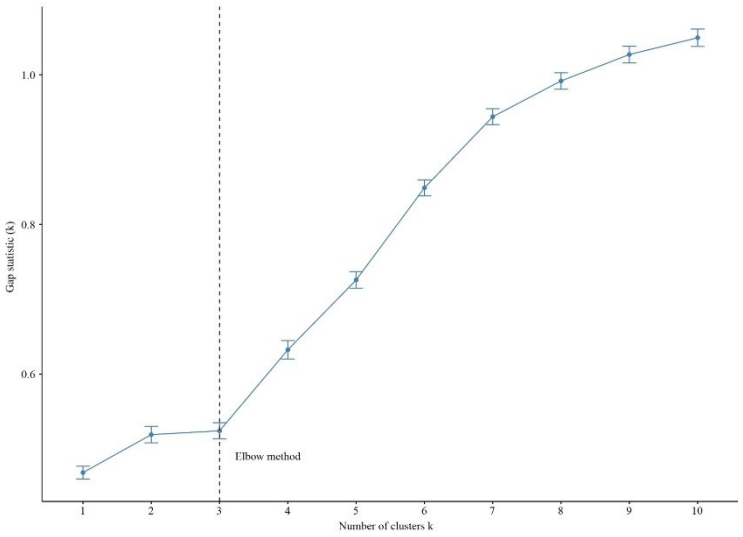

A **B**

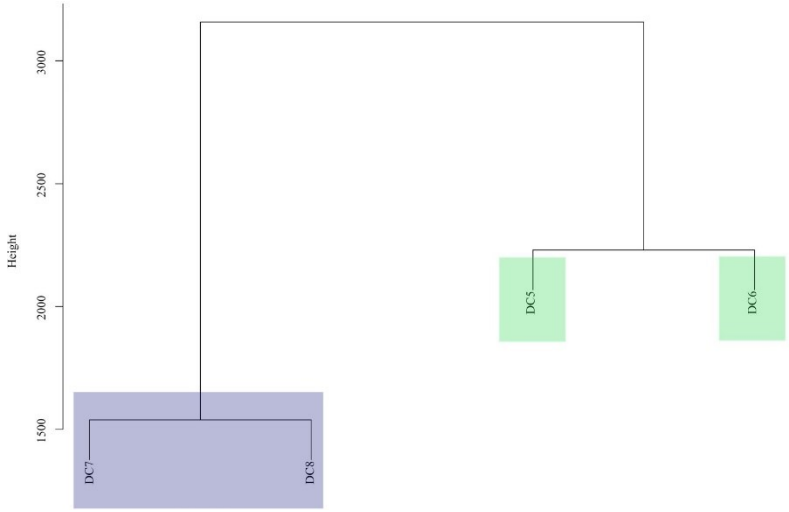

C

Supplementary Figure 4.8. A. NMDS biplot of the time zero samples. B. The "elbow method" used by the aid of Gap statistics for determining the number of optimum clusters and, C.

hierarchical tree designed based on the distance matrix of Manhattan, and clustering based on ward.d2 algorithm. In figure (A) large gray ovals separate the undisturbed (DC5 and DC6) (depicted with filled black circles) samples from disturbed (DC7 and DC8) (depicted with open circles) samples based on Bray-Curtis dissimilarity matrix. Small circles in green (DC5 and DC6) and purple (DC7 and DC8) separate the samples based on the optimum number of clusters based on the "elbow method" (determined based on C). In (B) the dashed line depicts the optimum number of clusters. In (C) the coloured boxes represent a cluster, which was determined based on (B).

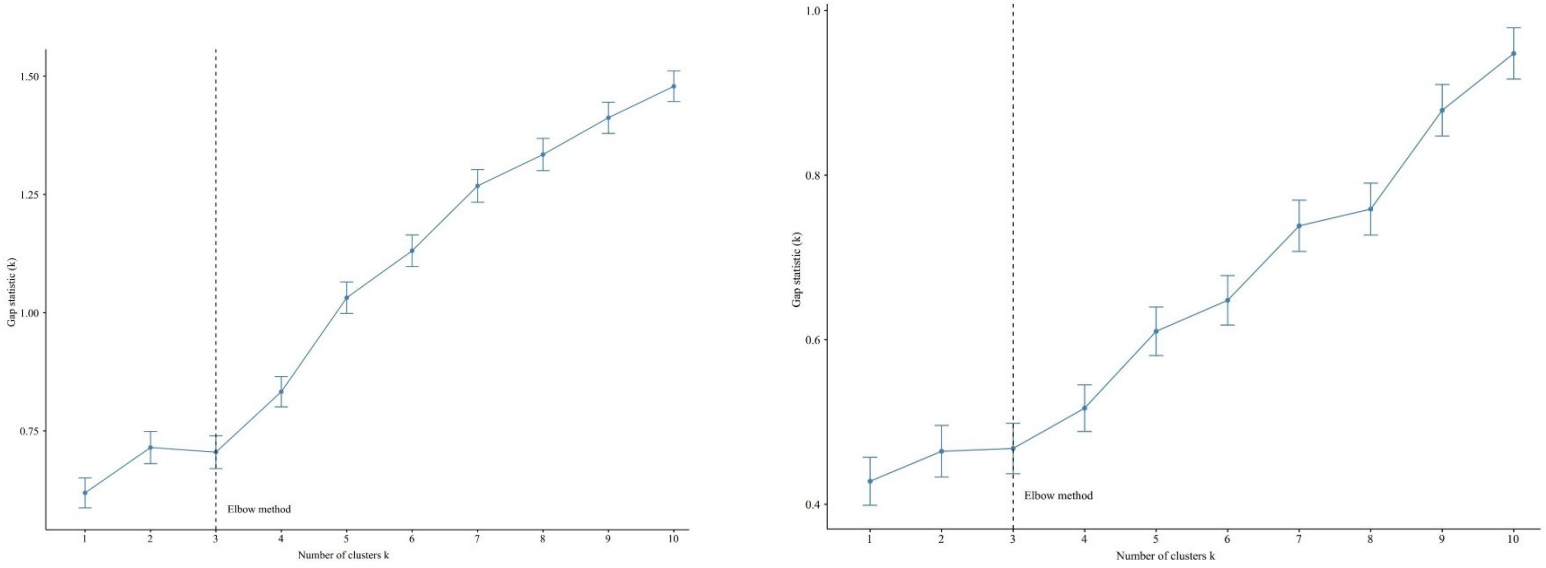

Supplementary Figure 4.9. The Gap statistics method used for evaluating the optimum number of clusters in the methanotroph dataset. The "elbow method" was used in order to cut the hierarchical trees of the methanotrophs dataset in undisturbed (DC5 and DC6) (A) and disturbed (DC7 and DC8) (B) active layer samples.

A

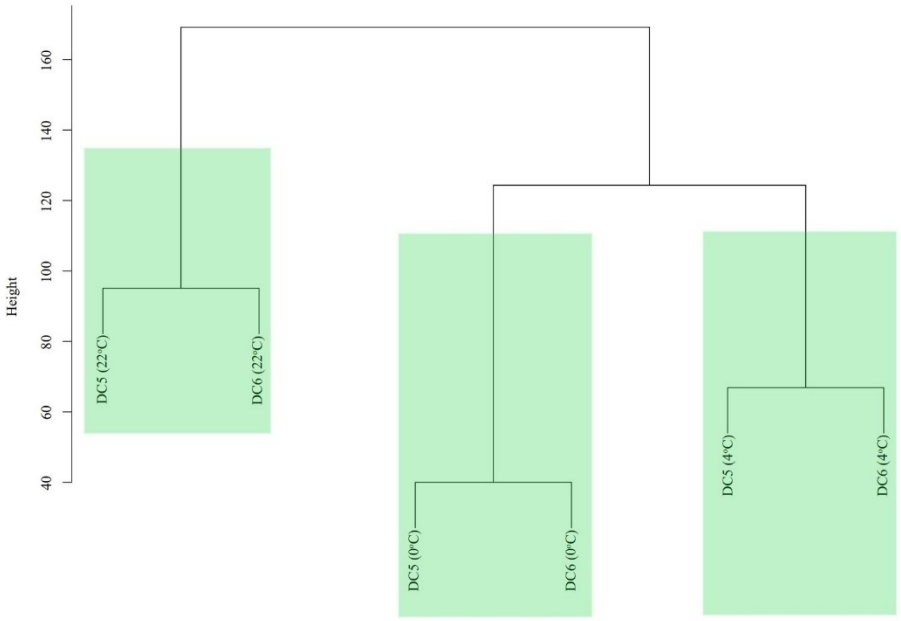

B

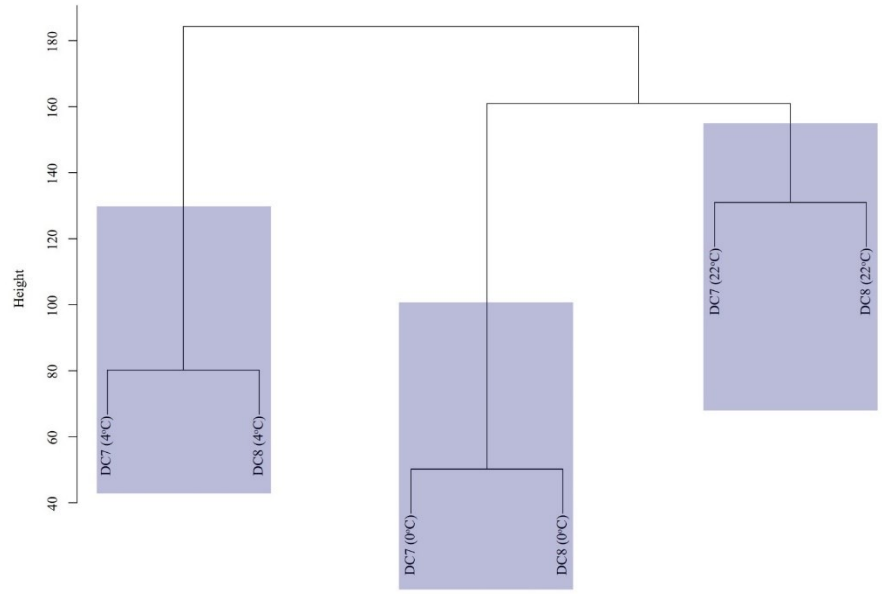

Supplementary Figure 4.10. Hierarchical cluster trees of the methanotroph dataset in (A) undisturbed (DC5 and DC6), and (B) disturbed (DC7 and DC8) active layer samples. In figure, the coloured boxes represent a cluster which was determined based on **Supplementary Figure 4.9 A, B.**

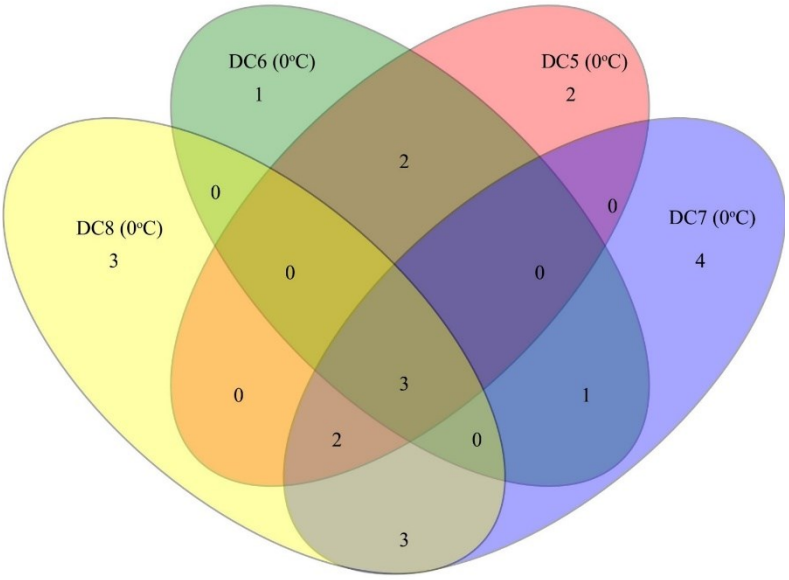

A

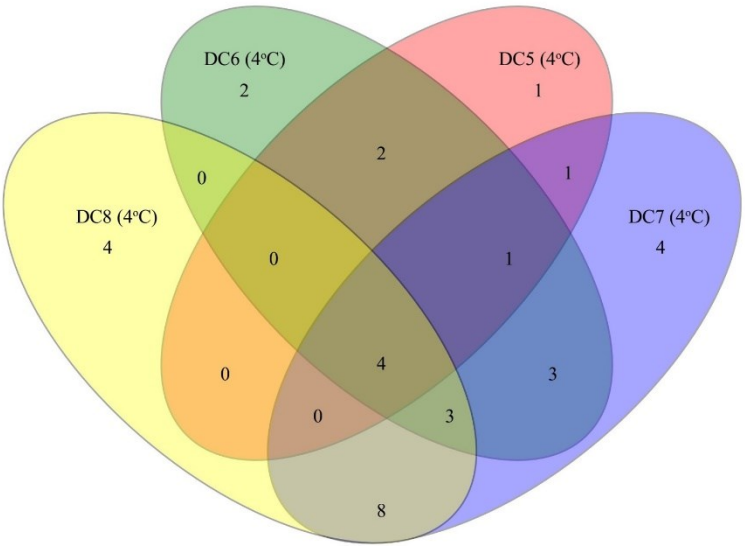

B

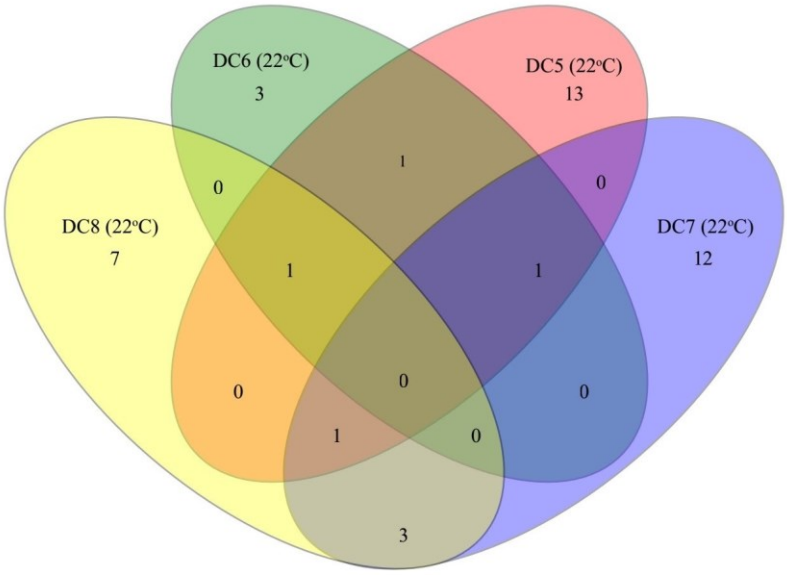

C

Supplementary Figure 4.11. Venn diagrams of methanotroph dataset based on observed ASVs. Shared and unique ASVs between undisturbed (DC5 and DC6) and disturbed (DC7 and DC8) samples incubated at 22 ºC (A), 4 ºC (B) and 0 ºC (C).

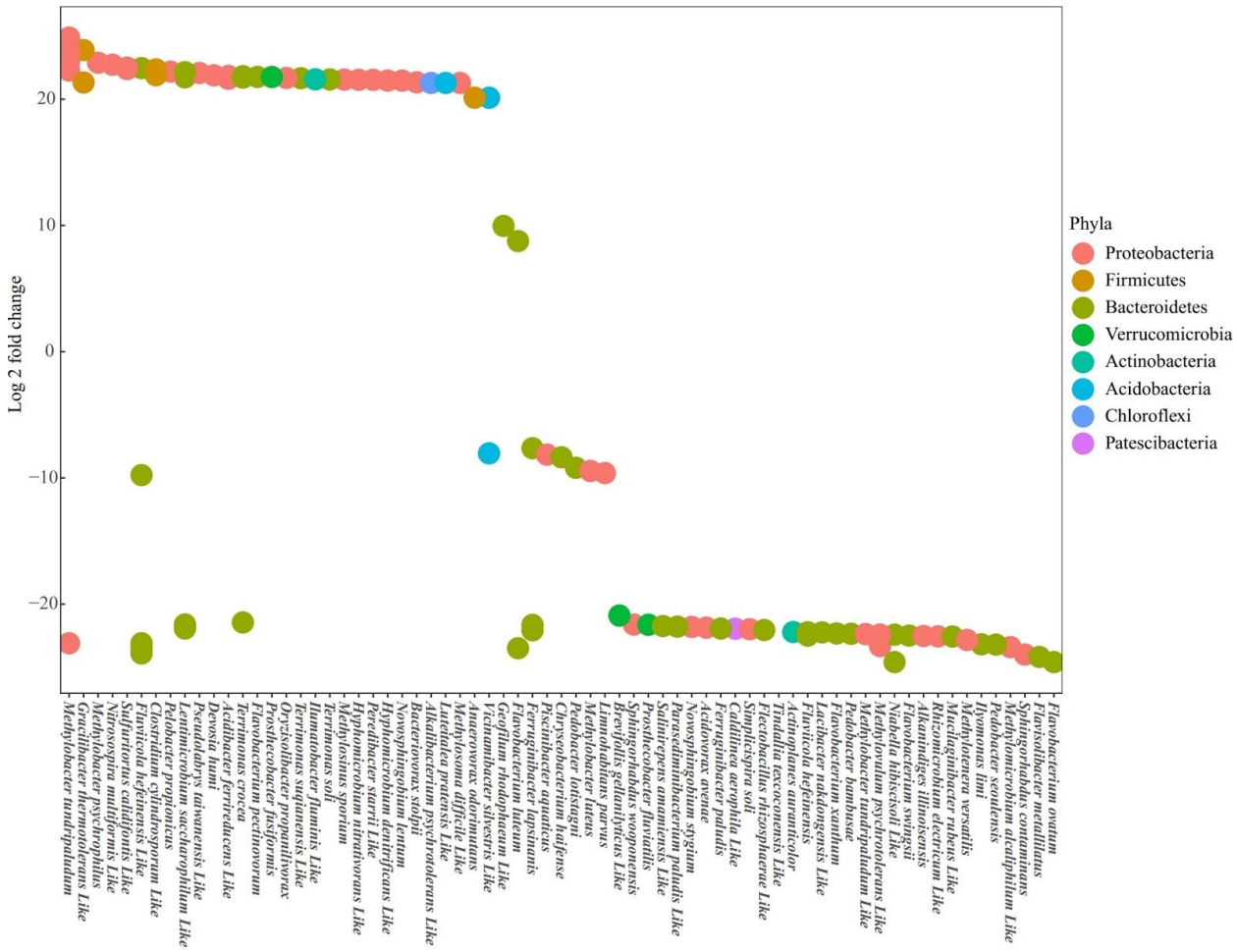
Log 2 fold change
20
10
0
−10
−20
Phyla
Proteobacteria
Firmicutes
Bacteroidetes
Verrucomicrobia
Actinobacteria
Acidobacteria
Chloroflexi
Patescibacteria
Methylobacter tundripaludum
Gracilibacter thermotolerans Like
Methylobacter psychrophilus
Nitrosospira multiformis Like
Sulfuritortus calidifontis Like
Flaviticola hefeinensis Like
Clostridium cylindrosporum Like
Pelobacter propionicus
Lentimicrobium saccharophilum Like
Pseudolabrys taiwanensis Like
Devosia hunt
Acidibacter ferrireducens Like
Terrimonas crocea
Flavobacterium pectinovorum
Prosthecobacter fusiformis
Oryzobacter propanilivorax
Terrimonas suqianensis Like
Humidibacter flaminis Like
Terrimonas soli
Methylosinus sporium
Hyphomicrobium nitrativorans Like
Percolibacter starrii Like
Hyphomicrobium denitrificans Like
Novosphingobium lentum
Bacterionoras stolpii
Alkalibacterium psychrotolerans Like
Luteitalea pratensis Like
Methylosoma difficile Like
Anaerovorax odorimutans
Vicinamibacter silvestris Like
Geoflium rhodophaeum Like
Flavobacterium luteum
Piscinibacter aquaticus
Ferruginibacter lapsinanis
Chryseobacterium halfense
Pedobacter lotistagni
Methylobacter luteus
Limnohabitans parvus
Brevifollis gellanilyticus Like
Sphingorhabdus wooponensis
Prosthecobacter flaviatilis
Salinirepens amamiensis Like
Parasediminibacterium paludis Like
Novosphingobium stygium
Acidovorax avenae
Ferruginibacter paludis
Caldilinea aerophila Like
Simplicispira soli
Flectobacillus rhizosphaerae Like
Tindallia texcoconensis Like
Actinoplanes auranticolor
Flaviticola hefeinensis
Lacibacter nakdongensis Like
Flavobacterium xanthum
Pedobacter humisuae
Methylobacter tundripaludum Like
Methylovulum psychrotolerans Like
Niabella hibiscisoli Like
Flavobacterium swingsii
Alkanindiges illinoisensis
Rhizomicrobium electricum Like
Mucilaginibacter rubeus Like
Methylotenera versatilis
Hyomonas limi
Pedobacter seoulensis
Methylomicrobium alcaliphilum Like
Sphingorhabdus contaminans
Flavisolibacter metallilatus
Flavobacterium ovatum

A

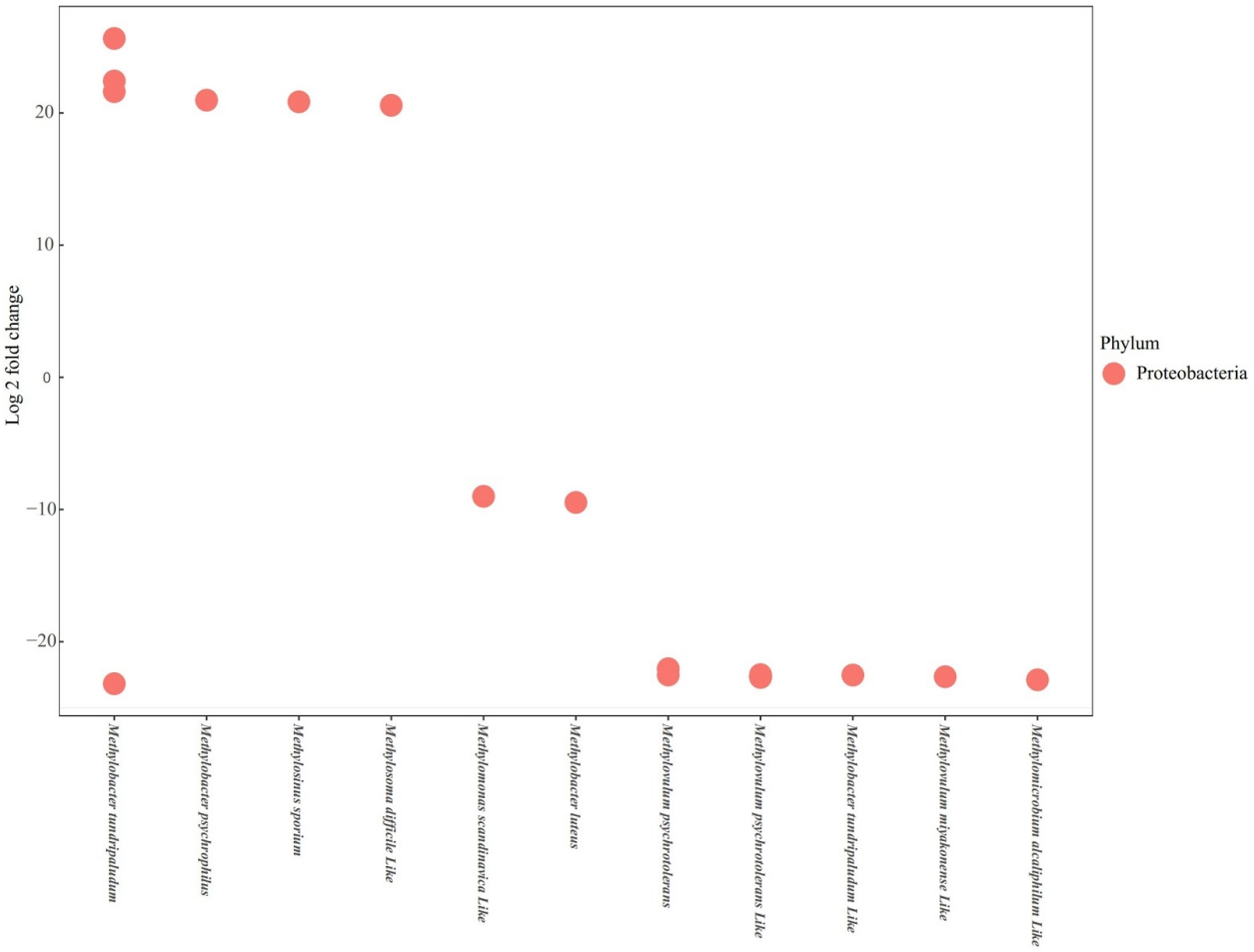

B

Supplementary Figure 4.12. DESeq2 differential abundance analysis of the entire dataset (A) and methanotroph dataset (B) based on soil disturbance. In both figures coloured circles depict species that were differentially abundant (log2 fold change) between soil types ($p < 0.01$). In A, colour of the circles shows the phylogenetic affiliation of a particular species to a phylum. Benjamini-Hochberg algorithm was used for controlling the false discovery rate of the analysis.

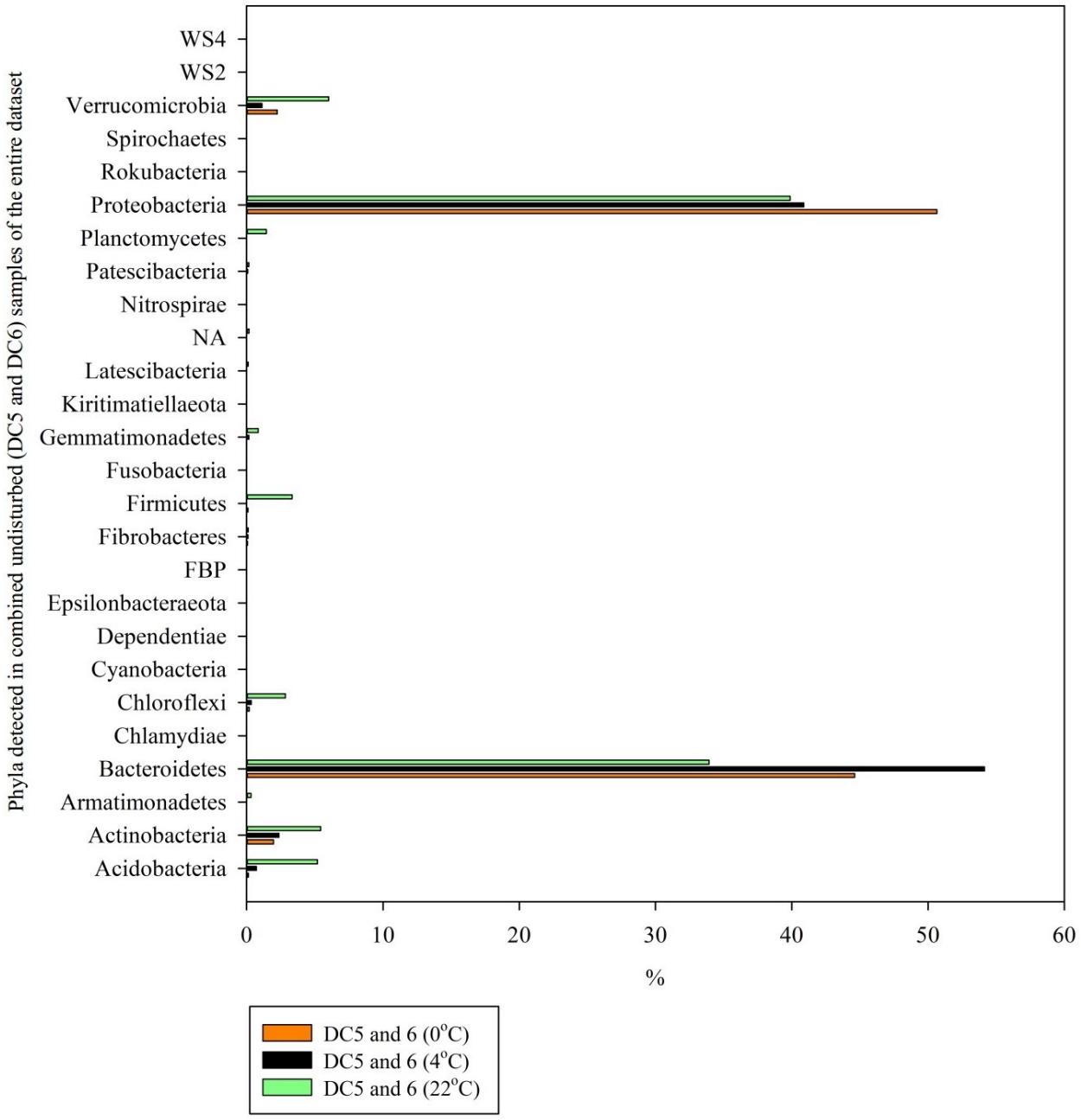
Phyla detected in combined undisturbed (DC5 and DC6) samples of the entire dataset
WS4
WS2
Verrucomicrobia
Spirochaetes
Rokubacteria
Proteobacteria
Planctomycetes
Patescibacteria
Nitrospirae
NA
Latescibacteria
Kiritimatiellaeota
Gemmatimonadetes
Fusobacteria
Firmicutes
Fibrobacteres
FBP
Epsilonbacteraeota
Dependentiae
Cyanobacteria
Chloroflexi
Chlamydiae
Bacteroidetes
Armatimonadetes
Actinobacteria
Acidobacteria
0
10
20
30
40
50
60
%
DC5 and 6 (0°C)
DC5 and 6 (4°C)
DC5 and 6 (22°C)

A

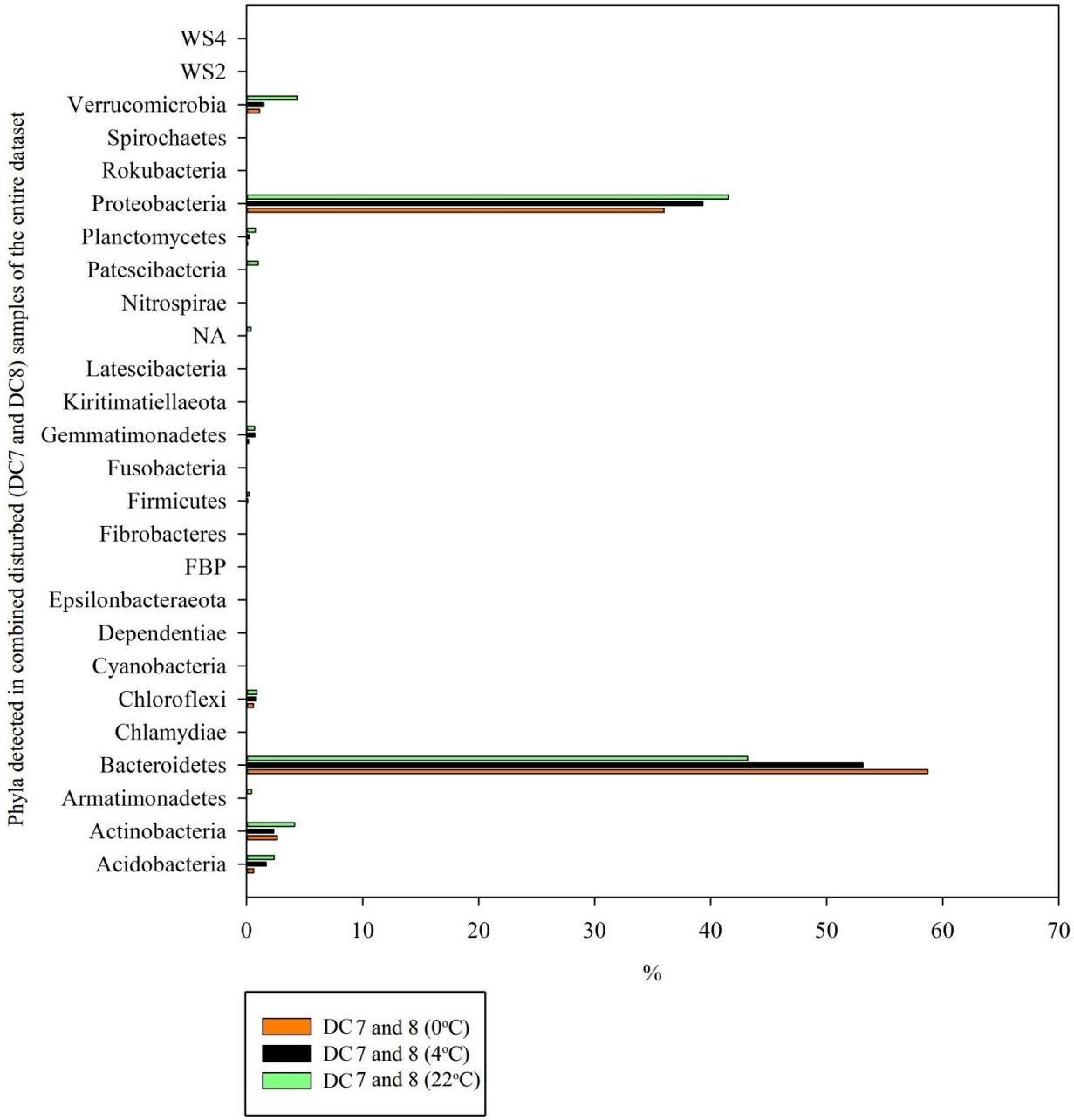

B

Supplementary Figure 4.13. Relative abundance analysis of the entire database (A) undisturbed (DC5 and DC6) and (B) disturbed samples (DC7 and DC8) at phylum level. In A and B the orange bars show 0 ºC, black bars 4 ºC and green bars 22 ºC samples. The "NA" group did not match any known phyla.

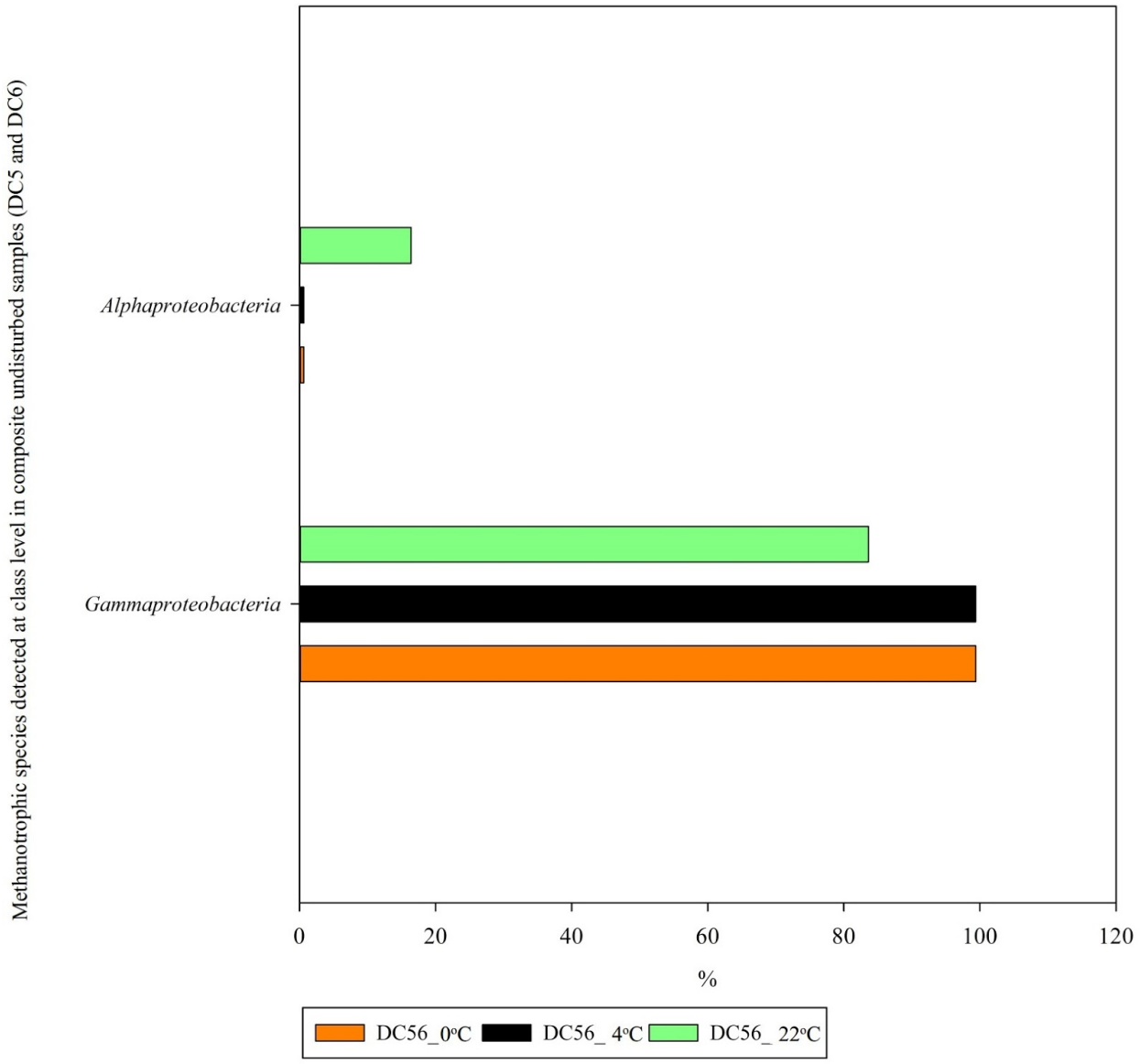
Methanotrophic species detected at class level in composite undisturbed samples (DC5 and DC6)
Alphaproteobacteria
Gammaproteobacteria
0
20
40
60
80
100
120
%
DC56_0°C
DC56_ 4°C
DC56_ 22°C

A

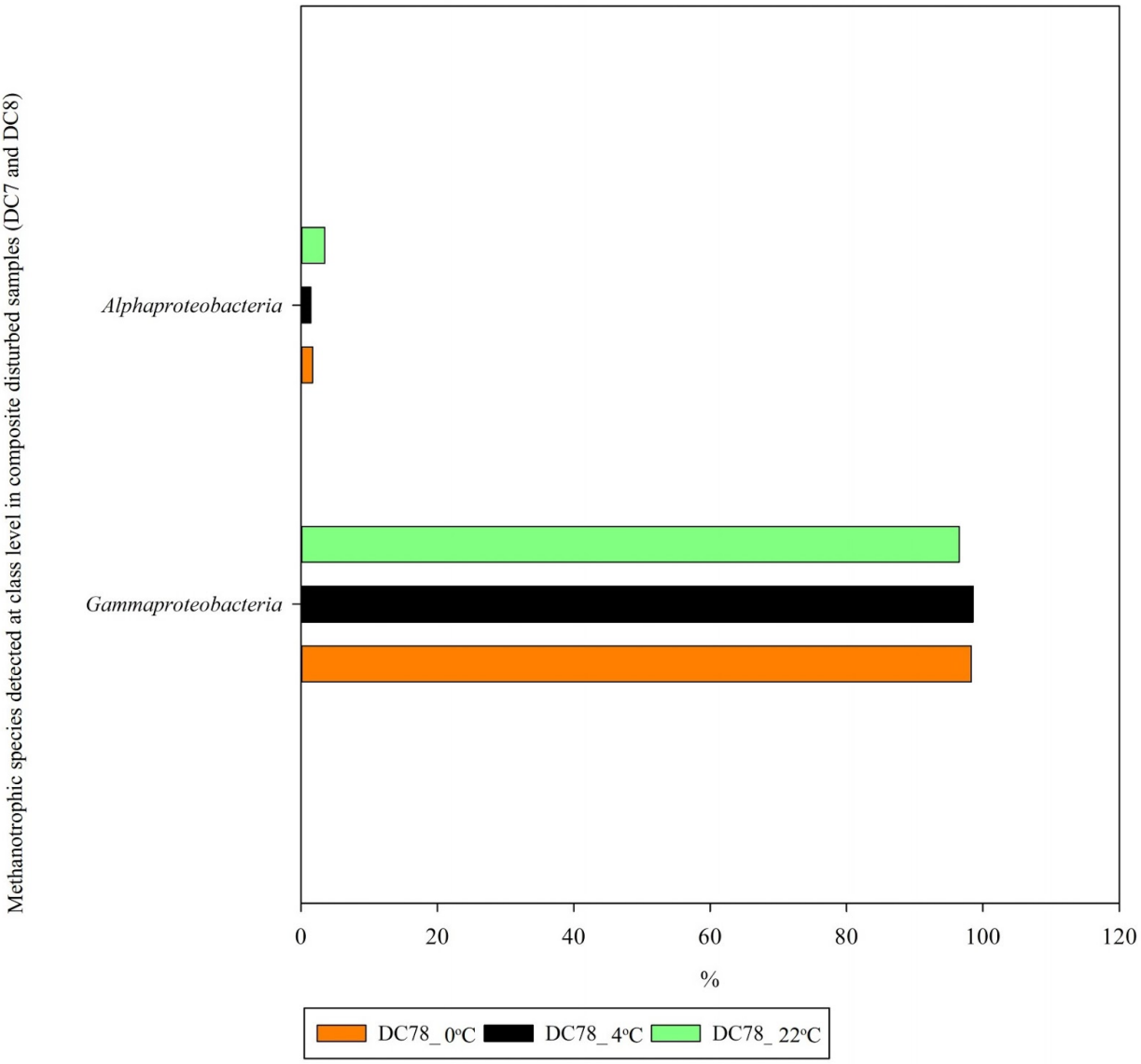

B

Supplementary Figure 4.14. Relative abundance analysis of the methanotroph dataset (A) undisturbed (DC5 and DC6) and (B) disturbed (DC7 and DC8) samples at class level. In A and B the orange bars show 0 ºC, black bars 4 ºC and green bars 22 ºC samples.

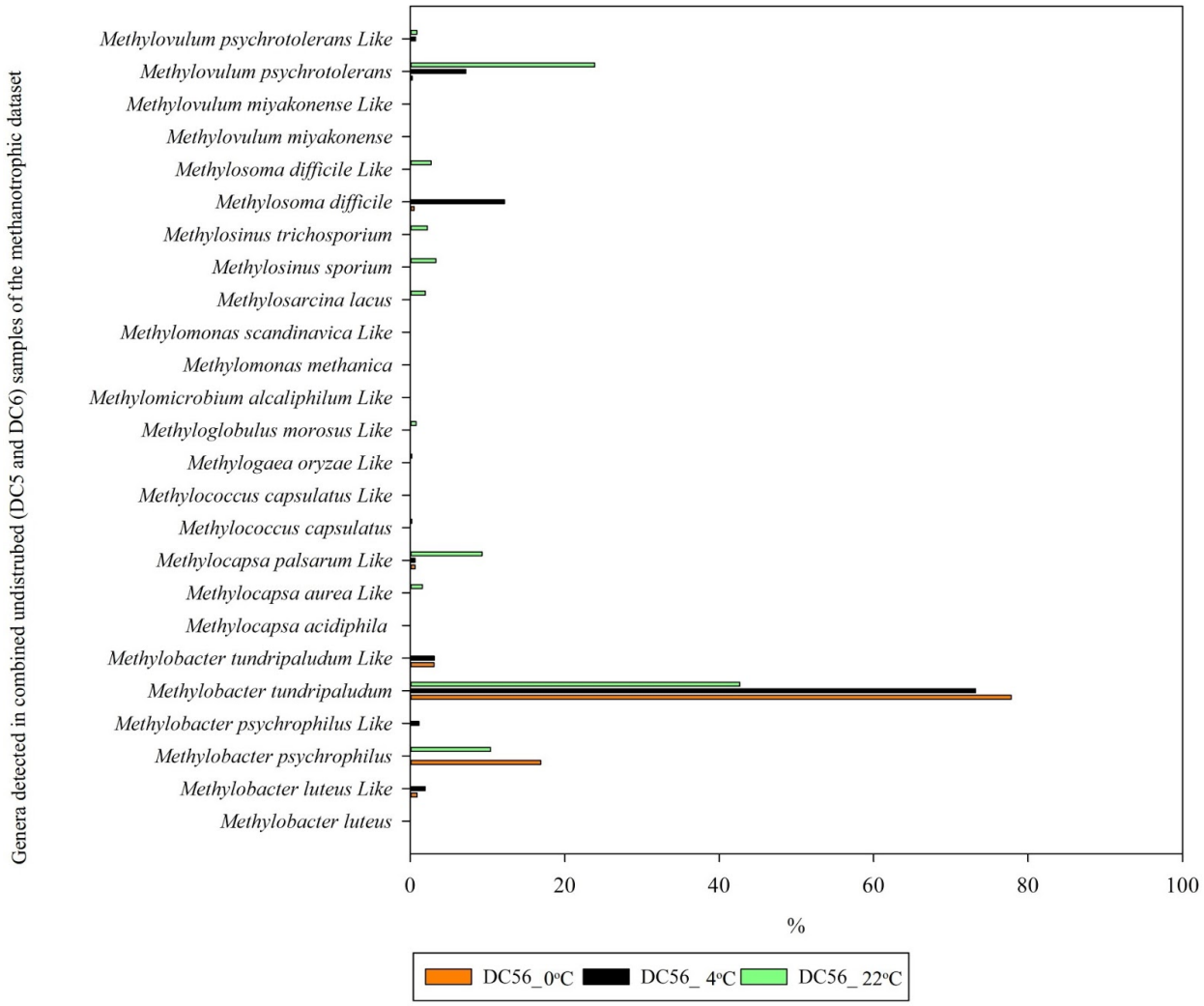
Genera detected in combined undistrubed (DC5 and DC6) samples of the methanotrophic dataset
Methylovulum psychrotolerans Like
Methylovulum psychrotolerans
Methylovulum miyakonense Like
Methylovulum miyakonense
Methylosoma difficile Like
Methylosoma difficile
Methylosinus trichosporium
Methylosinus sporium
Methylosarcina lacus
Methylomonas scandinavica Like
Methylomonas methanica
Methylomicrobium alcaliphilum Like
Methyloglobulus morosus Like
Methylogaea oryzae Like
Methylococcus capsulatus Like
Methylococcus capsulatus
Methylocapsa palsarum Like
Methylocapsa aurea Like
Methylocapsa acidiphila
Methylobacter tundripaludum Like
Methylobacter tundripaludum
Methylobacter psychrophilus Like
Methylobacter psychrophilus
Methylobacter luteus Like
Methylobacter luteus
0
20
40
60
80
100
%
DC56_0°C
DC56_ 4°C
DC56_ 22°C

A

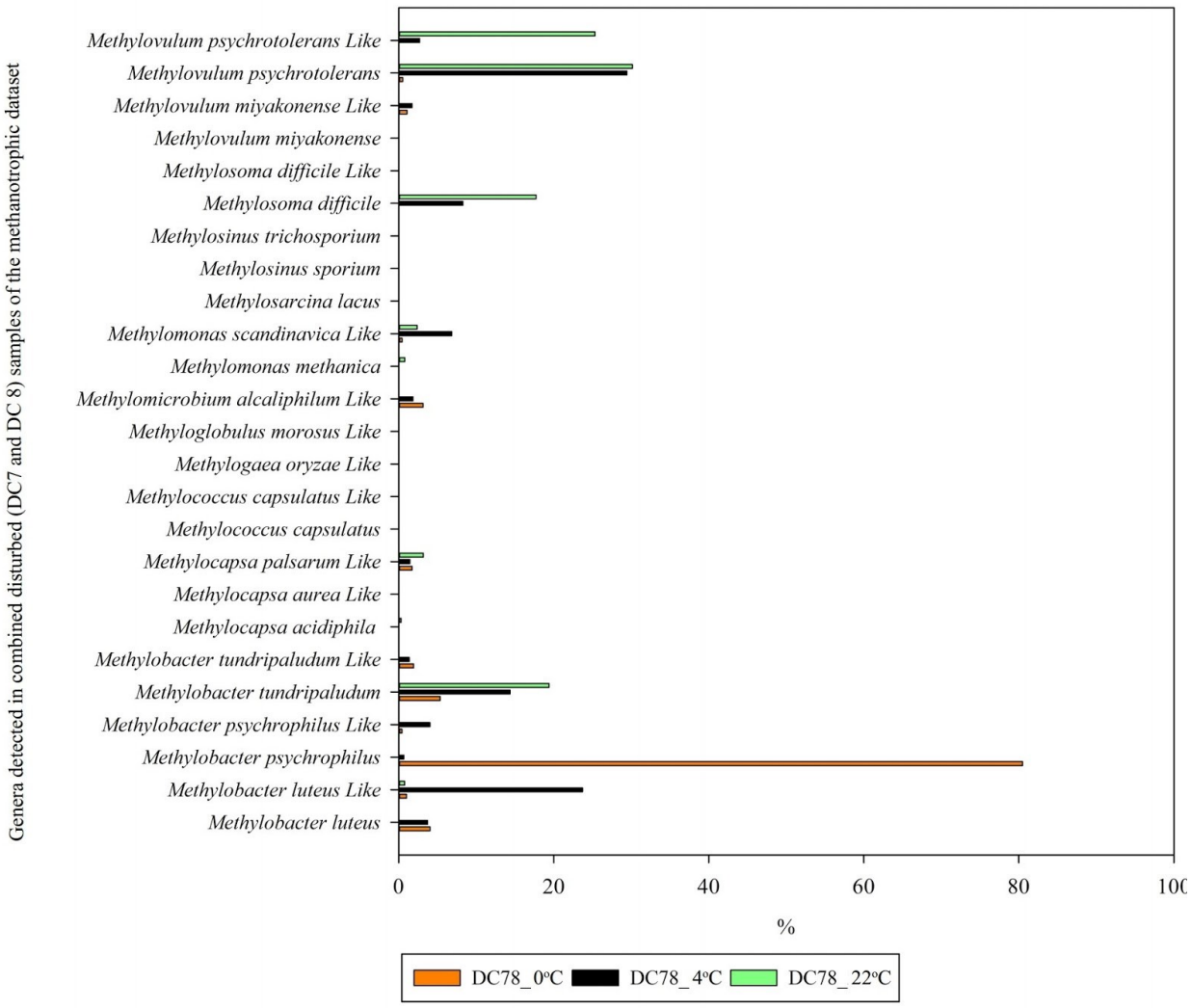

B

Supplementary Figure 4.15. Relative abundance analysis of the methanotroph dataset (A) undisturbed (DC5 and DC6) and (B) disturbed (DC7 and DC8) samples at genus level. In A and B the orange bars show 0 ºC, black bars 4 ºC and green bars 22 ºC samples.

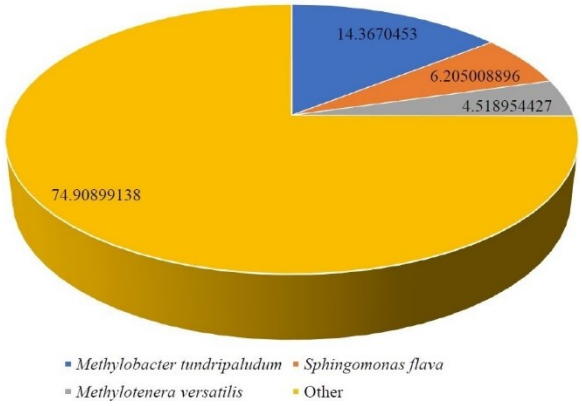
14.3670453
6.205008896
4.518954427
74.90899138
Methylobacter tundripaludum
Sphingomonas flava
Methylotenera versatilis
Other

A

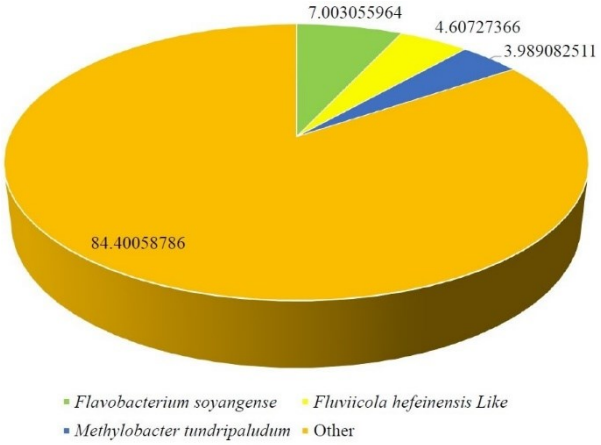
7.003055964
4.60727366
3.989082511
84.40058786
Flavobacterium soyangense
Fluviicola hefeinensis Like
Methylobacter tundripaludum
Other

B

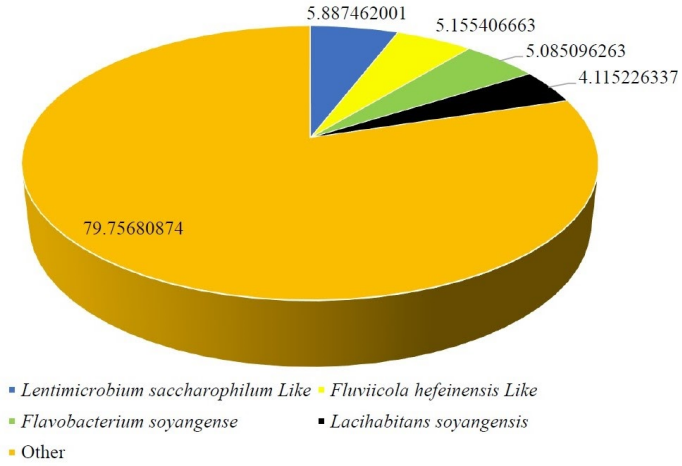
5.887462001
5.155406663
5.085096263
4.115226337
79.75680874
Lentimicrobium saccharophilum Like
Fluviicola hefeinensis Like
Flavobacterium soyangense
Lacihabitans soyangensis
Other

C

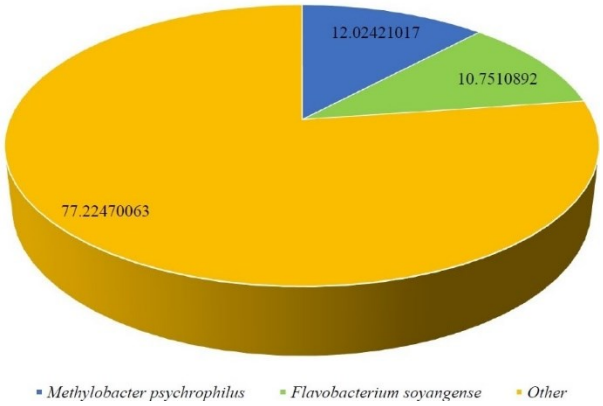
12.02421017
10.7510892
77.22470063
Methylobacter psychrophilus
Flavobacterium soyangense
Other

D

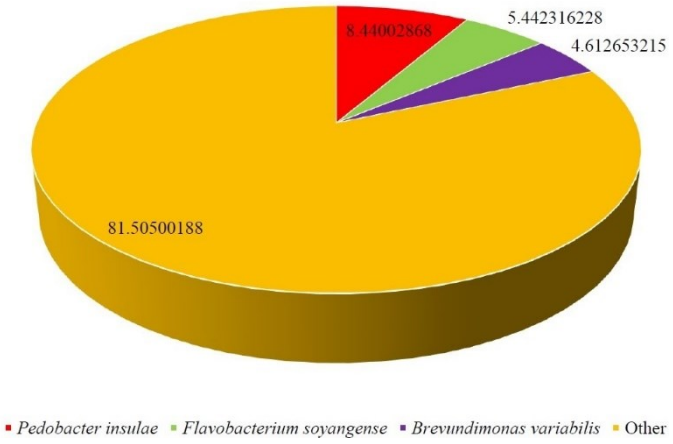
8.44002868
5.442316228
4.612653215
81.50500188
Pedobacter insulae
Flavobacterium soyangense
Brevundimonas variabilis
Other

E

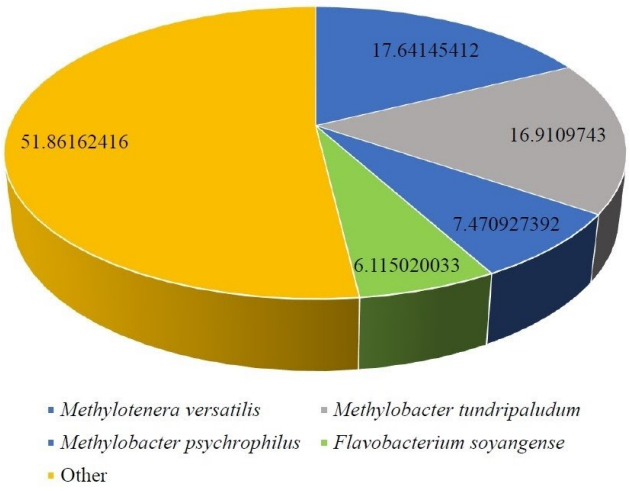
17.64145412
16.9109743
51.86162416
7.470927392
6.115020033
Methylotenera versatilis
Methylobacter tundripaludum
Methylobacter psychrophilus
Flavobacterium soyangense
Other

F

Supplementary Figure 4.16. The relative abundance of the strains detected in the heaviest ^{12}C fractions of the composite undisturbed (DC5 and DC6) (A-C) and composite disturbed (DC7 and DC8) (D-F) samples incubated at 0 ºC (A and D), 4 ºC (B and E) and 22 ºC (C and F). The group "Other" represents the composite relative abundance of the species with less than 4% abundance.

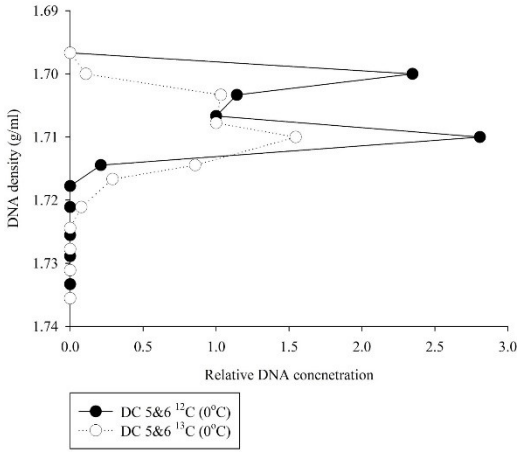

A

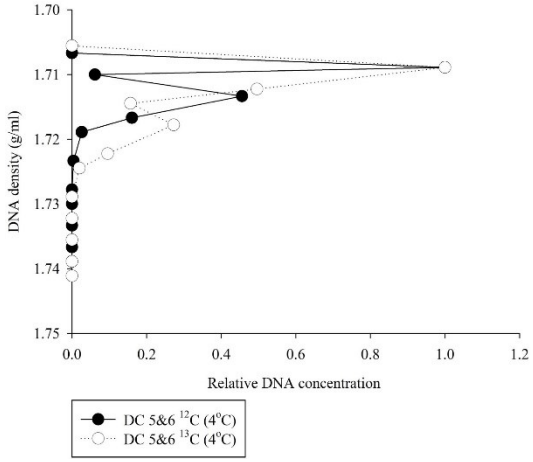

B

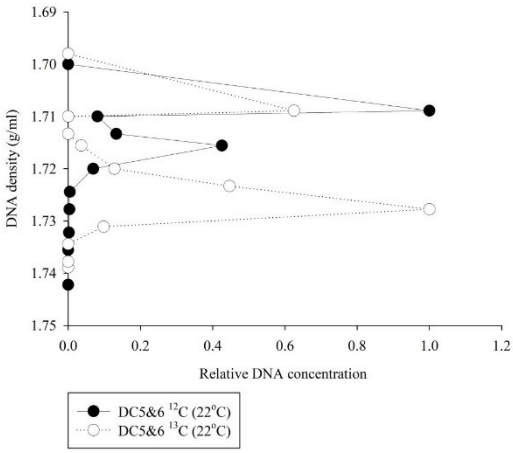

C

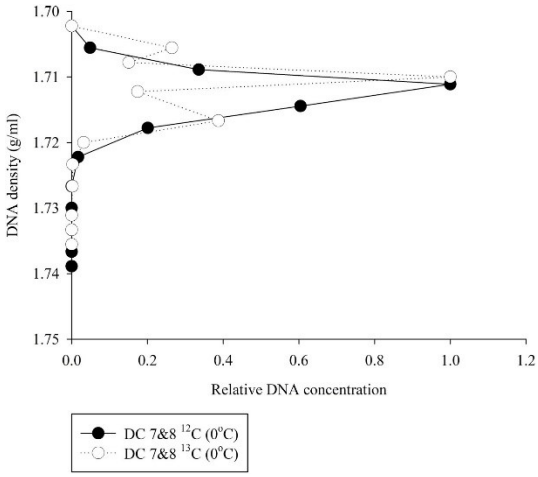

D

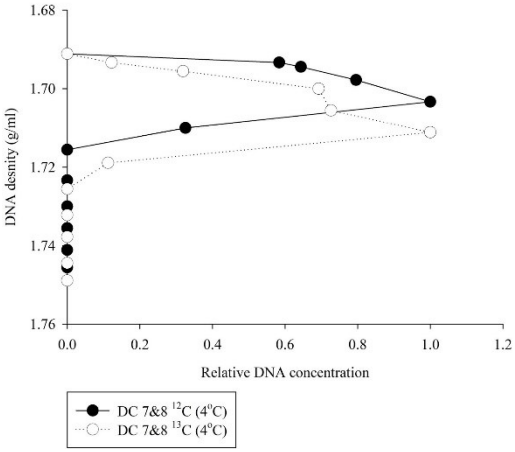

E

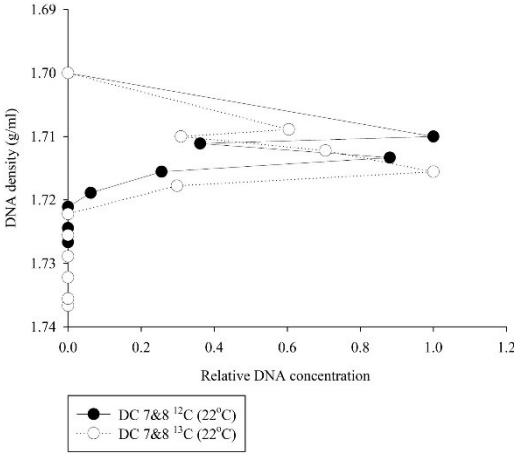

F

Supplementary Figure 4.17. DNA density gradients of composite undisturbed (DC5 and DC6) (A-C) and disturbed (DC7 and DC8) (D-F) samples incubated at 0 ºC (A and D), 4 ºC (B and E) and 22 ºC (C and F).

Supplementary Table 4.4. Average (n=3) measured basic soil edaphic parameters of undisturbed (DC5 and DC6) and disturbed (DC7 and DC8) active layer samples.

Samples [a]	OM (%)[d]	GW (%)[f]	pH*
DC 5 (UD)[b]	8.24 (1)[c]	81.8 (0.02)	7.21 (0.16)
DC6 (UD)	22.1 (0.66)	84.7 (0.01)	6.93 (0.17)
DC7 (D)[c]	11.3 (11.3)	70.8 (0.06)	6.57 (0.3)
DC8 (D)	13.6 (3.6)	80.8 (0.19)	6.1 (0.26)

[a] n=3, [b] UD = undisturbed active layer sample, [c] D = disturbed active layer sample, [d] OM = organic matter, [e] ± standard deviation, [f] gravimetric water, *$p < 0.01$ (DC5,6 vs DC7,8) measured based on Mann-Whitney U test.

Supplementary Table 4.5. The probability values calculated based on Wald's generalized estimating equation in the context of a many linear models.

Measured soil variables	The entire community	The methanotrophs
Soil type (disturbed/undisturbed)	0.018*	0.025*
Temperature (0 ºC-22 ºC)	0.005**	0.026*
CH_4 Oxidation rates	0.073	0.033*
pH	0.077	0.031*
OM[a]	0.195	0.521
GW[b]	0.3	0.119

[a]OM= organic matter, [b]GW = gravimetric water, *$p < 0.05$, **$p < 0.01$
Note: The residual degrees of freedom for all variables were 10 and differences in degrees of freedom attributed to each variable were 1.